University of Alberta

Molecular insights into SERCA regulation by endogenous peptide modulators

by

Przemyslaw Andrzej Gorski

A thesis submitted to the Faculty of Graduate Studies and Research
in partial fulfillment of the requirements for the degree of

Doctor of Philosophy

Department of Biochemistry

Fall 2013
Edmonton, Alberta

Abstract

In human cells, oscillations in calcium concentration serve as a mechanism for controlling a variety of physiological processes including muscle contraction and relaxation. The sarcoplasmic reticulum (SR) is a calcium storage organelle in muscle cells that contains a calcium pump (SERCA) required for the reuptake of calcium into the SR for muscle relaxation. The activity of SERCA is tightly regulated through reversible interactions with the short integral membrane proteins, phospholamban (PLN) and sarcolipin (SLN). Defects in the regulation of SERCA are a central determinant in end-stage heart failure. Consequently, the regulatory mechanisms imposed by PLN and SLN could have clinical implications for heart and skeletal muscle diseases. This thesis aims to provide functional insights into regulatory complexes formed between SERCA and its endogenous peptide modulators.

We sought to examine how SERCA activity is regulated by tissue-specific endogenous peptide modulators in order to meet the physiological needs of a specific cell type. Using alanine-scanning mutagenesis and chimeric PLN-SLN constructs, we identified the highly conserved luminal extension of SLN as a functionally important and transferrable domain that is a primary determinant for SERCA inhibition. Based on these findings, we concluded that SLN uses an inhibitory mechanism that is distinct from that of PLN. We also studied the ability of zebrafish phospholamban-like protein (zfPLN) to regulate SERCA. Functional analysis of zfPLN revealed that despite the high sequence diversity between zebrafish and human PLN, as well as the presence of a unique zfPLN luminal extension, zfPLN has inhibitory properties that are similar to human PLN. Finally, we examined the role of the 11^{th} transmembrane segment (TM11) of the ubiquitous SERCA2b in calcium transport. Our studies revealed that TM11 is a distinct and highly conserved functional region of SERCA2b that serves as a genuine regulator of

the calcium pump. Combined, the results provide novel insights into the different mechanisms of SERCA regulation by endogenous peptide modulators.

Acknowledgements

First and foremost, I would like to express my deepest gratitude to my supervisor, Dr. Howard Young, for his support, guidance and encouragement over the years. Thank you for giving me the opportunity to be a part of your lab.

I have been very fortunate to be surrounded by great people who have worked in the Young lab over the years. In particular, I would like to thank Drs. Cathy Trieber, Grant Kemp and John Paul Glaves for being great colleagues and becoming my close friends. It was a pleasure working with you! I have also met many amazing people during my stay in Edmonton who have made this journey very exciting. Thank you all!

My sincere thanks go to our collaborator and a good friend Dr. Peter Vangheluwe (K.U. Leuven) for his help and support for the past several years. I feel very fortunate to have had the opportunity to work with you. Your enthusiasm for research has definitely made me a better scientist.

I would like to thank my committee members, Dr. Marek Michalak and Dr. Mark Glover, for being very helpful and supportive throughout my graduate carrier as well as being a great source of advice. A special thanks to my internal examiner, Dr. Emmanuelle Cordat, and my external examiner, Dr. Todd Graham, for making the trip from Nashville.

Most importantly, I would like to thank my family. My fantastic parents, Marzena and Andrzej, have been there every step of the way and always encouraged me to pursue my dreams. Your unconditional love and support are a big reason for all of my successes. Without you none of this would have been possible! My wonderful sister Anna has always been a source of inspiration to me. Thank you for your love and making me believe that anything can be achieved if you put your mind to it. Lastly, I would like to thank my amazing girlfriend, Delaine, for her continuous support, patience, and love.

Table of Contents

List of Tables

Chapter 2

Chapter 3

Appendix I

List of Figures

Chapter1

Chapter 2

Chapter 3

Chapter 4

Chapter 5

Appendix I

List of Abbreviations

A-domain	actuator domain
ADP	adenosine diphosphate
AFA PLN	monomeric PLN construct (C36A, C41F, C46A)
Akt	protein kinase B
AMP	adenosine monophosphate
AMP-PCP	5'-adenylyl (beta,gamma-methylene)diphosphonate
ATP	adenosine triphosphate
BeF_3^-	beryllium fluoride
BHQ	dibutyl-dihydroxybenzene
$C_{12}E_8$	octaethylene glycol monododecyl ether
Ca^{2+}	calcium
CamKII	calcium/calmodulin-dependent protein kinase II
cAMP	cyclic adenosine monophosphate
COS cells	African green monkey kidney cells
CPA	cyclopiazonic acid
DCM	dilated cardiomyopathy
DHPR	L-type calcium channel
DPC	dodecylphosphocholine
DTT	dithiolthreitol
EGTA	ethylene glycol tetraacetic acid
EPR	electron paramagnetic resonance
ER	endoplasmic reticulum
EYPA	egg yolk phosphatidic acid
EYPC	egg yolk phosphatidylcholine

FITC	fluoroscein isothiocyanate
FRET	fluorescence resonance energy transfer
H^+	proton
HEK-293 cells	human embryonic kidney 293 cells
HPLC	high-performace liquid chromatography
HRC	histidine-rich calcium binding protein
I-1	inhibitor-1
I-2	inhibitor-2
IPTG	isopropyl β-D-1-thiogalactopyranoside
K_{Ca}	apparent calcium affinity
LE	luminal extension
MALDI-TOF	matrix-assisted laser desorption/ionisation-time of flight
Mg^{2+}	magnesium
NCX	sodium calcium exchanger
N-domain	nucleotide binding domain
n_H	Hill coefficient (cooperativity)
NMR	nuclear magnetic resonance
PDB	protein data bank accession number
P-domain	phosphorylation domain
PKA	protein kinase A
PKC	protein kinase C
PKI	protein kinase inhibitor
PLM	phospholemman
PLN	phospholamban
PMCA	plasma membrane calcium ATPase
PP-1	protein phosphatase-1

RyR	ryanodine receptor
SDS-PAGE	sodium dodecyl sulfate polyacrylamide gel electrophoresis
SERCA	sarco(endo)plasmic reticulum calcium ATPase
SLN	sarcolipin
SPCA	secretory-pathway calcium ATPase
SR	sarcoplasmic reticulum
STK16	Serine/Threonine Kinase 16
TCA	trichloroacetic acid
TEV	tobacco etch virus
TG	thapsigargin
TITU	1,3-dibromo-2,4,6-tri(methylisothiouronium)-benzene
TM	transmembrane domain
TM(num)	transmembrane helix number (num)
TNP-AMP	2',3'-O-(2,4,6-trinitrophenyl)adenosine 5'monophosphate
V_{max}	maximal activity

Standard Amino Acid Abbreviations

Glycine	Gly	G
Alanine	Ala	A
Valine	Val	V
Leucine	Leu	L
Isoleucine	Ile	I
Methionine	Met	M
Proline	Pro	P
Phenylalanine	Phe	F
Tryptophan	Trp	W
Serine	Ser	S
Threonine	Thr	T
Tyrosine	Tyr	Y
Asparagine	Asn	N
Glutamine	Gln	Q
Cysteine	Cys	C
Lysine	Lys	K
Arginine	Arg	R
Histidine	His	H
Aspartic Acid	Asp	D
Glutamic Acid	Glu	E

Chapter 1

Introduction

1-1. Calcium homeostasis

Calcium is a universal second messenger involved in diverse cellular processes such as fertilization, gene transcription, protein synthesis, neurotransmission, apoptosis, and excitation-contraction coupling in muscle tissue (1). Sustaining calcium homeostasis in the cell is central in allowing these processes to occur. This is achieved through movement of calcium across the membranes by various transporters and channels. For instance, in signal transduction pathways, changes in the intracellular calcium concentrations control the transcription of inducible genes through modification of transcription factors that interact with specific DNA regulatory elements in the promoter of the target gene. However, one of the most important roles of calcium is in muscle cells where its intracellular concentration oscillates as a mechanism for controlling muscle contraction and relaxation.

The contraction and relaxation of cardiac muscle cells are regulated by the cyclic movement of calcium primarily between the extracellular space, the cytoplasm and the sarcoplasmic reticulum (SR) (Fig. 1-1) (2). The process of muscle contraction begins with an action potential that depolarizes the plasma membrane and induces the L-type calcium channel (dihydropyranine receptor, DHPR) to open, allowing a minor calcium influx. In turn, this initiates a massive calcium release from the SR stores through the ryanodine receptor (RyR). The sudden increase in the cytosolic calcium concentration results in binding of calcium to troponin-C and initiation of muscle contraction. For muscle relaxation to occur, calcium concentration in the cytosol needs to be restored to resting levels. The rapid removal of calcium from the cytosol is primarily facilitated by the sarco(endo)plasmic reticulum calcium ATPase (SERCA) which pumps calcium back into the SR lumen and thereby controls the amount of calcium in the SR. To balance the influx of calcium via the DHPR, a small amount of calcium is moved into the

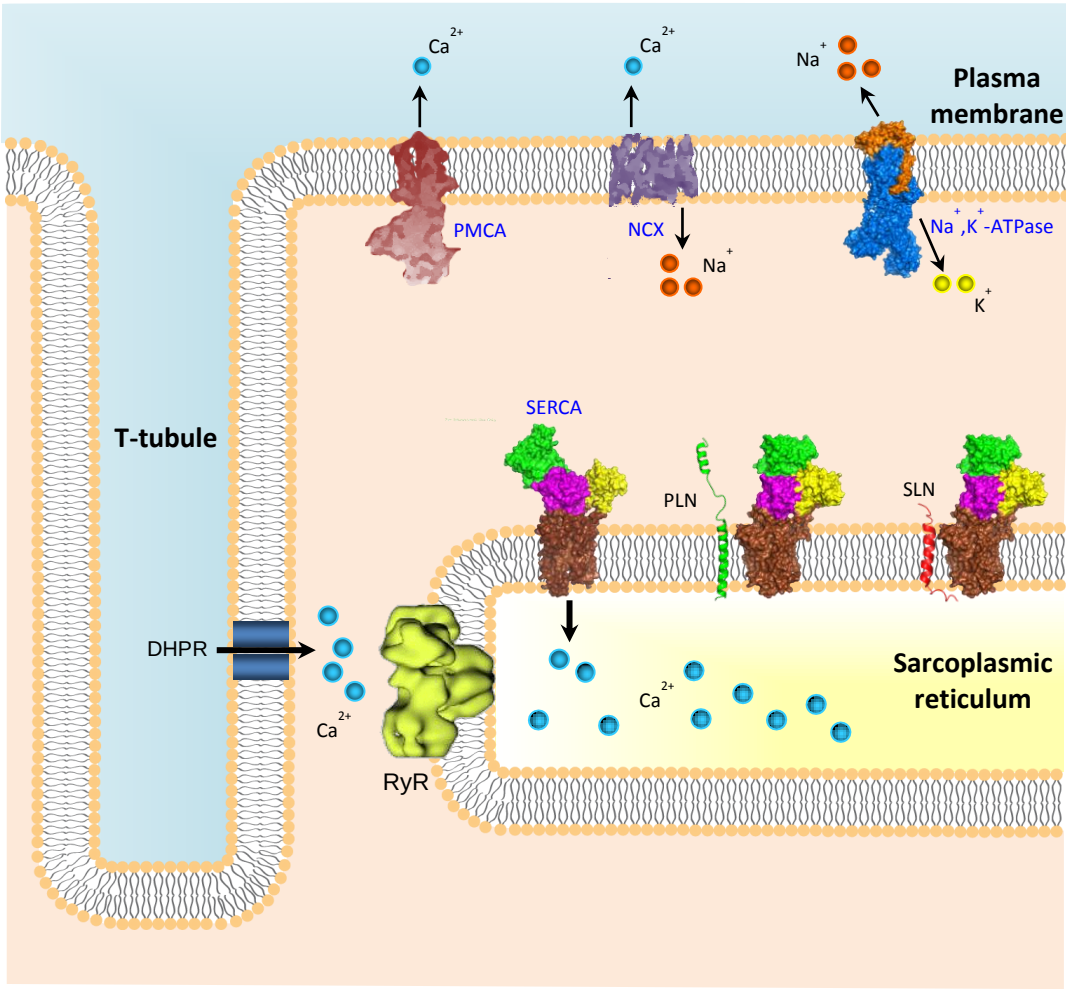

Figure 1-1. Schematic representation of ion homeostasis in cardiac muscle. The plasma membrane, T-tubule and sarcoplasmic reticulum of a cardiac myocyte are shown. Membrane channels and transporters important for muscle contraction and relaxation are shown along with their ion specificities. Models or structures of PMCA (plasma membrane calcium ATPase), NCX (sodium calcium exchanger, PDB 3V5U), Na^+,K^+-ATPase (PDB 3B8E), DHPR (dihydropyranine receptor), RyR (ryanodine receptor), SERCA (sarco(endo)plasmic reticulum calcium ATPase, PDB 1SU4 and 1IWO), PLN (phospholamban, PDB 1N7L) and SLN (sarcolipin PDB 1JDM) are shown.

extracellular space by sodium-calcium exchanger (NCX) and the plasma membrane calcium ATPase (PMCA). Therefore, SERCA is central in determining the rate of muscle relaxation and the strength of the subsequent contraction.

1-2. P-type ATPases

SERCA proteins are members of the P-type ATPase superfamily, a large and ubiquitous group of integral membrane proteins that are involved in many transport processes in all kingdoms of life (3). The P-type ATPase proteins generate and maintain electrochemical gradients by translocating cations, heavy metals and lipids across the cellular membranes at the expense of ATP and are named for the aspartyl-phosphate intermediate formed during their reaction cycle. The specific aspartate residue for auto-phosphorylation resides in a highly conserved sequence DKTGTLT shared by all P-type ATPase proteins. Members of the P-type ATPase family share many structural features and are thought to use similar mechanisms to transport their substrates.

Based solely on sequence homology, the P-type ATPase superfamily is divided into five distinct subfamilies, P1 through P5, which are further divided into a number of subgroups (4). P1 ATPases are presumably the simplest and most ancient ion transporters of the P-type ATPase family that can be further divided into two subgroups (3). The first subgroup, P1A is a small class of bacterial ATPases containing the KdpB-ATPase. KdpB-ATPase is rather a peculiar ATPase as it functions in complex with three other subunits (KdpF, KdpA, KdpC) in order to translocate K^+ across the membrane. Although KdpB has all the typical features of the P-type ATPases, it is the KdpA subunit that is thought to be responsible for K^+ transport (5). P1B-ATPases are found throughout all life forms and are the most common group of P-type ATPases in bacteria. They are primarily responsible for transporting monovalent and divalent heavy metal ions such as Cu^+, Ag^+,

Zn^{2+}, Cd^{2+} or Pb^{2+} across the plasma membrane into the extracellular space in order to prevent cell toxicity (6). Unlike the P1A-ATPases, P1B pumps are composed of a single polypeptide chain.

P2-ATPases are the most diverse and best characterized members of the P-type ATPase superfamily, and are divided into four subgroups (3). P2A-ATPases consist of Ca^{2+}-pumps found in the SR/ER (SERCAs) and Golgi (SPCAs) membranes, whereas plasma membrane Ca^{2+}-pumps (PMCAs) are of the P2B-type. The P2C subgroup of ATPases includes the Na^+/K^+-ATPase and the H^+/K^+-ATPase, where the latter is involved in gastric acidification. Members of this subgroup mostly form hetero-oligomers, composed of at least α- and β-subunits. Na^+/K^+-ATPase was the first P-type ATPase to be identified, and its discovery by Jens Christian Skou dates back to 1957 (7). After SERCA, Na^+/K^+-ATPase is the next best functionally and structurally characterized P-type ATPase. The Na^+/K^+-pump is involved in creating an electrochemical gradient across the plasma membrane by extruding three Na^+ ions for two K^+ ions (8). Finally, the P2D-type ATPases consists of eukaryotic Na^+-ATPases (3).

P3-ATPases are divided into two subgroups. The P3A-ATPases consist mainly of proton pumps found in the plasma membranes of bacteria, archea, fungi, and plants where they maintain intracellular pH. The P3B-ATPases consist of a small class of bacterial Mg^{2+} transporters (6).

The P4- and P5-ATPases are closely related to the P1-ATPases, although so far they have only been identified in eukaryotic organisms (4). It is interesting to note that together they make up over half of the P-type ATPase genes in the human genome. Despite their strong presence among the other groups of P-type ATPases, their function remains largely unknown. P4-ATPases have only recently been shown to be involved in

the translocation of phospholipids from the exoplasmic to the cytoplasmic leaflet of the plasma membrane in order to maintain the asymmetry of the lipid bilayer (hence the name 'lipid flippases') (9,10). The P5-type ATPases are the most elusive class of P-type ATPases because their substrate specificity and biological function have not yet been identified. There are some indications, however, that the P5-type pumps are located in the ER membranes and might be involved in cation transport (6).

1-3. SERCA isoforms and human disease

The SERCA pumps are highly conserved membrane proteins that have been identified in both prokaryotes and eukaryotes. In humans, three genes (*ATP2A1-3*) encode for multiple isoforms and splice variants of SERCA (SERCA1a-b, SERCA2a-c, SERCA3a-f), which allow for developmental and tissue-dependent expression patterns and alternative splicing (11). Due to the high sequence identity, all of the SERCA isoforms are predicted to have the same topology and virtually identical tertiary structure. Despite their high structural homology, these pumps significantly differ in their regulatory and kinetic properties, thereby accommodating cell or tissue specific calcium-handling requirements.

1-3.1. SERCA1

The SERCA1 gene (*ATP2A1*) can be alternatively spliced to generate the SERCA1a or SERCA1b isoforms, which are predominantly expressed in the adult and fetal fast-twitch skeletal muscles, respectively. SERCA1a is identical to SERCA1b, except the last C-terminal residue of SERCA1a (994 amino acids) is replaced by eight highly charged amino acids in SERCA1b (1001 amino acids) (12,13). Although the physiological role of SERCA1b remains elusive, this isoform was shown to be important for skeletal muscle development as it is expressed in the neonatal stages along with

SERCA2a but is completely replaced by SERCA1a in the adult muscle cells (14). The SERCA1a variant, on the other hand, has been extensively studied in different expression systems and animal models, and a plethora of functional and structural information is available. In this regard, SERCA1a has been a paradigm for the family of P-type ATPases. SERCA1a is highly abundant in the skeletal muscle where it is regulated by a single transmembrane peptide sarcolipin (SLN) (15). Compared to the cardiac SERCA2a isoform, SERCA1a appears to have the same affinity for calcium but a higher kinetic turnover rate (16). Because of its higher turnover rate, overexpression of SERCA1a in the cardiomyocytes of mice with ischemia-reperfusion injury was not only able to functionally substitute for SERCA2a but it also significantly enhanced the calcium transport and slowed down disease progression (17-19).

The gene encoding SERCA1 has been implicated in Brody disease, a rare inherited disorder of skeletal musculature (20). Several studies have indicated that mutations in the *ATP2A1* gene result in either a loss of function or a premature termination codon resulting in a truncated protein (21,22). As a result of dysfunctional SERCA1a, calcium is not properly transported back into the SR after its release into the cytoplasm, resulting in impaired muscle relaxation and stiffness. However, defects in genes encoding proteins other than SERCA have been linked to this disease implying that the origin of Brody disease is genetically heterogeneous (20).

1-3.2. SERCA2

The *ATP2A2* gene encodes for three splice variants of SERCA2 (a-c). The muscle specific isoform, SERCA2a, is expressed in cardiac and slow-twitch skeletal muscle, making it a key determinant of proper cardiac development and function (23). SERCA2a is 84% identical to SERCA1a, and is reversibly regulated by single

transmembrane proteins phospholamban (PLN) and sarcolipin (SLN) in cardiac muscle (24). SERCA2b is the most unique splice variant of all of the Ca^{2+}-ATPases, as it has a C-terminal extension that forms an eleventh transmembrane domain that protrudes into the ER lumen. It is referred to as the house-keeping form, as it is ubiquitously expressed in the ER of most cell types (25,26). Unlike SERCA2a, it is only sensitive to regulation by PLN (27). SERCA2c is a recently identified variant which has been found to be expressed at very low levels in monocytes and epithelial and hematopoietic cells (28,29).

The three SERCA2 splice variants display functional differences that can be attributed to the different C-terminal ends of the proteins. Overexpression studies have clearly demonstrated that SERCA2b has a two-fold higher affinity for calcium and a two-fold lower catalytic turnover rate as compared to SERCA2a (27). A more detailed explanation for the observed differences was given by in depth kinetic analysis of the SERCA2b isoform, which indicated that the C-terminal extension reduces the rate of calcium dissociation, phospho-enzyme intermediate conformational change, and dephosphorylation (30). SERCA2c was only recently shown to have the lowest apparent calcium affinity of the three SERCA2 variants, suggesting that it might serve its function in an environment with a locally high calcium concentration (29).

Although extremely rare, mutations in the SERCA2 gene have been linked to several human pathologies. Missense mutations in the SERCA2 gene cause Darier`s disease, a severe skin disorder characterized by loss of adhesion between epidermal cells, but do not effect cardiac function (31,32). More recently, mutations in the SERCA2 gene have been linked to lung and colon cancer (33). Studies in mice have shown that only one copy of the SERCA2 gene is necessary to maintain proper cardiac function but deletion of both genes is lethal (34). Heterozygous mice are viable but show a 35% decrease in SERCA levels (35). Defects in the regulation of SERCA2a as well as low activity or

expression levels of this isoform in the heart can lead to hypertrophy, cardiomyopathy, and end-stage heart failure and will be discussed in more detail in section 1-7.10.

1-3.3. SERCA3

SERCA3 is the most recently identified member of the SERCA family. Its primary sequence is ~75% identical to those of SERCA1 and SERCA2. Alternative splicing of the *ATP2A3* gene gives rise to six variants of SERCA3 that have been identified in humans (SERCA3a-f) (36). However, only three splice variants have so far been detected at the protein level (SERCA3a-c) (11).

The functional properties of this subfamily of calcium pumps are poorly understood. The hallmark of SERCA3 is its low affinity for calcium (5-fold lower than other SERCA isoforms) and its insensitivity to PLN (37,38). In addition, it has a significantly higher affinity for vanadate inhibition, and a higher pH optimum compared to other SERCA pumps (37). Just like the other SERCA isoforms, SERCA3 isoforms only vary at their C-termini, suggesting that the C-terminal tail region may contribute to the differences observed in the enzymatic activities (39).

SERCA3 isoforms are primarily expressed in hematopoietic cell lineages, epithelial cells, and endocrine pancreatic β-cells (40). Recently, SERCA3 expression was also observed in human cardiomyocytes (41). The SERCA3 expression profile often overlaps with the ubiquitous SERCA2b, although their relative subcellular locations are significantly different. Unique compartmentalization of the different SERCA isoforms might be crucial to their physiological role in maintaining calcium homeostasis within a cell. The high expression of SERCA3 in the pancreatic β-cells and mutations in the *ATP2A3* gene which have been associated with type II diabetes have suggested that SERCA3 plays a crucial role in metabolic homeostasis (42). Surprisingly, SERCA3

knock-out mice present normal glucose tolerance but display a smooth muscle relaxation defect (43). In addition, abnormal SERCA3 expression levels have been recently linked to gastric carcinoma (44).

1-4. Catalytic cycle of calcium transport by SERCA

It is well accepted that P-type ATPases undergo large conformational changes to transport ions or molecules across the membrane (3). These pumps cycle between a high affinity (E1) and low affinity (E2) state, both of which have phosphorylated intermediates (E1-P and E2-P). The E1-E2 model of active transport by P-type ATPase pumps was originally proposed by Post and Albers to describe the ion transport by Na^+/K^+-ATPase (45,46) and later adopted for the ion transport by SERCA (Fig. 1-2) (47). In the case of SERCA, the E1 state defines the high (micromolar) and E2 the low (millimolar) calcium affinity conformation of the enzyme (48). It is well established that calcium transport by SERCA is tightly coupled to ATP hydrolysis. The energy generated from one ATP molecule drives SERCA to pump two calcium ions in exchange for two to three protons. The E1 and E2 states do not indicate that the transporting enzyme is in either the "open" or "closed" conformation but rather represent two distinct SERCA states with high affinity for calcium and protons, respectively (49).

The mechanism of ATP dependent calcium transport by SERCA is summarized in Figure 1-2. The cycle begins in the high-affinity E1-ATP state where the two calcium binding sites are exposed to the cytosol. Successive binding of two calcium ions results in a release of two to three protons into the cytosol and formation of $(Ca^{2+})_2$-E1-ATP intermediate. Calcium binding triggers auto-phosphorylation by the γ-phosphate of ATP at the highly conserved aspartic acid residue, Asp^{351}. This results in the formation of a high-energy phospho-intermediate, $(Ca^{2+})_2$-E1-P-ADP, in which the bound calcium

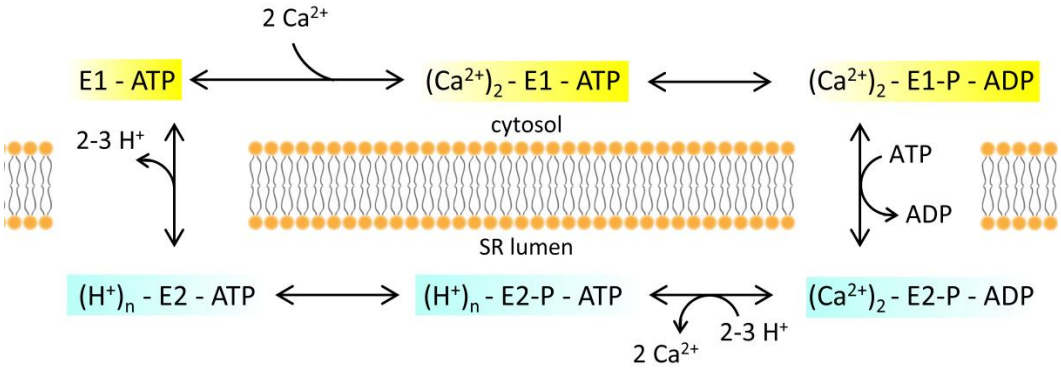

Figure 1-2. Post-Albers cycle. SERCA exists in either an E1 (high affinity for calcium; yellow) or E2 (low affinity for calcium; blue) state. Two cytosolic calcium ions are exchanged for two to three luminal protons. Nucleotide is always bound, either in a catalytic or modulatory mode, and SERCA is auto-phosphorylated at a conserved aspartic acid residue (Asp^{351}).

becomes occluded and is inaccessible to the cytosol or lumen (50). It is important to note that at this point in the transport cycle high ADP concentrations in the cytosol can reverse the reaction resulting in regeneration of ATP and release of calcium ions into the cytosol. The next step in the transport cycle involves exchange of ADP for ATP and transition into the low-energy $(Ca^{2+})_2$-E2-P-ADP state in which the calcium ions remain occluded. Conversion to the $(H^+)_{2\text{-}3}$-E2-P-ATP state results in a release of calcium ions into the lumen and binding of two to three protons to compensate for the net negative charge of the calcium binding sites (51). Subsequently, dephosphorylation of the enzyme leads to the formation of the $(H^+)_{2\text{-}3}$-E2-ATP state in which protons are occluded. The final step of the transport cycle is the release of the protons into the cytosol and reformation of the E1-ATP state with the ion binding sites primed for the binding of cytosolic calcium in the next reaction cycle (52).

The role of ATP in the calcium transport cycle has traditionally been described as catalytic, where nucleotide molecules were thought to be only associated with the E1 forms of the enzyme. More recently, however, ATP has been shown to not only play a catalytic but also a modulatory role in the transport cycle (53). At physiological concentrations, ATP appears to bind to SERCA at various intermediates and accelerate partial reaction steps involved in calcium binding (54,55), calcium translocation (56), and dephosphorylation of SERCA (57). Although the details of this stimulatory action of ATP on SERCA are still largely unexplained, some structural studies revealed that the modulatory binding site overlaps with the catalytic one (53,58,59). Therefore, it is now accepted that ATP (or ADP) is bound to every intermediate in the pump's transport cycle.

1-5. Structural studies of SERCA

SERCA is the best studied member of the P-type ATPase family as a result of numerous functional and structural studies carried out in the last few decades. The three dimensional structure of rabbit SERCA1a was the first to be determined and for a long time served as a model for the architecture and molecular mechanism of other P-type ATPases. Despite the difficulties associated with crystallization of membrane proteins, over forty high-resolution x-ray crystallographic structures have been solved, revealing the pump's structural complexity. These atomic models cover nearly all of the reaction intermediates, which correspond to the different conformations that the enzyme assumes during the calcium transport cycle.

1-5.1. First high-resolution structure of SERCA reveals its detailed architecture

In 1985 MacLennan and coworkers proposed a secondary-structure model of SERCA based on an amino acid sequence of rabbit SERCA1a (60). This model predicted the SERCA pump to consist of ten membrane spanning helices and three cytoplasmic domains. In the following years, extensive mutagenesis studies identified many important functional features of the pump and the involvement of transmembrane segments in calcium binding (61-65). Together with initial electron microscopy data (66-68), these early studies gave the first clues to the architecture and function of SERCA. In 1993, the first complete three dimensional structure of SERCA was obtained by cryo-electron microscopy (69). Tubular crystals of SERCA in the presence of vanadate, a key crystallization component which traps P-type ATPases in an E2 conformation, provided three dimensional maps to 14 Å resolution. This early structure revealed a large cytoplasmic domain connected to the transmembrane domain via a short stalk region. A more detailed view of the calcium pump was achieved in 1998 when an improved 8 Å

resolution structure of SERCA was obtained (70). This was mainly accomplished by crystallizing SERCA in the presence of a high-affinity inhibitor thapsigargin (TG), which is known to stabilize the transmembrane segments of the enzyme. The new structure of SERCA determined by electron microscopy provided an enhanced view of the transmembrane domain which was observed to be composed of ten transmembrane helices consistent with the previously proposed secondary-structure model (60).

The first high resolution structure of SERCA obtained by x-ray crystallography in 2000 by Toyoshima and coworkers represented a great milestone in the field (Fig. 1-3) (71). The structure was solved to 2.6 Å resolution and depicted a calcium bound $(Ca^{2+})_2$-E1 SERCA intermediate. The new SERCA structure largely confirmed previous models but allowed for examination of the calcium pump at an atomic level.

The SERCA x-ray structure confirmed that the transmembrane domain of SERCA indeed consists of ten transmembrane helices, two of which (TM4 and TM5) are long and extend from the membrane into the cytoplasmic domain. It also revealed two high affinity calcium binding sites (site I and II) in the transmembrane domain which are located side-by-side and close to the cytoplasmic surface of the membrane. Experimental evidence suggests sequential and cooperative mode of calcium binding to SERCA, where binding of the first calcium ion results in a conformational change in the enzyme leading to an increased affinity for the second calcium ion (72,73). This has been confirmed by mutagenesis studies which revealed that mutations in site I prevent binding of calcium at both sites, whereas mutation within site II only interfered with calcium binding to that site and not site I (74). The calcium ion at site I is coordinated mainly by residues on TM5 (Asn^{768} and Glu^{771}) and TM6 (Thr^{799} and Asp^{800}), with distal contributions from Glu^{908} on TM8. The neighboring calcium ion at site II is coordinated by Glu^{309} and main chain carbonyl groups of Val^{304}, Ala^{305} and Ile^{307} (all found on partially unwound TM4)

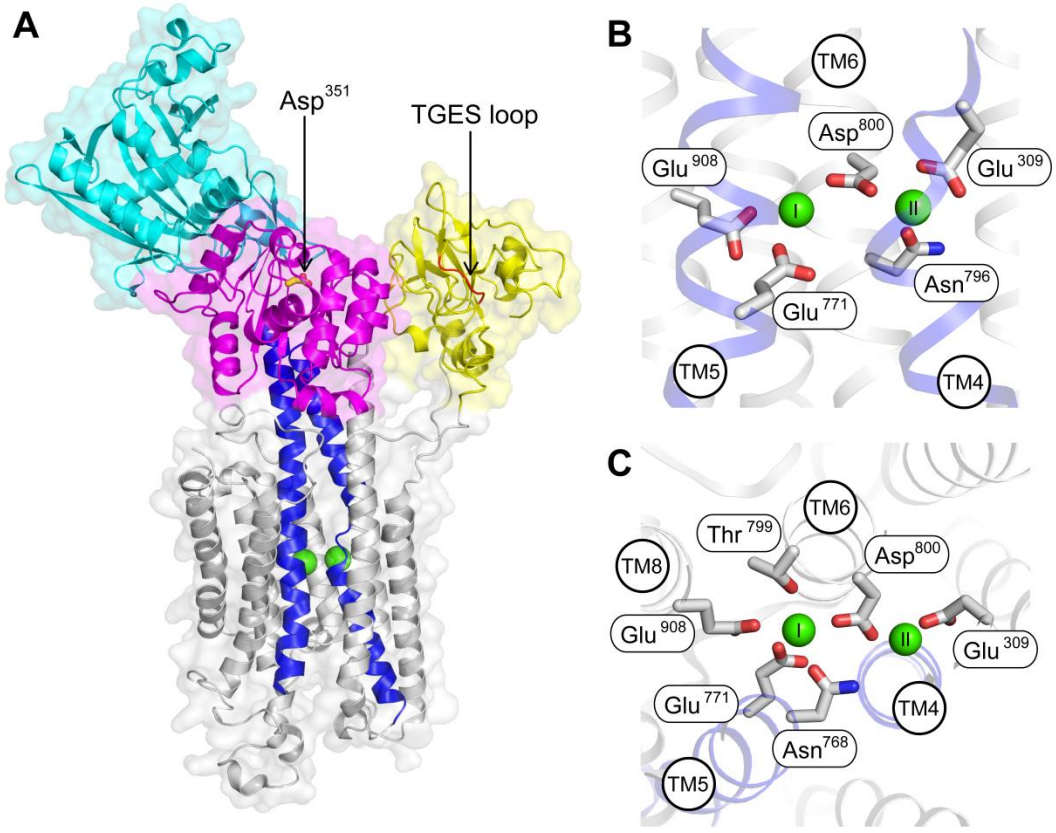

Figure 1-3. The first high-resolution structure of SERCA bound to two Ca^{2+} ions. **(A)** The $(Ca^{2+})_2$-E1 state of SERCA (PDB 1SU4) shown in transparent surface and cartoon with the P-domain in magenta, N-domain in cyan, A-domain in yellow, and helices TM1-10 in grey except TM4 and TM5 which are blue. The calcium ions are shown as green spheres. The TGES motif is shown in red and Asp^{351} is shown in yellow stick representation. **(B)** Close-up view of the calcium binding sites between TM4, TM5, TM6 and TM8 helices with key coordinating residue side chains shown as grey sticks. **(C)** Rotation of panel B by 90° around the x-axis (top-down view).

together with the side chains of Asn^{796} and Asp^{800} (both on TM6). Interestingly, the amino acids involved in calcium binding seen in this structure are in high agreement with previous mutagenesis studies (65).

The large cytoplasmic headpiece of the pump was visualized as three distinct domains: the nucleotide binding (N-), phosphorylation (P-), and actuator (A-) domains. The N-domain is the largest of the three cytoplasmic domains and is responsible for recruiting and positioning ATP to allow phosphorylation to occur. The nucleotide binding pocket within this domain contains a highly conserved residue, Phe^{487}, which interacts with the adenine ring of the ATP molecule. The N-domain is connected to the highly conserved P-domain via a flexible hinge region. Located in the top region of the P-domain is a conserved DKTGT motif, which includes an aspartate residue (Asp^{351} in SERCA) necessary for formation of the high energy aspartyl-phosphate intermediate. In this first $(Ca^{2+})_2$-E1 crystal structure, the phosphorylation site was located ~30 Å away from the nucleotide binding site, and thus provided little information as to how the phosphorylation event is coupled to calcium transport. Finally, the smallest cytosolic domain is the A-domain and it is well separated from the other cytosolic domains. Its role is to coordinate movements in the cytoplasmic domain that occur during the reaction cycle with movements in the membrane domain, allowing for calcium translocation to occur. The A-domain also controls the dephosphorylation reaction via the signature TGES sequence present in all P-type ATPases (50).

Comparison of the 8 Å resolution E2-TG structure of SERCA with the high resolution $(Ca^{2+})_2$-E1 structure suggested that large conformational changes take place during the reaction cycle. The most striking difference between these two structures was the wide open conformation of the cytoplasmic domains within the $(Ca^{2+})_2$-E1 structure. Since the N- and P-domains must come together for phosphorylation to take place, it was

proposed that the enzyme must assume a conformation similar to the compact headpiece formation of the calcium-free E2-TG state.

1-5.2. SERCA structure in the absence of calcium

Although the first high resolution structure of SERCA provided a detailed description of the enzyme, it also raised new questions; particularly, the relation of the large conformational changes in the cytoplasmic domains and how they might translate to changes in the transmembrane domain and in turn affect calcium binding and dissociation. Many of these questions were answered in 2002 when Toyoshima and coworkers released the second high resolution structure of SERCA in the calcium-free state (Fig. 1-4) (75). This x-ray crystal structure was solved to 3.1 Å resolution and represented the E2-TG intermediate. Comparison of the $(Ca^{2+})_2$-E1 SERCA structure with the new E2-TG structure allowed a direct comparison of the enzyme in two distinct conformations at an atomic level.

The new E2-TG SERCA structure revealed that in the absence of calcium the cytoplasmic domains drastically change their conformations and form a compact headpiece, consistent with the previous structures in the E2 state solved by electron microscopy (69,70). Comparing the $(Ca^{2+})_2$-E1 and the E2-TG structures, the N-domain inclines 60° relative to the P-domain and the P-domain inclines by about 30° with respect to the membrane assuming a more upright position. The A-domain undergoes a ~110° horizontal rotation between the two states. Despite the large conformational changes, the overall structure of each cytoplasmic domain remains relatively the same as SERCA transitions from the $(Ca^{2+})_2$-E1 to the E2-TG state. Therefore, the conformational changes are mainly restricted to the linker regions between the domains, strongly suggesting a

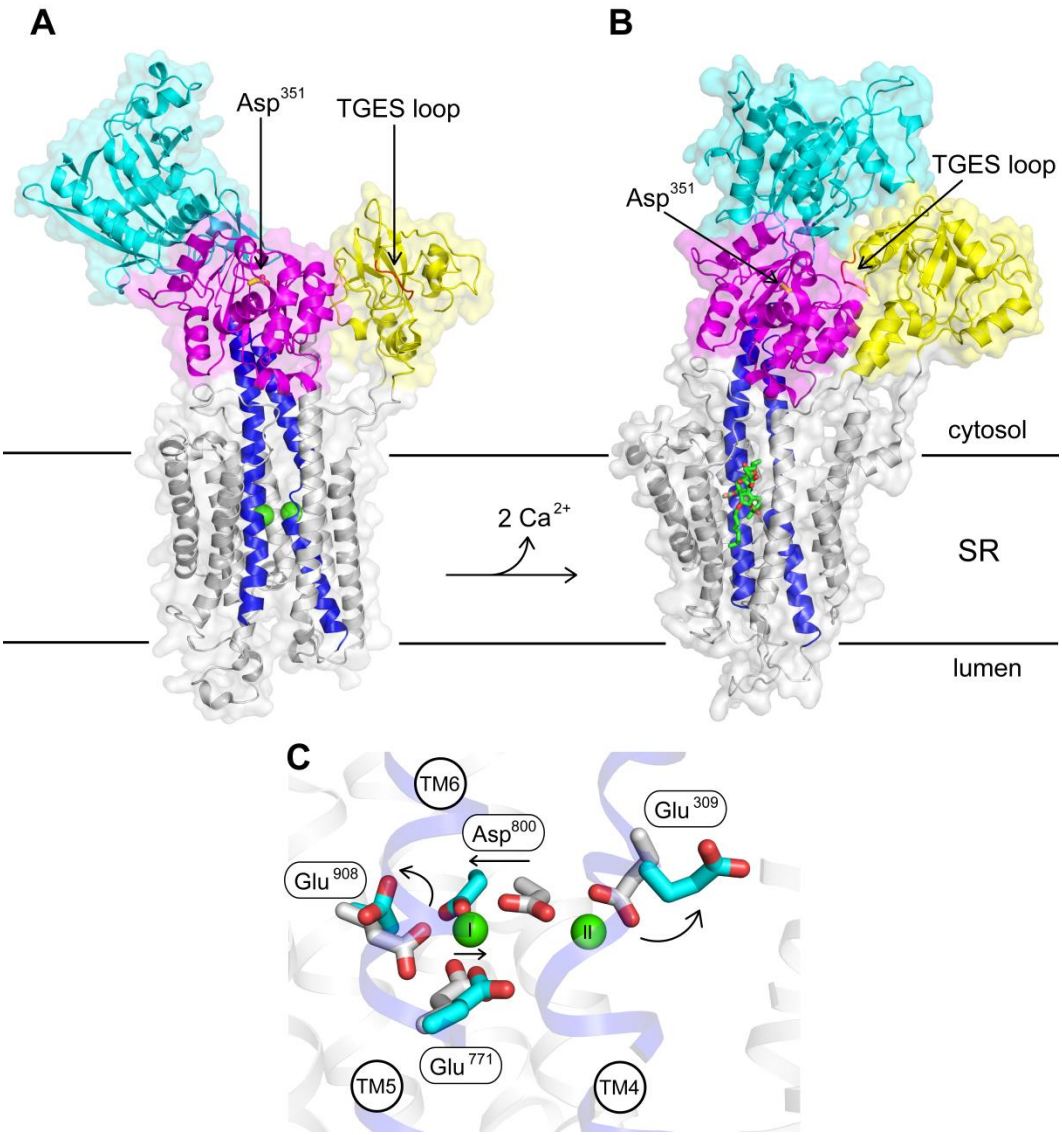

Figure 1-4. Conformational changes between the high resolution $(Ca^{2+})_2$-E1 and E2-TG structures of SERCA. (A) The $(Ca^{2+})_2$-E1 state of SERCA (PDB 1SU4) is shown in transparent surface and cartoon with the P-domain in magenta, N-domain in cyan, A-domain in yellow, and helices TM1-10 in grey except TM4 and TM5 which are blue. The calcium ions are shown as green spheres. **(B)** The E2-TG state of SERCA (PDB 1IWO) shown in transparent surface and cartoon colored as in panel A. TG molecule is shown in green stick representation. **(C)** Close-up view of the conformational changes around the calcium binding sites between the $(Ca^{2+})_2$-E1 and E2-TG states of SERCA. The side chains of calcium coordinating residues in the $(Ca^{2+})_2$-E1 state are shown as grey sticks and in the E2-TG state as cyan sticks. Changes in the position of the side chains of calcium coordinating residues when proceeding from the E1 to the E2 state are indicated by arrows.

critical role of the linker regions between the cytoplasmic and the transmembrane domains in proper SERCA function (76,77).

In addition to the information gained about the cytoplasmic domains of SERCA, the new structure revealed the arrangement of the transmembrane domain in the absence of calcium (75). The transition from the calcium bound to the calcium-free state is accompanied by complex movements of TM1 to TM6, while TM7 to TM10 remain relatively immobile. TM1 and TM2 move upward whereas TM3 and TM4 move downward with respect to the membrane. TM1 also makes a unique horizontal transition upon calcium dissociation. Located in the center of the enzyme, the TM4 helix shifts towards the luminal side of the membrane and the upper part of the TM5 helix is bent. The P-domain appears to play a major role in coordinating movements of TM1-2 and TM4-5 transmembrane segments through hydrogen bonding or direct interactions, respectively. As predicted, these movements have drastic effects on the coordination geometry of the two calcium binding sites. Site I rearrangement is mainly attributed to the movement of three crucial residues on TM6, which rotate by 90° away from the center of the molecule. In site II, as a result of the downward movement of TM4, the calcium coordinating Glu^{309} is facing away from the binding site. Together, these conformational changes clearly explain the decrease in affinity for calcium by SERCA in the E2-TG state (Fig. 1-4B).

1-5.3. Structural insights into the SERCA calcium transport cycle

Since 2002, the SERCA field has been overwhelmed with dozens of high resolution structures crystallized in the presence of many different inhibitors and nucleotide analogues (49). To date, we have a near complete understanding of reaction intermediates in the SERCA transport cycle. While there are many SERCA structures

available, only select ones will be discussed herein to briefly describe the structural changes that accompany calcium transport.

SERCA structures representing the key reaction intermediates of the calcium transport cycle are shown in Figure 1-5. The reaction cycle begins with the enzyme in the calcium-free state and bound nucleotide (E2-ATP) depicted by the E2-AMPPCP crystal structure (53). In the E2-ATP state, the A-domain is oriented in a manner suitable for close interactions with the P- and N-domains. The tight interactions of the cytoplasmic domains keep the TGES motif, the conserved sequence responsible for dephosphorylation, away from the phosphorylation site and the γ-phosphate of the N-domain-bound ATP molecule far (~10 Å) from the phosphorylatable Asp^{351}. Because SERCA is not subject to phosphorylation by ATP and the TGES loop is withdrawn from the phosphorylation site, the E2-ATP conformation represents a resting state. For the γ-phosphate of ATP to come into proximity with Asp^{351}, SERCA needs to change its conformation. This is achieved upon binding of two cytosolic calcium ions in exchange for 2-3 protons which results in the formation of $(Ca^{2+})_2$-E1-ATP state represented by the $(Ca_{2+})_2$-E1-AMPPCP structure (78). Binding of calcium ions leads to stabilization of the enzyme, and translational as well as rotational changes of the TM1-4 region that are later transmitted to cytoplasmic domains. In the $(Ca^{2+})_2$-E1-AMPPCP structure, the A-domain is rotated counterclockwise allowing a small movement of the N-domain towards the P-domain and in turn closer approximation of ATP to the catalytic Asp^{351}. In the following step, transfer of the γ-phosphate of ATP to Asp^{351} leads to the formation of the $(Ca^{2+})_2$-E1-P-ADP high-energy intermediate represented by the $(Ca^{2+})_2$-E1-ADP-AlF_4^- structure (78). Although the $(Ca^{2+})_2$-E1-AMPPCP and the $(Ca^{2+})_2$-E1-ADP-AlF_4^- structures are quite similar, subtle rearrangements lead to occlusion of calcium ions in the $(Ca^{2+})_2$-E1-P-ADP state as confirmed by experimental studies. Another important difference between

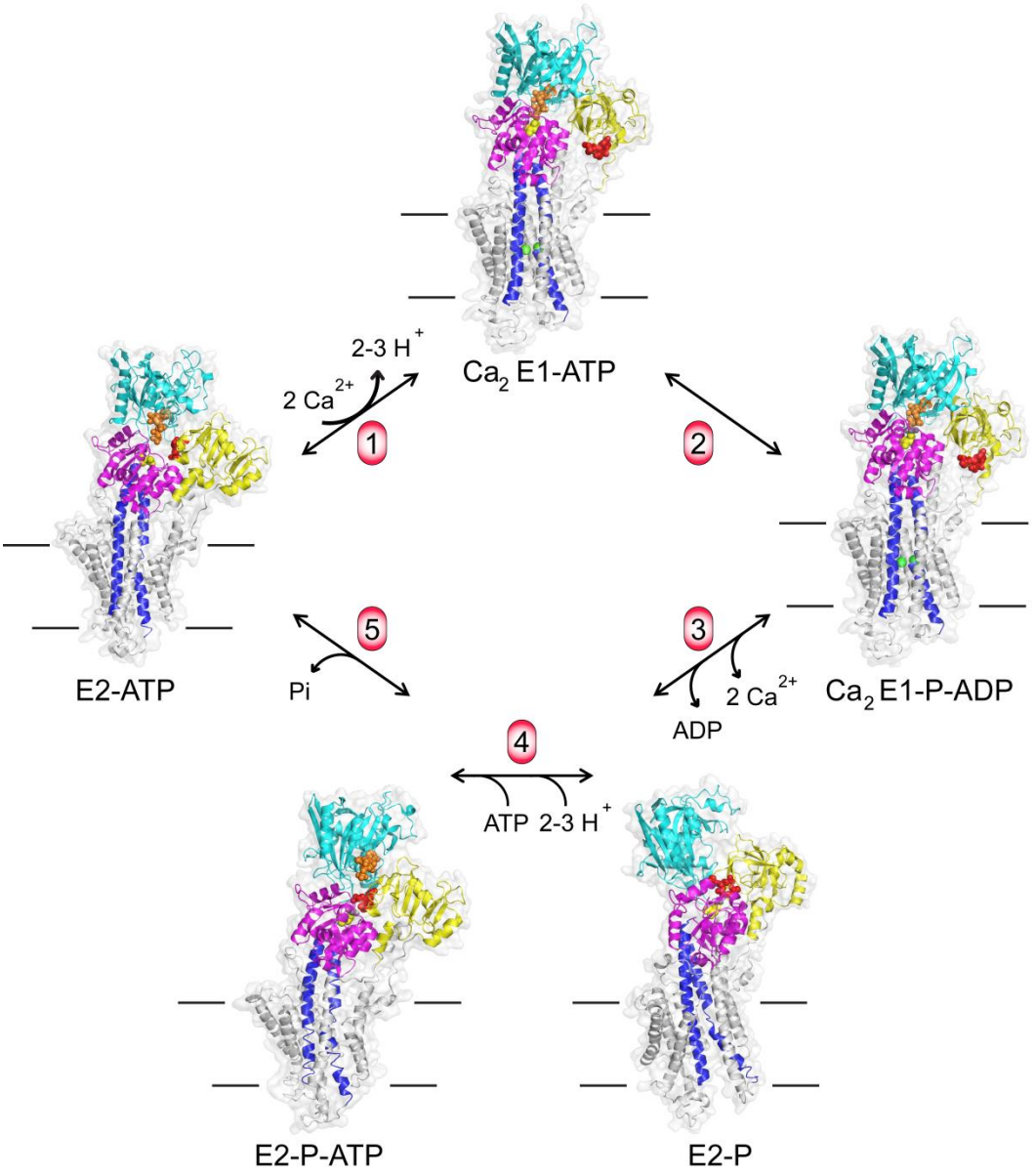

Figure 1-5. Structural basis of calcium transport. Transparent surface and cartoon representations of key structures of SERCA in the calcium transport cycle. P-domain of SERCA is magenta, N-domain is cyan, A-domain is yellow, and helices TM1-10 are grey except TM4 and TM5 which are blue. Calcium ions are shown as green spheres, nucleotide (ATP or ADP) is shown as orange spheres, and TGES motif residues are shown as red spheres (PDBs: 1T5T, 1T5S, 3B9B, 3B9R, 2C8K). Figure was adopted from (49).

these two complexes is related to the cation coordination of a nucleotide. Unlike the $(Ca^{2+})_2$-E1-AMPPCP structure where only one magnesium ion coordinates the γ-phosphate of the AMPPCP molecule, the $(Ca^{2+})_2$-E1-ADP-AlF_4^- structure reveals one magnesium coordinating AlF_4^- and another magnesium coordinates the α- and β-phosphates of the ADP. The second magnesium is only present in a transition state and is thought to lower the activation energy required for the phosphate transfer (49). Once the transfer of the γ-phosphate from ATP to Asp^{351} is complete, the enzyme transitions to the low energy E2-P-ATP state depicted by the E2-BeF_3^- structure. At this time bound ADP is exchanged with an ATP molecule. Direct comparison of the $(Ca^{2+})_2$-E1-ADP-AlF_4^- and the E2-BeF_3^- structures reveals a 50° rotation of the N-domain relative to the P-domain and a clockwise 108° rotation of the A-domain. This drastic movement of the A-domain causes a lateral movement of the TM1-2 and TM3-4 pairs relative to the TM5-10 complex, which results in the formation of a luminal access channel. This conformational change orients the side chains of the calcium binding residues towards the lumen allowing for the release of calcium ions to take place. It is important to mention that the E1-P to E2-P transition is thought to occur in two steps: formation of the calcium occluded $(Ca^{2+})_2$-E2-P intermediate followed by the opening of the channel (49). Unfortunately, the structure of the occluded $(Ca^{2+})_2$-E2-P intermediate has not yet been successfully determined. As the calcium ions leave the luminal channel, 2-3 protons are taken up to partially compensate for the negatively charged carboxylate groups at the ion binding site. This is followed by closure of the luminal channel and transition into the $(H^+)_{2\text{-}3}$-E2-P-ATP proton occluded state represented by the E2- AlF_4^--ATP structure (50). In this conformation the conserved TGES motif located on the A-domain docks into the phosphorylation site and coordinates water molecules for a hydrolytic cleavage of the phosphate group. Following dephosphorylation, the enzyme assumes a more relaxed state and the TGES motif is retracted from the phosphorylation site allowing release of the

bound phosphate. In the final step of the reaction cycle, SERCA returns to the E2-ATP state and is ready for the next pair of cytosolic calcium ions to bind.

1-5.4. Small molecule SERCA inhibitors

Several small molecules are known to inhibit SERCA by interfering with its ability to bind calcium. The first small molecule SERCA inhibitor to be discovered was thapsigargin (TG), a very potent and highly selective SERCA inhibitor (79). Other inhibitors such as cyclopiazonic acid (CPA) (80) and 2,5-di(*tert*-butyl)hydroquinone (BHQ) (81) were discovered in the following years. More recently 1,3-dibromo-2,4,6-tri(methylisothiouronium)-benzene (TITU) (82,83) and artemisinins (84) were also shown to act as SERCA inhibitors but their properties will not be discussed herein. Discovery of these small molecule inhibitors was a major breakthrough in the SERCA field, as they have been widely used as tools in physiological, biochemical and structural studies. Furthermore, they show potential to serve as important therapeutic agents (85).

TG is a compound extracted from the plant *Thapsia garganica* and is the best-studied SERCA inhibitor. It has sub-nanomolar affinity for the enzyme and is known to inhibit all mammalian SERCA isoforms with nearly equal potency (86,87). Other members of the P2A-type ATPase subgroup (SPCA pumps) have also been shown to be sensitive to TG, although to a much lower extent (88). As previously mentioned, TG has been an important tool in determining the first three dimensional SERCA structures by electron microscopy and x-ray crystallography. The high-resolution structures of SERCA in the presence of TG reveal that the inhibitor locks the enzyme in the E2-like calcium-free states (Fig. 1-6A) (89). TG binds in a hydrophobic cavity formed by TM3, TM5 and TM7 which prevents the movement of the transmembrane helices relative to each other (Fig. 1-6B). TG forms crucial interactions with Phe^{256} (TM3), Ile^{765} (TM5) and Tyr^{837}

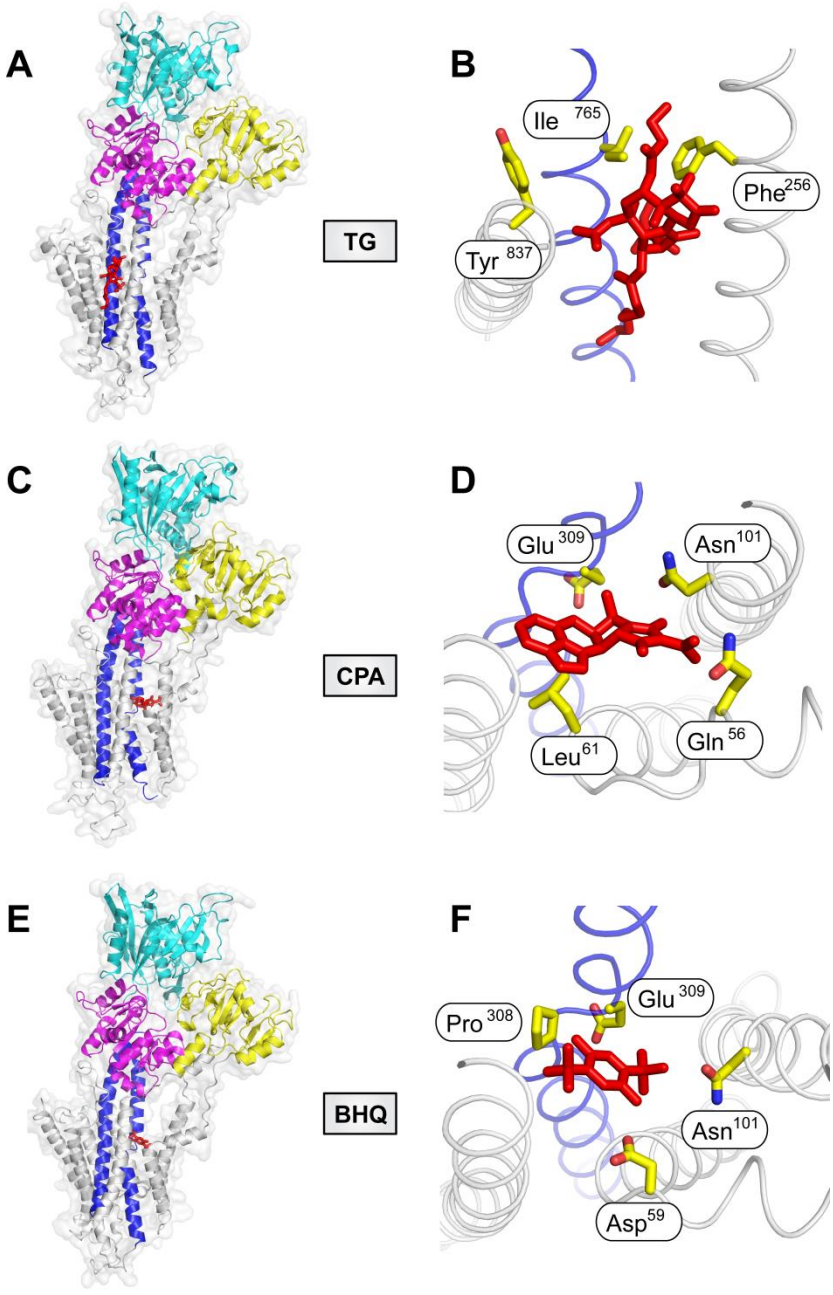

Figure 1-6. High-resolution structures of SERCA in complex with small molecule inhibitors. (A, C, E) Transparent surface and cartoon representations of SERCA in complex with TG (PDB 1IWO), CPA (PDB 2OJ9) and BHQ (PDB 2AGV), respectively. P-domain of SERCA is magenta, N-domain is cyan, A-domain is yellow, and helices TM1-10 are grey except TM4 and TM5 which are blue. The small molecule inhibitors are shown as red sticks. **(B, D, F)** Detailed views of the TG, CPA and BHQ binding sites, respectively. Residues important for inhibitor binding are shown as yellow sticks.

(TM7) as revealed by mutagenesis studies (90). Phe^{256} on TM3 appears to be the most important of the three residues as it is involved in a ring stacking interaction with the seven membered ring of TG that strengthens its binding with SERCA (91). Thus, TG inhibits SERCA by locking it in one conformation which prevents it from completing its transport cycle.

CPA is a toxic indole tetramic acid found in fungi and BHQ is a synthetic compound often used as an anti-oxidant (92,93). Like TG, both of these small molecules are potent inhibitors of SERCA with the binding affinities estimated to be in the nanomolar range (83). Interestingly, inhibition by CPA and BHQ can be reversed either by elevated calcium or ATP concentrations. Several high resolution crystal structures of SERCA in complex with CPA and BHQ revealed that, like TG, they lock the enzyme in the E2 conformation (Fig. 1-6 C and E) (58,94). CPA and BHQ share the same binding cavity which is formed by TM1-4 and is situated in the putative cytosolic calcium entry pathway. This cavity is distinct from that of TG, suggesting a different mechanism of inhibition (89). The structure of SERCA in complex with CPA indicated that this relatively planar molecule binds approximately 4 Å above the putative gating residue Glu^{309}, and stabilizes TM1 and TM2 in a locked conformation against TM4 (Fig. 1-6D). More specifically, the indole ring of CPA is stabilized by a hydrophobic platform and forms a bridge between TM1 and TM4, whereas the tetramic acid moiety binds within a polar pocket resulting in a displacement of TM2. BHQ inhibits SERCA in a similar manner to CPA. The SERCA-BHQ structure revealed that BHQ forms a bridge between TM1 and TM4 through interactions between its hydroxyl and butyl groups with residues within the BHQ binding site (Fig. 1-6F) (94). Similarly to CPA, BHQ sits above Glu^{309} and blocks the calcium access channel. Therefore, CPA and BHQ inhibit SERCA by

physically blocking calcium from accessing its binding site and immobilizing a subset of transmembrane segments.

1-6. Regulation of SERCA by phospholamban

1-6.1. Introduction to phospholamban

PLN is the predominant regulator of SERCA in cardiac, smooth and slow-twitch skeletal muscle (95-97). PLN is a 52 amino-acid type I integral membrane protein (98) that contains three distinct domains: a cytoplasmic domain Ia (residues 1-20) with two phosphorylation sites (Ser^{16} and Thr^{17}), a flexible linker domain Ib (residues 21-30), and a hydrophobic transmembrane domain II (residues 31-52) (Fig. 1-7) (24). PLN exists in a dynamic equilibrium between monomeric and pentameric states. While the monomer is considered the "active" inhibitory species, the pentamer is thought to be an "inactive" storage form of PLN (99). In its dephosphorylated state, PLN functionally interacts with SERCA and lowers its apparent affinity for calcium. This inhibition is reversed either by elevated cytosolic calcium or by phosphorylation of PLN at Ser^{16} by cAMP-dependent protein kinase A (PKA) or Thr^{17} by calcium/calmodulin-dependent protein kinase II (CaMKII) (100,101). Modeling of the NMR structure of PLN onto crystal structure of SERCA, with restraints imposed by mutagenesis and cross-linking studies, revealed a hydrophobic groove in the transmembrane domain of SERCA formed by helices TM2, TM4, TM6 and TM9 to which PLN is thought to bind (102,103). This groove is open in the E2 calcium-free state of SERCA and closed in the E1 calcium-bound state. Since PLN binds to the open groove in the E2 conformation of SERCA, this provides a probable mechanism by which PLN inhibits the E2-E1 transition in the catalytic cycle of SERCA.

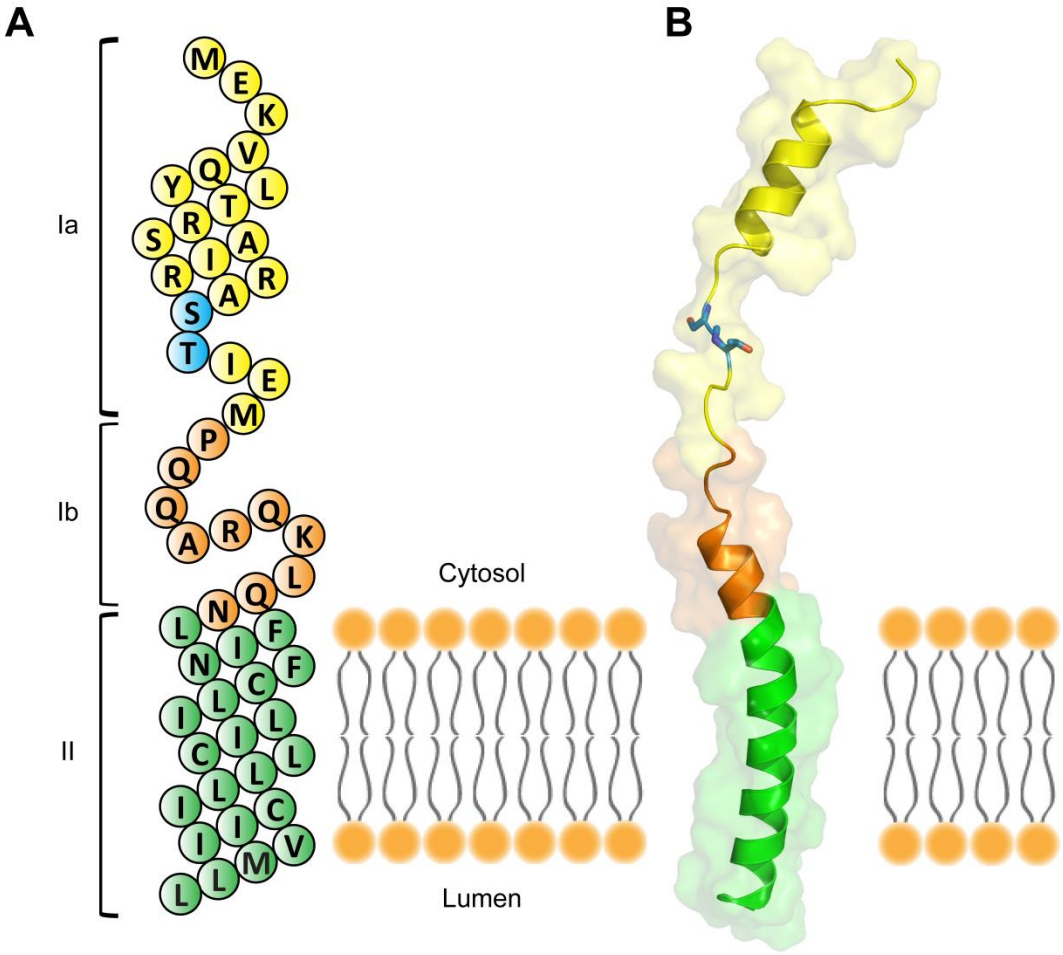

Figure 1-7. Topology model and structure of PLN. (A) Topology model for PLN. Domain Ia is yellow (residues 1 to 20), domain Ib is orange (residues 21 to 30) and domain II is green (residues 31 to 52). Phosphorylated residues (Ser^{16} and Thr^{17}) are blue. **(B)** Cartoon representation of the PLN structure (103). Domains Ia, Ib and II are colored as in panel A. Ser^{16} and Thr^{17} are shown as blue sticks.

1-6.2. Structural studies of phospholamban

Because of its small molecular weight (6080 Da) and highly hydrophobic nature, NMR spectroscopy quickly became the technique of choice for structural studies of PLN. Initial NMR studies used fully functional monomeric forms of PLN, such as C41F or AFA PLN (C36A, C41F, and C46A), to avoid possible complications associated with PLN's propensity to form oligomers, particularly a pentamer (104,105). The first NMR study of monomeric PLN in organic solvent revealed two alpha-helical regions connected by an unstructured loop (Fig. 1-7B). Overall, this structure would be consistent with later NMR studies in DPC detergent micelles and DOPC/DOPE lipid bilayers (106). Most recently, Traaseth and coworkers used solid-state NMR to determine the structure of monomeric PLN in lipid bilayers, an environment that closely resembles the native membrane (107). The structure assumes an L-shaped conformation and can be divided into three domains: α-helical cytoplasmic domain (residues 1-16), unstructured loop (residues 17-22), and transmembrane domain helix (residues 23-52). The cytoplasmic domain appears to interact with the lipid headgroups and the transmembrane helix traverses the membrane bilayer at an angle of 25°. This new structure provided important information on how lipid membranes influence the structure and domain dynamics of PLN.

In addition to the structural determination of the PLN monomer, efforts have been made to elucidate the pentameric structure of PLN. Many studies have contributed to the structural understanding of the PLN pentamer, which produced divergent results regarding the orientation of the cytoplasmic domains of PLN (108-111). Currently, the "bellflower" and "pinwheel" models are considered as the most accurate representations of the PLN pentamer (Fig. 1-8). The bellflower model was based on a solution NMR structure of wild-type PLN and shows the cytoplasmic helices to be oriented

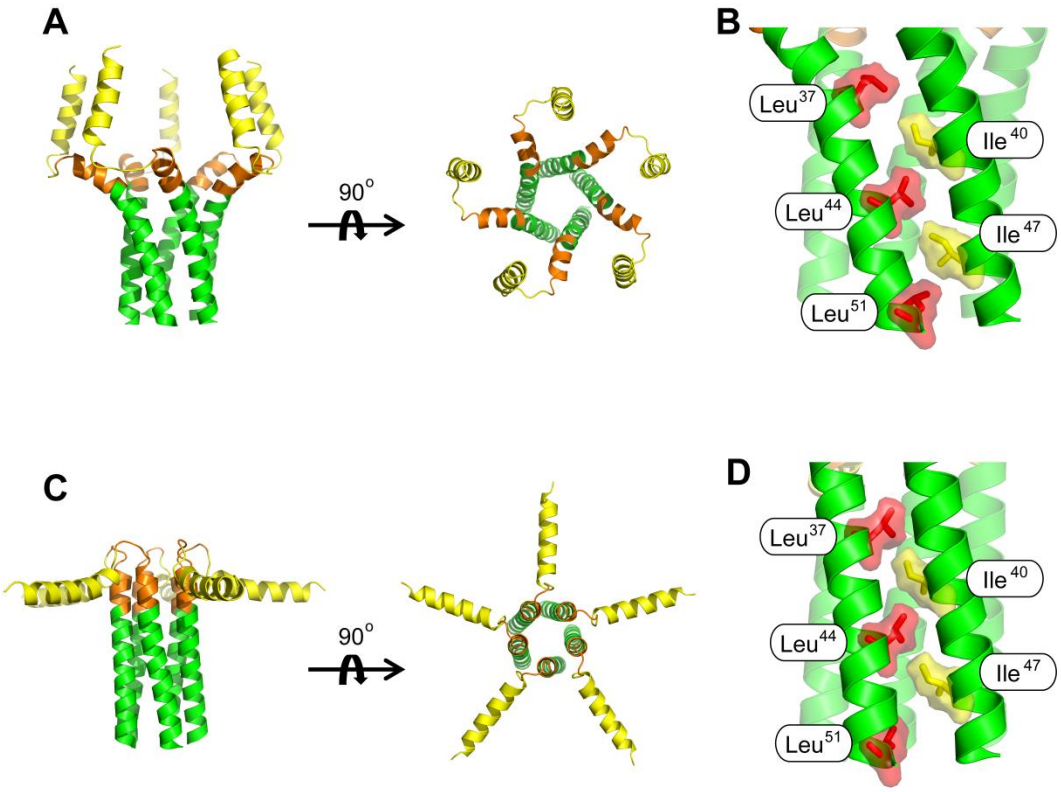

Figure 1-8. Structural models of the PLN pentamer. (A) The "bellflower" model of the PLN pentamer (left: side view, right: top-down view; PDB 1ZLL). **(C)** The "pinwheel" model of the PLN pentamer (left: side view, right: top-down view; PDB 2KYV). **(B and D)** Domain II leucine-isoleucine motif in the "bellflower" and "pinwheel" models, respectively. Leucine side chains (shown as stick and space filling representation in red) interact with isoleucine side chains (shown as stick and space filling representation in yellow) of the neighboring PLN monomer.

approximately 20° with respect to the membrane normal (112). The transmembrane helices cross the membrane at a 19° angle and form a coiled-coil conformation. In this conformation, the PLN pentamer has been suggested to be able to form initial recognition contacts with SERCA, but not a fully inhibitory interaction. In fact, PLN would have to "stretch" in order to satisfy proposed distance restraints between PLN and SERCA. The pinwheel model was originally proposed based on fluorescence studies and later confirmed by solution and solid-state NMR (113). In contrast to the bellflower model, the pinwheel structure shows the cytoplasmic helices to be oriented 90° relative to the bilayer normal and interacting with the membrane surface. The transmembrane helices are also arranged in a coiled-coil conformation and cross the membrane with a tilt angle of 11° with respect to the membrane normal. This model shows remarkable similarity to the L-shape structure of the monomeric AFA PLN. In spite of their structural differences, both models show that the pentamer is held together by the Leu-Ile zipper interactions, consistent with previous mutagenesis studies (Fig. 1-8 B and D). The models indicate that the transmembrane leucine residues (Leu^{37}, Leu^{44}, and Leu^{51}) in one transmembrane helix of PLN form hydrophobic interactions with isoleucine residues (Ile^{40} and Ile^{47}) in the neighboring PLN monomer. Furthermore, the models show interactions of transmembrane cysteines (Cys^{36} and Cys^{41}) with other residues at the interface of protomers, which is consistent with mutagenesis studies which show that substitution at these residues disrupts the pentamer.

1-6.3. Kinetics of SERCA inhibition by phospholamban

SERCA plays a major role in the contraction-relaxation cycle of heart muscle, as it is responsible for the removal of cytosolic calcium during relaxation and consequently determines the strength of the following contraction. PLN binds to and inhibits SERCA by decreasing its apparent calcium affinity and slowing the transition from the E2

(calcium-free state) to E1 (calcium-bound state) intermediate of the catalytic cycle. Inhibition of SERCA is reversed by elevated calcium concentration or upon phosphorylation of PLN (24). These effects of PLN on SERCA activity have been explained in terms of a well-characterized kinetic model for calcium transport by SERCA which assumes that calcium binding occurs in a cooperative two-step process (114).

$$E + Ca \underset{A_{rev}}{\overset{A_{for}}{\rightleftharpoons}} ECa \underset{B_{rev}}{\overset{B_{for}}{\rightleftharpoons}} E'Ca + Ca \underset{C_{rev}}{\overset{C_{for}}{\rightleftharpoons}} E'CaCa$$

This model postulates that binding of the first calcium ion induces a slow conformational change (ECa → E'Ca) that activates SERCA and increases the affinity of the enzyme for a second calcium ion, thereby accounting for the activation and cooperativity of SERCA. Kinetic analyses have found that PLN primarily affects this rate-limiting conformational transition, which manifests as an increase in B_{rev} and explains the increase in cooperativity and the shift in calcium affinity observed experimentally (115). While the principal effect of PLN is to lower the apparent calcium affinity of SERCA, PLN has also been shown to increase the maximal activity of the enzyme, although only under experimental conditions with high protein-to-lipid ratios (115,116). This stimulatory effect can be explained by a significant increase in the B_{for} rate constant observed in the presence of PLN. Since B_{for} represents a rate-limiting step in the SERCA calcium transport cycle, it is easy to envision how accelerating the formation of the E'Ca state would result in an increase in the maximal activity of SERCA. Kinetic analyses have also shed light on the mechanism of PLN phosphorylation. It has been determined that phosphorylation of PLN causes an increase in A_{for}, a reversal of B_{rev} to SERCA only levels, and a slight increase in C_{for}, as compared to non-phosphorylated PLN (117). These

changes reverse SERCA inhibition by PLN but maintain the increased maximal activity of SERCA, this latter effect manifests as a high B_{for}.

1-6.4. Phospholamban regulates SERCA through intramembrane interactions

The molecular mechanism by which PLN inhibits SERCA has been examined in great detail. The effects of wild-type and mutant forms of PLN on SERCA activity have been extensively studied in co-expression (118,119) and co-reconstitution (115,120) systems and have revealed important insights into the role of particular PLN residues in the inhibitory mechanism. Early studies demonstrated that deletion of the cytoplasmic domain of PLN had a minor effect on PLN inhibitory function while the cytoplasmic domain by itself did not inhibit SERCA, showing that the transmembrane domain of PLN plays a key inhibitory role (118). It is generally accepted that the transmembrane domain of PLN alone is responsible for approximately 80% of SERCA inhibition and that the cytoplasmic domain provides the remaining 20%. This simple assumption, however, contradicts other studies which have shown that mutations in the cytoplasmic domain of PLN cause a complete loss of inhibitory function (117,119).

The initial scanning alanine mutagenesis of the PLN transmembrane domain identified two faces on the PLN helix with distinct functional properties (99). Mutation of residues on one face of the transmembrane helix had little effect on PLN pentamer formation and resulted in loss of SERCA inhibition, whereas mutation of residues on the opposite face of the helix resulted in SERCA super-inhibition and pentamer destabilization. These results led the authors to propose that the PLN monomer is the active inhibitory species involved in the interaction with SERCA, while the pentamer must be a functionally inactive storage form of PLN. Thus, the mechanism of super-

inhibition could involve mass action via an increase in local concentration of the inhibitory PLN monomer (Fig. 1-9).

It is important to point out that several PLN mutants do not agree with the mass action theory of SERCA inhibition. For example, a transmembrane domain I40A mutation was initially assessed by SDS-PAGE to prevent pentamer formation, however, more recent FRET studies have demonstrated that this mutant does actually form pentamers, although they are more dynamic than wild-type PLN pentamers (121). In fact, several groups re-examined the transmembrane mutants of PLN that result in pentamer destabilization and concluded that SDS-PAGE is a poor method for accurate determination of PLN pentamer stability (121,122). Another striking example of a transmembrane mutation that opposes the mass action theory is C41F, which is completely monomeric but retains wild-type inhibitory activity (123). A more recent study has demonstrated that most residues along the circumference of the transmembrane helix of PLN contribute to SERCA inhibition (122). Interestingly, two mutations in domain Ib of PLN, K27A and N30A, have been shown to form pentamers to a similar (K27A PLN) or even greater (N30A PLN) degree than wild-type PLN, while exhibiting strong gain-of-function characteristics (124). This further suggests that PLN uses multiple mechanisms to inhibit SERCA. Together, these observed discrepancies clearly demonstrate that the mechanism of SERCA inhibition by PLN is more complex than initially suggested. Nevertheless, despite the evidence that opposes the mass action theory, this is still the currently accepted model for PLN inhibition of SERCA.

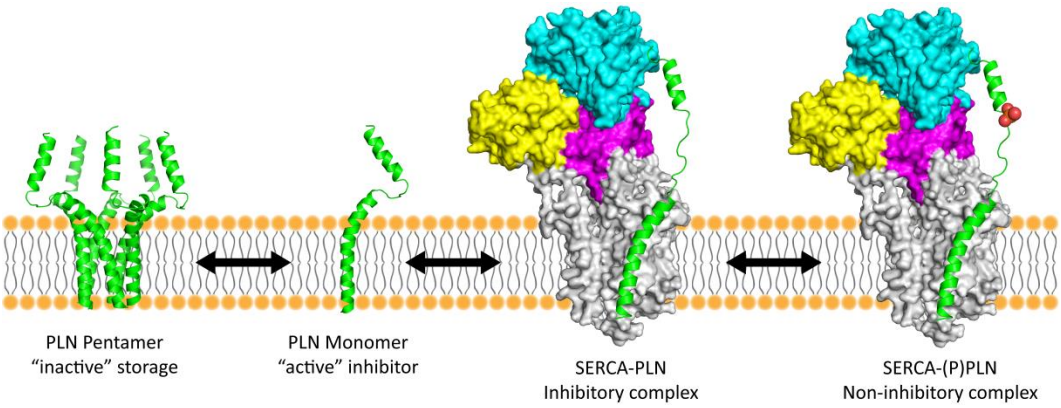

Figure 1-9. Mass action theory. SERCA is shown in surface representation (P-domain is magenta, N-domain is cyan, A-domain is yellow, and transmembrane domain is grey) and PLN as a cartoon (green) representation. Phosphorylated PLN is shown with orange spheres on the cytoplasmic domain. PLN exists in dynamic equilibrium between a pentameric state, which forms an inactive storage form, and monomeric state, which is an active inhibitor of SERCA. Monomeric dephosphorylated PLN functionally interacts with SERCA thereby inhibiting the pump. This inhibition can be relieved upon increased cytosolic calcium or phosphorylation of PLN by PKA or CaMKII.

1-6.5. The phospholamban pentamer – more than an inactive storage form

SERCA regulation by PLN is a dynamic process that depends on cytosolic calcium concentration, as well as the phosphorylation and oligomeric states of PLN. Most studies agree that the PLN monomer acts as the active inhibitory species (122) but the role of the PLN pentamer in cardiac muscle has remained ambiguous. While most of the early co-expression studies have declared it as a functionally inactive storage form (125), there is growing evidence supporting the PLN pentamer as an important player in SERCA regulation and calcium homeostasis. Several studies have reported the PLN pentamer to exhibit a channel-like activity (112,126). The pentameric assembly of the transmembrane helices of PLN has been proposed to conduct ions, such as calcium and chloride, across the SR membrane. In addition, recent cryo-electron microscopy studies have identified a physical interaction between the PLN pentamer and SERCA (Fig. 1-10) (127). In contrast to the previously proposed PLN binding cavity composed of TM2, TM4, TM6, and TM9, the pentamer was shown to interact at a distinct accessory site near TM3 (128). Most convincingly, the physiological role of the PLN pentamer has been inferred through a transgenic mouse model overexpressing a monomeric C41F mutant, which has the same inhibitory potency as wild-type PLN (129). These mice exhibited slower relaxation rates and calcium transients leading to depressed cardiac function, implying that the PLN pentamer-to-monomer balance is crucial for proper SERCA regulation in the cardiac muscle.

Although still highly debatable, phosphorylation of PLN also appears to influence functional and structural characteristics of the PLN pentamer. The initial model for SERCA regulation by MacLennan and co-workers suggested that phosphorylation of monomeric PLN disrupts the physical interaction with SERCA resulting in complete dissociation of the inhibitory complex and oligomerization of PLN (99). However, there

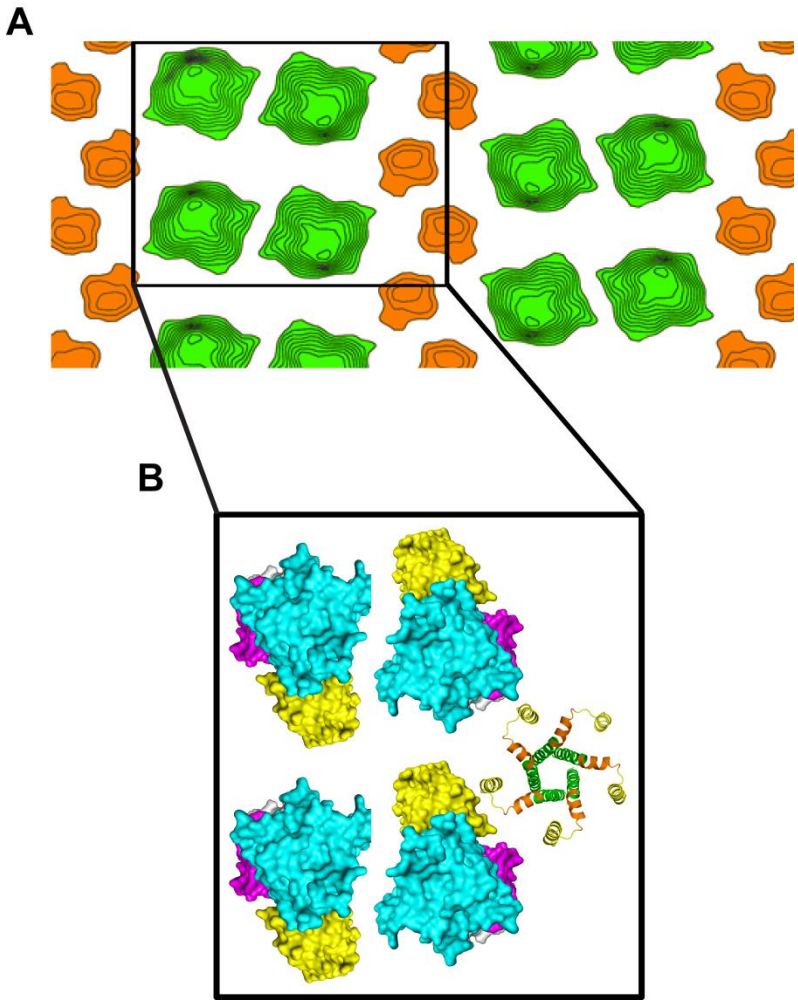

Figure 1-10. Structural interaction between SERCA and the PLN pentamer. (A) Projection map from cryo-electron microscopy of SERCA and PLN co-crystals. Positive contours are colored for the characteristic anti-parallel SERCA dimer ribbons (green) and the associated oligomeric PLN densities (orange). **(B)** Model for the interaction of SERCA (PDB 1KJU) with pentameric PLN (PDB 1ZLL) based on the projection map from 2D co-crystals. SERCA and PLN are in surface and cartoon representations, respectively.

is contradictory evidence about whether PLN dissociates from SERCA following phosphorylation. FRET (130) and cross-linking (131) experiments have shown that phosphorylation of PLN promotes dissociation of the SERCA-PLN complex and pentamer formation. In contrast, electron paramagnetic resonance (EPR) (132) and other biophysical studies (133) have demonstrated that PLN remains associated to SERCA following phosphorylation. In addition, SDS-PAGE analysis did not indicate any difference in the pentamer-to-monomer ratio upon phosphorylation (134). Numerous NMR studies have shown that phosphorylation induces a dynamically disordered state in the cytoplasmic domain of PLN, suggesting that the phosphorylated form of PLN remains bound to SERCA in a non-inhibitory state (135,136). A recent electron microscopy study provided a structure of a phosphorylated PLN pentamer bound to SERCA, which confirmed the selective disordering of the cytoplasmic domain and association of the transmembrane domain of PLN with SERCA (128). Additionally, the PLN pentamer was observed to form interactions with SERCA at an accessory site (TM3 of SERCA), away from the proposed binding site used by the PLN monomer for the inhibitory interaction. Based on these observations, the authors proposed that the PLN pentamer may play an active role in capturing a monomeric or phosphorylated PLN, thereby facilitating the exchange of PLN monomers to and from the SERCA inhibitory site in response to physiological cues.

1-6.6. Functional studies reveal key phospholamban residues responsible for SERCA regulation

Mutagenesis studies have proved to be a powerful tool in determining key functional interactions between SERCA and the transmembrane domain of PLN. As previously discussed, early alanine-scanning mutagenesis studies identified residues on one face of the transmembrane helix to be mainly involved in pentamer formation and

residues on the opposite face important for the inhibitory interactions with SERCA (99). It was shown that substitution of the pentamer-stabilizing residues (Leu^{37}, Leu^{44}, Leu^{51}, Ile^{40}, and Ile^{47}) in domain II of PLN by alanine resulted in monomeric mutants, which were more effective inhibitors of SERCA than wild-type PLN. Although these residues were initially thought to only be involved in PLN pentamer formation, some of them were later demonstrated to be involved in the inhibitory interactions with SERCA (122). This suggested that residues along most of the transmembrane domain of PLN were involved in SERCA inhibition. Furthermore, mutagenesis studies have identified eight essential residues (Leu^{31}, Asn^{34}, Phe^{35}, Ile^{38}, Leu^{42}, Ile^{48}, Val^{49}, and Leu^{52}) in the transmembrane domain of PLN, which are associated with loss of inhibitory function (99,115). Amongst these essential residues, Asn^{34} is the only polar residue and alanine substitution at this position results in complete loss of inhibitory function (99,120). In fact, the transmembrane domain of PLN is very hydrophobic with only four polar residues (Asn^{34} and three nonessential cysteines), and it is through hydrophobic interactions that PLN is thought to inhibit SERCA. Polar residues such as asparagine occur at low frequency in transmembrane helices, yet when present, they were shown to play an important role in protein-protein interactions and thermodynamic stability (137,138). To study the role of Asn^{34} in PLN, co-reconstitution studies using synthetic peptides to mimic the transmembrane domain of PLN were done (139). A model transmembrane peptide consisting of only the native leucine residues in PLN and all other residues substituted with alanine retained some of the inhibitory activity towards SERCA. Addition of Asn^{34} to this peptide resulted in super-inhibition, which could be expected considering the complete loss-of-function N34A PLN mutant. Finally, model peptides with the asparagine moved upstream or downstream by one residue or one turn of the helix from the native position further demonstrated the necessity of an asparagine residue at position 34 in PLN (140). Thus, a hydrophobic interface and a specifically

located asparagine residue in the transmembrane domain of PLN are two of the essential elements required for proper regulation of SERCA.

Mutagenesis studies have also identified residues outside of the transmembrane domain of PLN to be directly involved in interactions with SERCA. Substitution of Asn^{27} or Asn^{30} in domain Ib of PLN with alanine was shown to cause super-inhibition of SERCA, suggesting that these two residues form critical interactions with SERCA (124). The cytoplasmic domain Ia of PLN has also been revealed to modulate SERCA activity. In general, alanine-substitutions within the cytoplasmic domain Ia of PLN have been shown to exhibit only a minor effect on SERCA inhibition (117,119). However, mutation of Thr^{8}, Arg^{9}, and Ser^{10} to more hydrophobic amino acids resulted in a complete loss of function, suggesting that hydrophobic balance in the cytoplasmic domain of PLN is essential for proper inhibitory interaction with SERCA (117).

1-6.7. Insights into physical interactions within the SERCA-PLN inhibitory complex

Lack of high resolution structures of the SERCA-PLN complex has hindered our complete understanding of the physical interactions between SERCA and PLN. Fortunately, several structural models of the SERCA-PLN inhibitory complex have been constructed based on high resolution crystal structures of SERCA, NMR structures of PLN, and a plethora of biological data (102,103,141). While mutagenesis data provided important information about the functional interactions between SERCA and PLN, cross-linking studies have proven to be an effective method for establishing physical interaction sites between these proteins. The first evidence for a physical interaction between PLN and SERCA was the cross-linking of the ε-amino group of the N-terminal Lys^{3} of PLN to Lys^{397} and Lys^{400} of SERCA (142). The formation of this cross-link was prevented by calcium and phosphorylation of PLN. The close proximity of the cross-linked residues in

SERCA, Lys^{397} and Lys^{400}, to Asp^{351} led the authors to propose that PLN might interfere with formation of aspartyl-phosphate intermediate. Interestingly, several groups have attempted to reproduce this cross-link but they have not been successful, raising questions about the significance of this interaction. Subsequent cross-linking studies have provided more concrete evidence for a physical association between PLN and SERCA. Jones and coworkers were successful in identifying interactions between N27C of PLN and Lys^{328} of SERCA and N30C of PLN and Cys^{318}/Lys^{328} of SERCA (143,144). In addition, a cross-link between a loss-of-function N31C of PLN and Thr^{317}/Cys^{318} of SERCA was identified proving that a non-inhibitory form of PLN could in fact interact with SERCA without causing inhibition (145). Thus, these cross-links have confirmed domain Ib of PLN as an important site of physical and functional interaction with SERCA. Other studies reported a cross-link between the C-terminal V49C of PLN and Val^{89} in the TM2 of SERCA (102,146). Together, cross-links between residues of domain Ib of PLN and SERCA and Val^{49} of PLN and SERCA defined two well separated interaction sites between these two proteins that would be later helpful in modeling of the SERCA-PLN complex. Cross-linking between PLN and SERCA at these sites was prevented by micromolar calcium concentrations or the presence of SERCA specific inhibitors, such as TG or CPA. In contrast, cross-linking was greatly increased in the presence of ADP or ATP and in the absence of calcium. Based on these observations the authors proposed that PLN interacts with a nucleotide bound, calcium-free E2 state of SERCA.

The initial model of the SERCA-PLN complex by Toyoshima and co-workers showed that PLN binds to a groove formed by TM2, TM4, TM6, and TM9 of SERCA (Fig. 1-11) (102). In the calcium-free E2 state this groove is large enough to accommodate the transmembrane domain of PLN (Fig. 1-11C). However, as SERCA

transitions into the calcium bound $(Ca^{2+})_2$-E1 state, the lateral movement of TM2 narrows the binding grove and pushes PLN out of this inhibitory site (Fig. 1-11D). In addition to cross-linking studies, the proposed PLN binding groove was supported by mutagenesis studies of SERCA which showed several mutations on TM4 and TM6 to diminish the ability of wild-type PLN to inhibit SERCA activity (147). This model also revealed that there is enough space between SERCA and parts of the cytoplasmic domain of PLN, specifically domain Ib, for a kinase to bind and phosphorylate PLN. A more recent model of SERCA-PLN complex based on a solid state NMR structure of the monomeric AFA PLN mutant in the presence of SERCA was highly reminiscent of the model determined by Toyoshima and coworkers (Fig. 1-11 A and B) (103). Although these structural models satisfy most of the functional and cross-linking data they must be examined with caution, as they might not represent a physiological complex. It is important to point out that these models have been based on ATP free and TG-bound SERCA structures. Since most of the cross-linking between SERCA and PLN was largely dependent on the presence of ATP and prevented by TG or calcium, the conformation of SERCA and its interactions with PLN in these models might not be fully representative of the physiological complex.

1-6.8. Regulation of phospholamban by phosphorylation

During resting conditions, PLN acts as a physiological brake for calcium transport across the SR membrane in the heart (24). β-adrenergic stimulation relieves this brake by phosphorylation of PLN, stimulating calcium uptake activity of SERCA. This increased uptake of calcium into the SR results in accelerated relaxation and increased amplitude of the cardiomyocyte contraction. Thus, the ratio of phosphorylated to non-phosphorylated PLN is a key determinant of SERCA activity in the heart. It is now well established that PLN can be phosphorylated at Ser^{16} by PKA (24) and at Thr^{17} by

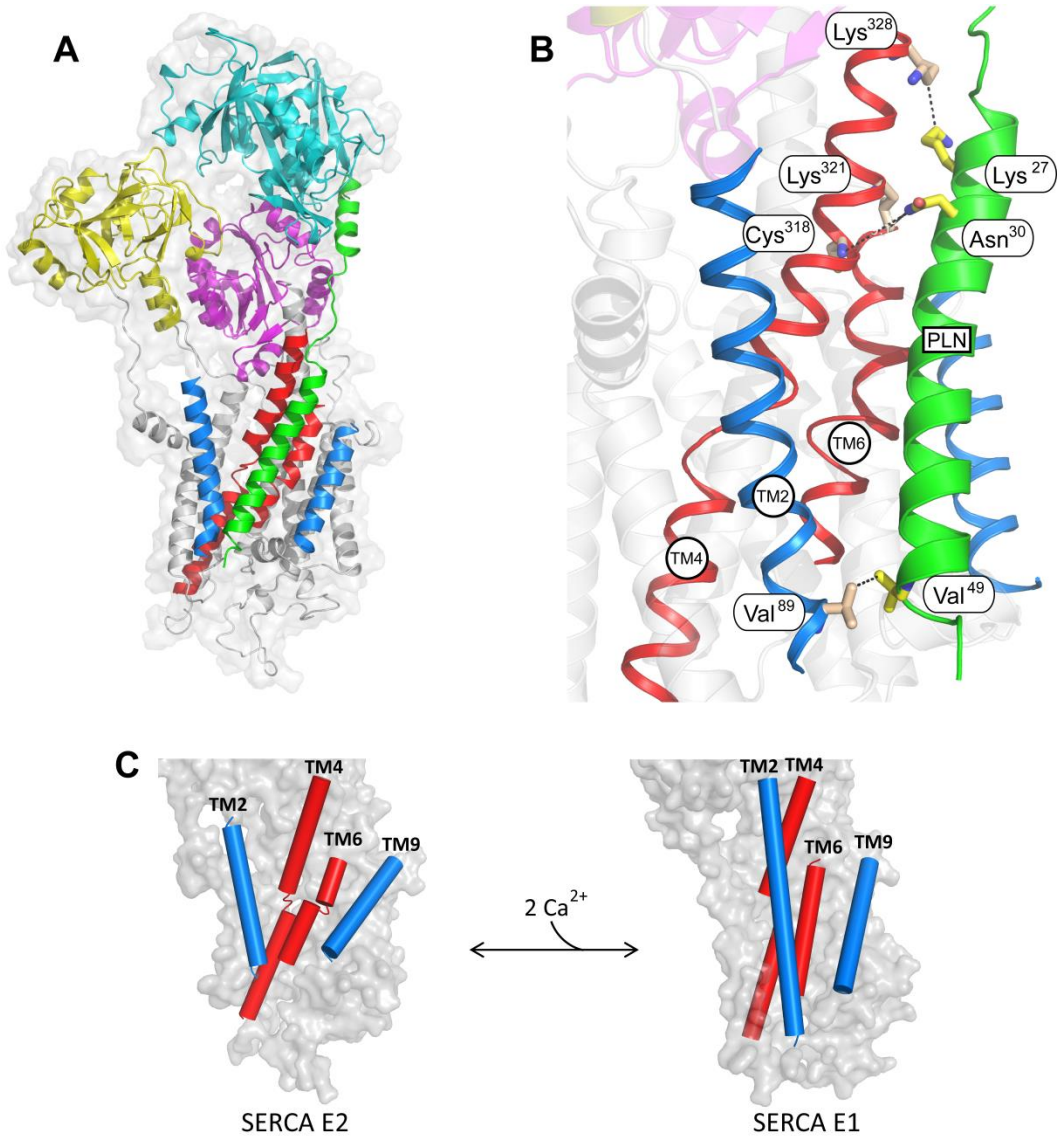

Figure 1-11. Model of the SERCA-PLN inhibitory complex. (A) A model of SERCA and PLN based on a solid-state NMR structure of AFA PLN (SERCA is in E2 state (103)). SERCA is shown in transparent surface and cartoon with the P-domain in magenta, N-domain in cyan, A-domain in yellow, TM2 and TM9 in blue, TM4 and TM6 in red and the rest of TM helices in grey. PLN is shown in green cartoon. **(B)** Close-up view of the interactions between PLN (green) and the transmembrane cavity formed by TM2 (blue), TM4, TM6 (both in red) and TM9 (blue). PLN and SERCA residues reported to form cross-links are shown as sticks. **(C)** Structural rearrangement of SERCA transmembrane helices involved in PLN binding between the E2 and E1 states (colored as in panel A and B). In the E2 state the cavity is in a wide-open conformation which allows PLN to bind (PDB 1IWO). In the calcium-bound E1 state the cavity is much narrower mainly due to lateral movement of TM2 (PDB 1SU4).

CaMKII or protein kinase B (Akt) (24,148). *In vitro* studies have also reported phosphorylation at Ser^{10} by protein kinase C (PKC) but this was never confirmed *in vivo (149)*. Since phosphorylation of PLN at either Ser^{16} or Thr^{17} has been demonstrated to be sufficient for complete reversal of SERCA inhibition, the functional significance and role of dual-site phosphorylation is not fully understood. Transgenic mice overexpressing the S16A PLN mutant showed diminished responses to β-adrenergic stimulation and lack of Thr^{17} phosphorylation (150). Conversely, mice overexpressing T17A PLN mutant showed normal Ser^{16} phosphorylation and response to β-adrenergic stimulation that was similar to that of wild-type mice (151). Moreover, overexpression of PLN with both S16A and T17A mutations resulted in maximal SERCA inhibition (152). Thus, based on these findings it was proposed that phosphorylation of Thr^{17} is dependent upon phosphorylation of Ser^{16}, and Ser^{16} is mainly responsible for β-adrenergic mediated cardiac response. However, Thr^{17} has been shown to be phosphorylated independently of Ser^{16} *in vivo* in the absence of β-adrenergic stimulation and under pathophysiological conditions, such as ischemia-reperfusion injury and acidosis (153,154). Furthermore, *in vitro* studies have provided evidence that Ser^{16} and Thr^{17} can be phosphorylated independent of any prior phosphorylation (155).

1-6.9. Phosphorylated (non-inhibitory) phospholamban remains associated with SERCA

While the effect of PLN phosphorylation on SERCA regulation has been clearly demonstrated by numerous functional studies, the molecular mechanism by which this occurs is less clear. Based mainly on crosslinking (131,142) and fluorescence studies (130), the original model for SERCA regulation by PLN suggested that phosphorylation of PLN completely disrupts interactions with SERCA. However, there is now compelling evidence implying that phosphorylated PLN retains interactions with the calcium pump.

Co-immunoprecipitation studies have shown that, unlike in the presence of high calcium concentration, phosphorylation of PLN does not disrupt the physical interaction between SERCA and PLN, suggesting that alleviation of SERCA inhibition by elevated calcium concentration and phosphorylation occur by distinct mechanisms (156). These findings were further supported by NMR studies (135,136). According to EPR and NMR studies, phosphorylation induces an order-to-disorder conformational change in the cytoplasmic domain of PLN (Fig. 1-12) (132,135). These different dynamic states of the cytoplasmic domain were attributed to the structural flexibility of the "hinge" region of domain Ib of PLN (157). In the ordered state, the cytoplasmic domain of PLN is thought to be directly interacting with the membrane surface, whereas it is detached in the disordered state. Interestingly, transition to the disordered state has also been observed in the presence of high concentrations of magnesium but not potassium, suggesting that magnesium ions specifically disrupt interactions between the negatively charged phospholipid headgroups and the positively charged cytoplasmic domain of PLN (157). More recent NMR studies revealed that phosphorylation of a monomeric AFA PLN influences partial unwinding of the PLN N-terminal alpha-helix around the phosphorylation site (136). In addition, phosphorylation was suggested to shift the conformational equilibrium toward the disordered state in the presence of SERCA. These findings led to the proposal that phosphorylation causes rearrangements in domains Ia and Ib, with the binding of domain II to SERCA only marginally affected, supporting the notion that phosphorylation does not result in dissociation of PLN from SERCA.

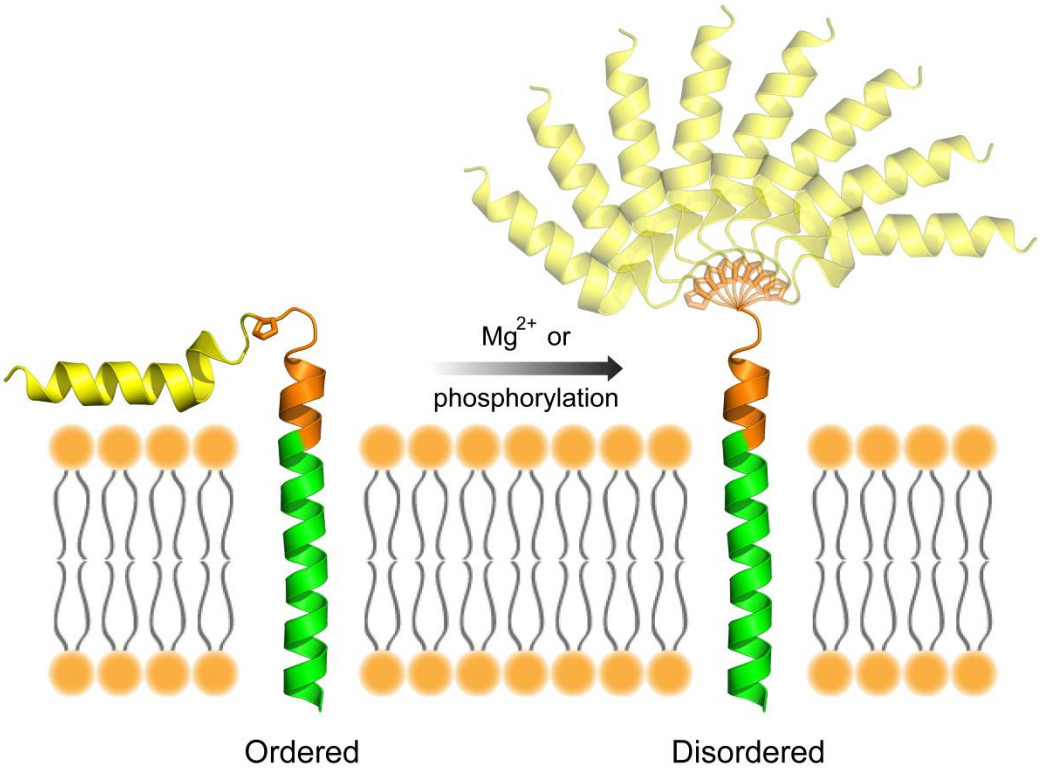

Figure 1-12. Order-to-disorder equilibrium in the cytoplasmic domain of PLN. Cartoon representation of PLN with domain Ia in yellow, domain Ib in orange and domain II in green . Pro^{21} (stick representation) of the "hinge" region allows for flexibility in domain Ib upon phosphorylation or increased magnesium concentration.

1-6.10. SERCA and phospholamban in heart failure

Altered calcium handling is a hallmark of heart disease and many studies have indicated that altered SR calcium handling is of particularly great pathophysiological relevance in human heart failure (158-160). It is well accepted that the levels of calcium binding (calsequestrin and calreticulin) and calcium releasing (RyR) proteins in the SR are unaltered under disease conditions (161). In contrast, studies in failing human myocardium and heart failure mouse models revealed SERCA levels to be decreased, contributing to impaired heart function (161-163). Furthermore, it has been shown that there is a decrease in PLN mRNA levels during heart failure (164), although several studies clearly demonstrated that the protein level of PLN remains unaltered (161,165). A decrease in SERCA levels relative to PLN results in higher ratios of PLN-to-SERCA which in turn leads to SERCA super-inhibition and prolonged muscle relaxation. In addition, the phosphorylation levels of PLN are decreased, further increasing the inhibition of SERCA (166). This reduced phosphorylation of PLN is thought to be a result of the β-adrenergic receptor down-regulation or desensitization, which is known to occur during heart failure (167,168). Moreover, increased protein phosphatase-1 (PP-1) activity could be another cause of diminished levels of phosphorylated PLN (169,170). Thus, alterations in the PLN-to-SERCA ratios and decrease in PLN phosphorylation contribute to depressed SR calcium uptake, leading to less calcium available for subsequent muscle contraction (Fig. 1-13).

Reversing the contractile dysfunction of cardiomyocytes by altering SERCA and/or PLN levels has been the focus of potential treatment for heart failure. Given the central role of SERCA in proper cardiac function, overexpression of SERCA2a by gene transfer using a recombinant adenovirus has been shown to enhance cardiac contractility in human cardiomyocytes (171,172) and improve function, metabolism and survival in

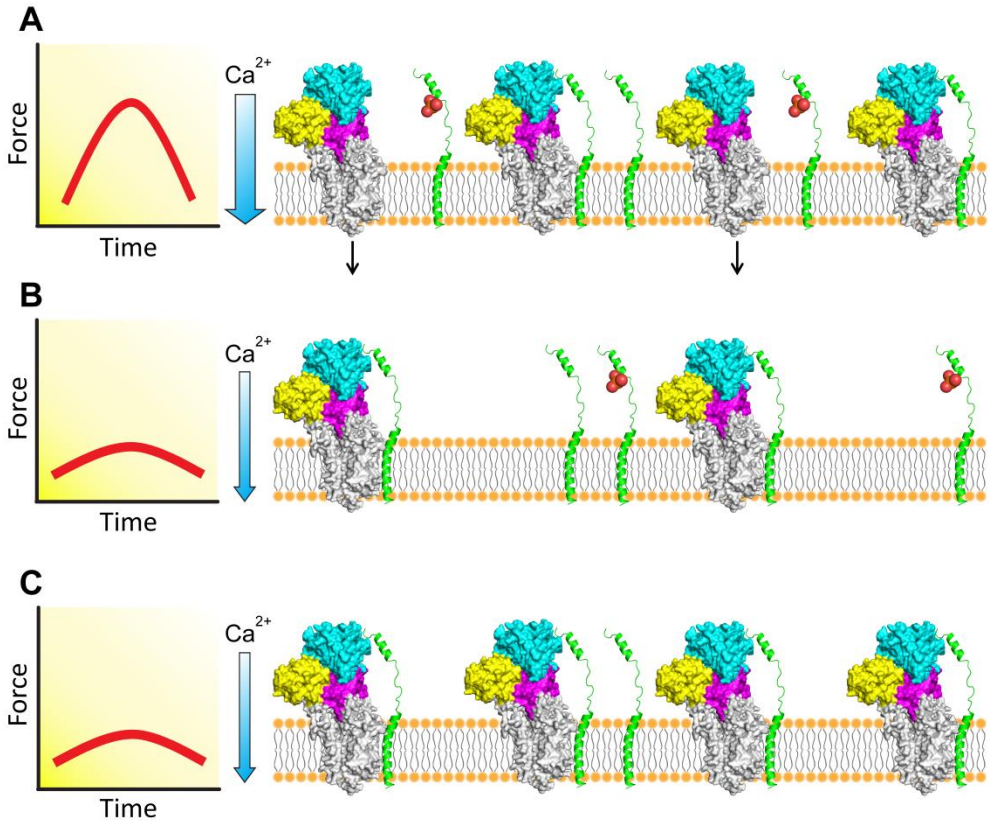

Figure 1-13. Model of the role of SERCA and PLN in heart disease. SERCA is shown as a surface (P-domain is magenta, N-domain is cyan, A-domain is yellow, and transmembrane domain is grey) and PLN as a cartoon (green) representation. Phosphorylated PLN is shown with orange spheres on the cytoplasmic domain. **(A)** In healthy resting individuals, approximately half of PLN is inhibitory (non-phosphorylated), giving rise to normal calcium transient and pumping capacity of the heart. **(B)** During heart failure, SERCA expression is diminished, giving rise to super-inhibition of SERCA, decreased calcium transients, and decreased pumping capacity of the heart. **(C)** Hereditary mutations in PLN cause decreased calcium transients and pumping capacity of the heart, leading to heart disease.

failing rat hearts (173,174). Based on the evidence that the adenovirus-mediated gene transfer of SERCA2a has positive effects in different models of heart failure, this treatment has been tested in clinical trials (175). While there are drawbacks to this therapy, such as immunity to the adenovirus, most treated patients demonstrated overall improvement in cardiac contractility (176).

Since impaired calcium handling can also be caused by super-inhibition of SERCA by PLN, several groups have examined different approaches to alter the SERCA-PLN interactions in heart failure. One potential approach to reduce SERCA inhibition by PLN is to decrease PLN expression. This was initially tested with PLN knockout mice which exhibited normal cardiac function (24), however, mice are highly insensitive to changes in PLN levels compared to larger mammals. For example, a slight increase in PLN levels in rabbits leads to severe muscular pathology (177) and homozygous expression of a null PLN mutant (truncation at Leu^{39} (L39stop)) results in heart failure in humans (178). Another way to influence the SERCA-PLN complex is to increase the levels of phosphorylated PLN by inhibiting PP-1. Recent studies have examined inhibition of PP-1 through its physiological regulators, inhibitor-1 (I-1) and inhibitor-2 (I-2). Adenoviral-mediated expression of the constitutively active I-1 or I-2 constructs in heart failure animal models resulted in enhanced contractility and PLN phosphorylation without any changes in the PKA mediated phosphorylation of the RyR (179-181). Thus, PP-1 inhibition appears to be a promising therapeutic approach to enhance cardiac function in a failing heart.

1-6.11. Human phospholamban mutations in heart failure

As discussed previously, PLN plays a fundamental role in proper calcium cycling within a cardiac myocyte. Alterations in the expression levels of PLN and its

phosphorylation strongly influence the activity of SERCA. In recent years, several naturally occurring mutations in the human PLN gene have been identified that lead to hereditary dilated cardiomyopathy (DCM) (178,182-184). These mutations use different mechanisms to alter SERCA activity and underline the importance of PLN in normal cardiac function.

In 2003, the first mutation in the human PLN gene implicated in lethal DCM was identified (182). A loss-of-function Arg^{9} to Cys (R9C) missense mutation in the cytoplasmic domain of PLN was found in a single large family with heart disease. All affected individuals were heterozygous for R9C PLN and developed severe cases of DCM with early symptom onset and quick progression to heart failure. Co-expression studies in HEK-293 cells revealed that R9C PLN did not inhibit SERCA and prevented phosphorylation of wild-type PLN by sequestering PKA, leading to enhanced inhibition of SERCA activity (182). Transgenic mice expressing wtPLN and the R9C PLN mutant developed lethal cardiomyopathy, whereas mice expressing only R9C PLN surprisingly had the highest survival rate (182,185). Therefore, in mice the disease-causing mechanism of the R9C mutant is dependent on the presence of wild-type PLN, suggesting that the phenotype in mice may not fully reflect the phenotype in humans. The disease-causing mechanism of R9C PLN was further examined in a recent FRET study where the authors demonstrated that R9C PLN forms much tighter pentamers than wild-type PLN, which explains the lower affinity of the R9C mutant for SERCA (186). In addition, mixed pentamers of R9C and wild-type PLN were also more stable than wild-type PLN homopentamers, implying that R9C impedes PLN deoligomerization and phosphorylation by PKA. Another view of the R9C inhibitory mechanism was presented in the most recent study in which the authors demonstrated that under heterozygous conditions the R9C mutant has a dominant negative effect on SERCA function (117).

This study concluded that the change in the hydrophobicity in the cytoplasmic domain of PLN resulting from the Arg^9 to Cys substitution is responsible for the loss of function and a persistent interaction with SERCA.

In a recent study, two other heterozygous mutations at Arg^9 position were identified within a large group of DCM patients (184). One patient had an Arg^9 to His (R9H) mutation and two had an Arg^9 to Leu (R9L) mutation. Studies in a co-reconstituted system revealed that R9H PLN exhibited normal inhibitory function but lost its ability to be phosphorylated by PKA while R9L PLN resulted in a complete loss of both inhibitory function and phosphorylation (117,187). These results indicated that the R9L mutation mimics the behavior of the R9C mutant, further confirming that hydrophobic imbalance in the cytoplasmic domain of PLN is a critical determinant of function and disease progression. Although the disease-causing mechanisms of the R9L and R9H mutants need further examination, the discovery of these point mutations demonstrates the importance of Arg^9 in proper SERCA inhibition and phosphorylation of PLN.

Deletion of Arg^{14} (R14del) in the cytoplasmic domain of PLN has been also found to lead to DCM in humans (183). A genetic screening of heart failure patients identified only heterozygous R14del individuals who developed either mild or severe cases of DCM (183,188,189). Similar to transgenic R9C PLN mice, transgenic mice overexpressing the R14del mutant developed cardiomyopathy which led to premature death. Co-expression of wild-type PLN with R14del PLN in HEK-293 cells resulted in super-inhibition of SERCA while expression of only R14del PLN resulted in a mild loss of SERCA inhibition. These differences in SERCA inhibition were proposed to be caused by an increase in the monomer concentration due to destabilization of the mixed wild-type and R14del PLN pentamers (183). This model was at least in part contradicted by a recent study in which R14del PLN was shown to be a mild loss-of-function mutant that

preferentially affects SERCA in the presence of wild-type PLN due to an increased hydrophobicity in the cytoplasmic domain of PLN (117). Furthermore, despite Arg^{14} being a part of the PKA recognition motif (^{13}RRAS^{16}) in PLN, R14del PLN was normally phosphorylated in HEK-293 cells (183) in contrast with co-reconstitution studies where the same mutant resulted in a complete loss of phosphorylation (187). Interestingly, in HEK-293 cells, R14del PLN failed to co-localize in the SR with SERCA in the absence of wild-type PLN (190). Instead, the R14del PLN mutant was misrouted to the plasma membrane where it was found to interact with and activate the Na^+,K^+-ATPase.

Thus far, only one disease-associated mutation (L39stop) has been identified in the transmembrane domain of PLN (178). This nonsense mutation in the PLN gene results in a premature stop codon which produces a truncated PLN protein. In heterozygous individuals, the L39stop mutation led to hypertrophy without diminished contractile performance while homozygous individuals developed DCM and heart failure during the teenage years. This was later explained by studies in HEK-293 cells which showed that the L39stop mutant had no effect on SERCA activity (178). Furthermore, the same study demonstrated that L39stop is a highly unstable protein which is misrouted to the plasma membrane or found in the insoluble fraction of ER microsomes, leaving SERCA in an uninhibited state. Based on this evidence, it was concluded that the homozygous patients can be compared to the PLN-null genotype that leads to DCM. This observation largely contradicts the PLN-null mouse models, where ablation of PLN results in normal cardiac function and does not lead to heart failure. Therefore, PLN mutations that are detrimental for humans might not show the same phenotype in mice, emphasizing the necessity to understand differences in physiology between human and mouse when studying cardiac diseases.

In addition to the mutations in the coding region of the PLN gene, mutations in the PLN promoter region and surrounding introns have been identified. These mutations are only found in the heterozygous form and are associated with altered promoter activity, leading to abnormal PLN expression levels (191). Recent *in vitro* studies revealed several of these mutations to either increase or decrease PLN promoter activity by 1.5-fold (192-194). Although the relevance of these mutations in heart disease is still largely controversial, these studies suggest that mutations in the promoter region of PLN may play an important role in aberrant calcium cycling within a cardiac myocyte leading to heart failure.

1-7. Regulation of SERCA by sarcolipin

1-7.1. Introduction to sarcolipin

SLN was first described as a low molecular-weight protein that co-purified with preparations of SERCA and was named to reflect its origin as a proteolipid of the SR (195). SLN is the predominant regulator of SERCA and calcium homeostasis in fast-twitch skeletal muscle (196,197). However, SLN is also expressed in the atria of the heart, where it can interact with PLN and lead to super-inhibition of SERCA (198-200). Structural similarities between the SLN and PLN genes as well as the significant sequence identity clearly suggest that these proteins are homologous members of the same gene family (15,24). SLN is a 31 residue type I integral membrane protein with a transmembrane domain and short cytoplasmic and luminal domains (Fig. 1-14) (195). Amino acid conservation in the transmembrane domains of SLN and PLN suggests that SLN inhibits SERCA by binding and lowering the apparent calcium affinity of the enzyme in a manner similar to PLN (197). Current models propose SLN and/or PLN might bind to SERCA and stabilize an E2 calcium-free state (201,202).

1-7.2. Regulatory mechanism of SERCA inhibition by sarcolipin

SLN inhibition of SERCA has been less well characterized than PLN, mainly due to the assumption that SLN inhibits SERCA in a similar manner as PLN. However, there are important differences in the way SLN inhibits SERCA. For example, it is well accepted that SLN lowers the apparent calcium affinity of SERCA to a lesser extent than PLN (197,203). In addition, some studies have found that SLN decreases the maximum reaction rate (V_{max}) of SERCA at micromolar calcium concentrations, indicating that SLN inhibition is not relieved by increased cytosolic calcium (204-206). Furthermore, it is not well established if phosphorylation of SLN is a physiologically relevant mechanism, although two kinases have been reported to target SLN (207,208). Finally, in contrast to PLN which is known to assemble into stable pentamers, SLN is thought to exist primarily as a monomer (197). However, evidence indicates that SLN can also form oligomers in detergent and lipid environments (209,210).

The differences in the amino acid composition between SLN and PLN are responsible for the structural changes that give these peptides their own unique functional properties. The N-terminal cytoplasmic domain of SLN (residues 1-7) is much shorter than that of PLN and lacks the corresponding phosphorylation sites. This region of SLN is poorly conserved among different species except for the highly conserved Thr^5 residue, considered as a putative phosphorylation site (Fig. 1-14) (15). The role of Thr^5 in phosphorylation mediated regulation of SLN was first demonstrated in heterologous co-expression studies with SERCA in which the phospho-mimetic T5E SLN mutant resulted in the expected complete loss of function, whereas T5A SLN was a gain-of-function mutation (197). The α-helical transmembrane domain of SLN (residues 8-27) is composed of 19 residues, 8 of which are identical and 8 are highly conserved as compared to the corresponding residues in the transmembrane domain of PLN. Despite

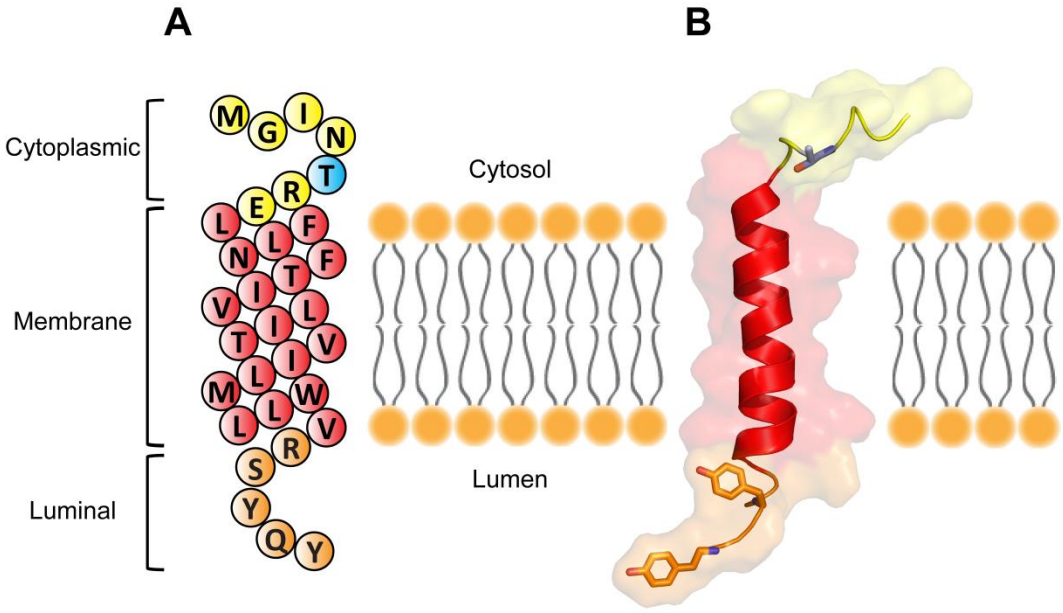

Figure 1-14. Topology model and structure of SLN. (A) Topology model for SLN. Cytoplasmic domain is yellow (residues 1 to 7), transmembrane domain is red (residues 8 to 26) and luminal domain is orange (residues 27 to 31). Phosphorylated residue (Thr^{5}) is blue. **(B)** Cartoon representation of the SLN structure (PDB 1JDM). SLN domains are colored as in panel A. Phosphorylated Thr^{5} and luminal Tyr^{29} and Tyr^{31} are shown as sticks.

the high sequence conservation between the transmembrane regions of SLN and PLN, alanine-scanning mutagenesis did not recapitulate the gain of function behavior associated with residues that destabilize the PLN pentamer (197). Nevertheless, mutation of Leu^{8} and Asn^{11} in SLN resulted in the expected loss of function observed for the comparable Leu^{31} and Asn^{34} in PLN, residues critical for proper PLN function. The last five residues of SLN are perfectly conserved among mammals and make up its luminal domain (residues 27-31) which extends into the SR lumen. The C-terminal regions of SLN and PLN represent a striking difference between these proteins, where the hydrophilic luminal tail of SLN (Arg^{27}-Ser-Tyr-Gln-Tyr^{31}) is substituted by the hydrophobic C-terminal end of PLN (Met^{50}-Leu-Leu^{52}). Early co-expression studies of SERCA and SLN identified Y29A as a gain-of-function mutation, suggesting that the luminal domain of SLN physically interacts with and regulates SERCA (197). More recently, solid-state NMR studies verified these results by demonstrating that the two tyrosine residues (Tyr^{29} and Tyr^{31}) are essential for proper SLN function (204). In addition to this functional role, the luminal domain was reported to be important for targeting or retention of SLN in the SR membrane (211).

1-7.3. Structure of sarcolipin

In contrast to PLN, there have been few structural studies of SLN. Considering its low molecular weight and highly hydrophobic nature, the structure of SLN has been predominantly studied by NMR in detergent and lipid environments. The initial 3D structure of SLN was determined in detergent (SDS) micelles and revealed that SLN forms a compact alpha-helical transmembrane domain (residues 9-27) with two short unstructured termini consisting of residues 1-8 in the cytoplasmic N-terminus and residues 27-31 in the luminal C-terminus (Fig. 1-14B) (104). Additionally, the orientation of SLN was found to be perpendicular to the membrane plane.

A subsequent NMR structure of SLN was determined in dodecylphosphocholine (DPC) micelles, conditions that more closely mimic the native membrane environment (212). The overall structure of SLN was highly similar to the initial SLN structure solved in the presence of detergent, indicating that this protein adopts the same conformation in detergent and lipid environments. However, contrasting what was observed in the initial structural study (104), SLN was determined to adopt a tilted orientation with the helix axis tilted by ~23° with respect to the membrane normal. In addition, spin relaxation measurements revealed four dynamic domains of SLN: an unstructured N-terminus (residues 1-6), a dynamic helix (residues 7-14), a highly rigid helix (residues 15-26), and an unstructured C-terminus (residues 27-31). The more hydrophilic N-terminal portion of the transmembrane domain of SLN is highly reminiscent of domain Ib of PLN, whereas the more hydrophobic and rigid segment resembles domain II of PLN, suggesting that sequence conservation between these two proteins is reflected in the conservation of both structure and dynamics. This study also indicated that the highly dynamic peptide backbone of the cytoplasmic and luminal domains of SLN become more structured in the presence of SERCA, suggesting that these regions of SLN might be stabilized through interactions with the pump.

1-7.4. Oligomeric state of sarcolipin

It is well documented that inhibitory PLN can assemble into stable pentamers (24). In contrast, SLN has been found to migrate primarily as a monomer in SDS-PAGE (197). However, several studies have since shown that SLN can form a mixture of oligomeric species. For example, SLN has been shown to aggregate after purification in non-ionic detergents as well as self-associate into higher order oligomers after chemical cross-linking in detergent micelles and in liposomes (209). Recently, a fluorescence study done in insect cells directly demonstrated that SLN monomers associate into dimers and

higher order oligomers, whereas mutant I17A SLN only formed monomers and dimers (210). The same study also revealed that the binding affinity of SLN for itself is very similar to that of SLN for SERCA.

Another interesting factor supporting the oligomerization of SLN came from recent studies which reported channel-like activity for SLN reconstituted into tethered bilayer lipid membranes (213,214). SLN was reported to form channels selective toward chloride and phosphate anions and impermeable to inorganic cations. This ion-channel activity was abolished by the T18A mutation in the transmembrane domain of SLN. In addition, the transport of phosphate by the SLN channel was found to be activated in the presence of ATP and inhibited by ADP. Intriguingly, the SLN channel shares some features with the unidentified phosphate transporter found in the SR, which is thought to enhance the level of accumulation of calcium ions in the SR when SERCA is activated by ATP (215,216). Although the physiological role of the SLN channel is still debatable, these studies suggest that SLN must oligomerize in order to exhibit channel-like activity.

1-7.5. Sarcolipin physically interacts with SERCA

Mutagenesis studies of both SLN and SERCA in combination with functional measurements and co-immunoprecipitation studies provided the first insights into where SLN binds on the SERCA pump (201). Since residues in the transmembrane domain of PLN responsible for interactions with SERCA are conserved in SLN, this study compared the effects of SLN mutation to the previously characterized mutations in PLN (147). With respect to binding SERCA, mutations in PLN had more dramatic effects on binding than SLN mutations, suggesting that PLN has higher affinity for SERCA than SLN. The most notable differences were that L8A SLN had no effect on binding to SERCA (the equivalent L31A PLN decreased binding by 73%) and I17A SLN decreased

binding by 18% (the equivalent I40A PLN increased binding by 145%). In addition, mutations in SERCA that reduced regulatory function with PLN had similar effects on SLN binding further suggesting that SLN binds in the same region of SERCA as PLN. Based on these results, the authors modeled the NMR structure of SLN onto the calcium-free crystal structure of SERCA. Modeling showed that the SERCA-SLN complex closely resembles the previously generated SERCA-PLN model (102), with the transmembrane domain of SLN occupying the same grove as the transmembrane of PLN, and the C-terminal luminal domain interacting with aromatic residues in the TM1-TM2 loop of SERCA.

A major breakthrough in understanding the interactions between SERCA and its regulator SLN came about with the recent publication of two high resolution crystal structures of the SERCA-SLN complex (Fig. 1-15) (217,218). These structures represent SLN bound to SERCA in a calcium-free state and for the first time provide detailed structural information explaining the mechanism of SERCA regulation by SLN. These structures reveal that SLN traps SERCA in a previously unobserved magnesium bound state, denoted as E1-Mg^{2+}, with the calcium binding sites exposed to the cytosol and the conformation of the pump being intermediate between the calcium-free (E2) and the calcium bound (E1-Ca^{2+}) states. Two magnesium ions appear to be bound at the second calcium binding site (site II) which is not fully formed in the E1-Mg^{2+} state (Fig. 1-15B). Therefore, it is possible that binding of a calcium ion at site I causes displacement of magnesium ions and complete formation of site II. This hypothesis is supported by functional studies which indicated that magnesium can access calcium binding sites from the cytosol and high magnesium concentrations can inhibit calcium binding to SERCA (219). The authors propose that SERCA utilizes magnesium ions to modulate the

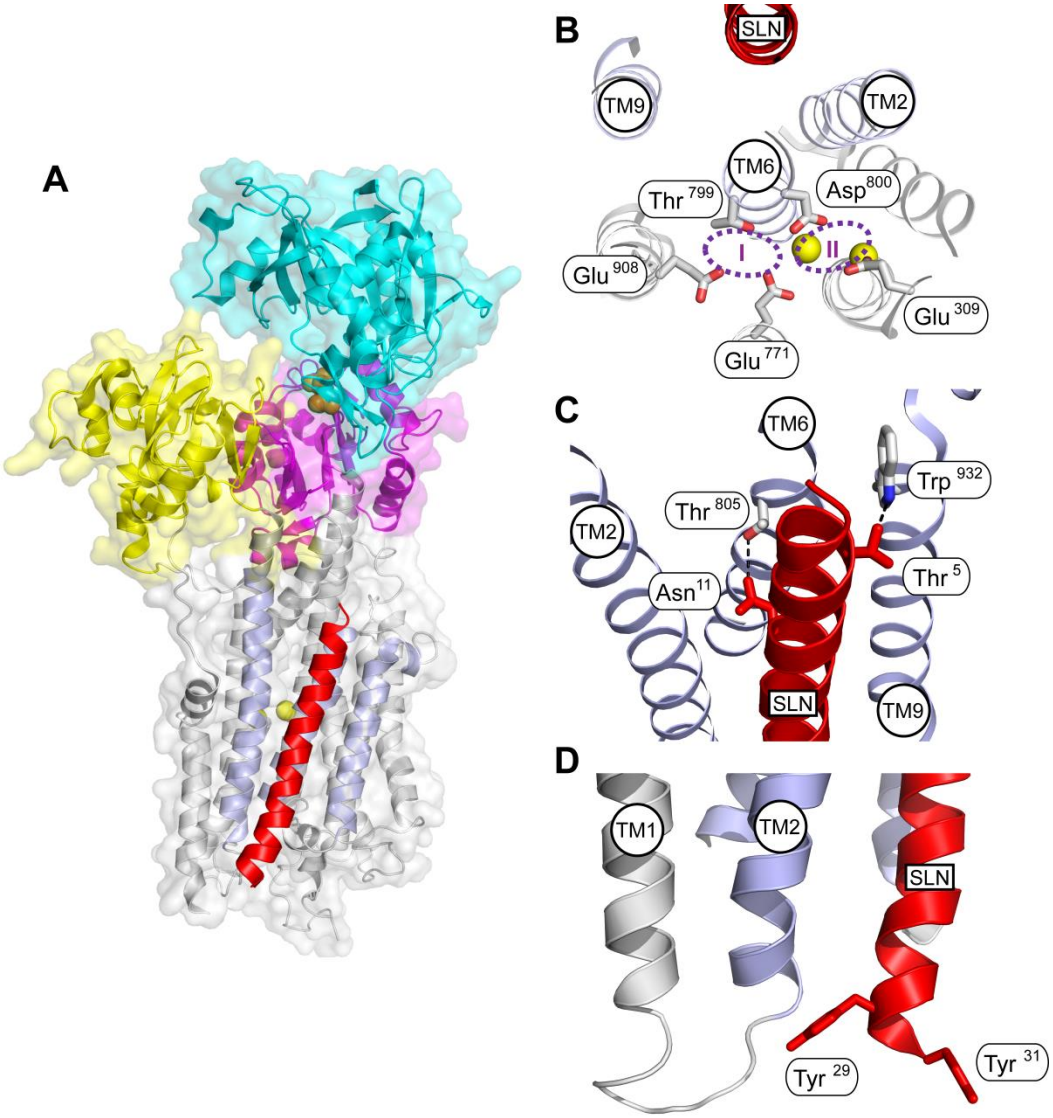

Figure 1-15. High-resolution structure of SERCA in complex with SLN. (A) SERCA is shown in transparent surface and cartoon with the P-domain in magenta, N-domain in cyan, A-domain in yellow, TM2 and TM9 in light purple and the rest of TM helices in grey. Magnesium ions are shown as yellow spheres. SLN is shown in red cartoon. **(B)** Close-up view of the calcium binding sites with two magnesium ions occupying site II. Calcium ion coordinating side chains are shown as grey sticks. **(C)** Close-up view of the interactions between the N-terminal part of SLN and TM2, TM6 and TM9 helices of SERCA. Asn^{11} and Thr^{5} (red sticks) of SLN are shown to interact with Thr^{805} and Trp^{932} (grey sticks) of SERCA, respectively. **(D)** Close-up view showing the proximity of Tyr^{29} and Tyr^{31} to the luminal end of TM1-TM2 of SERCA. (PDB 4H1W)

efficiency of calcium binding that may delay SERCA activation relative to the contractile filaments.

The structures of the SERCA-SLN complexes reveal SLN as a slightly bent α-helix bound in a groove surrounded by TM2, TM6, and TM9, which is highly consistent with previous models as well as cross-linking and mutagenesis studies (201,202). The SLN binding cleft appears particularly narrow in the cytoplasmic end where the putative SLN phosphorylation site, residue Thr^{5}, makes contacts with the pump (Fig. 1-15C). Thus, phosphorylation at this site would result in steric clash that relieves binding of SLN to SERCA. These structures also directly demonstrate the importance of the highly conserved Asn^{11} (Asn^{34} in PLN) as it clearly forms extensive interactions with Thr^{805} of SERCA, explaining why mutation of this residue to alanine results in loss of inhibitory function and weaker association of SLN with SERCA (Fig. 1-15C). Unfortunately, the amino- and carboxy-termini of SLN are poorly defined in both structures, preventing accurate assignment of the last three C-terminal residues (^{29}Tyr-Gln-Tyr^{31}). Nevertheless, the C-terminal domain of SLN appears to be in proximity to the aromatic residues in the TM1-TM2 loop (Fig. 1-15D). In summary, these structures suggest that by direct binding to the transmembrane domain of SERCA, SLN interferes with transition from the magnesium bound E1-Mg^{2+} state into the calcium bound E1-Ca^{2+} state, and thereby decreases the apparent affinity of SERCA for calcium.

1-7.6. Role of sarcolipin in the heart

Aside from being the primary regulator of SERCA1 in skeletal muscle, SLN is known to be an active regulator of cardiac SERCA2a. This was initially demonstrated in studies performed in HEK-293 cells, where co-expression of SLN with SERCA2a decreased the apparent calcium affinity of the calcium pump (203). Indeed, SLN mRNA

was shortly after demonstrated to be specifically expressed in the atria of mouse hearts but absent in the ventricles (198). In the same study, SLN mRNA was also detected in human atria. These findings were later confirmed with detection of SLN at the protein level in the atria of mouse and rat (199). Furthermore, several studies have shown that expression of SLN in the cardiac muscle appears to be differentially regulated under diverse physiological and pathophysiological states. For example, expression of SLN at both mRNA and protein levels have been shown to be down-regulated in the atria of patients with chronic atrial fibrillation (220,221) which appears to contribute to atrial remodeling (222). Similarly, down-regulation of SLN mRNA expression was reported in a transgenic mouse model of cardiac hypertrophy (198). Conversely, a more recent study showed that SLN mRNA is up-regulated approximately 50-fold in hypertrophied ventricles of Nkx2-5 null mice (223). In addition, one study reported a significant increase of SLN mRNA expression in the mouse atria during development (198).

Compared to PLN, the function of SLN in cardiac calcium homeostasis and contractility is not fully defined. Important insights into the physiological role of SLN in the heart were obtained with the help of transgenic mouse models with alterations in SLN protein levels. The first genetically engineered mice overexpressing SLN in the cardiac muscle displayed a decrease in SERCA2a affinity for calcium, a decrease in calcium transient amplitude and slowed muscle relaxation (206,224). The inhibitory effect of SLN was reversed by treatment with isoproterenol, suggesting that SLN is a reversible inhibitor of SERCA2a. Overall, these mice were very similar to a previously characterized mouse model overexpressing PLN. To investigate the independent role of SLN in the heart, mice overexpressing SLN in the PLN null background were generated (208). Overexpression of SLN in the absence of PLN caused a decrease in the apparent calcium affinity of SERCA2a, reduced calcium transient amplitude, and impaired

contractility as compared to PLN knockout mice. In agreement with previously studied SLN mouse models, isoproterenol treatment relieved SLN inhibition, further demonstrating that SLN can mediate the β-adrenergic response in the heart. These studies also identified Thr^5 as a potential phosphorylation site and directly demonstrated that SLN can be phosphorylated by Serine/Threonine Kinase 16 (STK16) (Fig. 1-16A). However, the physiological role of STK16 in the β-adrenergic pathway is yet to be defined.

The functional significance of SLN down-regulation in the cardiac muscle was later demonstrated with a SLN knockout mouse (225). In the atria, ablation of SLN resulted in increased apparent calcium affinity of SERCA2a, increased calcium transient amplitudes and enhanced cardiac contractility. SLN knockout mice did not exhibit any developmental abnormalities but were susceptible to arrhythmias and atrial remodeling upon old age, most likely due to enhanced SERCA2a activity (222,225). In addition, the absence of SLN in the atria showed blunted responses to isoproterenol, which implies that β-adrenergic stimulation in the atria is largely mediated by SLN. This was further supported by a study overexpressing SLN in rat ventricular myocytes which provided strong evidence that SLN can be phosphorylated at Thr^5 by CaMKII (Fig. 1-16A) (207). Taken together, these studies strongly suggest that SLN is an important regulator of SERCA2a function and cardiac contractility of the atria.

Since SLN and PLN are co-expressed in the heart, it is possible that the two regulators have a synergistic effect on SERCA activity. Interestingly, co-expression of SLN and PLN with SERCA2a in HEK-293 cell was shown to induce super-inhibition of SERCA2a activity (203). Initially, the authors of this study proposed that SLN mediates its inhibitory effect through PLN (201). According to their model SLN forms a stable binary complex with PLN that results in destabilization of PLN pentamers. This leads to

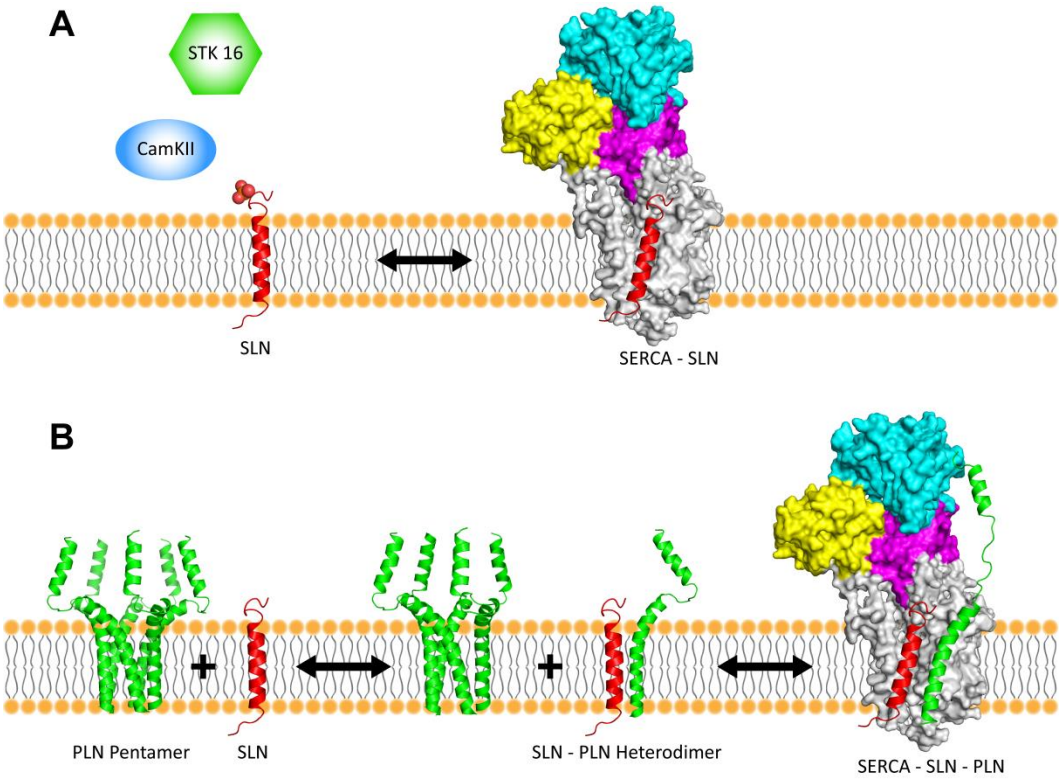

Figure 1-16. Regulation of SERCA by SLN. SERCA is shown as a surface (P-domain is magenta, N-domain is cyan, A-domain is yellow, and transmembrane domain is grey) and SLN (red) and PLN (green) as a cartoon representation. Phosphorylated SLN is shown with orange spheres on the cytoplasmic domain. **(A)** SLN exists mainly as a monomer and upon interaction with SERCA it inhibits its activity. This inhibition can be relieved upon increased cytosolic calcium or phosphorylation of SLN by CaMKII or STK16. **(B)** Super-inhibition of SERCA by the SLN-PLN heterodimers. SLN interferes with the PLN pentamer formation by direct interaction with PLN. The SLN-PLN heterodimers bind with higher affinity to SERCA than either SLN or PLN alone.

increased concentrations of PLN monomers, considered to be the active form of PLN, thus promoting super-inhibition of the SERCA pump. However, aside from the reduced apparent calcium affinity of SERCA, a reduction in maximal activity was also observed. This suggested that it is not only the increase in PLN monomers that causes super-inhibition of SERCA. On the basis of more recent mutagenesis and coimmunoprecipitation studies, the authors have proposed a modified model for the super-inhibition of SERCA (202). According to their data, hetero-dimeric interactions between SLN and PLN are stronger than homo-dimeric interactions between PLN monomers. Thus, a stable SLN-PLN hetero-dimer could form first and then fit into the PLN binding groove on SERCA causing super-inhibition (Fig. 1-16B). Indeed, according to a structural model of the PLN-SLN-SERCA ternary complex, the cavity formed by the TM2, TM4, TM6, and TM9 helices of SERCA in the calcium-free E2 state is large enough to accommodate SLN and PLN simultaneously but too narrow to bind two PLN monomers (201,202). Therefore, binding of the SLN-PLN hetero-dimer to SERCA forms a very stable ternary complex, which explains the observed super-inhibition of SERCA. It is noteworthy to point out, however, that strong evidence for a prominent super-inhibitory action of PLN and SLN in the cardiac muscle under normal physiological settings has never been reported.

1-8. Thesis outline

The primary goal of this thesis is to functionally examine SLN, zebrafish phospholamban-like protein (zfPLN) and the C-terminal TM11 segment of SERCA2b in order to obtain the molecular mechanisms by which they regulate SERCA activity. Chapter 2 examines the role of the luminal domain of SLN on the inhibition of SERCA. This work showed that the luminal extension of SLN is a distinct and transferrable

domain that encodes most of SLN's inhibitory properties. Based on these results, we concluded that SLN and PLN use different inhibitory mechanisms to regulate SERCA. Chapter 3 examines the ability of zfPLN to regulate SERCA. This work showed that despite the high sequence diversity between zebrafish and human PLN, as well as the presence of a unique zfPLN luminal extension, zfPLN has inhibitory properties that are similar to human PLN. Additionally, our results indicated that the luminal extensions of zfPLN and SLN have distinct functional effects, even though zfPLN appears to use a hybrid PLN-SLN inhibitory mechanism. Chapter 4 examines the functional role of the TM11 segment of the ubiquitous SERCA2b in calcium transport. This work demonstrated that TM11 is an independent and highly conserved functional region of SERCA2b that acts as a genuine regulating element of the calcium pump. Chapter 5 concludes the main body of work with a brief summary of the major findings and a discussion of the mechanisms used by the studied endogenous peptide regulators of SERCA.

This thesis also contains an appendix which examines specific sequence elements of SLN and PLN thought to be responsible for their propensity to form oligomers.

1-9. References

1. Carafoli, E. (2002) Calcium signaling: a tale for all seasons. *Proceedings of the National Academy of Sciences of the United States of America* **99**, 1115-1122

2. Bers, D. M. (2002) Cardiac excitation-contraction coupling. *Nature* **415**, 198-205

3. Kuhlbrandt, W. (2004) Biology, structure and mechanism of P-type ATPases. *Nature reviews. Molecular cell biology* **5**, 282-295

4. Axelsen, K. B., and Palmgren, M. G. (1998) Evolution of substrate specificities in the P-type ATPase superfamily. *Journal of molecular evolution* **46**, 84-101

5. Bertrand, J., Altendorf, K., and Bramkamp, M. (2004) Amino acid substitutions in putative selectivity filter regions III and IV in KdpA alter ion selectivity of the

KdpFABC complex from Escherichia coli. *Journal of bacteriology* **186**, 5519-5522

6. Palmgren, M. G., and Nissen, P. (2011) P-type ATPases. *Annual review of biophysics* **40**, 243-266

7. Skou, J. C. (1957) The influence of some cations on an adenosine triphosphatase from peripheral nerves. *Biochimica et biophysica acta* **23**, 394-401

8. Kaplan, J. H. (2002) Biochemistry of Na,K-ATPase. *Annual review of biochemistry* **71**, 511-535

9. Daleke, D. L. (2003) Regulation of transbilayer plasma membrane phospholipid asymmetry. *Journal of lipid research* **44**, 233-242

10. Pomorski, T., Lombardi, R., Riezman, H., Devaux, P. F., van Meer, G., and Holthuis, J. C. (2003) Drs2p-related P-type ATPases Dnf1p and Dnf2p are required for phospholipid translocation across the yeast plasma membrane and serve a role in endocytosis. *Molecular biology of the cell* **14**, 1240-1254

11. Periasamy, M., and Kalyanasundaram, A. (2007) SERCA pump isoforms: their role in calcium transport and disease. *Muscle & nerve* **35**, 430-442

12. Brandl, C. J., Green, N. M., Korczak, B., and MacLennan, D. H. (1986) Two Ca2+ ATPase genes: homologies and mechanistic implications of deduced amino acid sequences. *Cell* **44**, 597-607

13. Brandl, C. J., deLeon, S., Martin, D. R., and MacLennan, D. H. (1987) Adult forms of the Ca2+ATPase of sarcoplasmic reticulum. Expression in developing skeletal muscle. *The Journal of biological chemistry* **262**, 3768-3774

14. Anger, M., Samuel, J. L., Marotte, F., Wuytack, F., Rappaport, L., and Lompre, A. M. (1994) In situ mRNA distribution of sarco(endo)plasmic reticulum Ca(2+)-ATPase isoforms during ontogeny in the rat. *J Mol Cell Cardiol* **26**, 539-550

15. Bhupathy, P., Babu, G. J., and Periasamy, M. (2007) Sarcolipin and phospholamban as regulators of cardiac sarcoplasmic reticulum Ca2+ ATPase. *J Mol Cell Cardiol* **42**, 903-911

16. Sumbilla, C., Cavagna, M., Zhong, L., Ma, H., Lewis, D., Farrance, I., and Inesi, G. (1999) Comparison of SERCA1 and SERCA2a expressed in COS-1 cells and cardiac myocytes. *The American journal of physiology* **277**, H2381-2391

17. Ji, Y., Loukianov, E., Loukianova, T., Jones, L. R., and Periasamy, M. (1999) SERCA1a can functionally substitute for SERCA2a in the heart. *The American journal of physiology* **276**, H89-97

18. Loukianov, E., Ji, Y., Grupp, I. L., Kirkpatrick, D. L., Baker, D. L., Loukianova, T., Grupp, G., Lytton, J., Walsh, R. A., and Periasamy, M. (1998) Enhanced myocardial contractility and increased Ca2+ transport function in transgenic

hearts expressing the fast-twitch skeletal muscle sarcoplasmic reticulum Ca2+-ATPase. *Circulation research* **83**, 889-897

19. Lalli, M. J., Yong, J., Prasad, V., Hashimoto, K., Plank, D., Babu, G. J., Kirkpatrick, D., Walsh, R. A., Sussman, M., Yatani, A., Marban, E., and Periasamy, M. (2001) Sarcoplasmic reticulum Ca(2+) atpase (SERCA) 1a structurally substitutes for SERCA2a in the cardiac sarcoplasmic reticulum and increases cardiac Ca(2+) handling capacity. *Circulation research* **89**, 160-167

20. MacLennan, D. H. (2000) Ca2+ signalling and muscle disease. *European journal of biochemistry / FEBS* **267**, 5291-5297

21. Odermatt, A., Taschner, P. E., Khanna, V. K., Busch, H. F., Karpati, G., Jablecki, C. K., Breuning, M. H., and MacLennan, D. H. (1996) Mutations in the gene-encoding SERCA1, the fast-twitch skeletal muscle sarcoplasmic reticulum Ca2+ ATPase, are associated with Brody disease. *Nature genetics* **14**, 191-194

22. Odermatt, A., Barton, K., Khanna, V. K., Mathieu, J., Escolar, D., Kuntzer, T., Karpati, G., and MacLennan, D. H. (2000) The mutation of Pro789 to Leu reduces the activity of the fast-twitch skeletal muscle sarco(endo)plasmic reticulum Ca2+ ATPase (SERCA1) and is associated with Brody disease. *Human genetics* **106**, 482-491

23. Zarain-Herzberg, A., MacLennan, D. H., and Periasamy, M. (1990) Characterization of rabbit cardiac sarco(endo)plasmic reticulum Ca2(+)-ATPase gene. *The Journal of biological chemistry* **265**, 4670-4677

24. MacLennan, D. H., and Kranias, E. G. (2003) Phospholamban: a crucial regulator of cardiac contractility. *Nature reviews. Molecular cell biology* **4**, 566-577

25. Gunteski-Hamblin, A. M., Greeb, J., and Shull, G. E. (1988) A novel Ca2+ pump expressed in brain, kidney, and stomach is encoded by an alternative transcript of the slow-twitch muscle sarcoplasmic reticulum Ca-ATPase gene. Identification of cDNAs encoding Ca2+ and other cation-transporting ATPases using an oligonucleotide probe derived from the ATP-binding site. *The Journal of biological chemistry* **263**, 15032-15040

26. Vangheluwe, P., Louch, W. E., Ver Heyen, M., Sipido, K., Raeymaekers, L., and Wuytack, F. (2003) Ca2+ transport ATPase isoforms SERCA2a and SERCA2b are targeted to the same sites in the murine heart. *Cell calcium* **34**, 457-464

27. Verboomen, H., Wuytack, F., De Smedt, H., Himpens, B., and Casteels, R. (1992) Functional difference between SERCA2a and SERCA2b Ca2+ pumps and their modulation by phospholamban. *The Biochemical journal* **286 (Pt 2)**, 591-595

28. Gelebart, P., Martin, V., Enouf, J., and Papp, B. (2003) Identification of a new SERCA2 splice variant regulated during monocytic differentiation. *Biochem Biophys Res Commun* **303**, 676-684

29. Dally, S., Bredoux, R., Corvazier, E., Andersen, J. P., Clausen, J. D., Dode, L., Fanchaouy, M., Gelebart, P., Monceau, V., Del Monte, F., Gwathmey, J. K., Hajjar, R., Chaabane, C., Bobe, R., Raies, A., and Enouf, J. (2006) Ca2+-ATPases in non-failing and failing heart: evidence for a novel cardiac sarco/endoplasmic reticulum Ca2+-ATPase 2 isoform (SERCA2c). *The Biochemical journal* **395**, 249-258

30. Dode, L., Andersen, J. P., Leslie, N., Dhitavat, J., Vilsen, B., and Hovnanian, A. (2003) Dissection of the functional differences between sarco(endo)plasmic reticulum Ca2+-ATPase (SERCA) 1 and 2 isoforms and characterization of Darier disease (SERCA2) mutants by steady-state and transient kinetic analyses. *The Journal of biological chemistry* **278**, 47877-47889

31. Sakuntabhai, A., Ruiz-Perez, V., Carter, S., Jacobsen, N., Burge, S., Monk, S., Smith, M., Munro, C. S., O'Donovan, M., Craddock, N., Kucherlapati, R., Rees, J. L., Owen, M., Lathrop, G. M., Monaco, A. P., Strachan, T., and Hovnanian, A. (1999) Mutations in ATP2A2, encoding a Ca2+ pump, cause Darier disease. *Nature genetics* **21**, 271-277

32. Sakuntabhai, A., Burge, S., Monk, S., and Hovnanian, A. (1999) Spectrum of novel ATP2A2 mutations in patients with Darier's disease. *Human molecular genetics* **8**, 1611-1619

33. Korosec, B., Glavac, D., Rott, T., and Ravnik-Glavac, M. (2006) Alterations in the ATP2A2 gene in correlation with colon and lung cancer. *Cancer genetics and cytogenetics* **171**, 105-111

34. Periasamy, M., Reed, T. D., Liu, L. H., Ji, Y., Loukianov, E., Paul, R. J., Nieman, M. L., Riddle, T., Duffy, J. J., Doetschman, T., Lorenz, J. N., and Shull, G. E. (1999) Impaired cardiac performance in heterozygous mice with a null mutation in the sarco(endo)plasmic reticulum Ca2+-ATPase isoform 2 (SERCA2) gene. *The Journal of biological chemistry* **274**, 2556-2562

35. Ji, Y., Lalli, M. J., Babu, G. J., Xu, Y., Kirkpatrick, D. L., Liu, L. H., Chiamvimonvat, N., Walsh, R. A., Shull, G. E., and Periasamy, M. (2000) Disruption of a single copy of the SERCA2 gene results in altered Ca2+ homeostasis and cardiomyocyte function. *The Journal of biological chemistry* **275**, 38073-38080

36. Wuytack, F., Raeymaekers, L., and Missiaen, L. (2002) Molecular physiology of the SERCA and SPCA pumps. *Cell calcium* **32**, 279-305

37. Dode, L., Vilsen, B., Van Baelen, K., Wuytack, F., Clausen, J. D., and Andersen, J. P. (2002) Dissection of the functional differences between sarco(endo)plasmic reticulum Ca2+-ATPase (SERCA) 1 and 3 isoforms by steady-state and transient kinetic analyses. *The Journal of biological chemistry* **277**, 45579-45591

38. MacLennan, D. H., Toyofuku, T., and Lytton, J. (1992) Structure-function relationships in sarcoplasmic or endoplasmic reticulum type Ca2+ pumps. *Annals of the New York Academy of Sciences* **671**, 1-10

39. Bobe, R., Bredoux, R., Corvazier, E., Andersen, J. P., Clausen, J. D., Dode, L., Kovacs, T., and Enouf, J. (2004) Identification, expression, function, and localization of a novel (sixth) isoform of the human sarco/endoplasmic reticulum Ca2+ATPase 3 gene. *The Journal of biological chemistry* **279**, 24297-24306

40. Wuytack, F., Dode, L., Baba-Aissa, F., and Raeymaekers, L. (1995) The SERCA3-type of organellar Ca2+ pumps. *Bioscience reports* **15**, 299-306

41. Dally, S., Corvazier, E., Bredoux, R., Bobe, R., and Enouf, J. (2010) Multiple and diverse coexpression, location, and regulation of additional SERCA2 and SERCA3 isoforms in nonfailing and failing human heart. *J Mol Cell Cardiol* **48**, 633-644

42. Varadi, A., Lebel, L., Hashim, Y., Mehta, Z., Ashcroft, S. J., and Turner, R. (1999) Sequence variants of the sarco(endo)plasmic reticulum Ca(2+)-transport ATPase 3 gene (SERCA3) in Caucasian type II diabetic patients (UK Prospective Diabetes Study 48). *Diabetologia* **42**, 1240-1243

43. Liu, L. H., Paul, R. J., Sutliff, R. L., Miller, M. L., Lorenz, J. N., Pun, R. Y., Duffy, J. J., Doetschman, T., Kimura, Y., MacLennan, D. H., Hoying, J. B., and Shull, G. E. (1997) Defective endothelium-dependent relaxation of vascular smooth muscle and endothelial cell Ca2+ signaling in mice lacking sarco(endo)plasmic reticulum Ca2+-ATPase isoform 3. *The Journal of biological chemistry* **272**, 30538-30545

44. Xu, X. Y., Gou, W. F., Yang, X., Wang, G. L., Takahashi, H., Yu, M., Mao, X. Y., Takano, Y., and Zheng, H. C. (2012) Aberrant SERCA3 expression is closely linked to pathogenesis, invasion, metastasis, and prognosis of gastric carcinomas. *Tumour biology : the journal of the International Society for Oncodevelopmental Biology and Medicine* **33**, 1845-1854

45. Albers, R. W. (1967) Biochemical aspects of active transport. *Annual review of biochemistry* **36**, 727-756

46. Post, R. L., Hegyvary, C., and Kume, S. (1972) Activation by adenosine triphosphate in the phosphorylation kinetics of sodium and potassium ion transport adenosine triphosphatase. *The Journal of biological chemistry* **247**, 6530-6540

47. de Meis, L., and Vianna, A. L. (1979) Energy interconversion by the Ca2+-dependent ATPase of the sarcoplasmic reticulum. *Annual review of biochemistry* **48**, 275-292

48. Chevallier, J., and Butow, R. A. (1971) Calcium binding to the sarcoplasmic reticulum of rabbit skeletal muscle. *Biochemistry* **10**, 2733-2737

49. Moller, J. V., Olesen, C., Winther, A. M., and Nissen, P. (2010) The sarcoplasmic Ca2+-ATPase: design of a perfect chemi-osmotic pump. *Quarterly reviews of biophysics* **43**, 501-566

50. Olesen, C., Picard, M., Winther, A. M., Gyrup, C., Morth, J. P., Oxvig, C., Moller, J. V., and Nissen, P. (2007) The structural basis of calcium transport by the calcium pump. *Nature* **450**, 1036-1042

51. Yu, X., Hao, L., and Inesi, G. (1994) A pK change of acidic residues contributes to cation countertransport in the Ca-ATPase of sarcoplasmic reticulum. Role of H+ in Ca(2+)-ATPase countertransport. *The Journal of biological chemistry* **269**, 16656-16661

52. Moller, J. V., Nissen, P., Sorensen, T. L., and le Maire, M. (2005) Transport mechanism of the sarcoplasmic reticulum Ca2+ -ATPase pump. *Current opinion in structural biology* **15**, 387-393

53. Jensen, A. M., Sorensen, T. L., Olesen, C., Moller, J. V., and Nissen, P. (2006) Modulatory and catalytic modes of ATP binding by the calcium pump. *The EMBO journal* **25**, 2305-2314

54. Stahl, N., and Jencks, W. P. (1984) Adenosine 5'-triphosphate at the active site accelerates binding of calcium to calcium adenosinetriphosphatase. *Biochemistry* **23**, 5389-5392

55. Mintz, E., Mata, A. M., Forge, V., Passafiume, M., and Guillain, F. (1995) The modulation of Ca2+ binding to sarcoplasmic reticulum ATPase by ATP analogues is pH-dependent. *The Journal of biological chemistry* **270**, 27160-27164

56. Champeil, P., and Guillain, F. (1986) Rapid filtration study of the phosphorylation-dependent dissociation of calcium from transport sites of purified sarcoplasmic reticulum ATPase and ATP modulation of the catalytic cycle. *Biochemistry* **25**, 7623-7633

57. Champeil, P., Riollet, S., Orlowski, S., Guillain, F., Seebregts, C. J., and McIntosh, D. B. (1988) ATP regulation of sarcoplasmic reticulum Ca2+-ATPase. Metal-free ATP and 8-bromo-ATP bind with high affinity to the catalytic site of phosphorylated ATPase and accelerate dephosphorylation. *The Journal of biological chemistry* **263**, 12288-12294

58. Moncoq, K., Trieber, C. A., and Young, H. S. (2007) The molecular basis for cyclopiazonic acid inhibition of the sarcoplasmic reticulum calcium pump. *The Journal of biological chemistry* **282**, 9748-9757

59. Laursen, M., Bublitz, M., Moncoq, K., Olesen, C., Moller, J. V., Young, H. S., Nissen, P., and Morth, J. P. (2009) Cyclopiazonic acid is complexed to a divalent metal ion when bound to the sarcoplasmic reticulum Ca2+-ATPase. *The Journal of biological chemistry* **284**, 13513-13518

60. MacLennan, D. H., Brandl, C. J., Korczak, B., and Green, N. M. (1985) Amino-acid sequence of a Ca2+ + Mg2+-dependent ATPase from rabbit muscle sarcoplasmic reticulum, deduced from its complementary DNA sequence. *Nature* **316**, 696-700

61. Clarke, D. M., Loo, T. W., and MacLennan, D. H. (1990) Functional consequences of alterations to amino acids located in the nucleotide binding domain of the Ca2(+)-ATPase of sarcoplasmic reticulum. *The Journal of biological chemistry* **265**, 22223-22227

62. Clarke, D. M., Maruyama, K., Loo, T. W., Leberer, E., Inesi, G., and MacLennan, D. H. (1989) Functional consequences of glutamate, aspartate, glutamine, and asparagine mutations in the stalk sector of the Ca2+-ATPase of sarcoplasmic reticulum. *The Journal of biological chemistry* **264**, 11246-11251

63. Andersen, J. P., Vilsen, B., Leberer, E., and MacLennan, D. H. (1989) Functional consequences of mutations in the beta-strand sector of the Ca2(+)-ATPase of sarcoplasmic reticulum. *The Journal of biological chemistry* **264**, 21018-21023

64. Vilsen, B., Andersen, J. P., Clarke, D. M., and MacLennan, D. H. (1989) Functional consequences of proline mutations in the cytoplasmic and transmembrane sectors of the Ca2(+)-ATPase of sarcoplasmic reticulum. *The Journal of biological chemistry* **264**, 21024-21030

65. Clarke, D. M., Loo, T. W., Inesi, G., and MacLennan, D. H. (1989) Location of high affinity Ca2+-binding sites within the predicted transmembrane domain of the sarcoplasmic reticulum Ca2+-ATPase. *Nature* **339**, 476-478

66. Dux, L., and Martonosi, A. (1983) Two-dimensional arrays of proteins in sarcoplasmic reticulum and purified Ca2+-ATPase vesicles treated with vanadate. *The Journal of biological chemistry* **258**, 2599-2603

67. Castellani, L., Hardwicke, P. M., and Vibert, P. (1985) Dimer ribbons in the three-dimensional structure of sarcoplasmic reticulum. *J Mol Biol* **185**, 579-594

68. Taylor, K. A., Dux, L., and Martonosi, A. (1986) Three-dimensional reconstruction of negatively stained crystals of the Ca2+-ATPase from muscle sarcoplasmic reticulum. *J Mol Biol* **187**, 417-427

69. Toyoshima, C., Sasabe, H., and Stokes, D. L. (1993) Three-dimensional cryo-electron microscopy of the calcium ion pump in the sarcoplasmic reticulum membrane. *Nature* **362**, 467-471

70. Zhang, P., Toyoshima, C., Yonekura, K., Green, N. M., and Stokes, D. L. (1998) Structure of the calcium pump from sarcoplasmic reticulum at 8-A resolution. *Nature* **392**, 835-839

71. Toyoshima, C., Nakasako, M., Nomura, H., and Ogawa, H. (2000) Crystal structure of the calcium pump of sarcoplasmic reticulum at 2.6 A resolution. *Nature* **405**, 647-655

72. Dupont, Y. (1982) Low-temperature studies of the sarcoplasmic reticulum calcium pump. Mechanisms of calcium binding. *Biochimica et biophysica acta* **688**, 75-87

73. Lee, A. G., and East, J. M. (2001) What the structure of a calcium pump tells us about its mechanism. *The Biochemical journal* **356**, 665-683

74. Zhang, Z., Lewis, D., Strock, C., Inesi, G., Nakasako, M., Nomura, H., and Toyoshima, C. (2000) Detailed characterization of the cooperative mechanism of Ca(2+) binding and catalytic activation in the Ca(2+) transport (SERCA) ATPase. *Biochemistry* **39**, 8758-8767

75. Toyoshima, C., and Nomura, H. (2002) Structural changes in the calcium pump accompanying the dissociation of calcium. *Nature* **418**, 605-611

76. Holdensen, A. N., and Andersen, J. P. (2009) The length of the A-M3 linker is a crucial determinant of the rate of the Ca2+ transport cycle of sarcoplasmic reticulum Ca2+-ATPase. *The Journal of biological chemistry* **284**, 12258-12265

77. Yamasaki, K., Wang, G., Daiho, T., Danko, S., and Suzuki, H. (2008) Roles of Tyr122-hydrophobic cluster and K+ binding in Ca2+ -releasing process of ADP-insensitive phosphoenzyme of sarcoplasmic reticulum Ca2+ -ATPase. *The Journal of biological chemistry* **283**, 29144-29155

78. Sorensen, T. L., Moller, J. V., and Nissen, P. (2004) Phosphoryl transfer and calcium ion occlusion in the calcium pump. *Science* **304**, 1672-1675

79. Thastrup, O., Cullen, P. J., Drobak, B. K., Hanley, M. R., and Dawson, A. P. (1990) Thapsigargin, a tumor promoter, discharges intracellular Ca2+ stores by specific inhibition of the endoplasmic reticulum Ca2(+)-ATPase. *Proceedings of the National Academy of Sciences of the United States of America* **87**, 2466-2470

80. Seidler, N. W., Jona, I., Vegh, M., and Martonosi, A. (1989) Cyclopiazonic acid is a specific inhibitor of the Ca2+-ATPase of sarcoplasmic reticulum. *The Journal of biological chemistry* **264**, 17816-17823

81. Oldershaw, K. A., and Taylor, C. W. (1990) 2,5-Di-(tert-butyl)-1,4-benzohydroquinone mobilizes inositol 1,4,5-trisphosphate-sensitive and -insensitive Ca2+ stores. *FEBS letters* **274**, 214-216

82. Berman, M. C., and Karlish, S. J. (2003) Interaction of an aromatic dibromoisothiouronium derivative with the Ca(2+)-ATPase of skeletal muscle sarcoplasmic reticulum. *Biochemistry* **42**, 3556-3566

83. Tadini-Buoninsegni, F., Bartolommei, G., Moncelli, M. R., Tal, D. M., Lewis, D., and Inesi, G. (2008) Effects of high-affinity inhibitors on partial reactions, charge movements, and conformational States of the Ca2+ transport ATPase (sarco-endoplasmic reticulum Ca2+ ATPase). *Molecular pharmacology* **73**, 1134-1140

84. Uhlemann, A. C., Cameron, A., Eckstein-Ludwig, U., Fischbarg, J., Iserovich, P., Zuniga, F. A., East, M., Lee, A., Brady, L., Haynes, R. K., and Krishna, S. (2005) A single amino acid residue can determine the sensitivity of SERCAs to artemisinins. *Nature structural & molecular biology* **12**, 628-629

85. Yatime, L., Buch-Pedersen, M. J., Musgaard, M., Morth, J. P., Lund Winther, A. M., Pedersen, B. P., Olesen, C., Andersen, J. P., Vilsen, B., Schiott, B., Palmgren, M. G., Moller, J. V., Nissen, P., and Fedosova, N. (2009) P-type ATPases as drug targets: tools for medicine and science. *Biochimica et biophysica acta* **1787**, 207-220

86. Lytton, J., Westlin, M., and Hanley, M. R. (1991) Thapsigargin inhibits the sarcoplasmic or endoplasmic reticulum Ca-ATPase family of calcium pumps. *The Journal of biological chemistry* **266**, 17067-17071

87. Wootton, L. L., and Michelangeli, F. (2006) The effects of the phenylalanine 256 to valine mutation on the sensitivity of sarcoplasmic/endoplasmic reticulum Ca2+ ATPase (SERCA) Ca2+ pump isoforms 1, 2, and 3 to thapsigargin and other inhibitors. *The Journal of biological chemistry* **281**, 6970-6976

88. Dode, L., Andersen, J. P., Vanoevelen, J., Raeymaekers, L., Missiaen, L., Vilsen, B., and Wuytack, F. (2006) Dissection of the functional differences between human secretory pathway Ca2+/Mn2+-ATPase (SPCA) 1 and 2 isoenzymes by steady-state and transient kinetic analyses. *The Journal of biological chemistry* **281**, 3182-3189

89. Takahashi, M., Kondou, Y., and Toyoshima, C. (2007) Interdomain communication in calcium pump as revealed in the crystal structures with transmembrane inhibitors. *Proceedings of the National Academy of Sciences of the United States of America* **104**, 5800-5805

90. Yu, M., Zhong, L., Rishi, A. K., Khadeer, M., Inesi, G., and Hussain, A. (1998) Specific substitutions at amino acid 256 of the sarcoplasmic/endoplasmic reticulum Ca2+ transport ATPase mediate resistance to thapsigargin in thapsigargin-resistant hamster cells. *The Journal of biological chemistry* **273**, 3542-3546

91. Xu, C., Ma, H., Inesi, G., Al-Shawi, M. K., and Toyoshima, C. (2004) Specific structural requirements for the inhibitory effect of thapsigargin on the Ca2+ ATPase SERCA. *The Journal of biological chemistry* **279**, 17973-17979

92. Holzapfel, C. W. (1968) The isolation and structure of cyclopiazonic acid, a toxic metabolite of Penicillium cyclopium Westling. *Tetrahedron* **24**, 2101-2119

93. Khan, Y. M., Wictome, M., East, J. M., and Lee, A. G. (1995) Interactions of dihydroxybenzenes with the Ca(2+)-ATPase: separate binding sites for dihydroxybenzenes and sesquiterpene lactones. *Biochemistry* **34**, 14385-14393

94. Obara, K., Miyashita, N., Xu, C., Toyoshima, I., Sugita, Y., Inesi, G., and Toyoshima, C. (2005) Structural role of countertransport revealed in Ca(2+) pump crystal structure in the absence of Ca(2+). *Proceedings of the National Academy of Sciences of the United States of America* **102**, 14489-14496

95. Koss, K. L., and Kranias, E. G. (1996) Phospholamban: a prominent regulator of myocardial contractility. *Circulation research* **79**, 1059-1063

96. Damiani, E., Sacchetto, R., and Margreth, A. (2000) Variation of phospholamban in slow-twitch muscle sarcoplasmic reticulum between mammalian species and a link to the substrate specificity of endogenous Ca(2+)-calmodulin-dependent protein kinase. *Biochimica et biophysica acta* **1464**, 231-241

97. Lalli, J., Harrer, J. M., Luo, W., Kranias, E. G., and Paul, R. J. (1997) Targeted ablation of the phospholamban gene is associated with a marked decrease in sensitivity in aortic smooth muscle. *Circulation research* **80**, 506-513

98. Fujii, J., Ueno, A., Kitano, K., Tanaka, S., Kadoma, M., and Tada, M. (1987) Complete complementary DNA-derived amino acid sequence of canine cardiac phospholamban. *The Journal of clinical investigation* **79**, 301-304

99. Kimura, Y., Kurzydlowski, K., Tada, M., and MacLennan, D. H. (1997) Phospholamban inhibitory function is enhanced by depolymerization. *J. Biol. Chem.* **272**, 15061-15064

100. Simmerman, H. K., Collins, J. H., Theibert, J. L., Wegener, A. D., and Jones, L. R. (1986) Sequence analysis of phospholamban. Identification of phosphorylation sites and two major structural domains. *The Journal of biological chemistry* **261**, 13333-13341

101. Tada, M., Inui, M., Yamada, M., Kadoma, M., Kuzuya, T., Abe, H., and Kakiuchi, S. (1983) Effects of phospholamban phosphorylation catalyzed by adenosine 3':5'-monophosphate- and calmodulin-dependent protein kinases on calcium transport ATPase of cardiac sarcoplasmic reticulum. *J Mol Cell Cardiol* **15**, 335-346

102. Toyoshima, C., Asahi, M., Sugita, Y., Khanna, R., Tsuda, T., and MacLennan, D. (2003) Modeling of the inhibitory interaction of phospholamban with the Ca^{2+} ATPase. *Proc. Natl. Acad. Sci. U. S. A.* **100**, 467-472

103. Seidel, K., Andronesi, O. C., Krebs, J., Griesinger, C., Young, H. S., Becker, S., and Baldus, M. (2008) Structural Characterization of Ca^{2+}-ATPase-Bound Phospholamban in Lipid Bilayers by Solid-State Nuclear Magnetic Resonance (NMR) Spectroscopy. *Biochemistry* **47**, 4369-4376

104. Mascioni, A., Karim, C., Barany, G., Thomas, D. D., and Veglia, G. (2002) Structure and orientation of sarcolipin in lipid environments. *Biochemistry* **41**, 475-482

105. Zamoon, J., Mascioni, A., Thomas, D. D., and Veglia, G. (2003) NMR solution structure and topological orientation of monomeric phospholamban in dodecylphosphocholine micelles. *Biophys J* **85**, 2589-2598

106. Traaseth, N. J., Ha, K. N., Verardi, R., Shi, L., Buffy, J. J., Masterson, L. R., and Veglia, G. (2008) Structural and dynamic basis of phospholamban and sarcolipin inhibition of Ca(2+)-ATPase. *Biochemistry* **47**, 3-13

107. Traaseth, N. J., Shi, L., Verardi, R., Mullen, D. G., Barany, G., and Veglia, G. (2009) Structure and topology of monomeric phospholamban in lipid membranes

determined by a hybrid solution and solid-state NMR approach. *Proceedings of the National Academy of Sciences of the United States of America* **106**, 10165-10170

108. Tatulian, S. A., Jones, L. R., Reddy, L. G., Stokes, D. L., and Tamm, L. K. (1995) Secondary structure and orientation of phospholamban reconstituted in supported bilayers from polarized attenuated total reflection FTIR spectroscopy. *Biochemistry* **34**, 4448-4456

109. Arkin, I. T., Rothman, M., Ludlam, C. F., Aimoto, S., Engelman, D. M., Rothschild, K. J., and Smith, S. O. (1995) Structural model of the phospholamban ion channel complex in phospholipid membranes. *J Mol Biol* **248**, 824-834

110. Smith, S. O., Kawakami, T., Liu, W., Ziliox, M., and Aimoto, S. (2001) Helical structure of phospholamban in membrane bilayers. *J Mol Biol* **313**, 1139-1148

111. Robia, S. L., Flohr, N. C., and Thomas, D. D. (2005) Phospholamban pentamer quaternary conformation determined by in-gel fluorescence anisotropy. *Biochemistry* **44**, 4302-4311

112. Oxenoid, K., and Chou, J. J. (2005) The structure of phospholamban pentamer reveals a channel-like architecture in membranes. *Proceedings of the National Academy of Sciences of the United States of America* **102**, 10870-10875

113. Traaseth, N. J., Verardi, R., Torgersen, K. D., Karim, C. B., Thomas, D. D., and Veglia, G. (2007) Spectroscopic validation of the pentameric structure of phospholamban. *Proceedings of the National Academy of Sciences of the United States of America* **104**, 14676-14681

114. Cantilina, T., Sagara, Y., Inesi, G., and Jones, L. R. (1993) Comparative studies of cardiac and skeletal sarcoplasmic reticulum ATPases: effect of phospholamban antibody on enzyme activation. *J. Biol. Chem.* **268**, 17018-17025

115. Trieber, C. A., Afara, M., and Young, H. S. (2009) Effects of phospholamban transmembrane mutants on the calcium affinity, maximal activity, and cooperativity of the sarcoplasmic reticulum calcium pump. *Biochemistry* **48**, 9287-9296

116. Reddy, L., Cornea, R., Winters, D., McKenna, E., and Thomas, D. (2003) Defining the molecular components of calcium transport regulation in a reconstituted membrane system. *Biochemistry* **42**, 4585-4592

117. Ceholski, D. K., Trieber, C. A., and Young, H. S. (2012) Hydrophobic imbalance in the cytoplasmic domain of phospholamban is a determinant for lethal dilated cardiomyopathy. *The Journal of biological chemistry* **287**, 16521-16529

118. Kimura, Y., Kurzydlowski, K., Tada, M., and MacLennan, D. H. (1996) Phospholamban regulates the Ca^{2+}-ATPase through intramembrane interactions. *J. Biol. Chem.* **271**, 21726-21731

119. Toyofuku, T., Kurzydlowski, K., Tada, M., and MacLennan, D. H. (1994) Amino acids Glu2 to Ile18 in the cytoplasmic domain of phospholamban are essential for functional association with the Ca(2+)-ATPase of sarcoplasmic reticulum. *The Journal of biological chemistry* **269**, 3088-3094

120. Trieber, C. A., Douglas, J. L., Afara, M., and Young, H. S. (2005) The effects of mutation on the regulatory properties of phospholamban in co-reconstituted membranes. *Biochemistry* **44**, 3289-3297

121. Robia, S. L., Campbell, K. S., Kelly, E. M., Hou, Z., Winters, D. L., and Thomas, D. D. (2007) Forster transfer recovery reveals that phospholamban exchanges slowly from pentamers but rapidly from the SERCA regulatory complex. *Circulation research* **101**, 1123-1129

122. Cornea, R. L., Autry, J. M., Chen, Z., and Jones, L. R. (2000) Reexamination of the role of the leucine/isoleucine zipper residues of phospholamban in inhibition of the Ca2+ pump of cardiac sarcoplasmic reticulum. *The Journal of biological chemistry* **275**, 41487-41494

123. Simmerman, H. K., Kobayashi, Y. M., Autry, J. M., and Jones, L. R. (1996) A leucine zipper stabilizes the pentameric membrane domain of phospholamban and forms a coiled-coil pore structure. *The Journal of biological chemistry* **271**, 5941-5946

124. Kimura, Y., Asahi, M., Kurzydlowski, K., Tada, M., and MacLennan, D. H. (1998) Phospholamban domain Ib mutations influence functional interactions with the Ca^{2+}-ATPase isoform of cardiac sarcoplasmic reticulum. *J. Biol. Chem.* **273**, 14238-14241

125. Becucci, L., Cembran, A., Karim, C. B., Thomas, D. D., Guidelli, R., Gao, J., and Veglia, G. (2009) On the function of pentameric phospholamban: ion channel or storage form? *Biophys J* **96**, L60-62

126. Kovacs, R. J., Nelson, M. T., Simmerman, H. K., and Jones, L. R. (1988) Phospholamban forms Ca2+-selective channels in lipid bilayers. *The Journal of biological chemistry* **263**, 18364-18368

127. Stokes, D. L., Pomfret, A. J., Rice, W. J., Glaves, J. P., and Young, H. S. (2006) Interactions between Ca2+-ATPase and the pentameric form of phospholamban in two-dimensional co-crystals. *Biophys J* **90**, 4213-4223

128. Glaves, J. P., Trieber, C. A., Ceholski, D. K., Stokes, D. L., and Young, H. S. (2011) Phosphorylation and mutation of phospholamban alter physical interactions with the sarcoplasmic reticulum calcium pump. *Journal of molecular biology* **405**, 707-723

129. Chu, G., Li, L., Sato, Y., Harrer, J. M., Kadambi, V. J., Hoit, B. D., Bers, D. M., and Kranias, E. G. (1998) Pentameric assembly of phospholamban facilitates inhibition of cardiac function in vivo. *The Journal of biological chemistry* **273**, 33674-33680

130. Thomas, D., Reddy, L., Karim, C., Li, M., Cornea, R., Autry, J., Jones, L., and Stamm, J. (1998) Direct spectroscopic detection of molecular dynamics and interactions of the calcium pump and phospholamban. *Ann NY Acad Sci* **853**, 186-194

131. Chen, Z., Akin, B. L., and Jones, L. R. (2007) Mechanism of reversal of phospholamban inhibition of the cardiac Ca2+-ATPase by protein kinase A and by anti-phospholamban monoclonal antibody 2D12. *The Journal of biological chemistry* **282**, 20968-20976

132. Karim, C. B., Zhang, Z., Howard, E. C., Torgersen, K. D., and Thomas, D. D. (2006) Phosphorylation-dependent conformational switch in spin-labeled phospholamban bound to SERCA. *J Mol Biol* **358**, 1032-1040

133. Negash, S., Yao, Q., Sun, H., Li, J., Bigelow, D. J., and Squier, T. C. (2000) Phospholamban remains associated with the Ca2+- and Mg2+-dependent ATPase following phosphorylation by cAMP-dependent protein kinase. *The Biochemical journal* **351**, 195-205

134. Wegener, A. D., Simmerman, H. K., Liepnieks, J., and Jones, L. R. (1986) Proteolytic cleavage of phospholamban purified from canine cardiac sarcoplasmic reticulum vesicles. Generation of a low resolution model of phospholamban structure. *The Journal of biological chemistry* **261**, 5154-5159

135. Metcalfe, E. E., Traaseth, N. J., and Veglia, G. (2005) Serine 16 phosphorylation induces an order-to-disorder transition in monomeric phospholamban. *Biochemistry* **44**, 4386-4396

136. Traaseth, N. J., Thomas, D. D., and Veglia, G. (2006) Effects of Ser16 phosphorylation on the allosteric transitions of phospholamban/Ca(2+)-ATPase complex. *J Mol Biol* **358**, 1041-1050

137. Choma, C., Gratkowski, H., Lear, J. D., and DeGrado, W. F. (2000) Asparagine-mediated self-association of a model transmembrane helix. *Nature structural biology* **7**, 161-166

138. Zhou, F. X., Merianos, H. J., Brunger, A. T., and Engelman, D. M. (2001) Polar residues drive association of polyleucine transmembrane helices. *Proceedings of the National Academy of Sciences of the United States of America* **98**, 2250-2255

139. Afara, M. R., Trieber, C. A., Glaves, J. P., and Young, H. S. (2006) Rational design of peptide inhibitors of the sarcoplasmic reticulum calcium pump. *Biochemistry* **45**, 8617-8627

140. Afara, M. R., Trieber, C. A., Ceholski, D. K., and Young, H. S. (2008) Peptide inhibitors use two related mechanisms to alter the apparent calcium affinity of the sarcoplasmic reticulum calcium pump. *Biochemistry* **47**, 9522-9530

141. Hutter, M. C., Krebs, J., Meiler, J., Griesinger, C., Carafoli, E., and Helms, V. (2002) A structural model of the complex formed by phospholamban and the

calcium pump of sarcoplasmic reticulum obtained by molecular mechanics. *Chembiochem : a European journal of chemical biology* **3**, 1200-1208

142. James, P., Inui, M., Tada, M., Chiesi, M., and Carafoli, E. (1989) Nature and site of phospholamban regulation of the Ca2+ pump of sarcoplasmic reticulum. *Nature* **342**, 90-92

143. Chen, Z., Stokes, D. L., Rice, W. J., and Jones, L. R. (2003) Spatial and dynamic interactions between phospholamban and the canine cardiac Ca2+ pump revealed with use of heterobifunctional cross-linking agents. *The Journal of biological chemistry* **278**, 48348-48356

144. Jones, L. R., Cornea, R. L., and Chen, Z. (2002) Close proximity between residue 30 of phospholamban and cysteine 318 of the cardiac Ca2+ pump revealed by intermolecular thiol cross-linking. *The Journal of biological chemistry* **277**, 28319-28329

145. Chen, Z., Stokes, D. L., and Jones, L. R. (2005) Role of leucine 31 of phospholamban in structural and functional interactions with the Ca2+ pump of cardiac sarcoplasmic reticulum. *The Journal of biological chemistry* **280**, 10530-10539

146. Chen, Z., Akin, B., Stokes, D., and Jones, L. (2006) Cross-linking of C-terminal residues of phospholamban to the Ca^{2+} pump of cardiac sarcoplasmic reticulum to probe spatial and functional interactions within the transmembrane domain. *The Journal of biological chemistry* **281**, 14163-14172

147. Asahi, M., Kimura, Y., Kurzydlowski, K., Tada, M., and MacLennan, D. H. (1999) Transmembrane helix M6 in sarco(endo)plasmic reticulum Ca(2+)-ATPase forms a functional interaction site with phospholamban. Evidence for physical interactions at other sites. *The Journal of biological chemistry* **274**, 32855-32862

148. Catalucci, D., Latronico, M. V., Ceci, M., Rusconi, F., Young, H. S., Gallo, P., Santonastasi, M., Bellacosa, A., Brown, J. H., and Condorelli, G. (2009) Akt increases sarcoplasmic reticulum Ca2+ cycling by direct phosphorylation of phospholamban at Thr17. *The Journal of biological chemistry* **284**, 28180-28187

149. Edes, I., and Kranias, E. G. (1990) Phospholamban and troponin I are substrates for protein kinase C in vitro but not in intact beating guinea pig hearts. *Circulation research* **67**, 394-400

150. Luo, W., Chu, G., Sato, Y., Zhou, Z., Kadambi, V. J., and Kranias, E. G. (1998) Transgenic approaches to define the functional role of dual site phospholamban phosphorylation. *The Journal of biological chemistry* **273**, 4734-4739

151. Chu, G., Lester, J. W., Young, K. B., Luo, W., Zhai, J., and Kranias, E. G. (2000) A single site (Ser16) phosphorylation in phospholamban is sufficient in mediating its maximal cardiac responses to beta -agonists. *The Journal of biological chemistry* **275**, 38938-38943

152. Brittsan, A. G., Carr, A. N., Schmidt, A. G., and Kranias, E. G. (2000) Maximal inhibition of SERCA2 Ca(2+) affinity by phospholamban in transgenic hearts overexpressing a non-phosphorylatable form of phospholamban. *The Journal of biological chemistry* **275**, 12129-12135

153. Vittone, L., Mundina-Weilenmann, C., Said, M., Ferrero, P., and Mattiazzi, A. (2002) Time course and mechanisms of phosphorylation of phospholamban residues in ischemia-reperfused rat hearts. Dissociation of phospholamban phosphorylation pathways. *J Mol Cell Cardiol* **34**, 39-50

154. Mattiazzi, A., Mundina-Weilenmann, C., Guoxiang, C., Vittone, L., and Kranias, E. (2005) Role of phospholamban phosphorylation on Thr17 in cardiac physiological and pathological conditions. *Cardiovascular research* **68**, 366-375

155. Hagemann, D., and Xiao, R. P. (2002) Dual site phospholamban phosphorylation and its physiological relevance in the heart. *Trends in cardiovascular medicine* **12**, 51-56

156. Asahi, M., McKenna, E., Kurzydlowski, K., Tada, M., and MacLennan, D. H. (2000) Physical interactions between phospholamban and sarco(endo)plasmic reticulum Ca2+-ATPases are dissociated by elevated Ca2+, but not by phospholamban phosphorylation, vanadate, or thapsigargin, and are enhanced by ATP. *The Journal of biological chemistry* **275**, 15034-15038

157. Karim, C. B., Kirby, T. L., Zhang, Z., Nesmelov, Y., and Thomas, D. D. (2004) Phospholamban structural dynamics in lipid bilayers probed by a spin label rigidly coupled to the peptide backbone. *Proceedings of the National Academy of Sciences of the United States of America* **101**, 14437-14442

158. Morgan, J. P. (1991) Abnormal intracellular modulation of calcium as a major cause of cardiac contractile dysfunction. *The New England journal of medicine* **325**, 625-632

159. Beuckelmann, D. J., Nabauer, M., and Erdmann, E. (1992) Intracellular calcium handling in isolated ventricular myocytes from patients with terminal heart failure. *Circulation* **85**, 1046-1055

160. Hasenfuss, G., Mulieri, L. A., Leavitt, B. J., Allen, P. D., Haeberle, J. R., and Alpert, N. R. (1992) Alteration of contractile function and excitation-contraction coupling in dilated cardiomyopathy. *Circulation research* **70**, 1225-1232

161. Meyer, M., Schillinger, W., Pieske, B., Holubarsch, C., Heilmann, C., Posival, H., Kuwajima, G., Mikoshiba, K., Just, H., Hasenfuss, G., and et al. (1995) Alterations of sarcoplasmic reticulum proteins in failing human dilated cardiomyopathy. *Circulation* **92**, 778-784

162. Mercadier, J. J., Lompre, A. M., Duc, P., Boheler, K. R., Fraysse, J. B., Wisnewsky, C., Allen, P. D., Komajda, M., and Schwartz, K. (1990) Altered sarcoplasmic reticulum Ca2(+)-ATPase gene expression in the human ventricle during end-stage heart failure. *The Journal of clinical investigation* **85**, 305-309

163. Movsesian, M. A., Karimi, M., Green, K., and Jones, L. R. (1994) Ca(2+)-transporting ATPase, phospholamban, and calsequestrin levels in nonfailing and failing human myocardium. *Circulation* **90**, 653-657

164. Feldman, A. M., Ray, P. E., Silan, C. M., Mercer, J. A., Minobe, W., and Bristow, M. R. (1991) Selective gene expression in failing human heart. Quantification of steady-state levels of messenger RNA in endomyocardial biopsies using the polymerase chain reaction. *Circulation* **83**, 1866-1872

165. Hasenfuss, G., Reinecke, H., Studer, R., Meyer, M., Pieske, B., Holtz, J., Holubarsch, C., Posival, H., Just, H., and Drexler, H. (1994) Relation between myocardial function and expression of sarcoplasmic reticulum Ca(2+)-ATPase in failing and nonfailing human myocardium. *Circulation research* **75**, 434-442

166. Dash, R., Frank, K. F., Carr, A. N., Moravec, C. S., and Kranias, E. G. (2001) Gender influences on sarcoplasmic reticulum Ca2+-handling in failing human myocardium. *J Mol Cell Cardiol* **33**, 1345-1353

167. Barki-Harrington, L., Perrino, C., and Rockman, H. A. (2004) Network integration of the adrenergic system in cardiac hypertrophy. *Cardiovascular research* **63**, 391-402

168. Ferguson, S. S. (2001) Evolving concepts in G protein-coupled receptor endocytosis: the role in receptor desensitization and signaling. *Pharmacological reviews* **53**, 1-24

169. Park, I. K., and DePaoli-Roach, A. A. (1994) Domains of phosphatase inhibitor-2 involved in the control of the ATP-Mg-dependent protein phosphatase. *The Journal of biological chemistry* **269**, 28919-28928

170. Bibb, J. A., Nishi, A., O'Callaghan, J. P., Ule, J., Lan, M., Snyder, G. L., Horiuchi, A., Saito, T., Hisanaga, S., Czernik, A. J., Nairn, A. C., and Greengard, P. (2001) Phosphorylation of protein phosphatase inhibitor-1 by Cdk5. *The Journal of biological chemistry* **276**, 14490-14497

171. del Monte, F., Harding, S. E., Schmidt, U., Matsui, T., Kang, Z. B., Dec, G. W., Gwathmey, J. K., Rosenzweig, A., and Hajjar, R. J. (1999) Restoration of contractile function in isolated cardiomyocytes from failing human hearts by gene transfer of SERCA2a. *Circulation* **100**, 2308-2311

172. Giordano, F. J., He, H., McDonough, P., Meyer, M., Sayen, M. R., and Dillmann, W. H. (1997) Adenovirus-mediated gene transfer reconstitutes depressed sarcoplasmic reticulum Ca2+-ATPase levels and shortens prolonged cardiac myocyte Ca2+ transients. *Circulation* **96**, 400-403

173. Miyamoto, M. I., del Monte, F., Schmidt, U., DiSalvo, T. S., Kang, Z. B., Matsui, T., Guerrero, J. L., Gwathmey, J. K., Rosenzweig, A., and Hajjar, R. J. (2000) Adenoviral gene transfer of SERCA2a improves left-ventricular function in aortic-banded rats in transition to heart failure. *Proceedings of the National Academy of Sciences of the United States of America* **97**, 793-798

174. del Monte, F., Williams, E., Lebeche, D., Schmidt, U., Rosenzweig, A., Gwathmey, J. K., Lewandowski, E. D., and Hajjar, R. J. (2001) Improvement in survival and cardiac metabolism after gene transfer of sarcoplasmic reticulum Ca(2+)-ATPase in a rat model of heart failure. *Circulation* **104**, 1424-1429

175. Jessup, M., Greenberg, B., Mancini, D., Cappola, T., Pauly, D. F., Jaski, B., Yaroshinsky, A., Zsebo, K. M., Dittrich, H., Hajjar, R. J., and Calcium Upregulation by Percutaneous Administration of Gene Therapy in Cardiac Disease, I. (2011) Calcium Upregulation by Percutaneous Administration of Gene Therapy in Cardiac Disease (CUPID): a phase 2 trial of intracoronary gene therapy of sarcoplasmic reticulum Ca2+-ATPase in patients with advanced heart failure. *Circulation* **124**, 304-313

176. Kairouz, V., Lipskaia, L., Hajjar, R. J., and Chemaly, E. R. (2012) Molecular targets in heart failure gene therapy: current controversies and translational perspectives. *Annals of the New York Academy of Sciences* **1254**, 42-50

177. Pattison, J. S., Waggoner, J. R., James, J., Martin, L., Gulick, J., Osinska, H., Klevitsky, R., Kranias, E. G., and Robbins, J. (2008) Phospholamban overexpression in transgenic rabbits. *Transgenic research* **17**, 157-170

178. Haghighi, K., Kolokathis, F., Pater, L., Lynch, R. A., Asahi, M., Gramolini, A. O., Fan, G. C., Tsiapras, D., Hahn, H. S., Adamopoulos, S., Liggett, S. B., Dorn, G. W., 2nd, MacLennan, D. H., Kremastinos, D. T., and Kranias, E. G. (2003) Human phospholamban null results in lethal dilated cardiomyopathy revealing a critical difference between mouse and human. *The Journal of clinical investigation* **111**, 869-876

179. El-Armouche, A., Wittkopper, K., Degenhardt, F., Weinberger, F., Didie, M., Melnychenko, I., Grimm, M., Peeck, M., Zimmermann, W. H., Unsold, B., Hasenfuss, G., Dobrev, D., and Eschenhagen, T. (2008) Phosphatase inhibitor-1-deficient mice are protected from catecholamine-induced arrhythmias and myocardial hypertrophy. *Cardiovascular research* **80**, 396-406

180. Kawashima, H., Satoh, H., Saotome, M., Urushida, T., Katoh, H., and Hayashi, H. (2009) Protein phosphatase inhibitor-1 augments a protein kinase A-dependent increase in the Ca2+ loading of the sarcoplasmic reticulum without changing its Ca2+ release. *Circulation journal : official journal of the Japanese Circulation Society* **73**, 1133-1140

181. Yamada, M., Ikeda, Y., Yano, M., Yoshimura, K., Nishino, S., Aoyama, H., Wang, L., Aoki, H., and Matsuzaki, M. (2006) Inhibition of protein phosphatase 1 by inhibitor-2 gene delivery ameliorates heart failure progression in genetic cardiomyopathy. *FASEB journal : official publication of the Federation of American Societies for Experimental Biology* **20**, 1197-1199

182. Schmitt, J. P., Kamisago, M., Asahi, M., Li, G. H., Ahmad, F., Mende, U., Kranias, E. G., MacLennan, D. H., Seidman, J. G., and Seidman, C. E. (2003) Dilated cardiomyopathy and heart failure caused by a mutation in phospholamban. *Science* **299**, 1410-1413

183. Haghighi, K., Kolokathis, F., Gramolini, A. O., Waggoner, J. R., Pater, L., Lynch, R. A., Fan, G. C., Tsiapras, D., Parekh, R. R., Dorn, G. W., 2nd, MacLennan, D. H., Kremastinos, D. T., and Kranias, E. G. (2006) A mutation in the human phospholamban gene, deleting arginine 14, results in lethal, hereditary cardiomyopathy. *Proceedings of the National Academy of Sciences of the United States of America* **103**, 1388-1393

184. Medeiros, A., Biagi, D. G., Sobreira, T. J., de Oliveira, P. S., Negrao, C. E., Mansur, A. J., Krieger, J. E., Brum, P. C., and Pereira, A. C. (2011) Mutations in the human phospholamban gene in patients with heart failure. *American heart journal* **162**, 1088-1095 e1081

185. Schmitt, J. P., Ahmad, F., Lorenz, K., Hein, L., Schulz, S., Asahi, M., Maclennan, D. H., Seidman, C. E., Seidman, J. G., and Lohse, M. J. (2009) Alterations of phospholamban function can exhibit cardiotoxic effects independent of excessive sarcoplasmic reticulum Ca2+-ATPase inhibition. *Circulation* **119**, 436-444

186. Ha, K. N., Masterson, L. R., Hou, Z., Verardi, R., Walsh, N., Veglia, G., and Robia, S. L. (2011) Lethal Arg9Cys phospholamban mutation hinders Ca2+-ATPase regulation and phosphorylation by protein kinase A. *Proceedings of the National Academy of Sciences of the United States of America* **108**, 2735-2740

187. Ceholski, D. K., Trieber, C. A., Holmes, C. F., and Young, H. S. (2012) Lethal, hereditary mutants of phospholamban elude phosphorylation by protein kinase A. *The Journal of biological chemistry* **287**, 26596-26605

188. DeWitt, M. M., MacLeod, H. M., Soliven, B., and McNally, E. M. (2006) Phospholamban R14 deletion results in late-onset, mild, hereditary dilated cardiomyopathy. *Journal of the American College of Cardiology* **48**, 1396-1398

189. Posch, M. G., Perrot, A., Geier, C., Boldt, L. H., Schmidt, G., Lehmkuhl, H. B., Hetzer, R., Dietz, R., Gutberlet, M., Haverkamp, W., and Ozcelik, C. (2009) Genetic deletion of arginine 14 in phospholamban causes dilated cardiomyopathy with attenuated electrocardiographic R amplitudes. *Heart rhythm : the official journal of the Heart Rhythm Society* **6**, 480-486

190. Haghighi, K., Pritchard, T., Bossuyt, J., Waggoner, J. R., Yuan, Q., Fan, G. C., Osinska, H., Anjak, A., Rubinstein, J., Robbins, J., Bers, D. M., and Kranias, E. G. (2012) The human phospholamban Arg14-deletion mutant localizes to plasma membrane and interacts with the Na/K-ATPase. *J Mol Cell Cardiol* **52**, 773-782

191. Landstrom, A. P., Adekola, B. A., Bos, J. M., Ommen, S. R., and Ackerman, M. J. (2011) PLN-encoded phospholamban mutation in a large cohort of hypertrophic cardiomyopathy cases: summary of the literature and implications for genetic testing. *American heart journal* **161**, 165-171

192. Minamisawa, S., Sato, Y., Tatsuguchi, Y., Fujino, T., Imamura, S., Uetsuka, Y., Nakazawa, M., and Matsuoka, R. (2003) Mutation of the phospholamban promoter associated with hypertrophic cardiomyopathy. *Biochem Biophys Res Commun* **304**, 1-4

193. Medin, M., Hermida-Prieto, M., Monserrat, L., Laredo, R., Rodriguez-Rey, J. C., Fernandez, X., and Castro-Beiras, A. (2007) Mutational screening of phospholamban gene in hypertrophic and idiopathic dilated cardiomyopathy and functional study of the PLN -42 C>G mutation. *European journal of heart failure* **9**, 37-43

194. Haghighi, K., Chen, G., Sato, Y., Fan, G. C., He, S., Kolokathis, F., Pater, L., Paraskevaidis, I., Jones, W. K., Dorn, G. W., 2nd, Kremastinos, D. T., and Kranias, E. G. (2008) A human phospholamban promoter polymorphism in dilated cardiomyopathy alters transcriptional regulation by glucocorticoids. *Human mutation* **29**, 640-647

195. Wawrzynow, A., Theibert, J. L., Murphy, C., Jona, I., Martonosi, A., and Collins, J. H. (1992) Sarcolipin, the "proteolipid" of skeletal muscle sarcoplasmic reticulum, is a unique, amphipathic, 31-residue peptide. *Archives of biochemistry and biophysics* **298**, 620-623

196. Odermatt, A., Taschner, P. E., Scherer, S. W., Beatty, B., Khanna, V. K., Cornblath, D. R., Chaudhry, V., Yee, W. C., Schrank, B., Karpati, G., Breuning, M. H., Knoers, N., and MacLennan, D. H. (1997) Characterization of the gene encoding human sarcolipin (SLN), a proteolipid associated with SERCA1: absence of structural mutations in five patients with Brody disease. *Genomics* **45**, 541-553

197. Odermatt, A., Becker, S., Khanna, V. K., Kurzydlowski, K., Leisner, E., Pette, D., and MacLennan, D. H. (1998) Sarcolipin regulates the activity of SERCA1, the fast-twitch skeletal muscle sarcoplasmic reticulum Ca2+-ATPase. *The Journal of biological chemistry* **273**, 12360-12369

198. Minamisawa, S., Wang, Y., Chen, J., Ishikawa, Y., Chien, K. R., and Matsuoka, R. (2003) Atrial chamber-specific expression of sarcolipin is regulated during development and hypertrophic remodeling. *The Journal of biological chemistry* **278**, 9570-9575

199. Vangheluwe, P., Schuermans, M., Zador, E., Waelkens, E., Raeymaekers, L., and Wuytack, F. (2005) Sarcolipin and phospholamban mRNA and protein expression in cardiac and skeletal muscle of different species. *The Biochemical journal* **389**, 151-159

200. Babu, G. J., Bhupathy, P., Carnes, C. A., Billman, G. E., and Periasamy, M. (2007) Differential expression of sarcolipin protein during muscle development and cardiac pathophysiology. *J Mol Cell Cardiol* **43**, 215-222

201. Asahi, M., Sugita, Y., Kurzydlowski, K., De Leon, S., Tada, M., Toyoshima, C., and MacLennan, D. H. (2003) Sarcolipin regulates sarco(endo)plasmic reticulum Ca2+-ATPase (SERCA) by binding to transmembrane helices alone or in association with phospholamban. *Proceedings of the National Academy of Sciences of the United States of America* **100**, 5040-5045

202. Morita, T., Hussain, D., Asahi, M., Tsuda, T., Kurzydlowski, K., Toyoshima, C., and Maclennan, D. H. (2008) Interaction sites among phospholamban, sarcolipin,

and the sarco(endo)plasmic reticulum Ca(2+)-ATPase. *Biochem Biophys Res Commun* **369**, 188-194

203. Asahi, M., Kurzydlowski, K., Tada, M., and MacLennan, D. H. (2002) Sarcolipin inhibits polymerization of phospholamban to induce superinhibition of sarco(endo)plasmic reticulum Ca2+-ATPases (SERCAs). *The Journal of biological chemistry* **277**, 26725-26728

204. Hughes, E., Clayton, J. C., Kitmitto, A., Esmann, M., and Middleton, D. A. (2007) Solid-state NMR and functional measurements indicate that the conserved tyrosine residues of sarcolipin are involved directly in the inhibition of SERCA1. *The Journal of biological chemistry* **282**, 26603-26613

205. Tupling, A. R., Asahi, M., and MacLennan, D. H. (2002) Sarcolipin overexpression in rat slow twitch muscle inhibits sarcoplasmic reticulum Ca2+ uptake and impairs contractile function. *The Journal of biological chemistry* **277**, 44740-44746

206. Babu, G. J., Bhupathy, P., Petrashevskaya, N. N., Wang, H., Raman, S., Wheeler, D., Jagatheesan, G., Wieczorek, D., Schwartz, A., Janssen, P. M., Ziolo, M. T., and Periasamy, M. (2006) Targeted overexpression of sarcolipin in the mouse heart decreases sarcoplasmic reticulum calcium transport and cardiac contractility. *The Journal of biological chemistry* **281**, 3972-3979

207. Bhupathy, P., Babu, G. J., Ito, M., and Periasamy, M. (2009) Threonine-5 at the N-terminus can modulate sarcolipin function in cardiac myocytes. *J Mol Cell Cardiol* **47**, 723-729

208. Gramolini, A. O., Trivieri, M. G., Oudit, G. Y., Kislinger, T., Li, W., Patel, M. M., Emili, A., Kranias, E. G., Backx, P. H., and Maclennan, D. H. (2006) Cardiac-specific overexpression of sarcolipin in phospholamban null mice impairs myocyte function that is restored by phosphorylation. *Proceedings of the National Academy of Sciences of the United States of America* **103**, 2446-2451

209. Hellstern, S., Pegoraro, S., Karim, C. B., Lustig, A., Thomas, D. D., Moroder, L., and Engel, J. (2001) Sarcolipin, the shorter homologue of phospholamban, forms oligomeric structures in detergent micelles and in liposomes. *The Journal of biological chemistry* **276**, 30845-30852

210. Autry, J. M., Rubin, J. E., Pietrini, S. D., Winters, D. L., Robia, S. L., and Thomas, D. D. (2011) Oligomeric Interactions of Sarcolipin and the Ca-ATPase. *The Journal of biological chemistry* **286**, 31697-31706

211. Gramolini, A. O., Kislinger, T., Asahi, M., Li, W., Emili, A., and MacLennan, D. H. (2004) Sarcolipin retention in the endoplasmic reticulum depends on its C-terminal RSYQY sequence and its interaction with sarco(endo)plasmic Ca(2+)-ATPases. *Proceedings of the National Academy of Sciences of the United States of America* **101**, 16807-16812

212. Buffy, J. J., Traaseth, N. J., Mascioni, A., Gor'kov, P. L., Chekmenev, E. Y., Brey, W. W., and Veglia, G. (2006) Two-dimensional solid-state NMR reveals

two topologies of sarcolipin in oriented lipid bilayers. *Biochemistry* **45**, 10939-10946

213. Becucci, L., Guidelli, R., Karim, C. B., Thomas, D. D., and Veglia, G. (2007) An electrochemical investigation of sarcolipin reconstituted into a mercury-supported lipid bilayer. *Biophys J* **93**, 2678-2687

214. Becucci, L., Guidelli, R., Karim, C. B., Thomas, D. D., and Veglia, G. (2009) The role of sarcolipin and ATP in the transport of phosphate ion into the sarcoplasmic reticulum. *Biophys J* **97**, 2693-2699

215. Stefanova, H. I., East, J. M., and Lee, A. G. (1991) Covalent and non-covalent inhibitors of the phosphate transporter of sarcoplasmic reticulum. *Biochimica et biophysica acta* **1064**, 321-328

216. Stefanova, H. I., Jane, S. D., East, J. M., and Lee, A. G. (1991) Effects of Mg2+ and ATP on the phosphate transporter of sarcoplasmic reticulum. *Biochimica et biophysica acta* **1064**, 329-334

217. Winther, A. M., Bublitz, M., Karlsen, J. L., Moller, J. V., Hansen, J. B., Nissen, P., and Buch-Pedersen, M. J. (2013) The sarcolipin-bound calcium pump stabilizes calcium sites exposed to the cytoplasm. *Nature* **495**, 265-269

218. Toyoshima, C., Iwasawa, S., Ogawa, H., Hirata, A., Tsueda, J., and Inesi, G. (2013) Crystal structures of the calcium pump and sarcolipin in the Mg2+-bound E1 state. *Nature* **495**, 260-264

219. Henderson, I. M., Starling, A. P., Wictome, M., East, J. M., and Lee, A. G. (1994) Binding of Ca2+ to the (Ca(2+)-Mg2+)-ATPase of sarcoplasmic reticulum: kinetic studies. *The Biochemical journal* **297 (Pt 3)**, 625-636

220. Shanmugam, M., Molina, C. E., Gao, S., Severac-Bastide, R., Fischmeister, R., and Babu, G. J. (2011) Decreased sarcolipin protein expression and enhanced sarco(endo)plasmic reticulum Ca2+ uptake in human atrial fibrillation. *Biochem Biophys Res Commun* **410**, 97-101

221. Uemura, N., Ohkusa, T., Hamano, K., Nakagome, M., Hori, H., Shimizu, M., Matsuzaki, M., Mochizuki, S., Minamisawa, S., and Ishikawa, Y. (2004) Down-regulation of sarcolipin mRNA expression in chronic atrial fibrillation. *European journal of clinical investigation* **34**, 723-730

222. Xie, L. H., Shanmugam, M., Park, J. Y., Zhao, Z., Wen, H., Tian, B., Periasamy, M., and Babu, G. J. (2012) Ablation of sarcolipin results in atrial remodeling. *American journal of physiology. Cell physiology* **302**, C1762-1771

223. Pashmforoush, M., Lu, J. T., Chen, H., Amand, T. S., Kondo, R., Pradervand, S., Evans, S. M., Clark, B., Feramisco, J. R., Giles, W., Ho, S. Y., Benson, D. W., Silberbach, M., Shou, W., and Chien, K. R. (2004) Nkx2-5 pathways and congenital heart disease; loss of ventricular myocyte lineage specification leads to progressive cardiomyopathy and complete heart block. *Cell* **117**, 373-386

224. Asahi, M., Otsu, K., Nakayama, H., Hikoso, S., Takeda, T., Gramolini, A. O., Trivieri, M. G., Oudit, G. Y., Morita, T., Kusakari, Y., Hirano, S., Hongo, K., Hirotani, S., Yamaguchi, O., Peterson, A., Backx, P. H., Kurihara, S., Hori, M., and MacLennan, D. H. (2004) Cardiac-specific overexpression of sarcolipin inhibits sarco(endo)plasmic reticulum Ca2+ ATPase (SERCA2a) activity and impairs cardiac function in mice. *Proceedings of the National Academy of Sciences of the United States of America* **101**, 9199-9204

225. Babu, G. J., Bhupathy, P., Timofeyev, V., Petrashevskaya, N. N., Reiser, P. J., Chiamvimonvat, N., and Periasamy, M. (2007) Ablation of sarcolipin enhances sarcoplasmic reticulum calcium transport and atrial contractility. *Proceedings of the National Academy of Sciences of the United States of America* **104**, 17867-17872

Chapter 2

Sarco(endo)plasmic reticulum calcium ATPase (SERCA) inhibition by sarcolipin is encoded in its luminal tail

This research was originally published in The Journal of Biological Chemistry.

Gorski PA, Glaves JP, Vangheluwe P, and Young HS.

Sarco(endo)plasmic reticulum calcium ATPase (SERCA) inhibition by sarcolipin is encoded in its luminal tail

JBC. 2013; 287: 19876-19885.

Acknowledgements: Dr. C. Trieber purified SERCA for functional analysis. Dr. JP Glaves helped with cloning and purification of sarcolipin alanine mutants. Dr. P. Vangheluwe helped in designing and cloning of the PLN-SLN chimeras.

2-1. Introduction

Sarcolipin (SLN) was first described as a low molecular-weight protein that co-purified with preparations of SERCA and it was later named to reflect its origin as a proteolipid of the sarcoplasmic reticulum (SR) (1). SLN is the predominant regulator of SERCA and calcium homeostasis in fast-twitch skeletal muscle, where it may play an additional role in thermogenesis (2). However, SLN is also expressed with phospholamban (PLN) in the atria of the heart (3-6), which raises the possibility of an atrial-specific ternary complex that could lead to super-inhibition of SERCA (7). SLN is a 31 residue type I integral membrane protein with a transmembrane domain and short cytoplasmic and luminal domains (1). PLN is a 52 residue type I integral membrane protein with a transmembrane domain, a longer cytoplasmic domain and no luminal domain (8). Given the homology between the transmembrane domains of these proteins, it was hypothesized that SLN binds to SERCA and alters the apparent calcium affinity of the enzyme in a manner similar to PLN (9). Inhibition would result from SLN and/or PLN binding to SERCA and stabilizing an E2 calcium-free state (10). Mixed evidence exists on whether these regulatory subunits dissociate (11) or remain bound to SERCA (12-14) during calcium transport.

Historically, SLN inhibition of SERCA has been less well-characterized than PLN, owing in part to the assumption that SLN uses the same mechanism as PLN to inhibit SERCA. For PLN, SERCA inhibition is encoded by the transmembrane domain (15,16), while reversal of inhibition via phosphorylation is enabled by the cytoplasmic domain (8). For SLN, the transmembrane domain contains residues involved in inhibitory function (9), the cytoplasmic domain contains a phosphorylation site (17), and the luminal domain is important for SR retention (18) and SERCA inhibition (19). However, there are important differences in the way that SLN inhibits SERCA. For example, some

studies have found that SLN decreases the maximal activity (V_{max}) of SERCA at saturating calcium concentrations, indicating that SLN inhibition is not reversed by calcium (19-21). In addition, two kinases have been reported to target SLN (17,22), though it is not firmly established if phosphorylation of SLN is an important physiological mechanism. Finally, it is well documented that the inhibitory PLN monomer can self-associate to form pentamers. In contrast, SLN is thought to exist primarily as a monomer, though evidence suggests that SLN can also oligomerize in detergent and membrane environments (23,24).

The modeled site of interaction between SLN and the calcium-free state of SERCA was the same binding groove identified for PLN (TM2, TM4, TM6 and TM9). This was based on mutagenesis of both SERCA and SLN combined with functional measurements (9) and co-immunoprecipitation studies (7). Alanine-scanning mutagenesis of SLN revealed similarities and differences when compared to PLN. In general, mutagenesis of SLN had lesser effects on function and did not recapitulate the gain of function behavior associated with residues that destabilize the PLN pentamer. Nonetheless, key residues in both proteins were found to be important for physical association and function. Notably, mutation of Leu^{8} and Asn^{11} in SLN resulted in the expected loss of function seen for the comparable Leu^{31} and Asn^{34} of PLN, and mutation of the predicted phosphorylation site to glutamate (Thr^{5}-to-Glu) appeared to mimic phosphorylation and result in loss of function (17). While the remaining sampled residues were neutral or loss-of-function, there are mixed observations on the functional importance of SLN's unique luminal tail (Fig. 2-1) (9,18,19). The C-terminal sequences of PLN and SLN represent a marked difference between these two proteins, where the hydrophobic Met^{50}-Leu-Leu^{52} in PLN is replaced by the more polar Arg^{27}-Ser-Tyr-Gln-

Figure 2-1. Amino acid sequence alignments for primary structures of SLN and PLN from representative species. The cytoplasmic, transmembrane and luminal domains are indicated. Consensus sequences for SLN and PLN were generated based on all known sequences (ClustalW). Sequence variations in the luminal domains, as compared to human sequences, are indicated in bold.

Tyr^{31} in SLN. Importantly, this latter sequence is perfectly conserved among mammals (18).

Given the highly conserved nature of the SLN luminal tail and our incomplete understanding of its role in SERCA inhibition, we chose to investigate this domain by the co-reconstitution of SLN mutants with SERCA into proteoliposomes. Another motivating factor for this study was the observation that PLN and SLN can simultaneously bind to and regulate SERCA (7). While super-inhibition is thought to result from the tight fit of both PLN and SLN in the SERCA binding groove (TM2, TM4, TM6 & TM9), we hypothesized that the luminal domain of SLN may contribute to the strong inhibitory properties of the ternary complex. This prompted us to investigate chimeric PLN-SLN constructs. Herein, we provide new insights into the regulation of SERCA by the C-terminal domain of SLN. Alanine-scanning mutagenesis of this domain revealed at least partial loss of function associated with all residues (Arg^{27}-Ser-Tyr-Gln-Tyr^{31}), and the removal of the luminal tail in an Arg^{27}-stop construct also resulted in loss of function. Chimeric PLN variants possessing the luminal tail of SLN caused super-inhibition of SERCA reminiscent of studies of the PLN-SLN-SERCA ternary complex (7). Finally, transferring the SLN luminal tail onto a generic transmembrane helix resulted in a chimera that completely mimicked SERCA inhibition by wild-type SLN. We conclude that the highly conserved C-terminal tail of SLN is a primary determinant for SERCA inhibition, and that it is a distinct and transferrable functional domain.

2-2. Results

2-2.1. Wild-type PLN versus wild-type SLN. We first compared the reconstitution of SERCA in the absence and presence of recombinant human SLN (Fig. 2-2). The co-reconstitution method has been used extensively to study the functional regulation of

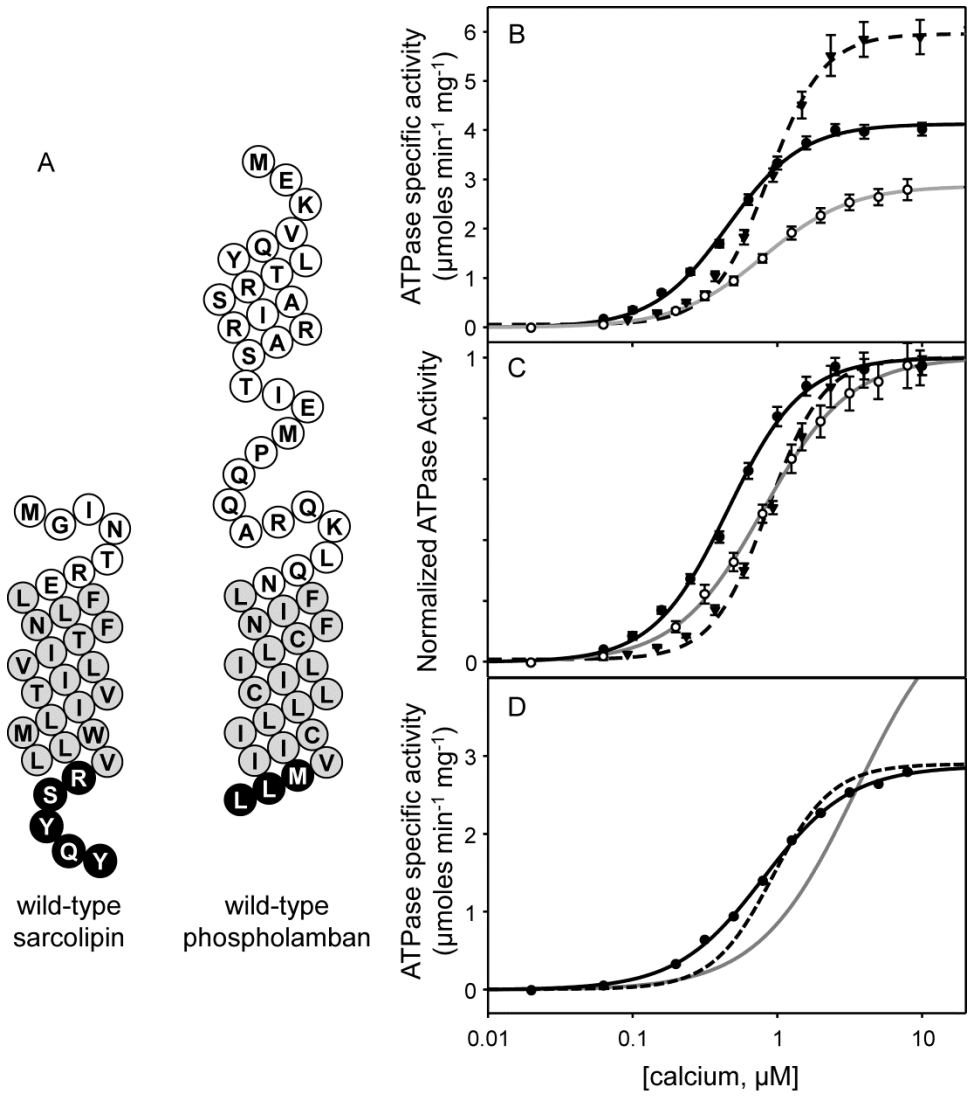

Figure 2-2. Functional data for wild-type SLN. (**A**) Topology models for wild-type SLN and wild-type PLN (white: cytosolic residues, grey: transmembrane residues, black: luminal residues). ATPase activity (**B**) and normalized ATPase activity (**C**) as a function of calcium concentration for SERCA alone (*solid black line*), SERCA in the presence of wild-type SLN (*solid grey line*) and SERCA in the presence of wild-type PLN (*dashed line*). The curves fitted to the experimental data are from a global nonlinear regression fit of SERCA reaction rate constants (25) to each plot of ATPase activity versus calcium concentration. The V_{max}, K_{Ca}, and Hill coefficients (n_H) are given in Table 2-1. Each data point is the mean ± SEM ($n \geq 4$). (**D**) Kinetic simulations highlighting the differences between PLN and SLN. Starting from values determined for wild-type PLN (Table 2-2 and (26)), simulations were performed allowing all reaction rate constants to vary (*solid black line*), allowing only B_{rev} to vary (Fit 1; *solid grey line*), or allowing only B_{for} and B_{rev} to vary (Fit 2; *dashed line*). The reaction rate constants are given in Table 2-2.

SERCA by PLN (26-32) and the same approach was used herein for detailed characterization of SLN. The reconstituted proteoliposomes contain low lipid to protein ratios that mimic the native SR membranes, which allows the direct correlation of functional data (26,28,30,31) with structural observations (33-35). As before, the proteoliposomes contained a lipid to protein molar ratio of approximately 120:1 and a SERCA to SLN molar ratio of ~4.5:1. For co-reconstitution of PLN, this molar ratio is similar to that found in cardiac SR (31,36,37); however, the SLN molar ratio used is higher than that found in skeletal SR (9). While there is growing evidence that SLN can form higher order oligomers (23,24,38), the primary reason for using a higher ratio of SLN was to facilitate comparison with PLN variants studied previously (26,28,31) and herein. We measured the calcium-dependent ATPase activity of SERCA in the absence and presence of SLN. Proteoliposomes containing SERCA alone yielded a K_{Ca} of 0.46 μM and a V_{max} of 4.1 μmol mg^{-1} min^{-1}. Incorporation of wild-type SLN into proteoliposomes with SERCA resulted in a K_{Ca} of 0.80 μM calcium and a V_{max} of 2.9 μmol mg^{-1} min^{-1} (Fig. 2-2 and Table 2-1). Thus, in the presence of SLN, SERCA had a lower apparent affinity for calcium (ΔK_{Ca} of 0.34) and a lower turnover rate (ΔV_{max} of -1.2). Comparative data for PLN indicated that it lowers the apparent calcium affinity of SERCA to a similar degree as SLN and it has the opposite effect on V_{max}. Nonetheless, the observed inhibitory activity of wild-type SLN in our system was consistent with previous observations (24,27,39) and served as a positive control for further studies.

2-2.2. Kinetic Simulations. In our previous studies, we have used kinetic reaction rate simulations to describe calcium transport by SERCA in the absence and presence of PLN (26,31). The reaction scheme assumes that the binding of calcium to SERCA occurs as two steps linked by a slow structural transition that establishes cooperativity (E + Ca ↔ ECa ↔ E'Ca + Ca ↔ E'2Ca) (25,40). The conformational change, represented by

Table 2-1. Kinetic parameters for SERCA in the absence and presence of various sarcolipin mutants, chimeras and peptides. The K_{Ca} (calcium concentration at half-maximal activity), the V_{max} (maximal activity), the n_H (Hill coefficient) and n (number of independent reconstitutions) are reported.

	V_{max} (μmoles mg^{-1} min^{-1})	K_{Ca} (μM)	n_H	n
SERCA	4.1 ± 0.1	0.46 ± 0.02	1.7 ± 0.1	32
wtSLN	2.9 ± 0.1*	0.80 ± 0.02*	1.4 ± 0.1	10
V26A	2.9 ± 0.1*	0.69 ± 0.03*	1.4 ± 0.1	7
R27A	3.4 ± 0.1*#	0.51 ± 0.01#	1.4 ± 0.1	6
S28A	3.5 ± 0.1*#	0.59 ± 0.03*#	1.5 ± 0.1	6
Y29A	3.2 ± 0.1*	0.63 ± 0.03*#	1.3 ± 0.1	13
Q30A	2.6 ± 0.1*	0.60 ± 0.04*#	1.4 ± 0.1	4
Y31A	4.6 ± 0.1*#	0.52 ± 0.02#	1.3 ± 0.1	5
Arg^{27}stop	3.4 ± 0.1*#	0.55 ± 0.02*#	1.6 ± 0.1	9
wtPLN	6.1 ± 0.1*#	0.88 ± 0.03*	2.0 ± 0.1	9
wtPLN + wtSLN	3.4 ± 0.1*#	1.36 ± 0.07*#	1.7 ± 0.1	3
$cPLN_{long}$	2.9 ± 0.1*	2.3 ± 0.09*#	1.6 ± 0.1	6
$cPLN_{short}$	2.2 ± 0.1*#	3.4 ± 0.20*#	1.9 ± 0.1	4
^{27}RSYQY	4.2 ± 0.1#	0.41 ± 0.02#	1.5 ± 0.1	5
Leu_9	4.4 ± 0.1#	0.61 ± 0.05*#	1.6 ± 0.1	5
Leu_9tail	3.0 ± 0.1*	0.81 ± 0.05*	1.5 ± 0.1	6

ANOVA (between-subjects, one-way analysis of variance) followed by the Holm-Sidak test for pairwise comparisons against SERCA in the absence (*) and presence (#) of wild-type SLN are indicated ($p < 0.05$). Note that the K_{Ca} value for SERCA in the presence of R^{27}stop was not significantly different from the values determined for R27A, S28A, Y29A, Q30A, and Y31A.

reaction rate constants B_{for} and B_{rev}, is the primary step affected by PLN, which manifests as a decrease in the apparent calcium affinity of SERCA and increased cooperativity for calcium binding. To provide a mechanistic framework for the function of SLN, we used the same approach to gain further insight into the subtle differences between SLN and PLN regulation of SERCA (Fig. 2-2 and Table 2-2). Our kinetic analyses revealed that wild-type SLN targets the first two reaction steps – binding of the first calcium ion (A_{for} and A_{rev}) and the subsequent conformational transition (B_{for} and B_{rev}).

$$E + Ca \underset{A_{rev}}{\overset{A_{for}}{\rightleftharpoons}} ECa \underset{B_{rev}}{\overset{B_{for}}{\rightleftharpoons}} E'Ca + Ca \underset{C_{rev}}{\overset{C_{for}}{\rightleftharpoons}} E'CaCa$$

A dramatic increase in A_{rev} was observed, indicating that SLN decreases the apparent calcium affinity of SERCA by driving the enzyme toward a calcium-free conformation. SLN also decreased the forward rate constant for the SERCA conformational change (B_{for}), indicating that SLN lowers the maximal activity of SERCA by making this reaction step less favorable. To test that our kinetic simulations for wild-type SLN were reliable, we ran additional simulations starting from the reaction rate constants determined for SERCA in the presence of wild-type PLN (25,26). Holding all reaction rates constant and allowing only B_{for} and B_{rev} to vary, we attempted to force the simulation to fit the wild-type SLN experimental data with reaction rate constants that were similar to those found for wild-type PLN. These simulations resulted in poor fits to the experimental data (Fig. 2-2D).

It is interesting to compare the kinetic simulations for SLN and PLN. The primary effect of SLN is to make binding of the first calcium ion less favorable, thereby stabilizing a calcium free conformation of SERCA. In contrast, the primary effect of PLN is to displace the SERCA ECa-E'Ca conformational equilibrium toward ECa, which has

Table 2-2. Rate Constants from Kinetic Simulations (s^{-1}).

	A_{for}	A_{rev}	B_{for}	B_{rev}	C_{for}	C_{rev}	Sum of squares
SERCA	190000	400	30	40	1810000	16	0.002
wtPLN	190000	400	45	25500	250000	16	0.004
wtSLN	156530	64736	22	135140	1810000	16	0.001
Alternate fits in Figure 2D[a]							
Fit 1	190000	400	45	**1133000**	250000	16	0.327
Fit 2	190000	400	**22**	**60562**	250000	16	0.03

[a] Only the values highlighted were allowed to vary in the kinetic simulations.

the additional consequence of enhancing cooperativity. In addition, our simulations indicate that the opposite effects that SLN and PLN have on the maximal activity of SERCA can be explained by an opposite effect on B_{for} (SLN decreased B_{for} and PLN increased B_{for}). This latter observation is consistent with the notion that PLN (12,14,41,42) and SLN (2) remain associated with SERCA at saturating calcium concentrations.

2-2.3. Alanine substitutions in the luminal domain of SLN. The presence of the unique luminal domain in SLN, as well as the high degree of conservation of its sequence, could suggest that all of these amino acids might be required for regulation of SERCA. As a first step in examining the role of the luminal tail of SLN, we systematically mutated residues 26-31 of SLN to alanine, co-reconstituted each mutant with SERCA, and measured the calcium-dependent ATPase activity of the proteoliposomes (Fig. 2-3 and Table 2-1). For effective comparison of the calcium-dependent ATPase activity of SERCA in the presence of SLN mutants, we wished to confirm that each of the mutants was reconstituted into proteoliposomes with the same efficiency as wild-type SLN. To that end, we used quantitative gel electrophoresis to monitor the levels of SERCA and SLN in the proteoliposomes (26,28). Incorporation of each of the SLN mutants did not significantly differ from wild-type (Fig. 2-3A), indicating that any observed differences in SERCA function could be attributed to the SLN mutation.

Alanine substitution of any residue within the ^{27}RSYQY motif had a negative impact on the ability of SLN to alter the apparent calcium affinity of SERCA, while substitution of the preceding residue, Val^{26}, had a lesser effect. While valine-to-alanine is a conservative substitution, we could compare our results with mutation of the homologous residue in PLN (Val^{49}; Fig. 2-1). The Val^{26}-to-Ala mutant also served as an

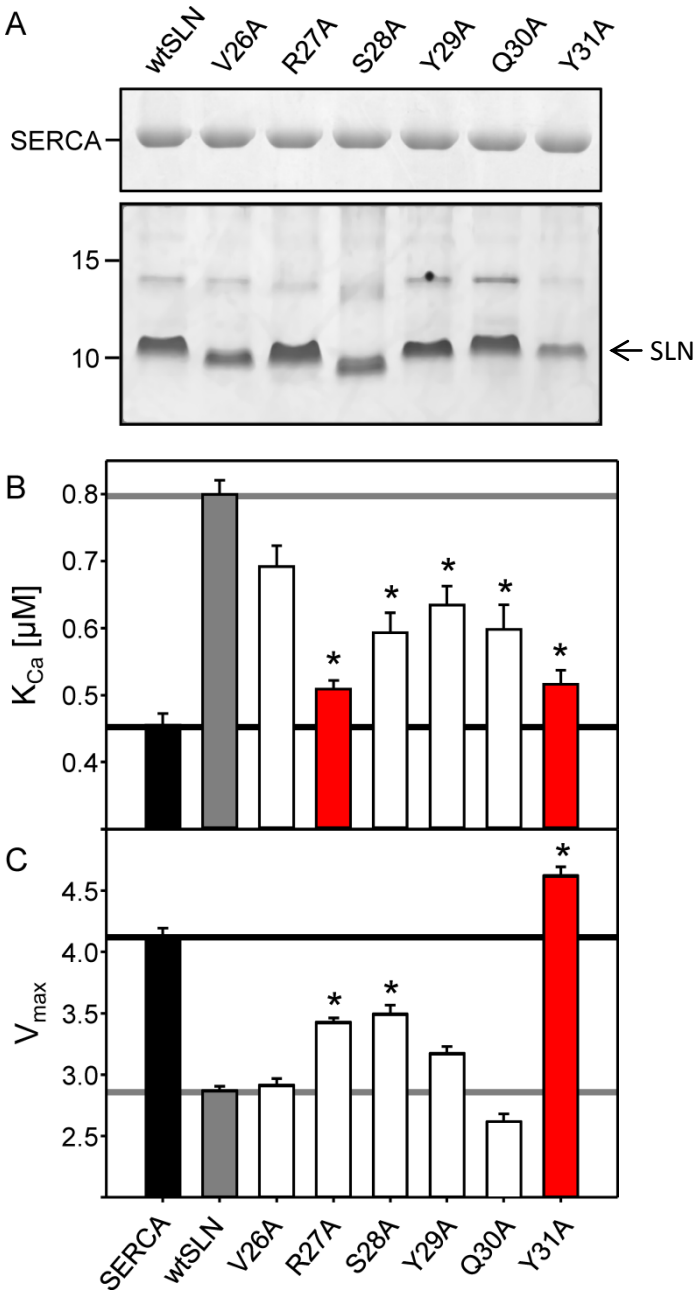

Figure 2-3. The effects of alanine mutation in the luminal domain of SLN on the K_{Ca} and V_{max} of SERCA. (**A**) SDS-PAGE of co-reconstituted proteoliposomes. The top gel shows the incorporation of SERCA (2µg of co-reconstituted proteoliposomes were loaded onto a 10% acrylamide gel and stained with Coomassie blue). The bottom gel shows the incorporation of wild-type and mutant SLN (2µg of co-reconstituted proteoliposomes were loaded onto a 16% acrylamide gel and silver stained). K_{Ca} (**B**) and V_{max} (**C**) values determined from ATPase activity measurements for SERCA in the absence and presence of wild-type and mutant forms of SLN. Each data point is the mean ± SEM ($n \geq 4$). The V_{max}, K_{Ca}, and Hill coefficients (n_H) are given in Table 2-1. *Asterisks* indicate comparisons against wild-type SLN ($p < 0.05$).

internal comparison for the luminal tail mutants described below. As expected, alanine substitution of Val^{26} had only a minor effect on the inhibitory properties of SLN resulting in mild loss-of-function (K_{Ca} was 0.69 μM compared to 0.80 μM calcium for wild-type; ΔK_{Ca} of 0.11). This compared well with findings for PLN, where alanine substitution of the homologous position, Val^{49}, has also been shown to have a mild effect on PLN function (26,43). Thus, we concluded that Val^{26} is part of the transmembrane domain and not the tail region of SLN. For mutations within the luminal tail domain, the two most severe alanine substitutions were Arg^{27}-to-Ala and Tyr^{31}-to-Ala, which resulted in nearly complete loss of SERCA inhibition (K_{Ca} of 0.51 and 0.52 μM calcium; ΔK_{Ca} of 0.05 and 0.06, respectively). These mutants were determined to be the strongest loss of function mutations in the luminal domain of SLN, indicating the importance of a positively charged residue at the membrane surface and a more distal aromatic residue. Interestingly, these mutants had distinct effects on the maximal activity of SERCA. Given the ability of wild-type SLN to reduce the maximal activity of SERCA (Fig. 2-3 and Table 2-1), the Arg^{27}-to-Ala mutant resulted in a slight loss of this behavior and the Tyr^{31}-to-Ala mutant resulted in a complete loss of this behavior. In fact, the Tyr^{31}-to-Ala mutant had the opposite effect in that it caused a slight increase in the maximal activity of SERCA. Compare the V_{max} values for SERCA alone (4.1 μmol mg^{-1} min^{-1}), SERCA in the presence of wild-type SLN (2.9 μmol mg^{-1} min^{-1}), SERCA in the presence of Arg^{27}-to-Ala SLN (3.4 μmol mg^{-1} min^{-1}), and SERCA in the presence of Tyr^{31}-to-Ala (4.6 μmol mg^{-1} min^{-1}).

Alanine mutants of the remaining residues (Ser^{28}, Tyr^{29}, and Gln^{30}) deviated from wild-type behavior, with variable effects on the apparent calcium affinity and maximal activity of SERCA (Fig. 2-3). In terms of their effects on the apparent calcium affinity of SERCA, the mutants resulted in a comparable partial loss of function. Ranking these

luminal tail residues in order of importance yielded $Ser^{28} \cong Tyr^{29} \cong Gln^{30}$. In terms of the maximal activity of SERCA, the mutants had differential effects with the rank order of importance being $Ser^{28} > Tyr^{29} > Gln^{30}$. Based on these observations, we concluded that alanine-substitution at any position in the SLN luminal tail results in loss of function, indicating a crucial role of each of the five luminal residues in proper regulation of SERCA. Clearly, Tyr^{31} was the most essential residue for altering the apparent calcium affinity and depressing the maximal activity of SERCA. This suggests that, in addition to contributing to SERCA inhibition, the residues Ser^{28}, Tyr^{29}, and Gln^{30} may play a role in the proper positioning of Tyr^{31}.

It should be noted that the SLN luminal tail was examined in a previous study using HEK-293 cells and co-expression with SERCA (9). Alanine substitution of the luminal tail residues was found to have a minimal impact on SERCA activity, which contrasts with our findings described above. However, it was later shown that mutations in the SLN tail affect the retention of SLN in the endoplasmic reticulum of HEK-293 cells (18), such that improper trafficking of SLN may have been an unappreciated factor in the previous study. In addition, the previous study measured calcium transport activity of SERCA, while we have measured ATPase activity. Recent evidence suggests that SLN may play a role in thermogenesis by uncoupling SERCA ATPase activity from calcium transport (2).

2-2.4. Removal of the SLN luminal tail (Arg^{27}stop). Since all of the alanine substitutions in the SLN luminal domain created defects in SERCA regulation, we next chose to remove the luminal tail and test the inhibitory capacity of SLN's transmembrane domain alone. For comparative purposes, recall that ~80% of the inhibitory activity of PLN is encoded by its transmembrane domain (26). To this end, a truncated variant of SLN, Arg^{27}stop, missing the last five C-terminal amino acids (^{27}RSYQY) was generated by

chemical synthesis. During synthesis, the C-terminus was amidated to avoid a free carboxyl at the end of the transmembrane domain. Incorporation of Arg^{27}stop into proteoliposomes with SERCA proceeded normally, and the final SERCA to peptide ratio was comparable to that for wild-type SLN (data not shown). The effect of this peptide on SERCA activity was measured in the same fashion as the alanine mutants described above. As one might expect given the results from alanine mutagenesis, the complete removal of the luminal tail resulted in major loss of SLN function (Fig. 2-4 and Table 2-1). The K_{Ca} of SERCA was 0.55 μM calcium in the presence of Arg^{27}stop, compared to 0.80 μM calcium in the presence of wild-type SLN (~26% of wild-type inhibitory capacity). Note that the K_{Ca} value for Arg^{27}stop is not significantly different from the alanine substitutions discussed above. Arg^{27}stop also resulted in a partial recovery of the maximal activity, with a V_{max} value halfway between that of SERCA alone and SERCA in the presence of wild-type SLN. The large change in the inhibitory potency of Arg^{27}stop agrees with the alanine-substitution data, and further demonstrates the necessity of the luminal domain of SLN in SERCA regulation. Interestingly, the luminal tail of SLN rather than the transmembrane domain appeared to encode most of the inhibitory properties of SLN. This contrasts with PLN where the inhibitory properties are encoded by the transmembrane domain. This was a surprising finding, given that SLN and PLN have homologous transmembrane domains, which are thought to interact with the same site on SERCA and use a similar mechanism of inhibition.

2-2.5. Adding the SLN luminal tail to PLN. If the luminal domain encodes the inhibitory properties of SLN, we wondered what would happen if the luminal tail were transferred to the homologous PLN. To test this idea, two chimeric peptides were constructed from wild-type PLN, one with the five luminal residues of SLN (^{27}RSYQY) added to the C-terminus ($cPLN_{long}$) and one with the luminal residues added after Val^{49} of PLN

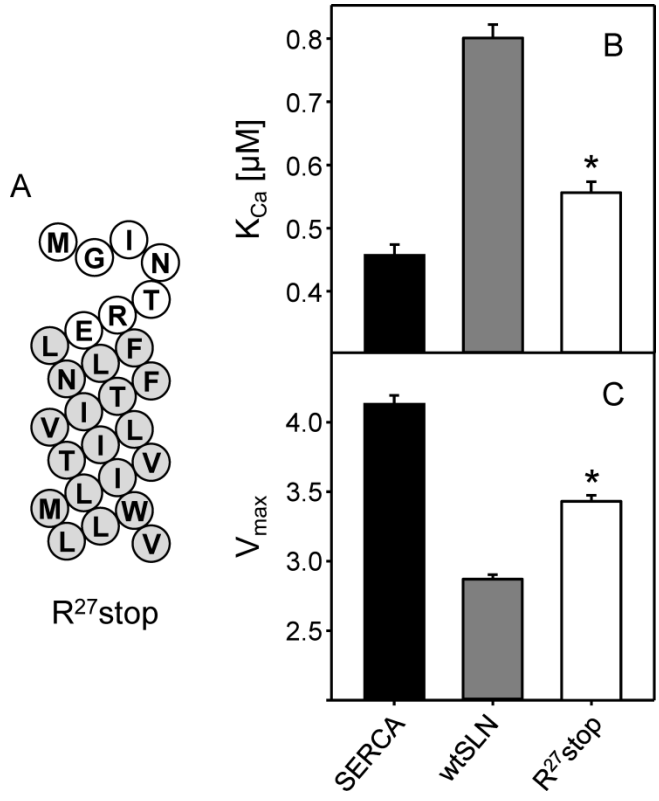

Figure 2-4. Removing the luminal tail of SLN. (**A**) Topology model for Arg^{27}stop SLN (white: cytosolic residues, grey: transmembrane residues). K_{Ca} (**B**) and V_{max} (**C**) values determined from ATPase activity measurements for SERCA in the absence and presence of Arg^{27}stop SLN. Each data point is the mean ± SEM ($n \geq 4$). The V_{max}, K_{Ca}, and Hill coefficients (n_H) are given in Table 2-1. *Asterisks* indicate comparisons against SERCA in the absence and presence of wild-type SLN ($p < 0.05$).

($cPLN_{short}$). This latter construct placed the luminal tail of SLN at the homologous position in PLN (Fig. 2-1 and Fig. 2-5). The calcium-dependent ATPase activity was measured for SERCA in the presence of the chimeras, where SERCA alone served as a negative control and SERCA in the presence of wild-type PLN served as a positive control (Fig. 2-5 and Table 2-1). Including wild-type PLN in proteoliposomes with SERCA resulted in the expected decrease in the apparent calcium affinity of SERCA (ΔK_{Ca} of 0.42 μM calcium) and increase in the maximal activity of SERCA (from 4.1 to 6.1 μmoles mg^{-1} min^{-1}). Compared to wild-type PLN, including the chimeras in proteoliposomes resulted in super-inhibition of SERCA (ΔK_{Ca} values were 1.84 μM calcium for $cPLN_{long}$ and 2.94 μM calcium for $cPLN_{short}$). Importantly, both chimeras also resulted in a decrease in the maximal activity of SERCA that was comparable to wild-type SLN. This was in marked contrast to the increase in SERCA maximal activity observed with wild-type PLN in the co-reconstituted proteoliposomes (26,28,31). Thus, adding the SLN luminal tail to PLN had a synergistic effect on the apparent calcium affinity of SERCA and a SLN-like effect on the maximal activity of SERCA. While both PLN chimeras were super-inhibitory, the cPLNshort construct resulted in a much larger shift in the apparent calcium affinity of SERCA. The potent inhibition by cPLNshort may be due to better positioning of the SLN luminal tail and the fact that this chimera appears to be monomeric by SDS-PAGE (Fig. 2-5D).

2-2.6. The SLN luminal tail is a distinct functional domain. The experiments thus far seemed to indicate that the luminal domain of SLN encodes most of its inhibitory activity. To test the inhibitory properties of this domain in isolation, we synthesized a peptide corresponding to ^{27}RSYQY with an acetylated N-terminus. Previous work by others has demonstrated that such a peptide can decrease the maximal activity of SERCA, albeit under excess peptide conditions (~1000-fold (19)). Herein, the soluble peptide was

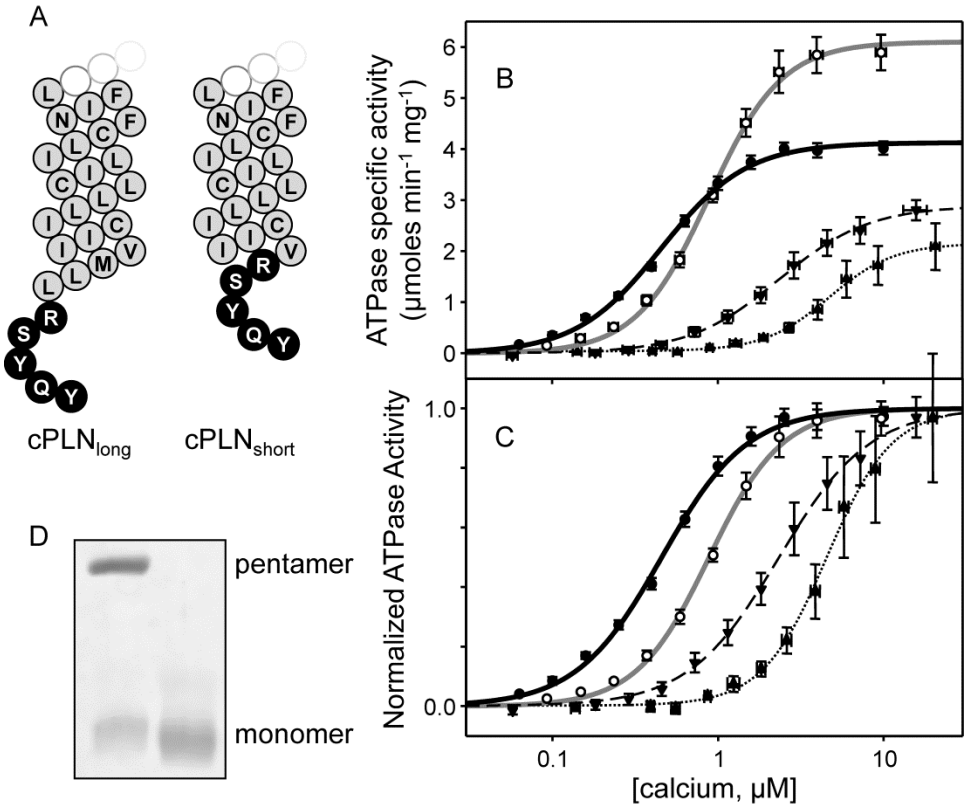

Figure 2-5. Transferring the luminal tail of SLN to PLN. (**A**) Topology models of $cPLN_{long}$ and $cPLN_{short}$ chimeras (*white*: cytosolic residues, *grey*: transmembrane residues, *black*: luminal residues). ATPase activity (**B**) and normalized ATPase activity (**C**) as a function of calcium concentration for SERCA alone (*solid black line*), SERCA in the presence of wild-type PLN (*solid grey line*), and SERCA in the presence of $cPLN_{long}$ (*dashed black line*) and $cPLN_{short}$ (*dotted black line*). Each data point is the mean ± SEM ($n \geq 4$). The V_{max}, K_{Ca}, and Hill coefficients (n_H) are given in Table 2-1. (**D**) SDS-PAGE of $cPLN_{long}$ (left lane) and $cPLN_{short}$ (right lane) chimeras (5µg per lane; 16% acrylamide gel). Pentameric and monomeric PLN chimeras are indicated.

co-reconstituted with SERCA such that the peptide was on the interior of the proteoliposomes with access to the luminal region of SERCA and excess peptide on the exterior of the proteoliposomes was removed by sucrose gradient purification. While SERCA was treated with up to a 100-fold molar excess of peptide prior to reconstitution, this had no effect on SERCA activity (Table 2-1). These data indicate that the ^{27}RSYQY peptide by itself did not result in the robust SERCA regulation observed for wild-type SLN or the PLN-SLN chimeras. Similar findings have been reported for the cytoplasmic domain of PLN, which does not appear to regulate SERCA as an isolated, soluble domain (16,44).

The transmembrane helix of SLN tethers the luminal domain to the membrane surface and provides a high local concentration relative to SERCA. As such, a soluble peptide may be a poor mimic of this domain. To bring the luminal domain to the membrane surface, we tethered the ^{27}RSYQY motif to a model transmembrane helix. We have previously characterized a synthetic leucine-alanine peptide that contains all of the naturally occurring leucine residues in the transmembrane domain of PLN, with all other residues substituted with alanine (designated Leu_9). A variety of generic transmembrane peptides including Leu_9 have been found to be weak inhibitors of SERCA (29,32). To test the action of the luminal tail of SLN on SERCA activity, we synthesized a peptide that contained the Leu_9 sequence with the five luminal residues of SLN at its C-terminus (Fig. 2-6; designated Leu_9tail). Since the Leu_9 peptide has been characterized (29), it served as a positive control for our studies of the Leu_9tail peptide. In the co-reconstituted proteoliposomes, Leu_9 had a slight effect on the apparent calcium affinity of SERCA (ΔK_{Ca} of 0.15 μM calcium; ~36% of wild-type PLN inhibitory activity) and a small effect on the maximal activity of SERCA. Inclusion of the SLN luminal tail significantly increased the inhibitory capacity of the Leu_9 peptide (ΔK_{Ca} of 0.35 μM calcium,

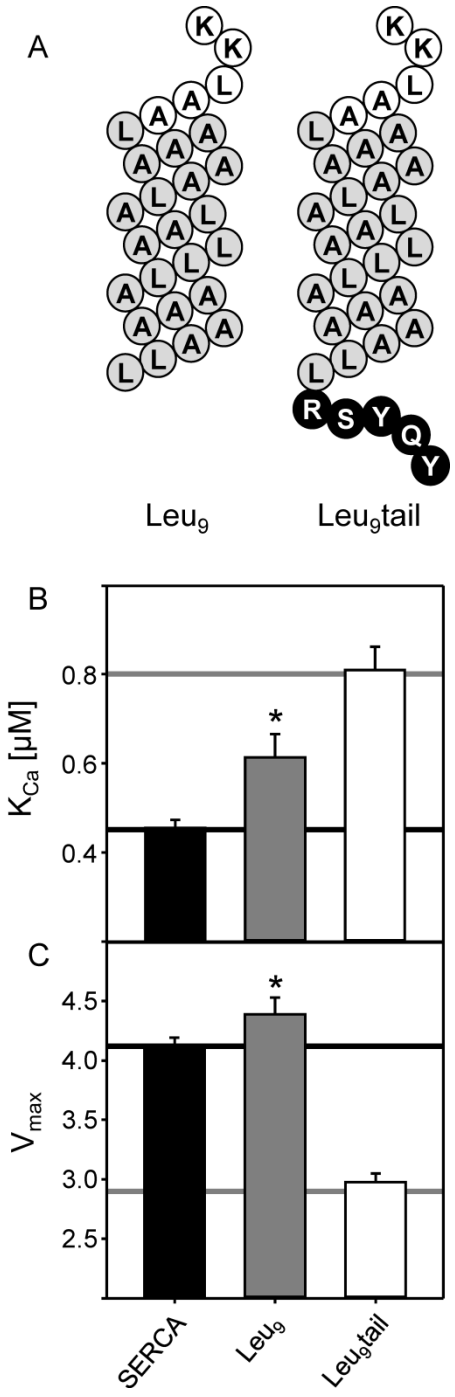

Figure 2-6. Transferring the luminal tail of SLN to a generic transmembrane helix. (**A**) Topology model of Leu_9 and Leu_9tail (*white*: cytosolic residues, *grey*: transmembrane residues, *black*: luminal residues). K_{Ca} (**B**) and V_{max} (**C**) values determined from ATPase activity measurements for SERCA in the absence and presence of Leu_9 and Leu_9tail. For comparative purposes, the black lines indicate the values for SERCA alone and the grey lines indicate values for SERCA in the presence of wild-type SLN. Notice that Leu_9tail closely recapitulates wild-type SLN. Each data point is the mean ± SEM ($n \geq 4$). The V_{max}, K_{Ca}, and Hill coefficients (n_H) are given in Table 2-1. *Asterisks* indicate comparisons against wild-type SLN ($p < 0.05$).

compared to ΔK_{Ca} of 0.34 μM for wild-type SLN) and reduced the maximal activity of SERCA to the same degree as wild-type SLN. Compare the V_{max} values for SERCA alone (4.1 μmol mg^{-1} min^{-1}), SERCA in the presence of Leu_9 (4.4 μmol mg^{-1} min^{-1}), SERCA in the presence of wild-type SLN (2.9 μmol mg^{-1} min^{-1}), and SERCA in the presence of Leu_9tail (3.0 μmol mg^{-1} min^{-1}). These observations support the notion that the luminal tail encodes much of the inhibitory properties of SLN and that it is a distinct and transferrable regulatory domain.

2-3. Discussion

2-3.1. Wild-type PLN versus wild-type SLN. Based on the available evidence, it was reasonable to assume that SLN and PLN would use similar inhibitory mechanisms to regulate SERCA. As such, SLN and PLN could represent redundant regulatory subunits separated by distinct tissue distributions – SLN primarily in skeletal muscle and PLN in cardiac and smooth muscle. As an endogenous inhibitor of SERCA, SLN plays a central role in regulating calcium transport in skeletal muscle. However, SLN is co-expressed in atrial muscle along with PLN (3-6), which raises questions about why redundant regulatory mechanisms would be required in this tissue. As has been shown for PLN, SLN alters the apparent calcium affinity of SERCA, albeit to a lesser degree (Fig. 2-2; (9)). PLN is highly conserved amongst mammalian species, with a transmembrane domain that encodes SERCA inhibition and a cytoplasmic domain that is a target for regulation. SLN is also highly conserved, with a transmembrane domain analogous to that in PLN, a short cytoplasmic domain that is a target for regulation, and a unique, highly-conserved luminal domain. Given these similarities and differences between SLN and PLN, it is important to understand the regulatory mechanism of SLN with potential relevance for heart and skeletal muscle diseases.

Since this is our first detailed characterization of SLN, it is important to consider aspects of the experimental system – namely, co-reconstituted proteoliposomes containing SERCA1a and recombinant SLN. Such proteoliposomes have been extensively used by us (26,28,30,31,33-35,45) and others (16,46-51) for the detailed characterization of PLN structure and function. They contain SERCA-lipid molar ratios that approximate SR membranes, and the inclusion of PLN in these proteoliposomes has the expected effect on the apparent calcium affinity of SERCA (25). At these low lipid-to-protein ratios, PLN has an additional effect on the maximal activity of SERCA (26,28,50). As shown herein, SLN is readily incorporated into the proteoliposomes and we observe the expected effect on the apparent calcium affinity of SERCA (Fig. 2-3) (9). In contrast to PLN, SLN has an opposite effect on the maximal activity of SERCA.

Using the proteoliposomes described above, we found that wild-type SLN altered the apparent calcium affinity of SERCA at a level equivalent to approximately 80% of the inhibitory capacity of wild-type PLN. Interestingly, the SERCA inhibition by wild-type SLN is comparable to what is observed for peptides encoding only the transmembrane domain of PLN (29,52,53). Nonetheless, in contrast to what is observed for PLN, SLN decreased the maximal activity of SERCA (Fig. 2-2 and Table 2-1). Given these differential effects on SERCA activity, we used kinetic simulations to identify SERCA reaction steps that may be altered by SLN. In this regard, PLN is known to alter a SERCA conformational change that follows binding of the first calcium ion, thereby establishing cooperativity for binding of a second calcium ion (25,26). Surprisingly, we found that SLN does not fit this kinetic model. Instead, SLN stabilizes a calcium free conformation of SERCA by altering the binding of the first calcium ion. Combined with the observed decrease in the maximal activity of SERCA, we concluded that SLN uses an inhibitory mechanism that is distinct from that used by PLN.

2-3.2. SLN structural elements involved in SERCA inhibition. Since SLN appeared to use a unique mechanism to regulate SERCA, it was important to identify the structural features that encode this behavior. There are nine invariant residues in SLN that mainly occur in the transmembrane domain (Fig. 2-1) and only four of these residues are invariant in the homologue PLN. The short cytoplasmic domain of SLN is variable across a wide range of species, while the luminal domain exhibits a high degree of conservation particularly amongst mammals. Alanine-scanning mutagenesis of the luminal domain revealed that Arg^{27} and Tyr^{31} are the two most essential residues for SERCA regulation; both residues are required for the effect on the apparent calcium affinity of SERCA and Tyr^{31} is required for the effect on the maximal activity of SERCA (Fig. 2-3). The interaction of Tyr^{31} with SERCA has been recognized (19), though another study did not identify luminal residues as important for SLN inhibitory function (9). Nonetheless, we found that mutation of either Arg^{27} or Tyr^{31} strongly suppressed SERCA inhibition by SLN. One might predict that Arg^{27} could reside at the membrane interface, and therefore aid in positioning of SLN relative to SERCA and the lipid bilayer. Alanine substitution would remove the positively charged side chain and extend the hydrophobic surface of SLN's transmembrane domain, thereby causing misalignment of SLN within the binding groove of SERCA (TM2, TM4, TM6 & TM9).

It is interesting to notice that the nature of the critical residues, Arg^{27} and Tyr^{31}, suggest that cation-π or π-π interactions might be involved in the SERCA-SLN inhibitory complex. By analogy with PLN, the C-terminus of SLN is thought to interact with the luminal end of the TM2 transmembrane segment of SERCA (54). Toward the luminal end of the TM1-TM2 region, there are five aromatic residues – Phe^{73}, Trp^{77} and Phe^{78} on TM1 and Phe^{88} and Phe^{92} on TM2. Phe^{88} and Phe^{92} on TM2 flank an interaction site identified for PLN, where Val^{89} of SERCA was cross-linked to Val^{49} of PLN (54,55).

Val^{49} of PLN is equivalent to Val^{26} of SLN, thus Arg^{27}, Tyr^{29} and Tyr^{31} of SLN may be proximal to Phe^{88} and Phe^{92} of SERCA (Fig. 2-7). Arg^{27} may form a cation-π interaction with Phe^{92}, while Tyr^{29} and/or Tyr^{31} may form a cation-π or π-stacking interactions with Phe^{88}. Given that the TM1-TM2 region of SERCA undergoes large structural rearrangements as the enzyme transitions from the calcium-free E2 state to the calcium-bound E1 state, these molecular interactions could explain the important inhibitory role of SLN's luminal residues.

2-3.3. The luminal extension of SLN is a distinct and transferrable regulatory domain. There are several roles that have been suggested for the luminal domain of SLN, including SR retention and functional interaction with SERCA. For PLN, SR retention occurs via the di-arginine motif in its cytoplasmic domain, as well as through the direct interaction with SERCA (56). The luminal ^{27}RSYQY sequence of SLN has been shown to be involved in SR retention, though the interaction with SERCA may also be a retention mechanism (18). There have been mixed reports on the inhibitory contributions of the SLN luminal domain (9,19). Co-expression of SERCA and SLN mutants in HEK-293 cells revealed minor contributions of the C-terminal residues, where loss of function occurred only when both Tyr^{29} and Tyr^{31} were mutated (9). ER retention may have been affected in this study (18). Another study highlighted the importance of the two luminal aromatic residues in regulating SERCA. Using solid-state NMR combined with functional measurements, a soluble ^{27}RSYQY peptide was shown to interact with SERCA and lower its maximal activity (19). There was no effect of this peptide on the apparent calcium affinity of SERCA. In contrast, our results indicate that the luminal domain of SLN alters both the maximal activity and apparent calcium affinity of SERCA. Given these disparate observations, we sought another experimental approach to elucidate the regulatory capacity of the SLN luminal domain.

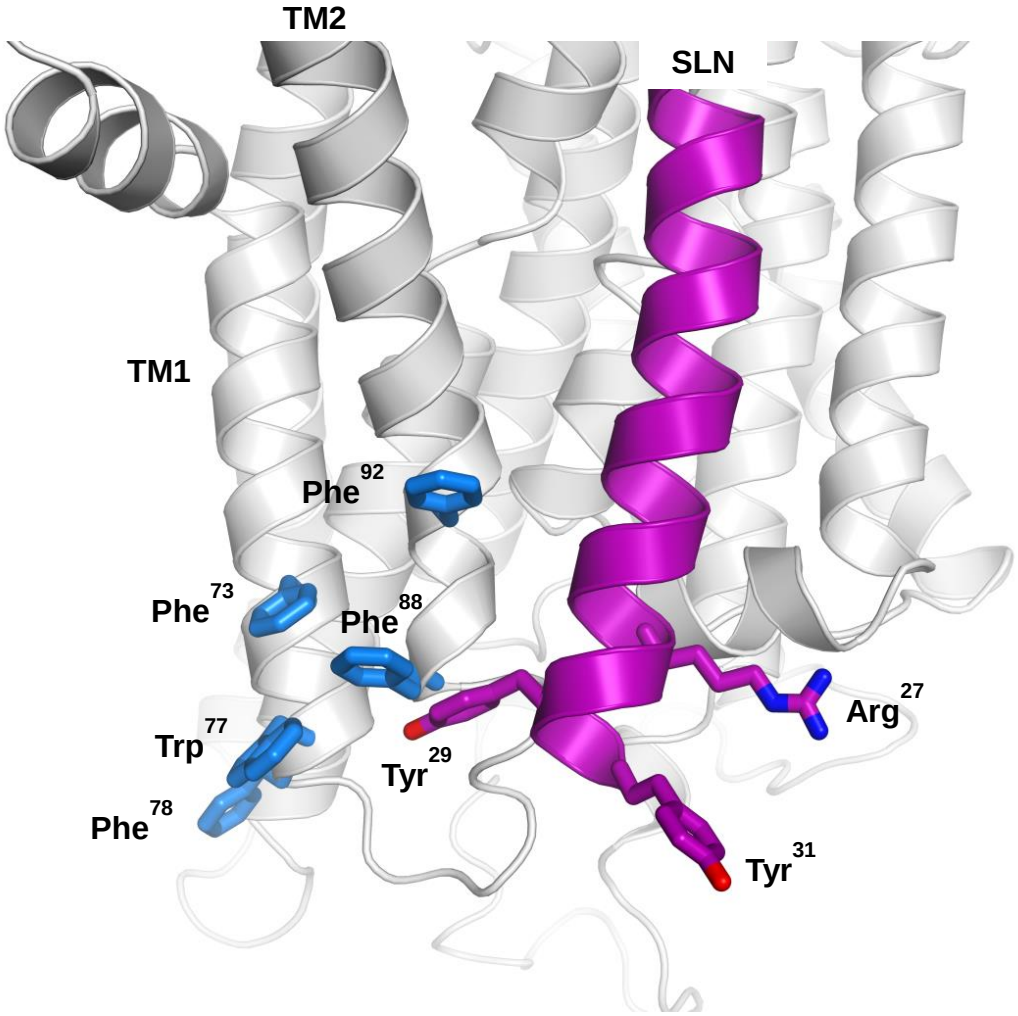

Figure 2-7. Model showing the proximity of the luminal domain of SLN (Arg^{27}, Tyr^{29} and Tyr^{31} are magenta) to the luminal end of TM1-TM2 of SERCA (particularly Phe^{88} and Phe^{92} are in blue). SERCA is in the E2 conformation (57). SLN is shown as a continuous α-helix, though we anticipate that the luminal tail may be partially unwound in the SERCA-SLN inhibitory complex. Based on models for the SERCA-PLN inhibitory complex (45,58), SLN was aligned in the TM2, TM4, TM6 & TM9 binding groove of SERCA. The positions of Arg^{27}, Tyr^{29} and Tyr^{31} are the approximate positions in the molecular model constructed by Asahi et al (7).

To test the functional contributions of this domain, two PLN-SLN chimeras were constructed. The first construct possessed the ^{27}RSYQY sequence added to the C-terminus of wild-type PLN. In the context of the chimera, the full length PLN sequence was expected to retain wild-type functional properties and the functional effects of the SLN luminal domain were expected to be additive. The second construct possessed the ^{27}RSYQY sequence added after Val^{49} of PLN, effectively replacing the C-terminal ^{50}MLL sequence. In the context of this chimera, the shortened PLN sequence might alter its functional properties, yet the SLN luminal domain would be optimally positioned for interaction with SERCA. To our surprise, both chimeras turned out to be potent super-inhibitors of SERCA, where the luminal domain of SLN had a synergistic effect on PLN inhibitory function. In fact, the chimeras were reminiscent of the super-inhibition observed for the ternary SERCA-PLN-SLN complex (7) thought to exist in the atria. These observations are consistent with the mutagenesis data described above and support the notion that the luminal domain of SLN possesses inhibitory activity. While the chimeras were reminiscent of the ternary complex, they were much more potent inhibitors of SERCA. Comparing the values in Table 2-1, the ΔK_{Ca} values were 0.9 μM calcium for the ternary complex, 1.84 μM calcium for the long chimera ($cPLN_{long}$), and 2.94 μM calcium for the short chimera ($cPLN_{short}$). In the ternary complex, PLN and SLN are thought to interact with SERCA as well as each other (7), and this may create steric restrictions that impact the proper positioning of critical regulatory domains – the transmembrane domain of PLN and the luminal domain of SLN. However, in the context of the chimeras, both the transmembrane domain of PLN and the luminal domain of SLN may be properly positioned in the SERCA binding groove (TM2, TM4 TM6 & TM9 (7)). Since these two domains use distinct mechanisms to regulate SERCA, the combined effect could result in the observed super-inhibition. It is also noteworthy that the short

chimera is largely monomeric by SDS-PAGE, which could contribute to the super-inhibition seen for this construct.

While the PLN-SLN chimeras were consistent with a functional role for SLN's luminal domain, this was one of several potential explanations for the observed super-inhibition. There are a variety of ways to convert PLN into a super-inhibitor of SERCA that might not reflect a functional contribution from the luminal ^{27}RSYQY sequence. PLN super-inhibition can result from mutation (28,59), depolymerisation of the PLN pentamer (43,60), and reverse-engineering of PLN peptides (29,32). If the luminal region of SLN is an independent functional and structural domain, it should be able to regulate SERCA in the absence of either the SLN or PLN transmembrane domain. However, a soluble ^{27}RSYQY peptide by itself did not alter SERCA activity over a range of excess concentrations. This may not be surprising, since the luminal ^{27}RSYQY sequence is normally tethered to the SR membrane. To further test the luminal domain as an independent functional entity, we tethered the ^{27}RSYQY sequence to a model transmembrane peptide designated Leu_9 (29). Using a reverse-engineering approach, Leu_9 was derived from the PLN transmembrane sequence where the nine leucine residues were retained and all other residues were mutated to alanine. This peptide is a weak inhibitor of SERCA, with ~36% of wild-type PLN inhibitory activity. Adding the luminal tail of SLN to Leu_9 generated a construct that was indistinguishable from wild-type SLN (Table 2-1 and Fig. 2-6). Compare the K_{Ca} and V_{max} values for SERCA in the presence of Leu_9tail (0.81 μM calcium and 3.0 μmol mg^{-1} min^{-1}) and SERCA in the presence of wild-type SLN (0.80 μM calcium and 2.9 μmol mg^{-1} min^{-1}). These data clearly demonstrate that the luminal region of SLN is a distinct structural and functional domain.

In summary, critical determinants for SLN inhibitory function are found in its unique and conserved luminal tail. The structural elements that may contribute to the

formation of a SERCA-SLN inhibitory complex include Arg^{27}, Tyr^{29} and Tyr^{31} of SLN and a series of aromatic residues at the base of TM1-TM2 of SERCA (particularly Phe^{88} and Phe^{92}). These molecular interactions account for much of SLN's inhibitory function, and this contrasts sharply with what is known for PLN. The transmembrane domain of PLN encodes ~80% of its inhibitory activity, whereas ~75% of SLN's inhibitory activity is encoded by the luminal tail. These distinct structural elements that are used by PLN and SLN to regulate SERCA translate into different inhibitory mechanisms. (25,26). PLN slows a SERCA conformational transition that follows binding of the first calcium ion and establishes cooperativity for binding of a second calcium ion. SLN alters binding of the first calcium ion, thereby stabilizing a calcium free conformation of SERCA. Given that these functional properties can be transferred to PLN or a generic transmembrane helix, we conclude that the luminal tail of SLN is a distinct, essential and transferrable regulatory domain.

2-4. Experimental Procedures

2-4.1. Expression and Purification of Recombinant SLN. Recombinant SLN and PLN chimeras were expressed and purified as previously described (32) with the exception of an additional organic extraction step for SLN purification. Briefly, following protease digestion of the maltose-binding protein and SLN fusion protein, trichloroacetic acid was added to a final concentration of 6%. This mixture was incubated on ice for 20 minutes. The precipitate was collected by centrifugation at 4°C and subsequently homogenized in a mixture of chloroform-isopropanol-water (4:4:1) and incubated at room temperature for 3 hours. The organic phase, highly enriched in recombinant SLN, was removed, dried to a thin film under nitrogen gas and resuspended in 7 M guanidine hydrochloride. Reverse-phase HPLC was performed as described (32) and the molecular mass was verified by

MALDI-TOF mass spectrometry (Institute for Biomolecular Design, University of Alberta).

2-4.2. Synthetic Peptide Handling. Synthetic peptides (Arg^{27}stop, Leu_9, Leu_9tail, and ^{27}RSYQY) were purchased from Biomatik (Wilmington, DE; 95% purity grade, HPLC and MS verified). Unless otherwise specified, all synthetic peptides were acetylated at the N-terminus and amidated at the C-terminus. Except for ^{27}RSYQY, which was solubilized in dH_2O, all peptides were solubilized in 3:1 chloroform:trifluoroethanol at a concentration of ~1 mg/ml. The peptide concentrations were verified by quantitative amino acid analysis.

2-4.3. Co-reconstitution of SERCA and Recombinant SLN. Routine procedures were used to purify SERCA1a from rabbit skeletal muscle SR vesicles and functionally reconstitute it into proteoliposomes with SLN. SERCA, SLN, egg yolk phosphatidylcholine (EYPC) and egg yolk phosphatidic acid (EYPA) were solubilized with octaethylene glycol monododecyl ether ($C_{12}E_8$) to achieve final molar stoichiometries of 1 SERCA, 6 SLN, and 195 lipids. The co-reconstituted proteoliposomes containing SERCA and SLN were formed by the slow removal of detergent (with SM-2 Biobeads, Bio-Rad) followed by purification on a sucrose step-gradient. The purified co-reconstituted proteoliposomes typically yield final molar stoichiometries of 1 SERCA, 4.5 SLN, and 120 lipids. This same procedure was used for the co-reconstitution of SERCA with PLN chimeras and synthetic transmembrane peptides. For the co-reconstitution of SERCA in the presence of ^{27}RSYQY peptide, the peptide in aqueous solution was added to the reconstitution mixture at a molar ratio of 1 SERCA to 100 ^{27}RSYQY, followed by detergent removal with SM-2 Biobeads to ensure incorporation of ^{27}RSYQY inside the proteoliposomes.

2-4.4. Activity Assays. Calcium-dependent ATPase activities of the co-reconstituted proteoliposomes were measured by a coupled-enzyme assay (61). The coupled enzyme assay reagents were of the highest purity available (Sigma-Aldrich, Oakville, ON). All co-reconstituted peptide constructs were compared to a negative control (SERCA reconstituted in the absence of SLN) and a matched positive control (SERCA co-reconstituted in the presence of either wild-type SLN, wild-type PLN or Leu_9 peptide). A minimum of three independent reconstitutions and activity assays were performed for each peptide, and the calcium-dependent ATPase activity was measured over a range of calcium concentrations (0.1 to 10 μM) for each assay. This method has been described in detail (28). The K_{Ca} (calcium concentration at half-maximal activity), the V_{max} (maximal activity) and the n_H (Hill coefficient) were calculated based on non-linear least-squares fitting of the activity data to the Hill equation using Sigma Plot software (SPSS Inc., Chicago, IL). Errors were calculated as the standard error of the mean for a minimum of three independent measurements. Comparison of K_{Ca}, V_{max} and n_H parameters was carried out using ANOVA (between-subjects, one-way analysis of variance) followed by the Holm-Sidak test for pairwise comparisons (Sigma Plot).

Throughout the Results and Discussion sections, we refer to SLN and PLN inhibition of SERCA. Inhibition is intended to reflect the effects that SLN and PLN have on the apparent calcium affinity of SERCA. The effects that SLN and PLN have on the maximal activity of SERCA are considered separately.

2-4.5. Kinetic Simulations. Reaction rate simulations have been described (25,26) for the transport cycle of SERCA in the absence and presence of PLN inhibition, and we have adopted this approach to understand SERCA inhibition by wild-type SLN. As before, we performed a global nonlinear regression fit of the model of Cantilina et al (25) to each plot of SERCA ATPase activity versus calcium concentration using Dynafit (Biokin Inc,

Pullman, WA). Such fits were performed for co-reconstituted wild-type SLN, which was compared to positive (SERCA co-reconstituted with wild-type PLN) and negative (SERCA alone) control samples. All reaction rate constants were allowed to vary in the kinetic simulations, though the SERCA activity in the presence of SLN was best fit with modifications to only the three calcium binding steps in the reaction cycle (26). Agreement between the simulated and experimental data is indicated by the lowest residual sum of squares.

2-5. References

1. Wawrzynow, A., Theibert, J. L., Murphy, C., Jona, I., Martonosi, A., and Collins, J. H. (1992) Sarcolipin, the "proteolipid" of skeletal muscle sarcoplasmic reticulum, is a unique, amphipathic, 31-residue peptide. *Archives of biochemistry and biophysics* **298**, 620-623

2. Bal, N. C., Maurya, S. K., Sopariwala, D. H., Sahoo, S. K., Gupta, S. C., Shaikh, S. A., Pant, M., Rowland, L. A., Goonasekera, S. A., Molkentin, J. D., and Periasamy, M. (2012) Sarcolipin is a newly identified regulator of muscle-based thermogenesis in mammals. *Nature medicine* **18**, 1575-1579

3. Minamisawa, S., Wang, Y., Chen, J., Ishikawa, Y., Chien, K. R., and Matsuoka, R. (2003) Atrial chamber-specific expression of sarcolipin is regulated during development and hypertrophic remodeling. *The Journal of biological chemistry* **278**, 9570-9575

4. Babu, G. J., Bhupathy, P., Carnes, C. A., Billman, G. E., and Periasamy, M. (2007) Differential expression of sarcolipin protein during muscle development and cardiac pathophysiology. *J Mol Cell Cardiol* **43**, 215-222

5. Odermatt, A., Taschner, P. E., Scherer, S. W., Beatty, B., Khanna, V. K., Cornblath, D. R., Chaudhry, V., Yee, W. C., Schrank, B., Karpati, G., Breuning, M. H., Knoers, N., and MacLennan, D. H. (1997) Characterization of the gene encoding human sarcolipin (SLN), a proteolipid associated with SERCA1: absence of structural mutations in five patients with Brody disease. *Genomics* **45**, 541-553

6. Vangheluwe, P., Schuermans, M., Zador, E., Waelkens, E., Raeymaekers, L., and Wuytack, F. (2005) Sarcolipin and phospholamban mRNA and protein expression in cardiac and skeletal muscle of different species. *The Biochemical journal* **389**, 151-159

7. Asahi, M., Sugita, Y., Kurzydlowski, K., De Leon, S., Tada, M., Toyoshima, C., and MacLennan, D. H. (2003) Sarcolipin regulates sarco(endo)plasmic reticulum

Ca2+-ATPase (SERCA) by binding to transmembrane helices alone or in association with phospholamban. *Proceedings of the National Academy of Sciences of the United States of America* **100**, 5040-5045

8. Simmerman, H. K., Collins, J. H., Theibert, J. L., Wegener, A. D., and Jones, L. R. (1986) Sequence analysis of phospholamban. Identification of phosphorylation sites and two major structural domains. *The Journal of biological chemistry* **261**, 13333-13341

9. Odermatt, A., Becker, S., Khanna, V. K., Kurzydlowski, K., Leisner, E., Pette, D., and MacLennan, D. H. (1998) Sarcolipin regulates the activity of SERCA1, the fast-twitch skeletal muscle sarcoplasmic reticulum Ca2+-ATPase. *The Journal of biological chemistry* **273**, 12360-12369

10. Waggoner, J. R., Huffman, J., Froehlich, J. P., and Mahaney, J. E. (2007) Phospholamban inhibits Ca-ATPase conformational changes involving the E2 intermediate. *Biochemistry* **46**, 1999-2009

11. Chen, Z., Akin, B. L., and Jones, L. R. (2010) Ca2+ binding to site I of the cardiac Ca2+ pump is sufficient to dissociate phospholamban. *The Journal of biological chemistry* **285**, 3253-3260

12. Negash, S., Yao, Q., Sun, H., Li, J., Bigelow, D. J., and Squier, T. C. (2000) Phospholamban remains associated with the Ca2+- and Mg2+-dependent ATPase following phosphorylation by cAMP-dependent protein kinase. *The Biochemical journal* **351**, 195-205

13. Traaseth, N. J., Thomas, D. D., and Veglia, G. (2006) Effects of Ser16 phosphorylation on the allosteric transitions of phospholamban/Ca(2+)-ATPase complex. *J Mol Biol* **358**, 1041-1050

14. Karim, C. B., Zhang, Z., Howard, E. C., Torgersen, K. D., and Thomas, D. D. (2006) Phosphorylation-dependent conformational switch in spin-labeled phospholamban bound to SERCA. *J Mol Biol* **358**, 1032-1040

15. Sasaki, T., Inui, M., Kimura, Y., Kuzuya, T., and Tada, M. (1992) Molecular mechanism of regulation of Ca2+ pump ATPase by phospholamban in cardiac sarcoplasmic reticulum. Effects of synthetic phospholamban peptides on Ca2+ pump ATPase. *The Journal of biological chemistry* **267**, 1674-1679

16. Reddy, L. G., Jones, L. R., Cala, S. E., O'Brian, J. J., Tatulian, S. A., and Stokes, D. L. (1995) Functional reconstitution of recombinant phospholamban with rabbit skeletal Ca(2+)-ATPase. *The Journal of biological chemistry* **270**, 9390-9397

17. Bhupathy, P., Babu, G. J., Ito, M., and Periasamy, M. (2009) Threonine-5 at the N-terminus can modulate sarcolipin function in cardiac myocytes. *J Mol Cell Cardiol* **47**, 723-729

18. Gramolini, A. O., Kislinger, T., Asahi, M., Li, W., Emili, A., and MacLennan, D. H. (2004) Sarcolipin retention in the endoplasmic reticulum depends on its C-

terminal RSYQY sequence and its interaction with sarco(endo)plasmic Ca(2+)-ATPases. *Proceedings of the National Academy of Sciences of the United States of America* **101**, 16807-16812

19. Hughes, E., Clayton, J. C., Kitmitto, A., Esmann, M., and Middleton, D. A. (2007) Solid-state NMR and functional measurements indicate that the conserved tyrosine residues of sarcolipin are involved directly in the inhibition of SERCA1. *The Journal of biological chemistry* **282**, 26603-26613

20. Tupling, A. R., Asahi, M., and MacLennan, D. H. (2002) Sarcolipin overexpression in rat slow twitch muscle inhibits sarcoplasmic reticulum Ca2+ uptake and impairs contractile function. *The Journal of biological chemistry* **277**, 44740-44746

21. Babu, G. J., Bhupathy, P., Petrashevskaya, N. N., Wang, H., Raman, S., Wheeler, D., Jagatheesan, G., Wieczorek, D., Schwartz, A., Janssen, P. M., Ziolo, M. T., and Periasamy, M. (2006) Targeted overexpression of sarcolipin in the mouse heart decreases sarcoplasmic reticulum calcium transport and cardiac contractility. *The Journal of biological chemistry* **281**, 3972-3979

22. Gramolini, A. O., Trivieri, M. G., Oudit, G. Y., Kislinger, T., Li, W., Patel, M. M., Emili, A., Kranias, E. G., Backx, P. H., and Maclennan, D. H. (2006) Cardiac-specific overexpression of sarcolipin in phospholamban null mice impairs myocyte function that is restored by phosphorylation. *Proceedings of the National Academy of Sciences of the United States of America* **103**, 2446-2451

23. Autry, J. M., Rubin, J. E., Pietrini, S. D., Winters, D. L., Robia, S. L., and Thomas, D. D. (2011) Oligomeric Interactions of Sarcolipin and the Ca-ATPase. *The Journal of biological chemistry* **286**, 31697-31706

24. Hellstern, S., Pegoraro, S., Karim, C. B., Lustig, A., Thomas, D. D., Moroder, L., and Engel, J. (2001) Sarcolipin, the shorter homologue of phospholamban, forms oligomeric structures in detergent micelles and in liposomes. *The Journal of biological chemistry* **276**, 30845-30852

25. Cantilina, T., Sagara, Y., Inesi, G., and Jones, L. R. (1993) Comparative studies of cardiac and skeletal sarcoplasmic reticulum ATPases: effect of phospholamban antibody on enzyme activation. *J. Biol. Chem.* **268**, 17018-17025

26. Trieber, C. A., Afara, M., and Young, H. S. (2009) Effects of phospholamban transmembrane mutants on the calcium affinity, maximal activity, and cooperativity of the sarcoplasmic reticulum calcium pump. *Biochemistry* **48**, 9287-9296

27. Douglas, J. L., Trieber, C. A., Afara, M., and Young, H. S. (2005) Rapid, high-yield expression and purification of Ca2+-ATPase regulatory proteins for high-resolution structural studies. *Protein Expr Purif* **40**, 118-125

28. Trieber, C. A., Douglas, J. L., Afara, M., and Young, H. S. (2005) The effects of mutation on the regulatory properties of phospholamban in co-reconstituted membranes. *Biochemistry* **44**, 3289-3297

29. Afara, M. R., Trieber, C. A., Glaves, J. P., and Young, H. S. (2006) Rational design of peptide inhibitors of the sarcoplasmic reticulum calcium pump. *Biochemistry* **45**, 8617-8627

30. Ceholski, D. K., Trieber, C. A., Holmes, C. F., and Young, H. S. (2012) Lethal, hereditary mutants of phospholamban elude phosphorylation by protein kinase a. *The Journal of biological chemistry* **287**, 26596-26605

31. Ceholski, D. K., Trieber, C. A., and Young, H. S. (2012) Hydrophobic imbalance in the cytoplasmic domain of phospholamban is a determinant for lethal dilated cardiomyopathy. *The Journal of biological chemistry* **287**, 16521-16529

32. Afara, M. R., Trieber, C. A., Ceholski, D. K., and Young, H. S. (2008) Peptide inhibitors use two related mechanisms to alter the apparent calcium affinity of the sarcoplasmic reticulum calcium pump. *Biochemistry* **47**, 9522-9530

33. Young, H. S., Jones, L. R., and Stokes, D. L. (2001) Locating phospholamban in co-crystals with Ca(2+)-ATPase by cryoelectron microscopy. *Biophys J* **81**, 884-894

34. Stokes, D. L., Pomfret, A. J., Rice, W. J., Glaves, J. P., and Young, H. S. (2006) Interactions between Ca2+-ATPase and the pentameric form of phospholamban in two-dimensional co-crystals. *Biophys J* **90**, 4213-4223

35. Glaves, J. P., Trieber, C. A., Ceholski, D. K., Stokes, D. L., and Young, H. S. (2011) Phosphorylation and mutation of phospholamban alter physical interactions with the sarcoplasmic reticulum calcium pump. *J Mol Biol* **405**, 707-723

36. Ferrington, D., Yao, Q., Squier, T., and Bigelow, D. (2002) Comparable levels of Ca-ATPase inhibition by phospholamban in slow-twitch skeletal and cardiac sarcoplasmic reticulum. *Biochemistry* **41**, 13289-13296

37. Negash, S., Chen, L., Bigelow, D., and Squier, T. (1996) Phosphorylation of phospholamban by cAMP-dependent protein Kinase enhances interactions between Ca-ATPase polypeptide chains in cardiac sarcoplasmic reticulum membranes. *Biochemistry* **35**, 11247-11259

38. Becucci, L., Guidelli, R., Karim, C. B., Thomas, D. D., and Veglia, G. (2009) The role of sarcolipin and ATP in the transport of phosphate ion into the sarcoplasmic reticulum. *Biophys J* **97**, 2693-2699

39. Buck, B., Zamoon, J., Kirby, T. L., DeSilva, T. M., Karim, C., Thomas, D., and Veglia, G. (2003) Overexpression, purification, and characterization of recombinant Ca-ATPase regulators for high-resolution solution and solid-state NMR studies. *Protein Expression and Purification* **30**, 253-261

40. Inesi, G., Kurzmack, M., and Lewis, D. (1988) Kinetic and equilibrium characterization of an energy-transducing enzyme and its partial reactions. *Methods in enzymology* **157**, 154-190

41. Fowler, C., Huggins, J. P., Hall, C., Restall, C. J., and Chapman, D. (1989) The Effects of Calcium, Temperature, and Phospholamban Phosphorylation on the Dynamics of the Calcium-Stimulated ATPase of Canine Cardiac Sarcoplasmic Reticulum. *Biochimica Biophysica Acta* **980**, 348-356

42. Bidwell, P., Blackwell, D. J., Hou, Z., Zima, A. V., and Robia, S. L. (2011) Phospholamban binds with differential affinity to calcium pump conformers. *The Journal of biological chemistry* **286**, 35044-35050

43. Kimura, Y., Kurzydlowski, K., Tada, M., and MacLennan, D. H. (1997) Phospholamban inhibitory function is enhanced by depolymerization. *J. Biol. Chem.* **272**, 15061-15064

44. Lockwood, N. A., Tu, R. S., Zhang, Z., Tirrell, M. V., Thomas, D. D., and Karim, C. B. (2003) Structure and function of integral membrane protein domains resolved by peptide-amphiphiles: application to phospholamban. *Biopolymers* **69**, 283-292

45. Seidel, K., Andronesi, O. C., Krebs, J., Griesinger, C., Young, H. S., Becker, S., and Baldus, M. (2008) Structural Characterization of Ca^{2+}-ATPase-Bound Phospholamban in Lipid Bilayers by Solid-State Nuclear Magnetic Resonance (NMR) Spectroscopy. *Biochemistry* **47**, 4369-4376

46. Reddy, L. G., Jones, L. R., Pace, R. C., and Stokes, D. L. (1996) Purified, reconstituted cardiac Ca^{2+}-ATPase is regulated by phospholamban but not by direct phosphorylation with Ca^{2+}/calmodulin-dependent protein kinase. *JBC* **271**, 14964-14970

47. Thomas, D., Reddy, L., Karim, C., Li, M., Cornea, R., Autry, J., Jones, L., and Stamm, J. (1998) Direct spectroscopic detection of molecular dynamics and interactions of the calcium pump and phospholamban. *Ann NY Acad Sci* **853**, 186-194

48. Reddy, L., Jones, L., and Thomas, D. (1999) Depolymerization of phospholamban in the presence of calcium pump: a fluorescence energy transfer study. *Biochemistry* **38**, 3954-3962

49. Karim, C. B., Paterlini, M. G., Reddy, L. G., Hunter, G. W., Barany, G., and Thomas, D. D. (2001) Role of cysteine residues in structural stability and function of a transmembrane helix bundle. *The Journal of biological chemistry* **276**, 38814-38819

50. Reddy, L., Cornea, R., Winters, D., McKenna, E., and Thomas, D. (2003) Defining the molecular components of calcium transport regulation in a reconstituted membrane system. *Biochemistry* **42**, 4585-4592

51. Reddy, L., Autry, J., Jones, L., and Thomas, D. (1999) Co-reconstitution of phospholamban mutants with the Ca-ATPase reveals dependence of inhibitory function on phospholamban structure. *J. Biol. Chem.* **274**, 7649-7655

52. Karim, C., Marquardt, C., Stamm, J., Barany, B., and Thomas, D. (2000) Synthetic null-cysteine phospholamban analogue and the corresponding transmembrane domain inhibit the Ca-ATPase. *Biochemistry* **39**, 10892-10897

53. Kimura, Y., Kurzydlowski, K., Tada, M., and MacLennan, D. H. (1996) Phospholamban regulates the Ca^{2+}-ATPase through intramembrane interactions. *J. Biol. Chem.* **271**, 21726-21731

54. Morita, T., Hussain, D., Asahi, M., Tsuda, T., Kurzydlowski, K., Toyoshima, C., and Maclennan, D. H. (2008) Interaction sites among phospholamban, sarcolipin, and the sarco(endo)plasmic reticulum Ca(2+)-ATPase. *Biochem Biophys Res Commun* **369**, 188-194

55. Chen, Z., Akin, B., Stokes, D., and Jones, L. (2006) Cross-linking of C-terminal residues of phospholamban to the Ca^{2+} pump of cardiac sarcoplasmic reticulum to probe spatial and functional interactions within the transmembrane domain. *The Journal of biological chemistry* **281**, 14163-14172

56. Sharma, P., Ignatchenko, V., Grace, K., Ursprung, C., Kislinger, T., and Gramolini, A. O. (2010) Endoplasmic reticulum protein targeting of phospholamban: a common role for an N-terminal di-arginine motif in ER retention? *PloS one* **5**, e11496

57. Toyoshima, C., and Nomura, H. (2002) Structural changes in the calcium pump accompanying the dissociation of calcium. *Nature* **418**, 605-611

58. Toyoshima, C., Asahi, M., Sugita, Y., Khanna, R., Tsuda, T., and MacLennan, D. (2003) Modeling of the inhibitory interaction of phospholamban with the Ca^{2+} ATPase. *Proc. Natl. Acad. Sci. U. S. A.* **100**, 467-472

59. Kimura, Y., Asahi, M., Kurzydlowski, K., Tada, M., and MacLennan, D. H. (1998) Phospholamban domain Ib mutations influence functional interactions with the Ca^{2+}-ATPase isoform of cardiac sarcoplasmic reticulum. *J. Biol. Chem.* **273**, 14238-14241

60. Cornea, R. L., Jones, L. R., Autry, J. M., and Thomas, D. D. (1997) Mutation and phosphorylation change the oligomeric structure of phospholamban in lipid bilayers. *Biochemistry* **36**, 2960-2967

61. Warren, G. B., Toon, P. A., Birdsall, N. J., Lee, A. G., and Metcalfe, J. C. (1974) Reconstitution of a calcium pump using defined membrane components. *Proceedings of the National Academy of Sciences of the United States of America* **71**, 622-626

Chapter 3

Zebrafish phospholamban-like protein is an active regulator of the sarcoplasmic reticulum calcium pump

Acknowledgements: Dr. C. Trieber purified SERCA for functional analysis and helped with cloning and purification of various phospholamban constructs. G. Ashrafi performed initial characterization of zebrafish phospholamban.

3-1. Introduction

The regulation of calcium transport across the sarcoplasmic reticulum (SR) membrane plays a central role in the muscle contraction-relaxation cycle. Following the release of calcium from the SR during muscle contraction, the reuptake of calcium into the SR lumen determines the rate of relaxation as well as the force of subsequent contractions. Reuptake involves the active transport of calcium into the SR, which is accomplished by an ATP-dependent calcium pump, SERCA (1). In cardiac and smooth muscle, SERCA is regulated by phospholamban (PLN), a 52 amino acid integral membrane protein (2,3). The interaction between SERCA and PLN is controlled by the β-adrenergic pathway (4) where the phosphorylation of PLN by cAMP-dependent protein kinase (PKA) reverses SERCA inhibition and regulates the overall SR calcium load (5). In fast-twitch skeletal muscle and the atria of the heart, SERCA is regulated by sarcolipin (SLN), a 31 amino acid homologue of PLN (6-8). There is a high degree of sequence homology in the transmembrane regions of PLN and SLN, suggesting a similar mode of interaction with SERCA (9,10). However, recent studies have demonstrated that PLN and SLN use different mechanisms to regulate SERCA (11) and crystal structures of the SERCA-SLN complex (12,13) deviate from molecular models of the SERCA-PLN complex (14,15).

The topology of PLN is organized into three domains: an α-helical cytoplasmic domain IA (residues 1-20), an extended linker domain IB (residues 21-30), and a highly hydrophobic and α-helical domain II (residues 31-52) that makes up the transmembrane region of PLN (16,17). The cytoplasmic domain makes a small contribution to SERCA inhibition, yet it has two phosphorylation sites (Ser^{17} and Thr^{17}) that play a critical role in the regulation of PLN inhibitory functions. Indeed, several hereditary mutations in this domain are associated with early-onset, lethal heart failure in humans (18,19). The linker

domain of PLN can also interact with SERCA, though residues such as Lys^{27}, Gln^{29}, and Asn^{30} appear to modulate the physical interaction with SERCA rather than making a direct contribution to inhibition (20). Finally, the transmembrane domain of PLN encodes most of its inhibitory properties, which manifests as a decrease in the apparent calcium affinity of SERCA and a shift from the E1 calcium-bound state to the E2 calcium-free state in the catalytic cycle (21,22). The PLN transmembrane domain is highly hydrophobic and contains residues that are either critical for inhibitory function (e.g. Leu^{31} and Asn^{34}) or involved in self-association to form a pentamer (leucine-isoleucine zipper) (23-26). Comparatively, SLN has a short cytoplasmic domain (residues 1-7), a transmembrane domain homologous to that of PLN (residues 8-26), and a short, unique luminal domain (residues 27-31). Like PLN, the cytoplasmic domain of SLN is involved in regulating the interaction with SERCA (27). However, unlike PLN, the inhibitory properties of SLN are encoded by its unique luminal domain rather than its transmembrane domain (11).

Because of its implications in heart disease, most structural and functional studies of PLN have concentrated primarily on the mammalian forms. Nevertheless, PLN has been shown to be expressed in many non-mammalian vertebrates, including birds, amphibians, and fish (28,29). This ubiquitous expression underlines the importance of PLN as a regulator of calcium transport in the cardiac muscle of many organisms. There is a remarkable degree of sequence homology between the mammalian forms of PLN with predominantly as few as one or two amino acid substitutions between them all. In birds and fish, however, PLN shows much greater divergence (Fig. 3-1). For example, chicken PLN and zebrafish PLN isoform 2 (zfPLN) are 83% and 68% identical to human PLN (hPLN), respectively. In fact, the primary sequence of zfPLN is the most divergent PLN sequence identified to date. Compared to hPLN, the zebrafish protein contains 13

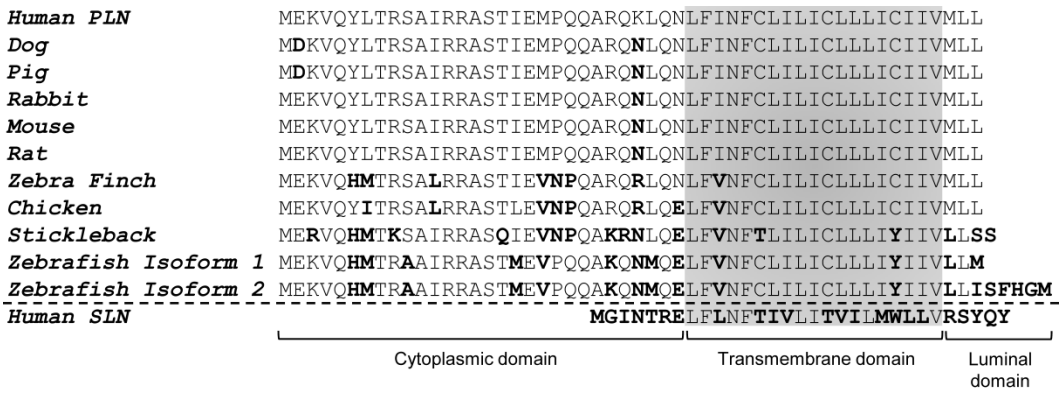

Figure 3-1. Amino acid sequence alignments for primary structures of PLN and SLN from representative species. The cytoplasmic, transmembrane, and luminal domains are indicated. Sequence variations, as compared to human PLN, are indicated in bold.

sequence variations and five additional residues at the C-terminus. Most of the residue differences between human and zfPLN cluster in three distinct regions, suggesting that these more complex sequence changes could alter PLN function. The most intriguing variation in zfPLN is the addition of a C-terminal tail (residues 53-57). Unlike other PLN proteins, zfPLN has an additional five amino acids that extend into the SR lumen (Fig. 3-1). It is important to note that the C-terminal sequence of PLN in all mammals and birds is perfectly conserved (Met^{50}-Leu-Leu^{52}). In zfPLN, this sequence is modified to the longer and more polar Ile^{52}-Ser-Phe-His-Gly-Met^{57}, which is reminiscent of the luminal Arg^{27}-Ser-Tyr-Gln-Tyr^{31} sequence of SLN. So far, it is not known if zfPLN can regulate SERCA and whether this regulation resembles that of hPLN or SLN.

Given the high sequence diversity between zebrafish and human PLN, as well as the presence of a unique zfPLN luminal extension, we characterized the ability of zfPLN to regulate SERCA. Full-length zfPLN, as well as zebrafish-human chimeras and point mutants were co-reconstituted with SERCA into proteoliposomes. To summarize our findings, full-length zfPLN had inhibitory properties that were similar to hPLN, with comparable effects on the apparent calcium affinity and maximal activity of SERCA. In addition, PKA-mediated phosphorylation of zfPLN was found to reverse SERCA inhibition as is known to occur for hPLN. hPLN chimeras containing the cytoplasmic or linker domains of zfPLN resulted in mild loss of inhibitory function or gain of function, respectively. Thus, despite similar functions, the human and zebrafish sequences are not synonymous. To investigate the unique luminal domain of zfPLN, a C-terminal truncation and a chimera with hPLN were constructed. A truncated zfPLN lacking the Ser^{53}-Phe-His-Gly-Met^{57} luminal extension resulted in loss of function, while adding the zfPLN luminal extension to hPLN had a minimal effect on SERCA inhibition. These data indicate that the luminal extension is required for SERCA inhibition, but only in the

context of the sequence variations in zfPLN. Finally, replacing the luminal extension of zfPLN with the SLN tail resulted in a chimera with super-inhibitory, SLN-like properties. We conclude that the luminal extensions of zfPLN and SLN have distinct functional effects, even though zfPLN appears to use a hybrid PLN-SLN inhibitory mechanism.

3-2. Results

3-2.1. Human versus zebrafish PLN. Our first objective was to characterize the physical and functional properties of the wild-type zfPLN. To accomplish this, we compared the reconstitution of SERCA alone and in the presence of wild-type hPLN or wild-type zfPLN. The co-reconstitution system has been used extensively to study the functional regulation of SERCA1a by PLN (23-25,30-33) and the same approach was used herein for detailed characterization of zfPLN. The reconstituted proteoliposomes at high protein to lipid ratios mimic the native SR membrane, which allows for functional and structural characterization of SERCA in the absence and presence of PLN (23,30,32-36). The final molar ratio of the proteoliposomes was 1 SERCA: 4.5 zfPLN: 120 lipids and there was no observable difference in the reconstitution efficiency of human versus zebrafish PLN. It is well established that hPLN has high propensity to form homo-oligomers in the SR membrane (2). Using quantitative SDS-PAGE, we also determined zfPLN to be primarily in a pentameric form and not significantly different from hPLN (data not shown).

We next measured the calcium-dependent ATPase activity of SERCA in the absence and presence of hPLN or zfPLN. As expected, proteoliposomes containing SERCA alone yielded a K_{Ca} of 0.46 μM and a V_{max} of 4.1 μmol mg^{-1} min^{-1}. Inclusion of hPLN in proteoliposomes decreased the apparent calcium affinity (0.88 μM calcium; ΔK_{Ca} of 0.42) and increased the maximal activity (6.3 μmol mg^{-1} min^{-1}; ΔV_{max} of 2.2) of SERCA. Incorporation of zfPLN in proteoliposomes with SERCA resulted in a K_{Ca} value

similar to that for hPLN (0.85 μM calcium; ΔK_{Ca} of 0.39) and a slightly higher V_{max} value (6.9 μmol mg^{-1} min^{-1}; ΔV_{max} of 2.8). Thus, despite the sequence variation in zfPLN, it has similar regulatory properties as hPLN (Fig. 3-2 and Table 3-1).

A hallmark of mammalian PLNs is the ability to reverse SERCA inhibition by PKA-mediated phosphorylation of PLN at Ser^{16} (16,37). To test this, we phosphorylated zfPLN with PKA followed by co-reconstitution into proteoliposomes with SERCA. As expected, phosphorylation of zfPLN restored the apparent calcium affinity of SERCA (Fig. 3-2 and Table 3-1; K_{Ca} value of 0.55 μM; ΔK_{Ca} of 0.09). This compared well with findings for hPLN, where phosphorylation resulted in complete reversal of SERCA inhibition (K_{Ca} of 0.45 μM) (32).

3-2.2. Functional contributions of zebrafish PLN sequence variation. The primary sequence of wild-type zfPLN can be divided into three distinct regions (designated: zfHEAD, zfMIDDLE, zfTAIL), as well as three transmembrane residue changes at Tyr^{46}, Leu^{50} and Ile^{52} (Fig. 3-2, A and B). Each of the three regions contains a cluster of residues that differ from the hPLN sequence. There are three residue changes in the N-terminal helix (Tyr^{6}-to-His, Leu^{7}-to-Met and Ser^{10}-to-Ala), seven residue changes in the linker region (Ile^{18}-to-Met, Met^{20}-to-Val, Arg^{25}-to-Lys, Arg^{27}-to-Asn, Leu^{28}-to-Met, Asn^{30}-to-Glu, and Ile^{33}-to-Val), and five residues added to the C-terminus (Ser^{53}-Phe^{54}-His^{55}-Gly^{56}-Met^{57}). While many of the residue changes are conservative, they represent more global sequence variations compared to the traditional single-site mutants that have been used to study PLN function. To study the functional consequences of these sequence variations, we created chimeric peptides that consisted of hPLN containing each of the zebrafish regions. We first focused on the cytoplasmic domain chimeras (zfHEAD and

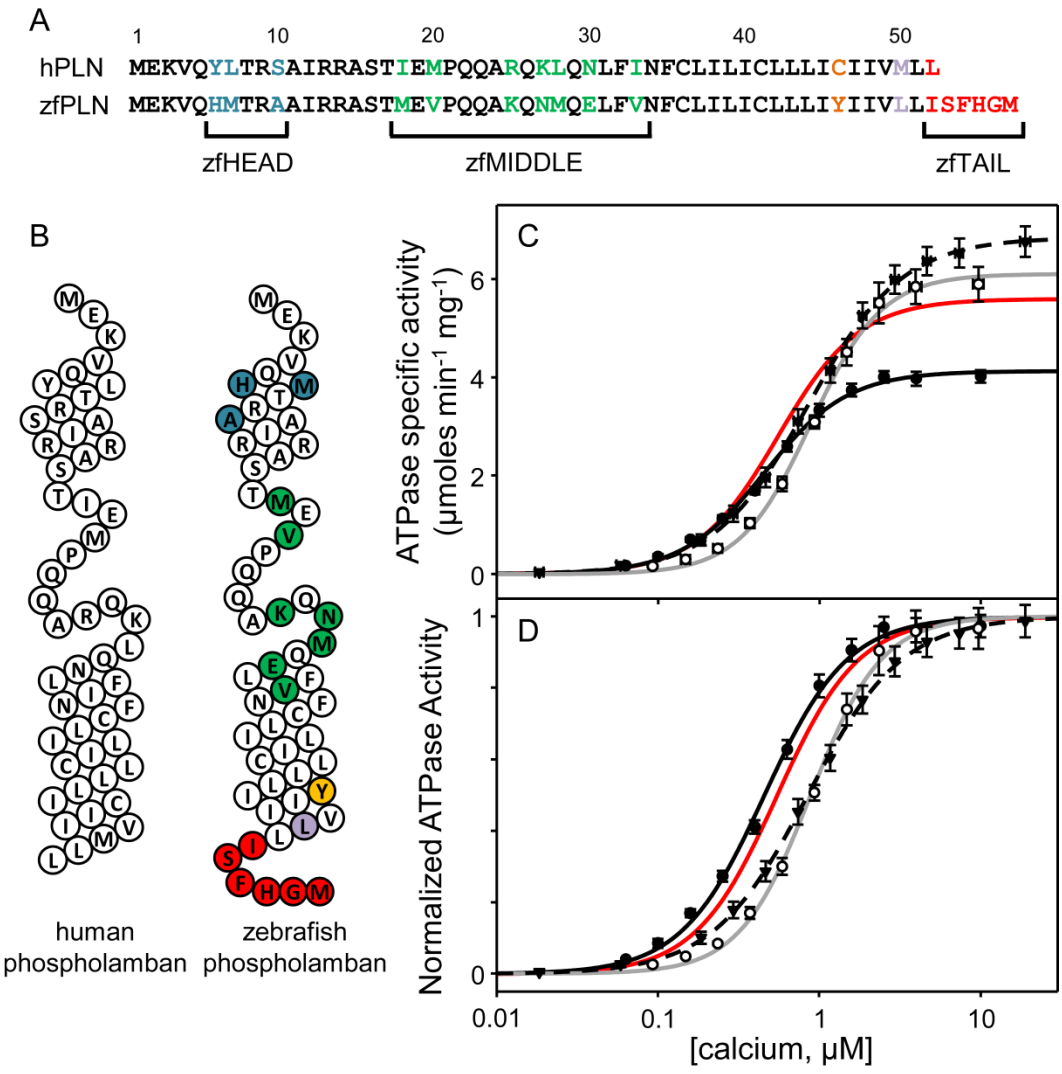

Figure 3-2. Functional data for wild-type human and zebrafish PLN. (**A**) Amino acid sequence alignment for human and zebrafish PLN. The differences in sequence composition are color coded based on their location (zfHEAD (blue), zfMIDDLE (green), Tyr[46] (orange), Leu[50] (purple), and zfTAIL (red). (**B**) Topology models for wild-type human and wild-type zebrafish PLN (*white*, conserved residues, variant residues are color coded to match the primary sequences in panel (A). Shown are ATPase activity (**C**) and normalized ATPase activity (**D**) as a function of calcium concentration for SERCA alone (*solid black line*), SERCA in the presence of wild-type human PLN (*solid gray line*), SERCA in the presence of wild-type zebrafish PLN (*dashed line*), and SERCA in the presence of phosphorylated form of wild-type zebrafish PLN (*solid red line*). The V_{max}, K_{Ca}, and n_H are given in Table 3-1. Each data point is the mean ± S.E. (*error bars*) ($n \geq 3$).

Table 3-1. Kinetic parameters for SERCA in the absence and presence of various phospholamban variants. Between-subjects one-way analysis of variance followed by the Holm-Sidak test was used for pairwise comparisons against SERCA in the absence and presence of wild-type human PLN.

	V_{max} (μmoles mg^{-1} min^{-1})	K_{Ca} (μM)	n_H	n
SERCA	4.1 ± 0.1	0.46 ± 0.02	1.7 ± 0.1	32
hPLN	6.1 ± 0.1[a]	0.88 ± 0.03[a]	2.0 ± 0.1	9
ph-hPLN	6.3 ± 0.1[a]	0.45 ± 0.02[b]	1.7 ± 0.1	4
zfPLN	6.9 ± 0.1[a,b]	0.85 ± 0.01[a]	1.5 ± 0.1	12
ph-zfPLN	5.6 ± 0.1[a]	0.55 ± 0.01[b]	1.7 ± 0.1	3
zfHEAD	4.3 ± 0.1[b]	0.94 ± 0.04[a]	1.6 ± 0.1	7
zfMID	5.9 ± 0.1[a]	1.1 ± 0.05[a,b]	1.4 ± 0.1	8
C46Y	6.6 ± 0.1[a,b]	0.89 ± 0.03[a]	1.6 ± 0.1	4
zfPLN (-5)	7.2 ± 0.1[a,b]	0.70 ± 0.03[a,b]	1.6 ± 0.1	8
zfPLN (-6)	6.4 ± 0.1[a]	0.67 ± 0.03[a,b]	1.6 ± 0.1	6
hPLN (+5)	5.7 ± 0.1[a,b]	0.94 ± 0.02[a,b]	1.6 ± 0.1	8
hPLN (+6)	6.8 ± 0.1[a,b]	0.76 ± 0.02[a,b]	1.6 ± 0.1	6
zfPLN-SLN_{tail}	4.7 ± 0.1[a,b]	1.5 ± 0.06[a,b]	2.0 ± 0.1	5

[a] $p < 0.05$ in the absence of wild-type human or zebrafish PLN.
[b] $p < 0.05$ in the presence of wild-type human PLN.

zfMID) and a residue change in the transmembrane domain (Cys^{46}-to-Tyr; Fig. 3-3 and Table 3-1). The calcium-dependent ATPase activity was measured for SERCA in the presence of each peptide, where SERCA alone served as a negative control and SERCA in the presence of hPLN served as a positive control. Inclusion of the zfHEAD chimera in proteoliposomes with SERCA resulted in a similar increase in K_{Ca} as seen for hPLN (K_{Ca} values of 0.94 and 0.88 μM, respectively). Surprisingly, the zfHEAD chimera did not increase the maximal activity of SERCA as observed for hPLN. Compare V_{max} values for SERCA alone (4.1 μmol mg^{-1} min^{-1}), SERCA in the presence of zfHEAD (4.3 μmol mg^{-1} min^{-1}) and SERCA in the presence of hPLN (6.1 μmol mg^{-1} min^{-1}).

Next we tested the zfMID chimera in proteoliposomes with SERCA. Compared to hPLN, the zfMID chimera was a super-inhibitor of SERCA (K_{Ca} of 1.1 μM) while maintaining the characteristic increase in maximal activity. Compare the V_{max} values for SERCA in the presence of zfMID (5.9 μmol mg^{-1} min^{-1}) and SERCA in the presence of hPLN (6.1 μmol mg^{-1} min^{-1}). Finally, the Cys^{46}-to-Tyr mutation did not change the ability of hPLN to alter the apparent calcium affinity (K_{Ca} values of 0.89 and 0.88 μM, respectively) or maximal activity of SERCA (V_{max} values of 6.6 and 6.1 μmol mg^{-1} min^{-1}, respectively). It is interesting to note that the Cys^{46}-to-Tyr substitution resulted in a monomeric variant of hPLN by SDS-PAGE (data not shown), despite the fact that both human and zebrafish PLN can form pentamers.

3-2.3. Removal of the zebrafish PLN tail. A distinctive feature of zfPLN is the unique luminal extension at the C-terminal end of the protein (Ser^{53}-Phe-His-Gly-Met^{57}, which is lacking in all other known PLN sequences. While SLN contains a luminal domain that contributes to SERCA inhibition (11), the key question was whether or not the luminal extension of zfPLN contributes to its inhibitory properties. To test this, we created two truncation variants of zfPLN, one with the last five C-terminal residues removed and one

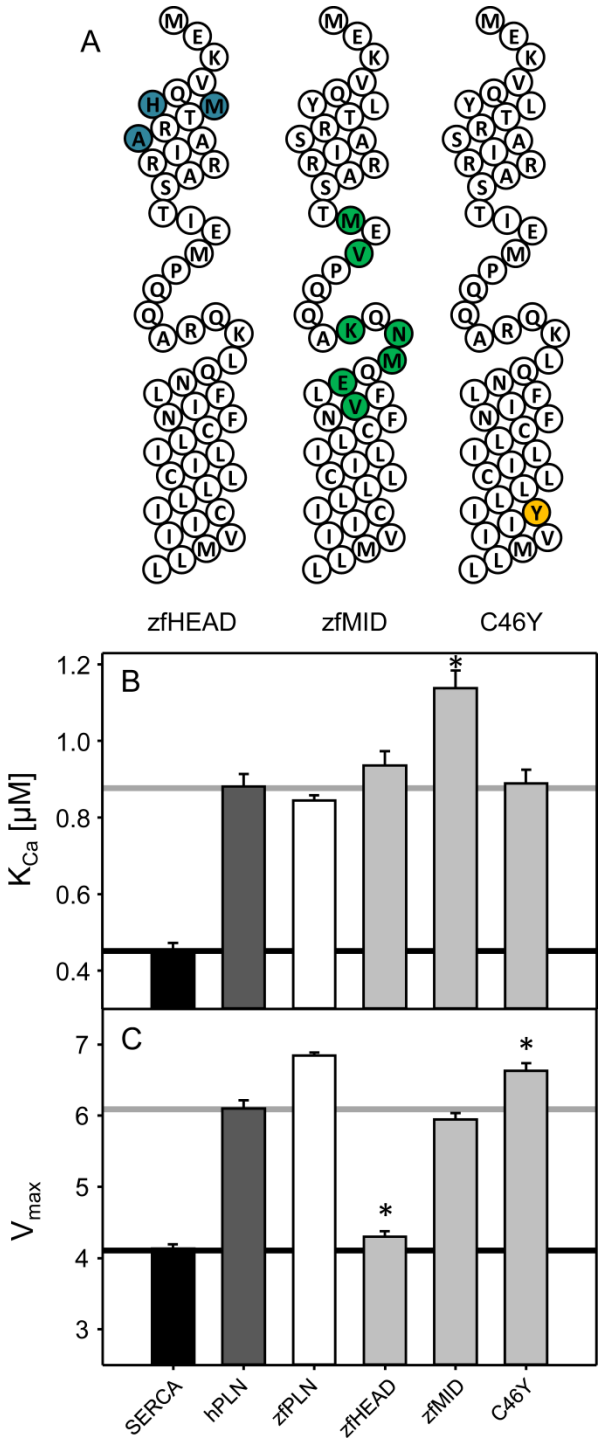

Figure 3-3. Cytoplasmic and transmembrane hPLN-zfPLN chimeras. (**A**) Topology model for zfHEAD, zfMIDDLE, and C46Y chimeras (*white*, conserved residues; *colored*, variant zfPLN residues). K_{Ca} (**B**) and V_{max} (**C**) values were determined from ATPase activity measurements for SERCA in the absence and presence of zfHEAD, zfMIDDLE, and C46Y chimeras. Each data point is the mean ± S.E. (*error bars*) ($n \geq 4$). The V_{max}, K_{Ca}, and n_H are given in Table 3-1. *Asterisks* indicate comparisons against SERCA in the presence of wild-type hPLN ($p \geq 0.05$).

with the last six residues removed (designated zfPLN(-5) and zfPLN(-6), respectively; Fig. 3-4A). It should be mentioned that removal of the luminal tail did not affect the ability of either of the truncated peptides to form pentamers by SDS-PAGE (data not shown). Inclusion of zfPLN (-5) in proteoliposomes resulted in a significant loss of SERCA inhibition (K_{Ca} of 0.70 μM calcium; ~62% of zfPLN inhibitory capacity) and its effect on V_{max} did not significantly differ from that of zfPLN (V_{max} of 7.2 and 6.9 μmol mg^{-1} min^{-1}, respectively; Fig. 3-4 and Table 3-1). The zfPLN(-6) truncation behaved in a similar manner, with a K_{Ca} of 0.67 μM calcium (~54% of zfPLN inhibitory capacity) and a V_{max} of 6.4 μmol mg^{-1} min^{-1} for SERCA. Thus, the luminal extension of zfPLN appeared to encode ~40% of its inhibitory activity. This contrasts with what is known for PLN and SLN, where the inhibitory activity of PLN is encoded by its transmembrane domain (~80% (30)) and the inhibitory activity of SLN is encoded by its luminal tail (~75% (11)). Nonetheless, there is an interesting parallel between the luminal extensions of zfPLN and SLN in that they both contribute to SERCA inhibition. The different magnitudes of SERCA inhibition attributable to the zfPLN and SLN luminal domains (~40% versus ~75%, respectively) suggest that zfPLN may be a hybrid PLN-SLN regulator of SERCA.

3-2.4. Adding the zebrafish PLN luminal tail to human PLN. In order to further characterize the significance of the zfPLN tail on SERCA inhibition, we wondered what would happen if the luminal tail were transferred to hPLN. To this end, two chimeric constructs were developed, one with the last five C-terminal residues and one with the last six residues of zfPLN added to the C-terminus of hPLN (designated hPLN (+5) and hPLN (+6), respectively; Fig. 3-5A). Two different lengths of the zfPLN luminal tail were added in order to ensure we tested the effects of a complete luminal domain. We hoped that the addition of the zfPLN tail region to hPLN would confirm the involvement

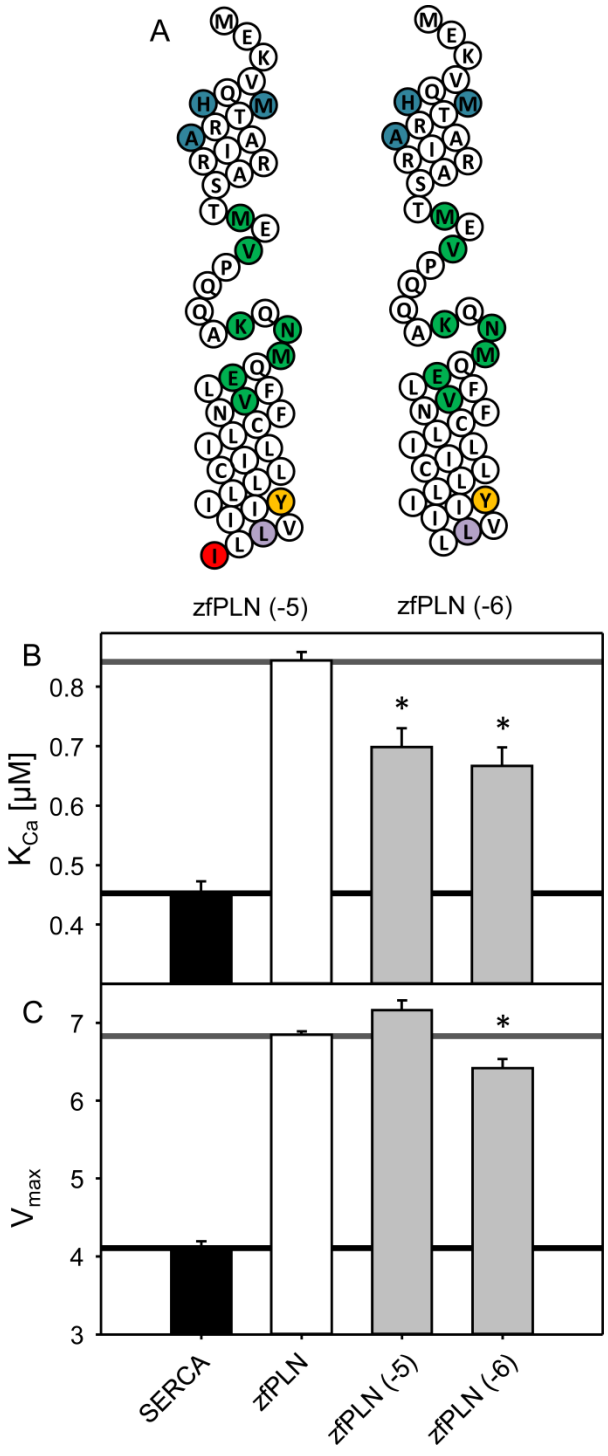

Figure 3-4. Removal of the zfPLN luminal tail. (**A**) Topology model for zfPLN (-5) and zfPLN (-6) (*white*, conserved residues; *colored*, variant zfPLN residues). K_{Ca} (**B**) and V_{max} (**C**) values were determined from ATPase activity measurements for SERCA in the absence and presence of zfPLN (-5) and zfPLN (-6) truncation variants. Each data point is the mean ± S.E. (*error bars*) ($n \geq 4$). The V_{max}, K_{Ca}, and n_H are given in Table 3-1. *Asterisks* indicate comparisons against SERCA in the presence of wild-type zfPLN ($p \geq 0.05$).

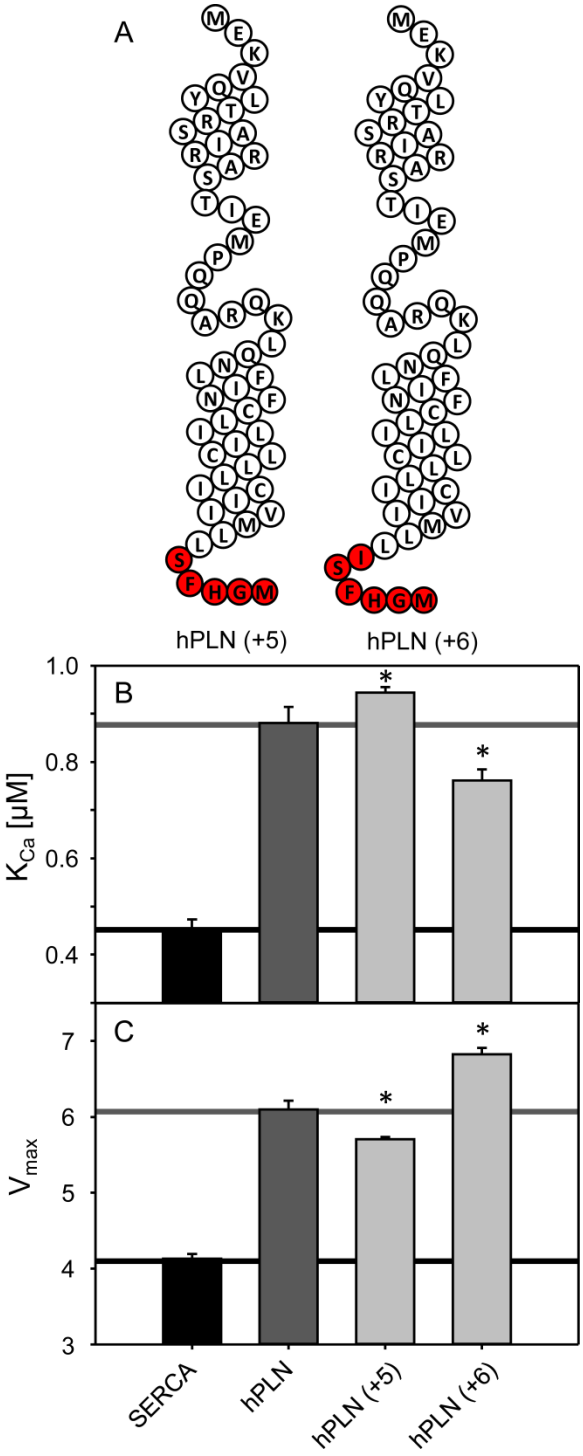

Figure 3-5. Transferring the luminal tail of zfPLN to hPLN. (**A**) Topology model for hPLN (+5) and hPLN (+6) (*white*, hPLN residues; *red*, zfPLN luminal domain). K_{Ca} (**B**) and V_{max} (**C**) values were determined from ATPase activity measurements for SERCA in the absence and presence of hPLN (+5) and hPLN (+6) truncation variants. Each data point is the mean ± S.E. (*error bars*) ($n \geq 4$). The V_{max}, K_{Ca}, and n_H are given in Table 3-1. *Asterisks* indicate comparisons against SERCA in the presence of wild-type hPLN ($p \geq 0.05$).

of the tail in SERCA inhibition. In the co-reconstituted proteoliposomes, hPLN (+5) resulted in a slight increase in the apparent calcium affinity (K_{Ca} of 0.94 μM calcium) and a decrease in the maximal activity (V_{max} of 5.7 μmol mg^{-1} min^{-1}) of SERCA, as compared to hPLN (Fig. 3-5 and Table 3-1). Inclusion of hPLN (+6) chimera into proteoliposomes also had minor effects on K_{Ca} (K_{Ca} of 0.76 μM calcium) and the maximal activity (V_{max} of 6.8 μmol mg^{-1} min^{-1}) of SERCA, but these effects were opposite to those found in the presence of hPLN (+5). Thus, these observations are in agreement with the zfPLN truncation constructs and further demonstrate that the zfPLN luminal extension functions as an inhibitory domain. In addition, they show that the zfPLN luminal domain needs to be properly positioned for effective SERCA inhibition.

3-2.5. Replacing the luminal tail of zebrafish PLN with the luminal tail of SLN. In a previous study (11), we demonstrated that the luminal extension of SLN is a distinct and transferrable functional domain. Seeing the structural parallels between zfPLN and SLN, despite the differences in the tail sequences, we decided to test whether substituting the zfPLN tail with the luminal domain of SLN would result in a peptide which would retain zfPLN inhibitory characteristics. We constructed a chimera with the last five residues of SLN (Arg^{27}-Ser-Tyr-Gln-Tyr^{31}) added after Ile^{52} of zfPLN (designated zfPLN-SLN_{tail}; Fig. 3-6A). The calcium-dependent ATPase activity was measured for SERCA in the presence of this chimera, where SERCA alone served as a negative control and SERCA in the presence of wild-type zfPLN and wild-type SLN served as positive controls (Fig. 3-6 and Table 3-1). Compared to zfPLN, including zfPLN-SLN_{tail} in proteoliposomes resulted in super-inhibition of SERCA (ΔK_{Ca} of 1.04 μM). The chimera also resulted in a drastic decrease in the maximal activity of SERCA that was comparable to that of SERCA alone (ΔV_{max} of 0.6). Thus, replacing the zfPLN luminal domain with that of SLN had a synergistic effect on the apparent calcium affinity and the maximal activity of

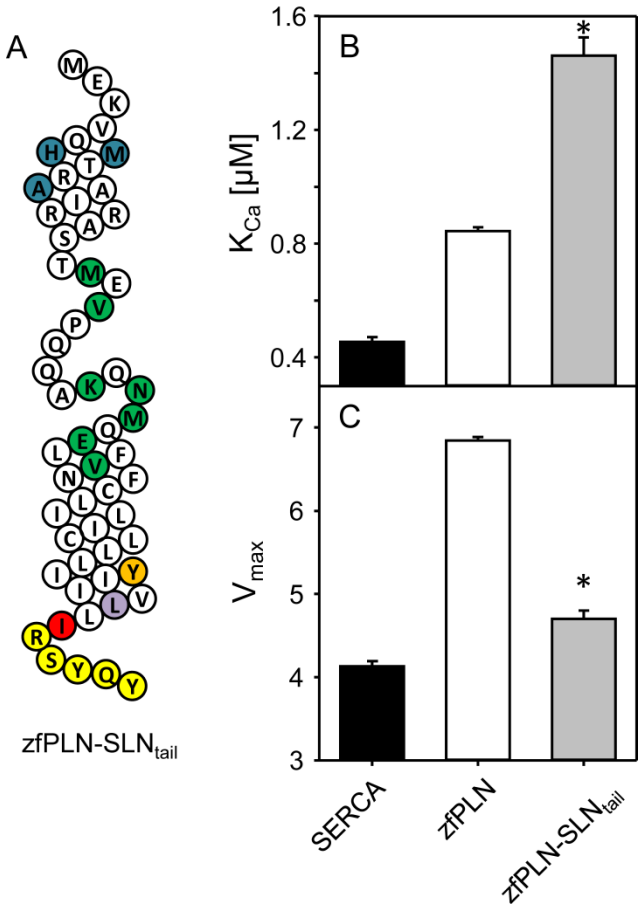

Figure 3-6. Replacing the luminal tail of zfPLN with the luminal tail of SLN. (**A**) Topology model for zfPLN-SLN_{tail} (*white*, conserved PLN residues; *colored*, variant zfPLN residues; *yellow*, SLN luminal domain). K_{Ca} (**B**) and V_{max} (**C**) values were determined from ATPase activity measurements for SERCA in the absence and presence of zfPLN-SLN_{tail} chimera. Each data point is the mean ± S.E. (*error bars*) ($n \geq 4$). The V_{max}, K_{Ca}, and n_H are given in Table 3-1. *Asterisks* indicate comparisons against SERCA in the presence of wild-type zfPLN ($p \geq 0.05$).

SERCA. This correlated well with the previously characterized PLN-SLN chimeras (11) which also exhibited the same inhibitory characteristics on SERCA (large increase in K_{Ca} and decrease in V_{max}). These observations indicate that the luminal domain of zfPLN cannot be replaced by the luminal domain of SLN and that both of these domains have distinct regulatory functions.

3-3. Discussion

3-3.1. Human versus zebrafish PLN. As shown in Fig. 3-1, the various primary sequences of PLN are highly conserved among vertebrates, unequivocally confirming the important function that this protein has in SERCA regulation. Despite the high homology, there are significant differences in the sequence composition of PLN found in mammalian and non-mammalian species. The mammalian forms of PLN only differ at one or two positions (Glu^{2}-to-Asp and Lys^{27}-to-Asn), whereas the non-mammalian forms have as many as eighteen residues which differ from the human counterpart. It is necessary to mention that zebrafish contain two genes for phospholamban (Fig. 3-1), one on chromosome 17 (isoform 1) and the other on chromosome 20 (isoform 2). The only difference between the two isoforms is the C-terminal extension present in isoform 2. It is unknown whether both of these proteins are expressed and under what conditions. In this study we decided to functionally characterize zfPLN isoform 2 for several reasons. First, it has the highest degree of sequence variation among all of the known PLN sequences. Second, it has a unique luminal extension that resembles the luminal domain of SLN and which might be involved in SERCA regulation from the luminal side of the SR membrane. Third, studying the SERCA regulation by zfPLN can provide insights into the mechanism of SERCA regulation by other forms of non-mammalian PLN, as all of them seem to contain sequence variations in the same regions of the protein. Moreover, it

allows us to examine more complex sequence changes in PLN, beyond the usual single missense mutations. Because this is the first detailed characterization of a non-mammalian form of PLN, we wanted to understand whether there are differences in how PLN from lower organisms regulate SERCA activity. We wished to identify similarities and differences between these two regulators as PLN is a major determinant of cardiac muscle contractility, making it a target for heart disease therapy.

Using the co-reconstituted proteoliposomes described above, we found that wild-type zfPLN altered the apparent calcium affinity of SERCA to an equivalent magnitude as wild-type hPLN (Fig. 3-2 and Table 3-1). This inhibition was almost completely alleviated by phosphorylation of zfPLN by PKA, indicating that it also responds to β-adrenergic stimulation. It is important to note a presence of several amino acid differences around the phosphorylation and PKA recognition sites, such as Leu^{7}-to-Met, Ser^{10}-to-Ala and Ile^{18}-to-Met, and the fact that none of them seemed to have a negative effect on the efficiency of phosphorylation. At the low lipid to protein ratios used herein, hPLN has a stimulatory effect on the maximal activity of SERCA (23,30). The same trend was observed in the presence of zfPLN, although it was ~25% higher than seen for hPLN. Interestingly, the physical behaviour of zfPLN did not differ from that of its human homologue. zfPLN was readily incorporated into the proteoliposomes and formed stable homopentamers. Therefore, we concluded that despite the high sequence variations between the zebrafish and human homologues of PLN, zfPLN very closely resembles the functional characteristics of hPLN.

3-3.2. Effects of the cytoplasmic and transmembrane regions of zfPLN on SERCA activity. Because there is a high degree of sequence variation between zebrafish and human PLN, it was important to investigate whether any of these structural differences had an effect on how zfPLN regulates SERCA. In order to better understand the role of

domain Ia of zfPLN, we mutated three cytoplasmic residues (Tyr^{6}-to-His, Leu^{7}-to-Met, Ser^{10}-to-Ala) in hPLN to match the ones in zfPLN (zfHEAD; Fig. 3-3A). Therefore, any changes in the inhibitory properties of PLN would be attributed to the three mutations present in the zfHEAD chimera. We found that there was no effect of this peptide on the apparent calcium affinity of SERCA as compared to wild-type hPLN, but the V_{max} effect was restored to SERCA levels. Previous mutagenesis work found that alanine substitutions of Tyr^{6} and Ser^{10} had little effect on K_{Ca}; however, Leu^{7}-to-Ala mutation resulted in loss of function, presumably because this amino acid side chain is facing the SERCA pump as opposed to the other two (Fig. 3-7) (20,23,32). Moreover, the maximal activity of SERCA was significantly decreased in the presence of Tyr^{6}-to-His and Leu^{7}-to-Met. Since in hPLN, Leu^{7} seems to form the strongest interactions with SERCA, it is reasonable to assume that methionine at this position is mainly responsible for the drastic decrease in V_{max}.

zfPLN contains a cluster of residues that differ from the hPLN sequence in the Ib linker region and the N-terminal part of the transmembrane helix. As these regions of PLN contain several essential residues, we created a chimera with these seven substitutions on the wild-type hPLN background (zfMID; Fig. 3-3A) to see if they affect the inhibitory properties of PLN. Inclusion of the zfMID chimera resulted in gain of inhibitory function and no significant change in the maximal activity of SERCA, as compared to wild-type hPLN (Fig. 3-3B and C). This indicated that at least some of these residues must be necessary for SERCA regulation. Early mutagenesis studies found that Ile^{18}-to-Ala and Met^{20}-to-Ala did not have an effect on PLN inhibition (20), allowing us to assume that amino acid substitutions at these positions do not contribute to the inhibitory properties of zfMID chimera. For the remaining five residues, we divided them into two categories: residues facing SERCA (Asn^{27}, Glu^{30}, Val^{33}; Fig. 3-7C) and residues

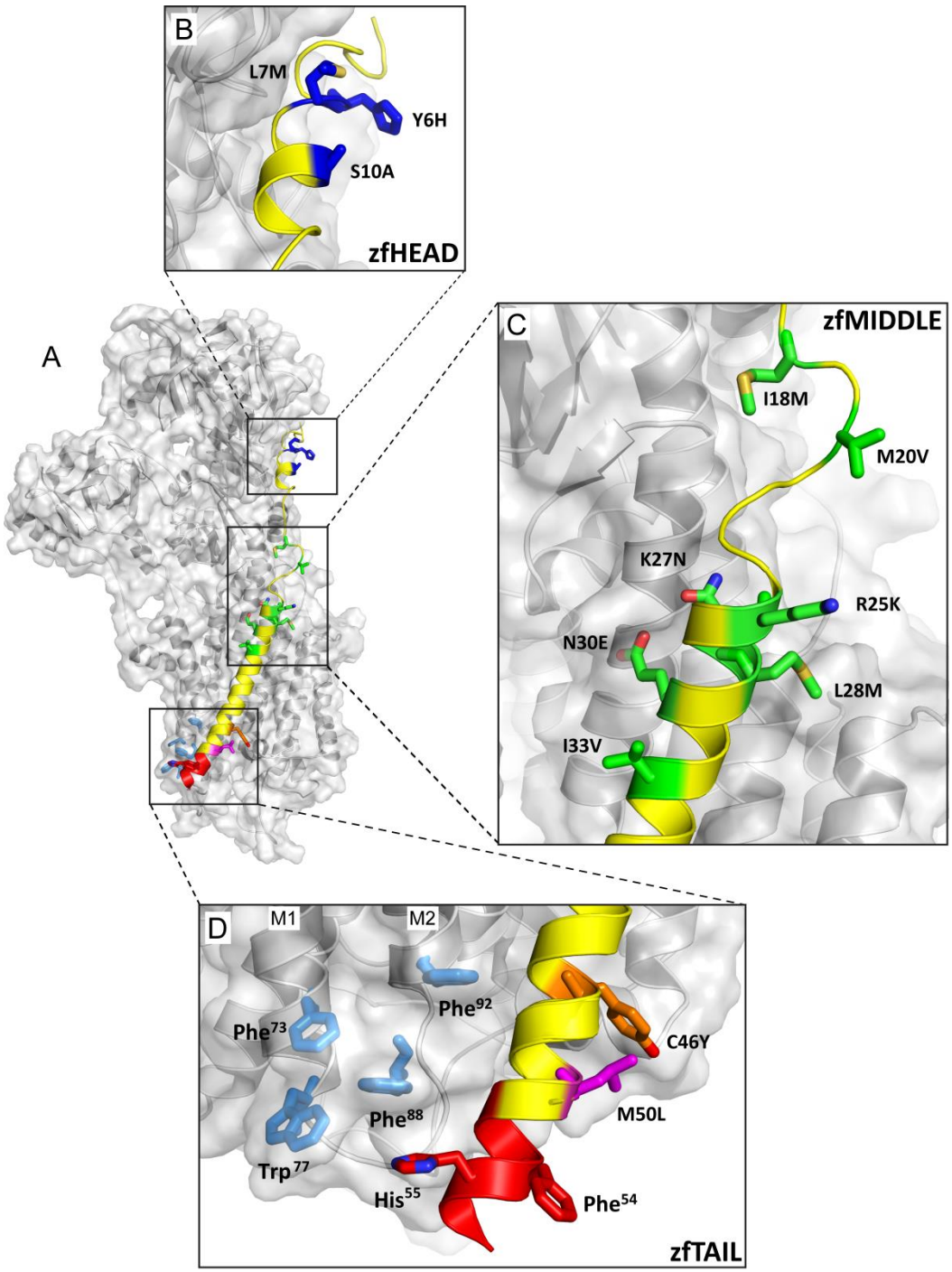

Figure 3-7. Molecular model showing the interactions of zfPLN with SERCA. (**A**) SERCA (*grey*) is in the E2 conformation (15). Residues that differ from the hPLN sequence are shown as stick representation and are color coded based on Figure 3-1A. (**B-D**) Close-up views of the zfHEAD (**B**), zfMIDDLE (**C**), and zfTAIL (**D**) regions of zfPLN. Phe^{54} and His^{55} (*red*) are in proximity to the luminal end of TM1-TM2 of SERCA (particularly Phe^{88} and Phe^{92}, which are in light blue). The zfTAIL region of zfPLN is shown as a continuous α-helix, although we anticipate that it may be partially unwound in the SERCA-zfPLN inhibitory complex.

facing away from SERCA (Lys^{25}, Met^{28}; Fig. 3-7C). The pair of residues facing away from SERCA is unlikely to have significant contribution to inhibitory properties of PLN, as alanine substitutions at these positions have been shown to have minor effects on SERCA activity (20). In addition, Arg^{25}-to-Lys is a highly conservative substitution, making it unlikely to have different interactions with SERCA. Lastly, we have to consider the final three substitutions found on the side of PLN that faces the calcium pump. Mutagenesis studies in co-expression and co-reconstitution systems have shown all three residues to be essential for proper SERCA regulation by PLN (20,23). Mutation of any of these residues to alanine resulted in gain of inhibition. Furthermore, modeling studies based on functional and cross-linking data indicated that Lys^{27} interacts with Leu^{321} of SERCA, and Asn^{30} is involved in hydrogen bonding with Thr^{317} of SERCA (Fig. 3-7C) (38). Asn^{27} is found in many mammalian forms of PLN (Fig. 3-1), and it has been shown that substitution of Lys^{27} in hPLN results in a mild gain of inhibition (20). Asn^{30}-to-Glu is a charge reversal substitution, which might result in different interaction with SERCA. Therefore, we conclude that the gain of inhibition seen for zfMID chimera is most likely due to interaction of Asn^{27}, Glu^{30} and Val^{33} with SERCA.

The final three residues in the transmembrane domain of zfPLN that differ from the human sequence are Tyr^{46}, Leu^{50} and Ile^{52}. We wanted to investigate the role of an aromatic tyrosine on the function of PLN, thus we mutated Cys^{46} in hPLN to Tyr. We found that Cys^{46}-to-Tyr had wild-type like properties but it was unable to form stable pentamers. The PLN pentamer is thought to be predominantly formed by a leucine-isoleucine zipper with all five monomers of the pentamer contributing. Mutation of any of these residues to alanine prevents pentamer formation, indicating their important role in the oligomer assembly. Additionally, the three cysteines (Cys^{36}, Cys^{41} and Cys^{46}) found in the transmembrane domain of PLN have also been shown to be essential for

pentamer stability (33,39-42), explaining the effects of Cys^{46}-to-Tyr mutation. It is intriguing that SLN does not readily form higher order oligomers and also has an aromatic residue at the equivalent position (Trp^{23}). Aside from the luminal extension, this is another feature of zfPLN which resembles the SLN sequence. Since we did not detect any difference in the ability of full-length zfPLN and hPLN to form pentamers, it must be the unique zfPLN features that enhance pentamer stability (e.g. Leu^{50} instead of Met at this position might enhance the pentamer formation).

3-3.3. The luminal extension of zebrafish PLN is a functional regulatory domain. The C-terminal end of mammalian and avian PLN is perfectly conserved (Fig. 3-1), implying that this region of the protein has important functional and structural features. Therefore, it is surprising that the PLN homologues in fish, especially the zfPLN, significantly differ in the amino acid composition in this region. In fact, the C-terminal end of zfPLN is reminiscent of the C-terminal end of SLN, suggesting the possibility of co-evolution of SLN and PLN. The luminal domain of SLN has been shown to play important roles in the SR retention as well as inhibition of the calcium pump (11,43,44). For PLN, SR retention occurs via the di-arginine motif in its cytoplasmic domain as well as through the direct interaction with SERCA (45). Because this di-arginine motif is perfectly preserved in zfPLN, it is difficult to envision the necessity of having the luminal domain to perform the same task. While we did not investigate zfPLN targeting, our results indicate that the removal of as many as six residues from the C-terminal end of zfPLN did not have an effect on its ability to be incorporated or retained in the proteoliposomes. Given these observations, we sought to examine the regulatory capacity of the zfPLN luminal domain.

To test the inhibitory contributions of the luminal extension of zfPLN, two truncation variants were first constructed. The first construct was missing the last five (zfPLN(-5)) and the second the last six (zfPLN(-6)) C-terminal residues (Fig. 3-4A). We

hypothesized that if the luminal extension of zfPLN plays a role in regulating SERCA, its complete removal would alter its functional properties. Indeed, the truncation variants lost their ability to properly regulate calcium affinity of SERCA, lowering its inhibitory properties to ~54-62% of zfPLN (Fig. 3-4, B and C; Table 3-1). Interestingly, there was little difference in the extent to which these chimeras regulated SERCA, suggesting that Ile^{52} is not part of this regulatory domain but the last hydrophobic amino acid in the transmembrane domain of zfPLN. To further test the luminal domain as an independent functional entity, we added the last five and six residues of zfPLN to the C-terminus of the hPLN sequence (Fig. 3-5A). In the context of these chimeras, the full-length hPLN sequence was expected to retain wild-type functional properties, and the functional effects of the zfPLN luminal domain were expected to be additive. These two chimeras had opposite effect on the apparent calcium affinity of SERCA. The shorter chimera (zfPLN(+5)) resulted in a significant gain of inhibitory function as expected, whereas the long chimera (zfPLN(+6)) resulted in an unexpected mild loss of function (Fig. 3-5, B and C; Table 3-1). These opposite effects can be explained by taking the positioning of the luminal residues into account. In the short chimera, the luminal residues are in the same positions as in the wild-type zfPLN, assuring identical spatial orientation of the luminal amino acid side chains. On the other hand, the long chimera has an additional residue between the end of the transmembrane domain and the beginning of the luminal domain, resulting in a shift of the tail one position down. Such a shift may not allow for the necessary side chains to interact with residues on SERCA, therefore rendering a dysfunctional luminal tail. Functional and structural analyses of SLN indicate that the two aromatic residues in the luminal domain are crucial for proper inhibition of SERCA (11,44). Although there is little similarity between the luminal domains of SLN and zfPLN, the zfPLN tail also has two aromatic amino acids in its sequence, Phe^{54} and His^{55}. Interestingly, based on the sequence alignment, Phe^{54} of zfPLN assumes the same

position as the essential Tyr^{31} of SLN (Fig. 3-1). Therefore, it is possible for Phe^{54} and His^{55} to form important molecular interactions with at least some of the aromatic residues at the base of TM1-TM2 of SERCA (particularly Phe^{88} and Phe^{92}, Fig. 3-7D).

The striking difference between the way zfPLN and SLN luminal domains regulate SERCA is the potent inhibition associated with the SLN tail. Nevertheless, we decided to replace the luminal domain of zfPLN with that of SLN and examine the effect on SERCA inhibition. A zfPLN-SLN_{tail} chimera with ^{53}Ser-Phe-His-Gly-Met^{57} sequence replaced by SLN's Arg^{27}-Ser-Tyr-Gln-Tyr^{31} was constructed (Fig. 3-6A). As expected, zfPLN-SLN_{tail} chimera turned out to be a potent super-inhibitor of SERCA (Fig. 3-6, B and C; Table 3-1). This correlated well with our previous study, in which hPLN-SLN_{tail} chimera was shown to alter K_{Ca} and V_{max} to a similar extent (11). It is important to note that addition of the SLN tail to zfPLN altered K_{Ca} of SERCA to a lesser degree than in the hPLN-SLN_{tail} chimera (ΔK_{Ca} of 1.04μM calcium for zfPLN-SLN_{tail} versus 1.38μM calcium for hPLN-SLN_{tail}). This supports our truncation data, which indicate that zfPLN missing the luminal tail partly lost its ability to lower the apparent calcium affinity of SERCA.

Another interesting aspect of the luminal domain of zfPLN is that it is not involved in regulation of the maximal activity of SERCA. This was demonstrated by the above mentioned truncation and chimeric variants for which in most part V_{max} values did not significantly differ from the wild-type controls. This is another striking difference between the SLN luminal tail which has been shown to be responsible for suppression of V_{max} (11). Together, the data discussed above clearly demonstrate the specificity of the luminal domain of zfPLN. In marked contrast to mammalian PLNs, the sequence variations throughout the cytoplasmic and transmembrane domains of zfPLN render it dependent on a unique luminal domain for proper SERCA regulation.

3-3.4. Conclusions. In summary, by performing a detailed analysis of the most divergent PLN sequence known, we demonstrated that despite many sequence variations between zfPLN and hPLN, both peptides regulate SERCA in a similar fashion. We have identified residues in each domain of zfPLN that affect its physical properties as well as ones which influence a functional effect on SERCA activity. Most importantly, we identified the unique C-terminal tail as a functional domain of zfPLN capable of regulating the apparent calcium affinity of SERCA. Thus, we conclude that the sequence variations among the different PLN homologues are balanced in a way that results in an almost identical functional effect.

3-4. Experimental Procedures

3-4.1. Expression and Purification of Recombinant PLN. Human and zebrafish PLN variants were expressed and purified as previously described (31). Mutants were confirmed by DNA sequencing (TAGC Sequencing, University of Alberta) and by MALDI-TOF mass spectrometry (Institute for Biomolecular Design, University of Alberta). To phosphorylate PLN, detergent solubilized PLN was treated with the catalytic subunit of PKA (Sigma Aldrich) (23).

3-4.2. Co-reconstitution of SERCA and Recombinant PLN. Routine procedures were used to purify SERCA1a from rabbit skeletal muscle SR vesicles (46,47) and functionally reconstitute it into proteoliposomes with PLN as previously described (23). The purified co-reconstituted proteoliposomes typically yielded final molar stoichiometries of 1 SERCA, 4.5 SLN, and 120 lipids. The SERCA and PLN concentrations were determined by BCA assay and quantitative SDS-PAGE (34).

3-4.3. Activity Assays. Calcium-dependent ATPase activities of the co-reconstituted proteoliposomes were measured by a coupled-enzyme assay (48). The coupled enzyme assay reagents were of the highest purity available (Sigma-Aldrich, Oakville, ON). All co-reconstituted peptide constructs were compared to a negative control (SERCA reconstituted in the absence of PLN) and a matched positive control (SERCA co-reconstituted in the presence of either wild-type hPLN or wild-type zfPLN). A minimum of three independent reconstitutions and activity assays were performed for each peptide, and the calcium-dependent ATPase activity was measured over a range of calcium concentrations (0.1 to 10 μM) for each assay. This method has been described in detail (23). The K_{Ca} (calcium concentration at half-maximal activity), the V_{max} (maximal activity) and the n_H (Hill coefficient) were calculated based on non-linear least-squares fitting of the activity data to the Hill equation using Sigma Plot software (SPSS Inc., Chicago, IL). Errors were calculated as the standard error of the mean for a minimum of three independent measurements. Comparison of K_{Ca}, V_{max} and n_H parameters was carried out using ANOVA (between-subjects, one-way analysis of variance) followed by the Holm-Sidak test for pairwise comparisons (Sigma Plot).

3-5. References

1. Moller, J. V., Olesen, C., Winther, A. M., and Nissen, P. (2010) The sarcoplasmic Ca2+-ATPase: design of a perfect chemi-osmotic pump. *Quarterly reviews of biophysics* **43**, 501-566

2. MacLennan, D. H., and Kranias, E. G. (2003) Phospholamban: a crucial regulator of cardiac contractility. *Nature reviews. Molecular cell biology* **4**, 566-577

3. Kirchberber, M. A., Tada, M., and Katz, A. M. (1975) Phospholamban: a regulatory protein of the cardiac sarcoplasmic reticulum. *Recent advances in studies on cardiac structure and metabolism* **5**, 103-115

4. Katz, A. M., Repke, D. I., Kirchberger, M. A., and Tada, M. (1974) Calcium-binding sites and calcium uptake in cardiac microsomes: effects of varying Ca++ concentration, and of an adenosine-3',5'- monophosphate-dependent protein

kinase. *Recent advances in studies on cardiac structure and metabolism* **4**, 427-436

5. Tada, M., and Kirchberger, M. A. (1976) Significance of the membrane protein phospholamban in cyclic AMP-mediated regulation of calcium transport by sarcoplasmic reticulum. *Recent advances in studies on cardiac structure and metabolism* **11**, 265-272

6. Odermatt, A., Taschner, P. E., Scherer, S. W., Beatty, B., Khanna, V. K., Cornblath, D. R., Chaudhry, V., Yee, W. C., Schrank, B., Karpati, G., Breuning, M. H., Knoers, N., and MacLennan, D. H. (1997) Characterization of the gene encoding human sarcolipin (SLN), a proteolipid associated with SERCA1: absence of structural mutations in five patients with Brody disease. *Genomics* **45**, 541-553

7. Odermatt, A., Becker, S., Khanna, V. K., Kurzydlowski, K., Leisner, E., Pette, D., and MacLennan, D. H. (1998) Sarcolipin regulates the activity of SERCA1, the fast-twitch skeletal muscle sarcoplasmic reticulum Ca2+-ATPase. *The Journal of biological chemistry* **273**, 12360-12369

8. Wawrzynow, A., Theibert, J. L., Murphy, C., Jona, I., Martonosi, A., and Collins, J. H. (1992) Sarcolipin, the "proteolipid" of skeletal muscle sarcoplasmic reticulum, is a unique, amphipathic, 31-residue peptide. *Archives of biochemistry and biophysics* **298**, 620-623

9. Asahi, M., Sugita, Y., Kurzydlowski, K., De Leon, S., Tada, M., Toyoshima, C., and MacLennan, D. H. (2003) Sarcolipin regulates sarco(endo)plasmic reticulum Ca2+-ATPase (SERCA) by binding to transmembrane helices alone or in association with phospholamban. *Proceedings of the National Academy of Sciences of the United States of America* **100**, 5040-5045

10. Morita, T., Hussain, D., Asahi, M., Tsuda, T., Kurzydlowski, K., Toyoshima, C., and Maclennan, D. H. (2008) Interaction sites among phospholamban, sarcolipin, and the sarco(endo)plasmic reticulum Ca(2+)-ATPase. *Biochem Biophys Res Commun* **369**, 188-194

11. Gorski, P. A., Glaves, J. P., Vangheluwe, P., and Young, H. S. (2013) Sarco/endoplasmic reticulum calcium ATPase (SERCA) inhibition by sarcolipin is encoded in its luminal tail. *The Journal of biological chemistry*

12. Winther, A. M., Bublitz, M., Karlsen, J. L., Moller, J. V., Hansen, J. B., Nissen, P., and Buch-Pedersen, M. J. (2013) The sarcolipin-bound calcium pump stabilizes calcium sites exposed to the cytoplasm. *Nature* **495**, 265-269

13. Toyoshima, C., Iwasawa, S., Ogawa, H., Hirata, A., Tsueda, J., and Inesi, G. (2013) Crystal structures of the calcium pump and sarcolipin in the Mg2+-bound E1 state. *Nature* **495**, 260-264

14. Toyoshima, C., Asahi, M., Sugita, Y., Khanna, R., Tsuda, T., and MacLennan, D. H. (2003) Modeling of the inhibitory interaction of phospholamban with the

Ca2+ ATPase. *Proceedings of the National Academy of Sciences of the United States of America* **100**, 467-472

15. Seidel, K., Andronesi, O. C., Krebs, J., Griesinger, C., Young, H. S., Becker, S., and Baldus, M. (2008) Structural Characterization of Ca^{2+}-ATPase-Bound Phospholamban in Lipid Bilayers by Solid-State Nuclear Magnetic Resonance (NMR) Spectroscopy. *Biochemistry* **47**, 4369-4376

16. Simmerman, H. K., Collins, J. H., Theibert, J. L., Wegener, A. D., and Jones, L. R. (1986) Sequence analysis of phospholamban. Identification of phosphorylation sites and two major structural domains. *The Journal of biological chemistry* **261**, 13333-13341

17. Zamoon, J., Mascioni, A., Thomas, D. D., and Veglia, G. (2003) NMR solution structure and topological orientation of monomeric phospholamban in dodecylphosphocholine micelles. *Biophys J* **85**, 2589-2598

18. Haghighi, K., Kolokathis, F., Gramolini, A. O., Waggoner, J. R., Pater, L., Lynch, R. A., Fan, G. C., Tsiapras, D., Parekh, R. R., Dorn, G. W., 2nd, MacLennan, D. H., Kremastinos, D. T., and Kranias, E. G. (2006) A mutation in the human phospholamban gene, deleting arginine 14, results in lethal, hereditary cardiomyopathy. *Proceedings of the National Academy of Sciences of the United States of America* **103**, 1388-1393

19. Medeiros, A., Biagi, D. G., Sobreira, T. J., de Oliveira, P. S., Negrao, C. E., Mansur, A. J., Krieger, J. E., Brum, P. C., and Pereira, A. C. (2011) Mutations in the human phospholamban gene in patients with heart failure. *American heart journal* **162**, 1088-1095 e1081

20. Kimura, Y., Asahi, M., Kurzydlowski, K., Tada, M., and MacLennan, D. H. (1998) Phospholamban domain Ib mutations influence functional interactions with the Ca^{2+}-ATPase isoform of cardiac sarcoplasmic reticulum. *J. Biol. Chem.* **273**, 14238-14241

21. Cantilina, T., Sagara, Y., Inesi, G., and Jones, L. R. (1993) Comparative studies of cardiac and skeletal sarcoplasmic reticulum ATPases: effect of phospholamban antibody on enzyme activation. *J. Biol. Chem.* **268**, 17018-17025

22. Kimura, Y., Kurzydlowski, K., Tada, M., and MacLennan, D. H. (1996) Phospholamban regulates the Ca^{2+}-ATPase through intramembrane interactions. *J. Biol. Chem.* **271**, 21726-21731

23. Trieber, C. A., Douglas, J. L., Afara, M., and Young, H. S. (2005) The effects of mutation on the regulatory properties of phospholamban in co-reconstituted membranes. *Biochemistry* **44**, 3289-3297

24. Afara, M. R., Trieber, C. A., Glaves, J. P., and Young, H. S. (2006) Rational design of peptide inhibitors of the sarcoplasmic reticulum calcium pump. *Biochemistry* **45**, 8617-8627

25. Afara, M. R., Trieber, C. A., Ceholski, D. K., and Young, H. S. (2008) Peptide inhibitors use two related mechanisms to alter the apparent calcium affinity of the sarcoplasmic reticulum calcium pump. *Biochemistry* **47**, 9522-9530

26. Kimura, Y., Kurzydlowski, K., Tada, M., and MacLennan, D. H. (1997) Phospholamban inhibitory function is enhanced by depolymerization. *J. Biol. Chem.* **272**, 15061-15064

27. Bhupathy, P., Babu, G. J., and Periasamy, M. (2007) Sarcolipin and phospholamban as regulators of cardiac sarcoplasmic reticulum Ca2+ ATPase. *J Mol Cell Cardiol* **42**, 903-911

28. Will, H., Kuttner, I., Vetter, R., Will-Shahab, L., and Kemsies, C. (1983) Early presence of phospholamban in developing a chick heart. *FEBS letters* **155**, 326-330

29. Will, H., Kuttner, I., Kemsies, C., Vetter, R., and Schubert, E. (1985) Comparative analysis of phospholamban phosphorylation in crude membranes of vertebrate hearts. *Experientia* **41**, 1052-1054

30. Trieber, C. A., Afara, M., and Young, H. S. (2009) Effects of phospholamban transmembrane mutants on the calcium affinity, maximal activity, and cooperativity of the sarcoplasmic reticulum calcium pump. *Biochemistry* **48**, 9287-9296

31. Douglas, J. L., Trieber, C. A., Afara, M., and Young, H. S. (2005) Rapid, high-yield expression and purification of Ca2+-ATPase regulatory proteins for high-resolution structural studies. *Protein Expr Purif* **40**, 118-125

32. Ceholski, D. K., Trieber, C. A., and Young, H. S. (2012) Hydrophobic imbalance in the cytoplasmic domain of phospholamban is a determinant for lethal dilated cardiomyopathy. *The Journal of biological chemistry* **287**, 16521-16529

33. Ceholski, D. K., Trieber, C. A., Holmes, C. F., and Young, H. S. (2012) Lethal, hereditary mutants of phospholamban elude phosphorylation by protein kinase A. *The Journal of biological chemistry* **287**, 26596-26605

34. Young, H. S., Jones, L. R., and Stokes, D. L. (2001) Locating phospholamban in co-crystals with Ca(2+)-ATPase by cryoelectron microscopy. *Biophys J* **81**, 884-894

35. Stokes, D. L., Pomfret, A. J., Rice, W. J., Glaves, J. P., and Young, H. S. (2006) Interactions between Ca2+-ATPase and the pentameric form of phospholamban in two-dimensional co-crystals. *Biophys J* **90**, 4213-4223

36. Glaves, J. P., Trieber, C. A., Ceholski, D. K., Stokes, D. L., and Young, H. S. (2011) Phosphorylation and mutation of phospholamban alter physical interactions with the sarcoplasmic reticulum calcium pump. *Journal of molecular biology* **405**, 707-723

37. Drago, G. A., and Colyer, J. (1994) Discrimination between two sites of phosphorylation on adjacent amino acids by phosphorylation site-specific antibodies to phospholamban. *The Journal of biological chemistry* **269**, 25073-25077

38. Toyoshima, C., Asahi, M., Sugita, Y., Khanna, R., Tsuda, T., and MacLennan, D. (2003) Modeling of the inhibitory interaction of phospholamban with the Ca^{2+} ATPase. *Proc. Natl. Acad. Sci. U. S. A.* **100**, 467-472

39. Fujii, J., Maruyama, K., Tada, M., and MacLennan, D. H. (1989) Expression and site-specific mutagenesis of phospholamban. Studies of residues involved in phosphorylation and pentamer formation. *The Journal of biological chemistry* **264**, 12950-12955

40. Karim, C., Marquardt, C., Stamm, J., Barany, B., and Thomas, D. (2000) Synthetic null-cysteine phospholamban analogue and the corresponding transmembrane domain inhibit the Ca-ATPase. *Biochemistry* **39**, 10892-10897

41. Karim, C. B., Paterlini, M. G., Reddy, L. G., Hunter, G. W., Barany, G., and Thomas, D. D. (2001) Role of cysteine residues in structural stability and function of a transmembrane helix bundle. *The Journal of biological chemistry* **276**, 38814-38819

42. Chu, G., Li, L., Sato, Y., Harrer, J. M., Kadambi, V. J., Hoit, B. D., Bers, D. M., and Kranias, E. G. (1998) Pentameric assembly of phospholamban facilitates inhibition of cardiac function in vivo. *The Journal of biological chemistry* **273**, 33674-33680

43. Gramolini, A. O., Kislinger, T., Asahi, M., Li, W., Emili, A., and MacLennan, D. H. (2004) Sarcolipin retention in the endoplasmic reticulum depends on its C-terminal RSYQY sequence and its interaction with sarco(endo)plasmic Ca(2+)-ATPases. *Proceedings of the National Academy of Sciences of the United States of America* **101**, 16807-16812

44. Hughes, E., Clayton, J. C., Kitmitto, A., Esmann, M., and Middleton, D. A. (2007) Solid-state NMR and functional measurements indicate that the conserved tyrosine residues of sarcolipin are involved directly in the inhibition of SERCA1. *The Journal of biological chemistry* **282**, 26603-26613

45. Sharma, P., Ignatchenko, V., Grace, K., Ursprung, C., Kislinger, T., and Gramolini, A. O. (2010) Endoplasmic reticulum protein targeting of phospholamban: a common role for an N-terminal di-arginine motif in ER retention? *PloS one* **5**, e11496

46. Eletr, S., and Inesi, G. (1972) Phospholipid orientation in sarcoplasmic membranes: spin-label ESR and proton MNR studies. *Biochimica et biophysica acta* **282**, 174-179

47. Stokes, D. L., and Green, N. M. (1990) Three-dimensional crystals of CaATPase from sarcoplasmic reticulum. Symmetry and molecular packing. *Biophys J* **57**, 1-14

48. Warren, G. B., Toon, P. A., Birdsall, N. J., Lee, A. G., and Metcalfe, J. C. (1974) Reconstitution of a calcium pump using defined membrane components. *Proceedings of the National Academy of Sciences of the United States of America* **71**, 622-626

Chapter 4

Transmembrane helix 11 is a genuine regulator of the endoplasmic reticulum Ca^{2+} pump and acts as a functional parallel of β-subunit on α-Na^+,K^+-ATPase

This research was originally published in The Journal of Biological Chemistry.

Gorski PA, Trieber CA, Larivière E, Schuermans M, Wuytack F, Young HS, and Vangheluwe P.

Transmembrane helix 11 is a genuine regulator of the endoplasmic reticulum Ca^{2+} pump and acts as a functional parallel of β-subunit on α-Na^+,K^+-ATPase.

JBC. 2012; 287: 19876-19885.

Acknowledgements: Dr. C. Trieber purified SERCA for functional analysis. E. Larivière and M. Schuermans performed COS cell experiments. Dr. P. Vangheluwe performed phylogenetic analysis and helped with the functional characterization of TM11 constructs.

4-1. Introduction

The sarco(endo)plasmic reticulum Ca^{2+} ATPase (SERCA) generates and maintains a 1000-fold Ca^{2+} gradient over the endo/sarcoplasmic reticulum (ER/SR) membrane ensuring a high luminal Ca^{2+} concentration. This is vital to control cellular activities like contraction, secretion, growth, proliferation, differentiation and cell death (1).

Atomic resolution structures of the fast-twitch skeletal muscle SERCA1a isoform show that the SERCA Ca^{2+} ATPases cycle between an E1 conformation with high-affinity Ca^{2+}-binding sites facing the cytosol, and an E2 conformation with low-affinity Ca^{2+}-binding sites facing the lumen of the endoplasmic reticulum (2,3). SERCA consists of three cytosolic domains for ATP hydrolysis and one transmembrane (TM) domain for Ca^{2+} binding and transport. ATP hydrolysis in the cytosolic domain drives the conformational changes in the TM region that lead to the opening or closing of the gates to the Ca^{2+}-binding sites. The TM region is divided into a highly mobile part (TM1-6) that controls the access to the Ca^{2+}-binding sites, and a relatively immobile part (TM7-10) that is thought to serve as the anchoring region of the pump in the lipid bilayer (2,3).

Humans evolved three SERCA genes (SERCA1-3, human gene nomenclature *ATP2A1-3*) (4). Although their exon-intron layout is nearly entirely conserved, the 3' ends of the primary gene transcripts are subjected to alternative processing. This generates a plethora of SERCA splice variants with a specific tissue distribution and activity range (5,6). With the additional aid of tissue-specific SERCA regulators, the SERCA activity is tightly adjusted to the physiological needs of each specific cell type (6). However, how these extrinsic regulatory proteins or the intrinsic C-terminal variations alter the enzymatic properties of the Ca^{2+} ATPase remains poorly understood.

Here, we focus on the regulation of SERCA2, the oldest and most wide-spread isoform, which is alternatively processed to form the muscle-specific SERCA2a (cardiac, slow-twitch skeletal and smooth muscle) or the housekeeping SERCA2b (7). In the heart, SERCA2a is regulated by a small TM protein called phospholamban (PLN), which reduces its apparent affinity for Ca^{2+} (8). PLN occupies a hydrophobic groove in between the mobile and anchoring part of the TM domain of SERCA2a (TM2, 4, 6 and 9), leading to a stabilization of the low Ca^{2+} affinity E2 conformation (9). This interaction is relieved by phosphorylation of PLN during β-adrenergic stimulation (8). SERCA2b, on the other hand, uniquely differs from the other SERCA1-3 splice variants by housing a 49 amino acid long C-terminus (2b-tail) that imposes the unusual enzymatic properties on this pump, *i.e.* a two-fold higher apparent affinity for Ca^{2+} (K_{Ca}) and lower catalytic turnover rate (V_{max}) as compared to the muscle isoforms SERCA1a or SERCA2a (7,10). The 2b-tail increases the pump's apparent Ca^{2+} affinity, whereas PLN decreases it through a different mechanism (11,12). The 2b-tail consists of a cytosolic part (19 amino acids, Gly^{994}-Asp^{1012}), a transmembrane segment (TM11, 18 amino acids, Gly^{1013}-Tyr^{1030}), and a luminal extension (LE, 12 amino acids, Ser^{1031}-Ser^{1042}) (see Fig. 4-1A). Earlier work pointed to the luminal extension as the sole functional region of the 2b-tail (13). TM11 would interact with the anchoring part of the pump at the periphery of TM7 and TM10 (12). The short luminal extension would then follow a path from this remote site, running between luminal loops L5-6 and L7-8, towards a luminal binding site for the last four residues (^{1039}MFWS^{1042}) (see Fig. 4-1B). This functional C-terminal tetrapeptide stretch would here interact with a pocket formed in the E1 state by the upstream luminal loops. The interaction therefore stabilizes the E1 conformation, which at least partially accounts for the increased apparent Ca^{2+} affinity of SERCA2b (12).

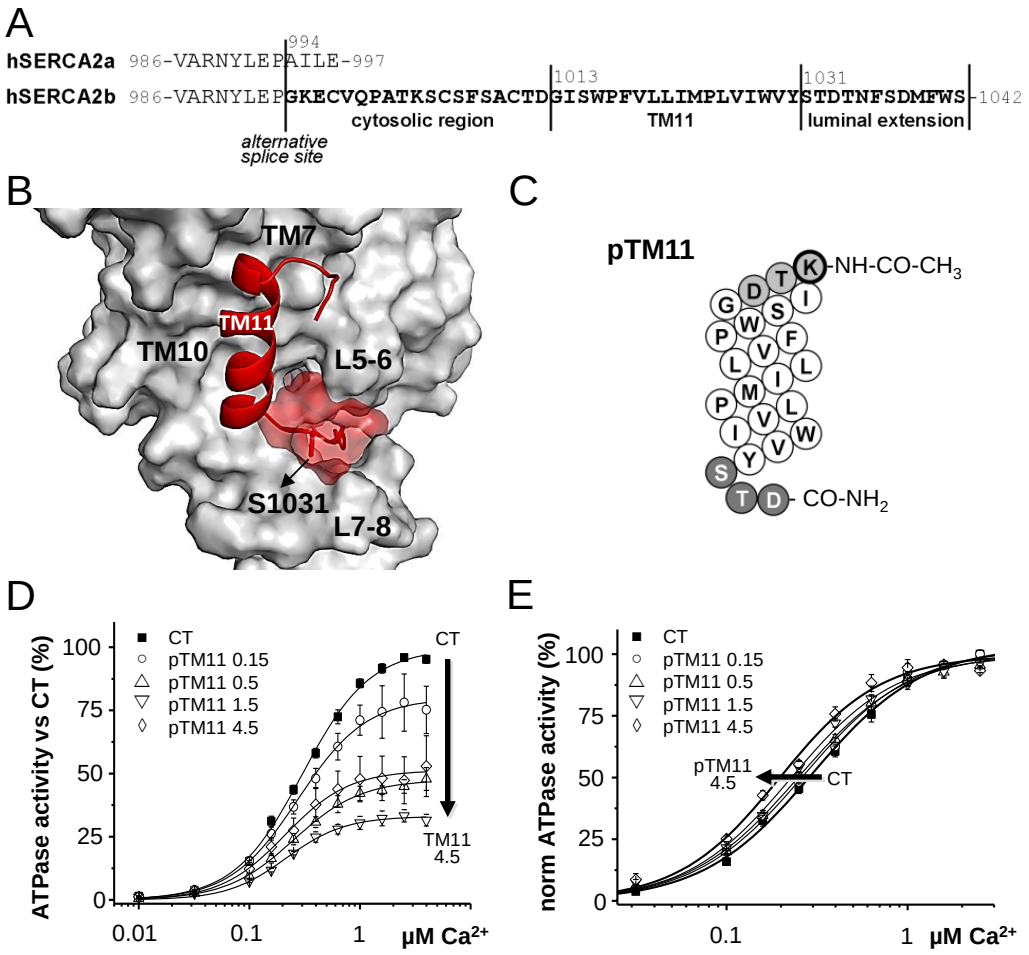

Figure 4-1. Reconstitution of SERCA1a with pTM11. (**A**) Amino acid sequence of the C-terminal part of the human SERCA2 splice variants. The 49 amino acids of the SERCA2b-tail are indicated in bold. The 4 unique amino acids of the SERCA2a-tail are shown as a comparison. (**B**) Structural model of SERCA2b shows that TM11 (*red*) descends along TM7 and TM10, with Ser^{1031} at the border of the luminal extension. S1031 might open the groove formed between L5/6 and L7/8 to allow the passage of the luminal extension. (**C**) Sequence of the synthetic pTM11 peptide (white: predicted TM11 residues; dark grey: predicted luminal residues; light grey: cytosolic residues, the incorporation of an extra lysine is indicated by the thicker circle). The peptide is N-terminally acetylated and amidated at its C-terminus. (**D**) Ca^{2+}-dependent ATPase activity of SERCA1a in the absence (control, CT) or presence of increasing amounts of pTM11 (pTM11/SERCA1a molar ratios 0.15 – 4.5). (**E**) Normalized Ca^{2+}-dependent ATPase activity of SERCA1a in the absence (CT) or presence of increasing amounts of pTM11 (pTM11/SERCA1a molar ratios 0.15 – 4.5). n = 3-10 independent reconstitutions. *Error bars*, S.E.

However, two observations indicate that the interaction of LE with its luminal interaction site does not fully explain the 2b-tail effect and that TM11 plays a more active role than simply providing a passive membrane passage. First, there remains a clear functional effect of the 2b-tail upon truncation of its last 11 residues (Thr^{1032*}). But removal of one additional residue (Ser^{1031*}) completely abolishes the effect of the 2b-tail (12,13). It is thus clear that Ser^{1031} takes a key position in the function of the 2b-tail. Second, an affinity-increasing effect is also seen in the SERCA1a context, *i.e.* when the 2b-tail is coupled to SERCA1a (SERCA1a2b chimera) (12). Because the SERCA1a luminal domain does not present the right interface for interaction with the last four residues of LE, the affinity modulation must by elimination be attributed to a more upstream region of the 2b-tail, presumably Ser^{1031} or TM11. Using peptides corresponding to TM11, we will here convincingly demonstrate that TM11 is the second functional region of the 2b-tail acting independently from Ser^{1031} and LE.

4-2. Results

4-2.1. Peptides corresponding to TM11 region of 2b-tail modulate SERCA1a activity. We showed previously that when the 2b-tail is coupled to the SERCA1a isoform, it increases the apparent Ca^{2+} affinity of the pump (12). We therefore used purified SERCA1a reconstituted in proteoliposomes as a model system (15) to address the role of TM11 and Ser^{1031}.

First, SERCA1a was reconstituted into proteoliposomes in the presence or absence of pTM11, *i.e.* a peptide that corresponds to the predicted TM11 region (Thr^{1011}-Tyr^{1030}) of the 2b-tail, but which also includes the first three residues of the luminal extension (Ser^{1031}-Asp^{1033}) (Fig. 4-1C). Several reconstitutions were carried out with

increasing molar ratios of pTM11 to SERCA1a (ratios 0.15-15; Fig. 4-1, D and E, and Fig. 4-2).

We first verified whether pTM11 was incorporated in the SERCA1a vesicles via gel electrophoresis using a 16% Tricine SDS polyacrylamide gel with 6 M urea to separate the small 2.6-kDa peptide. The dose-dependent increase of pTM11 incorporation is illustrated in supplemental Fig. 4-1A. We then determined the orientation of the peptide in the membrane. To that end, we incorporated a lysine at the N-terminus of pTM11 as an acceptor for biotin. Lysines residing at the luminal side of the vesicles remain protected against biotinylation unless the vesicles are treated with detergent (*n*-octyl-β-D-glucopyranoside), which would lead to a complete labeling of pTM11. The ratio of biotinylated pTM11 in the absence and presence of detergent at molar ratios 1.5 and 4.5 is approximately 50%, in line with an expected random orientation of pTM11 in the membrane (Fig. 4-2B).

To test whether pTM11 alters the activity of SERCA1a in the proteoliposomes, we measured via an enzyme-coupled assay the Ca^{2+}-dependent ATPase activity of SERCA1a in the presence and absence of pTM11. Our data clearly demonstrate that extrinsically added pTM11 mimics the effect of the 2b-tail (7,10), causing significant changes in V_{max} and K_{Ca} in a dose-dependent manner (Fig. 4-1, D and E). The differences between the V_{max} effects at molar ratios 0.5 to 10 are not significant (Fig. 4-1D and supplemental Fig. 4-1C). Therefore, the maximal effect of TM11 on V_{max} is observed at molar ratio 0.5 and higher. With increasing molar ratios there is a continuous increase in the apparent Ca^{2+} affinity with a maximal effect on K_{Ca} at molar ratio 4.5 and higher (Fig. 4-1E and Fig. 4-2D). The Hill coefficient remained unaffected (data not shown).

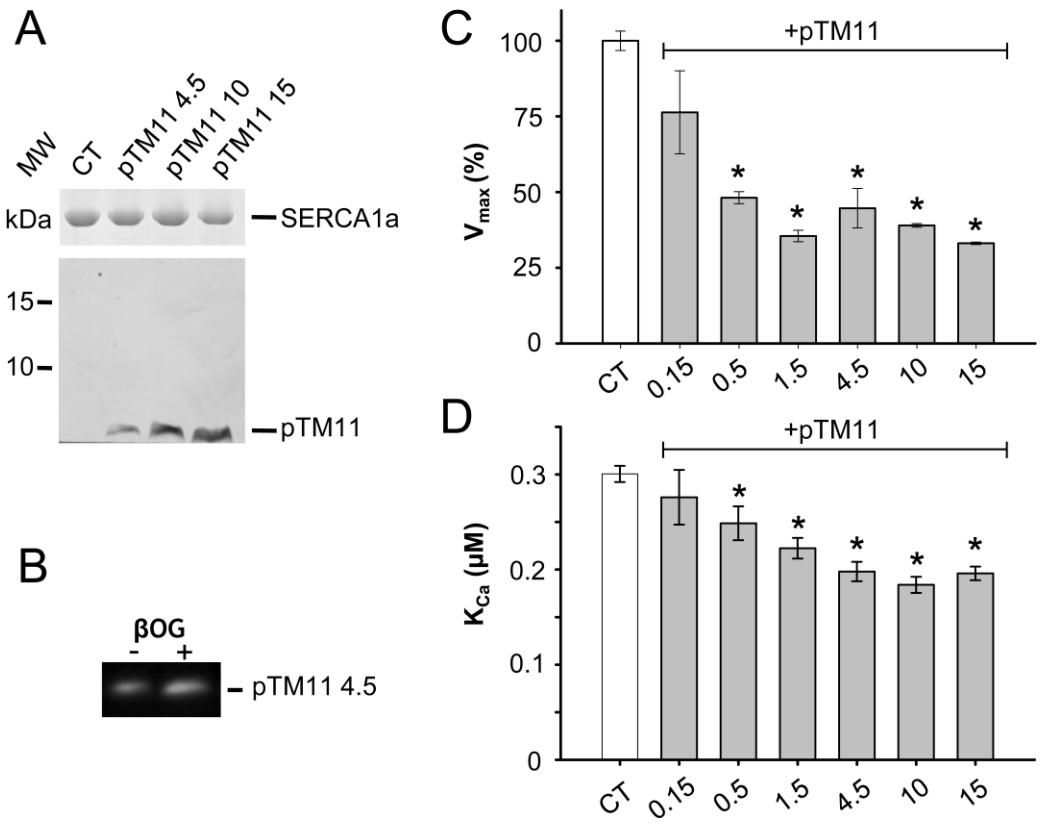

Figure 4-2. Reconstitution of SERCA1a with high concentrations of pTM11. (**A**) (top) SDS-PAGE (10% acrylamide, Coomassie blue stained gel) of 3 µg of co-reconstituted proteoliposomes shows the incorporation of SERCA. (bottom) SDS-PAGE (16% acrylamide, silver-stained gel) of 3 µg of proteoliposomes shows the incorporation of increasing amounts of pTM11 (pTM11/SERCA1a molar ratios 4.5-15) compared to control (CT). (**B**) Biotinylation of 5 µg of proteoliposomes containing pTM11 and SERCA1a treated with or without detergent n-octyl-β-D-glucopyranoside (β-OG). Equal amounts of protein were separated on SDS-PAGE and blotted on PVDF membrane for streptavidin staining. (**C**) Maximal turnover rate of the Ca^{2+}-dependent ATPase activity (V_{max}) of SERCA1a in the absence (CT) or presence of increasing amounts of pTM11 (pTM11/SERCA1a molar ratios 0.15 – 15). (**D**) K_{Ca} of the Ca^{2+}-dependent ATPase activity of SERCA1a in the absence (CT) or presence of increasing amounts of pTM11 (pTM11/SERCA1a molar ratios 0.15 – 15). n = 3-10 independent reconstitutions; *, $p < 0.05$. *Error bars*, S.E.

4-2.2. Modulation by TM11 peptides is specific. Importantly, we found a combined maximal effect of pTM11 on V_{max} (65% reduction) and K_{Ca} (35% reduction) at a 4.5 molar ratio of pTM11 to SERCA1a (Fig. 4-2, C and D). The lack of complete inhibition points to a specific 2b-tail-like effect and suggests that at molar ratio 4.5, the interaction site of pTM11 is saturated.

To exclude possible side effects of the peptide, we tested two peptide variants of pTM11 with alanine substitution at sites Pro^{1017} or Trp^{1028} (Fig. 4-3A). We showed previously that mutation of these residues in SERCA2b reduced the apparent Ca^{2+} affinity of the pump (12). Both peptide variants were successfully co-reconstituted with SERCA1a into proteoliposomes at levels comparable with pTM11 (Fig. 4-3B). At this point, we switched to a higher throughput method of measuring the ATPase activity based on an end point measurement of the produced inorganic phosphate at different free Ca^{2+} concentrations. Our results indicate that alanine substitutions at Pro^{1017} and Trp^{1028} reduce the impact of pTM11 on the K_{Ca} of SERCA1a (Fig. 4-3D). Note that the pP1017A substitution has no effect on V_{max}, whereas the V_{max} effect of pW1028A is only seen at molar ratio 10, indicating that the pump has a lower affinity for pW1028A than pTM11 (Fig. 4-3C).

To rule out that the pTM11 effect on pump activity is not merely due to an aspecific hydrophobic interaction with the Ca^{2+} pump, we also tested the effect of a randomized pTM11 peptide (pTM11rand, Fig. 4-4). pTM11rand is predicted to be a TM-spanning peptide (predicted by the TMHMM software). Different molar ratios of pTM11rand to SERCA1a were tested (0.5-10, Fig. 4-4, B-D), *i.e.* in the same range as for the WT TM11 peptide. Although we confirmed that pTM11rand is incorporated into the proteoliposomes (Fig. 4-4B), we found in contrast to pTM11 no significant effect of

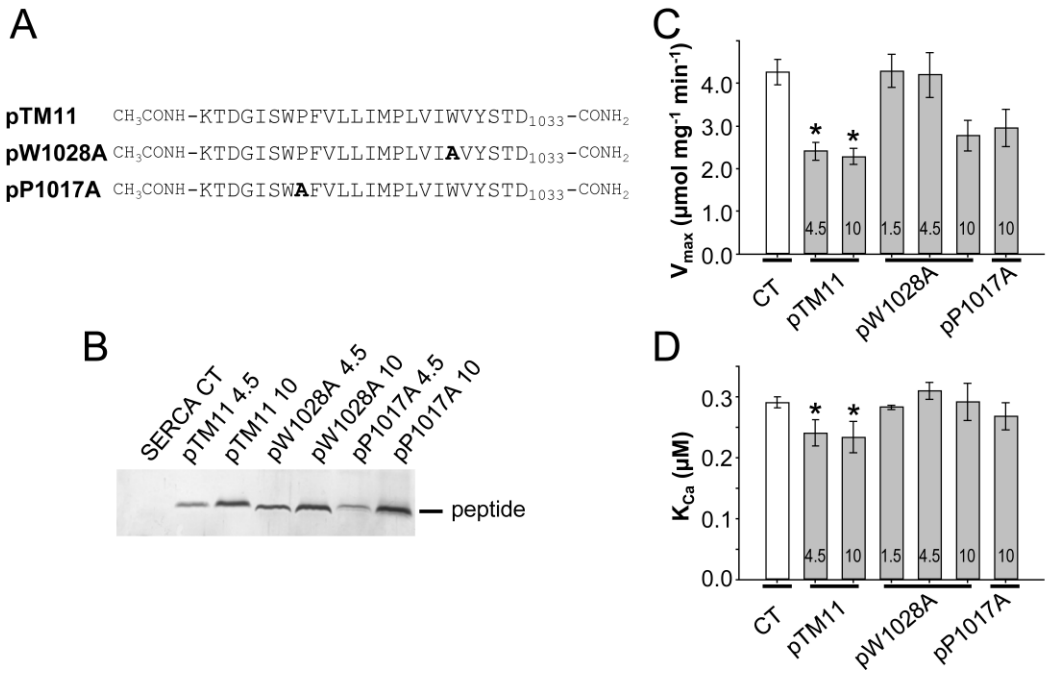

Figure 4-3. Specificity of the SERCA1a regulation by pTM11. (**A**) Amino acid sequence of synthetic mutated pTM11 peptides (substitution indicated in bold). The peptides are N-terminally acetylated and amidated at their C-termini. (**B**) SDS-PAGE of 3 µg of proteoliposomes shows the incorporation of comparable amounts of pTM11, W1028A and P1017A. (**C**) Average ± S.E. of the maximal Ca^{2+}-dependent ATPase activity (V_{max}) of SERCA1a in the absence (control, CT) or presence of increasing amounts of pTM11, W1028A or P1017A peptides (peptide/SERCA1a molar ratios between 1.5 – 10). (**D**) Average ± S.E. K_{Ca} value of the Ca^{2+}-dependent ATPase activity of SERCA1a in the absence (CT) or presence of increasing amounts of pTM11, W1028A or P1017A peptides (peptide/SERCA1a molar ratios between 1.5 – 10). n = 3-7 independent reconstitutions; *, $p < 0.05$. *Error bars*, S.E.

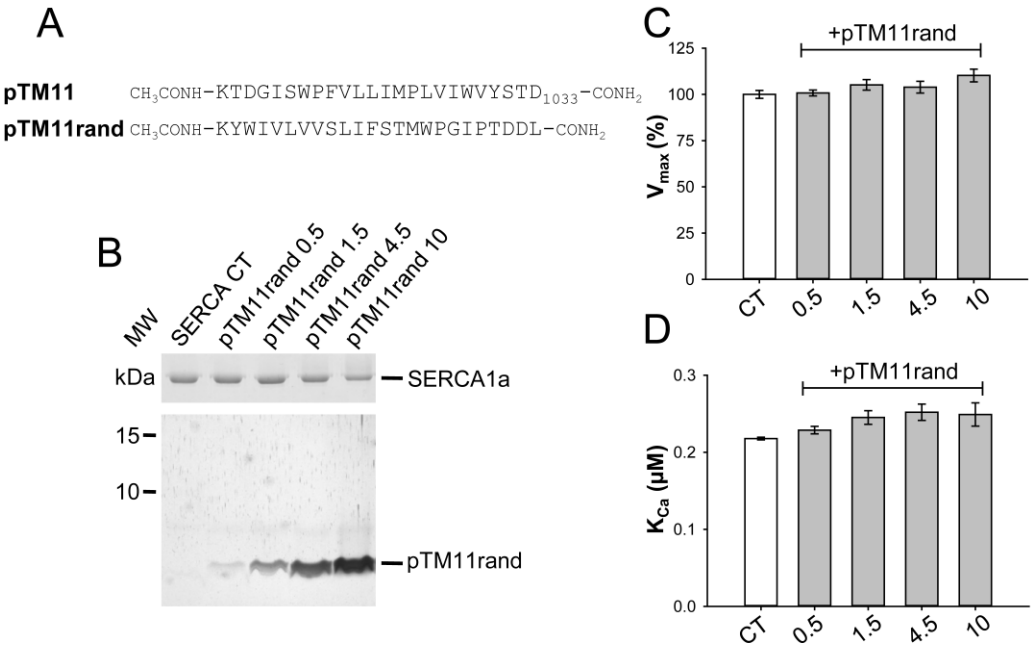

Figure 4-4. A randomized pTM11 peptide has no functional effect on the enzymatic properties of SERCA1a. (**A**) Amino acid sequence of synthetic wild-type and randomized pTM11 peptides. The peptides are N-terminally acetylated and amidated at their C-termini. (**B**) (top) SDS-PAGE (10% acrylamide, Coomassie blue stained gel) of 3 µg of co-reconstituted proteoliposomes shows the incorporation of SERCA. (bottom) SDS-PAGE (16% acrylamide, silver-stained gel) of 3 µg of proteoliposomes shows the incorporation of increasing amounts of pTM11rand (pTM11rand/SERCA1a molar ratios 0.5 – 10) compared to control (CT). (**C**) Maximal turnover rate of the Ca^{2+}-dependent ATPase activity (V_{max}) of SERCA1a in the absence (CT) or presence of increasing amounts of pTM11rand (pTM11rand/SERCA1a molar ratios 0.5 – 10). (**D**) K_{Ca} of the Ca^{2+}-dependent ATPase activity of SERCA1a in the absence (CT) or presence of increasing amounts of pTM11rand (pTM11rand/SERCA1a molar ratios 0.5 – 10). n = 3 independent reconstitutions. *Error bars,* S.E.

pTM11rand on the maximal SERCA1a activity (Fig. 4-4C) and a modest, but not significant increase in K_{Ca} (Fig. 4-4D).

The specificity of the reconstitution system is further corroborated by the opposite effect of adding pTM11 or PLN on the SERCA1a apparent Ca^{2+} affinity. pTM11 peptides increase the apparent Ca^{2+} affinity, whereas addition of PLN lowers it. This is in line with their respective expected physiological performance (15,17).

Therefore, we can conclude that in our reconstituted system, pTM11 is a specific regulator of SERCA1a that recapitulates the action of the 2b-tail on the V_{max} and K_{Ca} of the Ca^{2+} pump. This method now allows the exploration of the functional role of TM11 by site-specific amino acid replacement in pTM11.

4-2.3. TM11 regulates SERCA1a independently from its luminal extension. Our next experiments addressed the specific role of Ser^{1031}, *i.e.* a residue found at the border between the hydrophobic TM11 segment and the more hydrophilic LE. Clearly, Ser^{1031} occupies a key position in the 2b-tail. We knew that removing the last twelve amino acids (Ser^{1031*}) results in a full loss of the 2b-tail effect rendering a pump with SERCA2a-like properties (12,13), whereas truncation at position Thr^{1032*} displays a Ca^{2+} affinity in-between that of SERCA2a and SERCA2b (12).

Here, we wanted to recapitulate the findings of the SERCA2b truncation mutant Ser^{1031*} by comparing the maximal effect of shorter pTM11 peptides in our reconstituted system. First, we tested the amidated peptides pS1031-CN and pT1032-CN, which, respectively, correspond to fragments of the 2b-tail that are found in the SERCA2b Ser^{1031*} and Thr^{1032*} mutants (Fig. 4-5A). Unexpectedly, the pS1031-CN variant altered the K_{Ca} and V_{max} to the same extent as the longer variants pTM11 and pT1032-CN (Fig. 4-5, C and D). This demonstrates that pTM11, and therefore also the corresponding

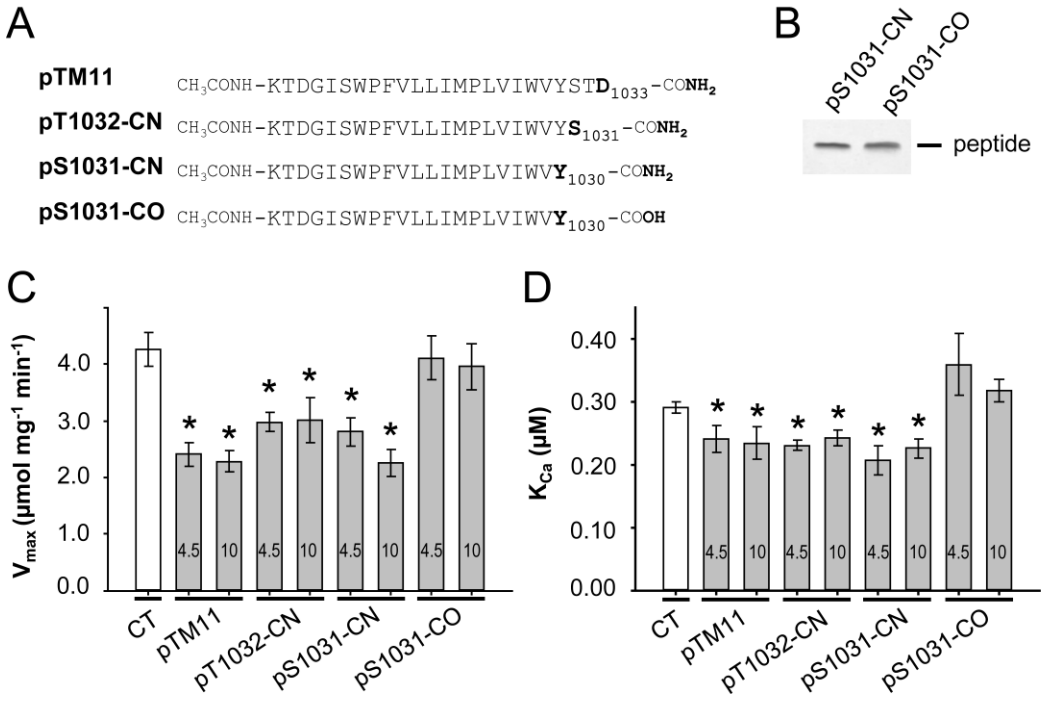

Figure 4-5. TM11 is a second functional region of the 2b-tail, acting independently from the luminal extension. (**A**) Amino acid sequence of synthetic truncated pTM11 peptides. The carboxyl terminus is either amidated (CN) or free (CO). (**B**) SDS-PAGE of 3 µg of proteoliposomes shows the incorporation of comparable amounts of S1031-CN and S1031-CO. (**C**) Average ± S.E. of the maximal Ca^{2+}-dependent ATPase activity (V_{max}) of SERCA1a in the absence (control, CT) or presence of pTM11 or truncated variants (peptide/SERCA1a molar ratios 4.5 and 10). (**D**) Average ± S.E. K_{Ca} value of the Ca^{2+}-dependent ATPase activity of SERCA1a in the absence (CT) or presence of pTM11 or truncated variants (peptide/SERCA1a molar ratios 4.5 and 10). n = 3-7 independent reconstitutions; *, $p < 0.05$. *Error bars*, S.E.

TM11 stretch of the 2b-tail, represents a second, previously unrecognized functional region that acts independently from Ser^{1031} and the LE. However, this contrasts with our earlier conclusion that LE would be the only functionally important element in the 2b-tail (13).

Note that the SERCA2b truncation mutant Ser^{1031*} contains a free C-terminus, whereas with the peptide approach we used the peptide pS1031-CN that is amidated at the C-terminus to better mimic the original peptide backbone. We therefore hypothesized that the presence of the free C-terminus might lead to the complete loss of 2b-tail function in the SERCA2b truncation mutant Ser^{1031*}. To test this, we also determined the effect of the non-amidated synthetic peptide pS1031-CO (Fig. 4-5A), which ends with a free C-terminus. Indeed, we could show that in contrast to pS1031-CN, pS1031-CO does not alter the V_{max} and K_{Ca} of SERCA1a, indicating that it is no longer active (Fig. 4-5, C and D). The possibility that the presence of a C-terminal carboxyl group on the pS1031-CO peptide might have precluded proper membrane insertion appears unlikely because we could detect equally high levels of pS1031-CO and pS1031-CN peptides in the proteoliposomes (Fig. 4-5B).

Together, we provide strong evidence for TM11 as a second, independent functional region of the 2b-tail and show that introducing a free C-terminus at position Ser^{1031} of the 2b-tail completely abolishes the function of TM11, explaining why earlier experiments led to the false assumption that LE would be the only functional region of the 2b-tail.

4-2.4. TM11, the oldest and most conserved feature of 2b-tail. Of all known vertebrate SERCA variants, the presence of an 11^{th} TM segment is confined to SERCA2b. SERCA2 is also the oldest SERCA isoform in vertebrates as it is most related to the sole

invertebrate SERCA isoform. In animal evolution, the 2b-tail appears early as a conserved feature of the SERCA/SERCA2 pump. It is not found in the SERCA orthologue of Choanoflagellata, Porifera, Cnidaria or Placozoa (Fig. 4-6A), but is present in most Bilateria (Fig. 4-6B). Importantly, topology analysis using the TMHMM software predicts that all of the 2b-tail sequences of the Bilateria possess an 11th TM segment (Fig. 4-6B). Most likely, TM11 in invertebrates alters the enzymatic properties of the pump as it does in the vertebrate SERCA2b. SERCAa and SERCAb splice forms were indeed reported for *Artemia franciscana* (18) and *Caenorhabditis elegans* (19). At least in *C. elegans*, these variants showed structural and functional conservation to the vertebrate SERCA2a/b proteins (19).

In Fig. 4-6B, we attempted to reconstruct the phylogeny of the 2b-tail to pinpoint the most conserved regions of TM11. At least three different forms of the 2b-tail can be recognized in Bilateria (Fig. 4-7, A-C): a very short 2b-tail in Protostomia consisting of mainly a predicted TM11 region (Fig. 4-7A), an intermediate long 2b-tail in vertebrates with a TM11 helix, slightly longer cytosolic and short luminal extensions (Fig. 4-7B), and a much longer 2b-tail in Nematoda with the most extended luminal and cytosolic parts (Fig. 4-7C). Thus, a LE, which, as we documented earlier, is a functional region in the vertebrate 2b-tail, is only found in vertebrates and Nematoda and is absent in Protostomia and lower Deuterostomia. This suggests that it is not an essential feature of the 2b-tail and that it evolved independently in Nematoda and Chordata. The pronounced difference in the peptide sequence and length of the LE supports this.

In contrast, the 11th TM helix forms the essential and ancestral part of the 2b-tail (Fig. 4-6B). Despite remarkable sequence differences, TM11 seems to have originated from a common ancestral sequence, since the TM11 sequences of *Strongylocentrotus purpuratus* (Echinodermata) and *Saccoglossus kowalevskii* (Hemichordata) resemble

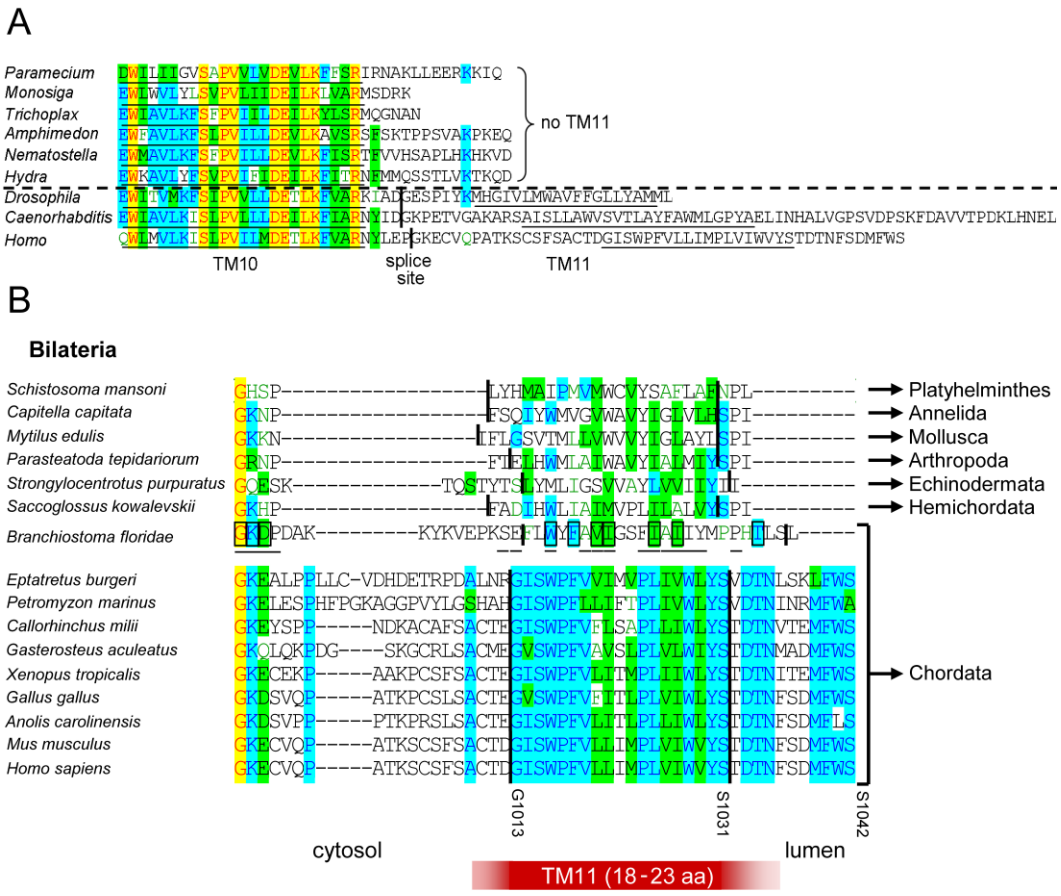

Figure 4-6. An 11th TM helix is found in the 2b-tail of all Bilateria. (**A**) Amino acid sequence alignment of the C-terminus starting from TM10 of the invertebrate SERCA versus the human SERCA2b sequence (AlignX, Invitrogen). A longer C-terminus with an 11th TM helix (underlined) is only found in SERCA of the Bilateria. The alternative splice site is indicated if present. (**B**) Amino acid sequence alignment of the alternative SERCA(2) C-terminus in representative invertebrate and vertebrate species (sequence starts from the alternative splice site, AlignX). The residue numbering follows the hSERCA2b sequence. The 2b-tail amino acid sequence of the primitive chordate *Branchiostoma floridae* partially resembles that of higher vertebrates (squares) and partially that of the lower Bilateria (underlined). Note that the urochordata (*Ciona savigny* and *Ciona intestinalis*) appear to have lost TM11-like sequences (data not shown). All sequences contain an extra TM helix as predicted with the TMHMM software (between vertical lines). Yellow: 100% identical, blue: 50% identical, green: 50% conserved.

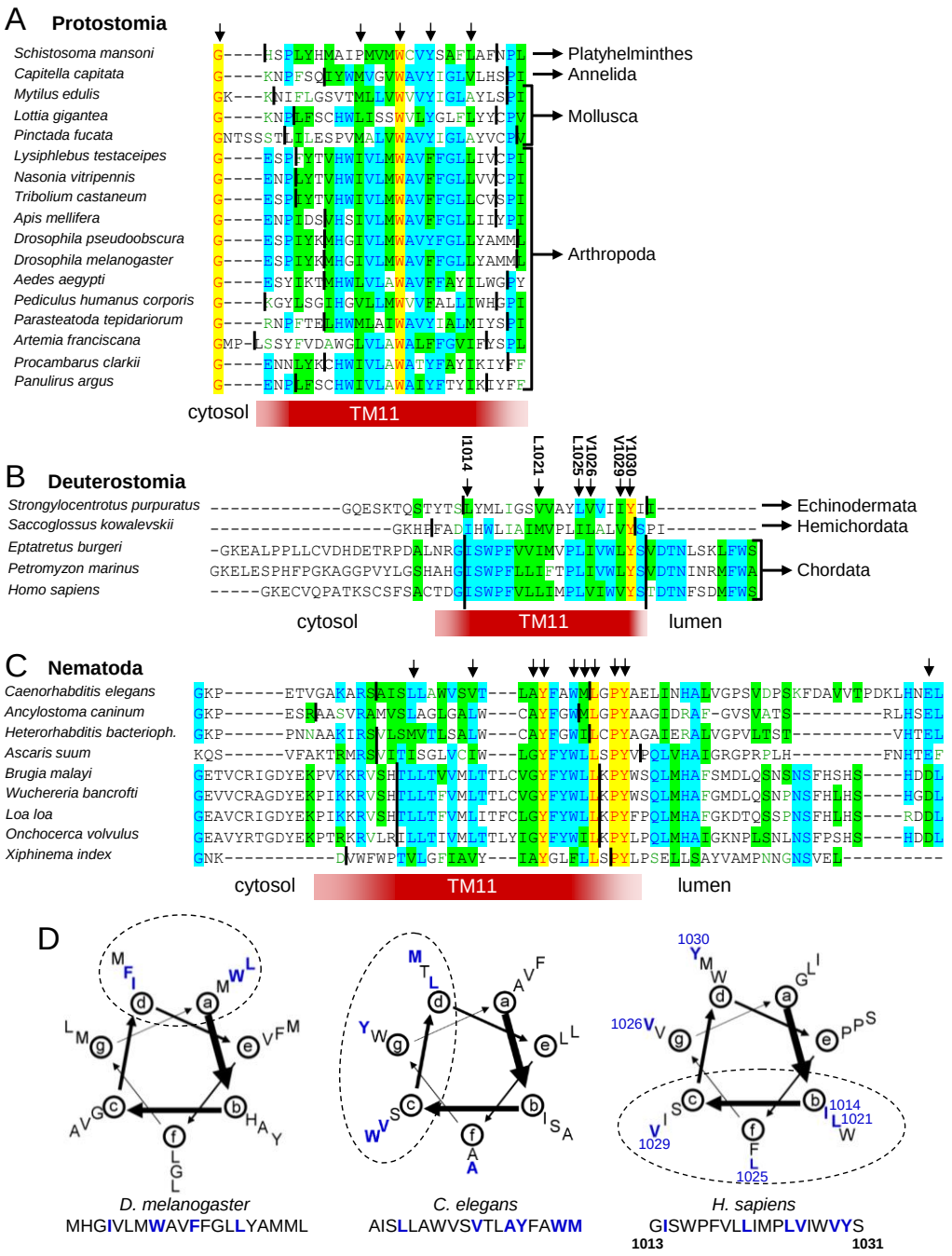

Figure 4-7. The 2b-tail and TM11 in Protostomia, Deuterostomia and Nematoda. Sequence alignment starting from the alternative splice site of the SERCAb C-terminus in Protostomia (**A**), Deuterostomia (**B**) and Nematoda (**C**) (AlignX, Life Technologies). All sequences contain an extra TM helix as predicted by the TMHMM software (in-between vertical lines). Arrows highlight highly conserved residues. Yellow: 100% identical, blue: 50% identical, green: 50% conserved. (**D**) Helical wheel plot analysis of representative TM11 sequences of Protostomia (*D. melanogaster*), Nematoda (*C. elegans*) and Chordata (*H. sapiens*). Bold residues in blue correspond to the highly conserved residues indicated by arrows in panels A-C. The most conserved residues are mainly found on one side of the helix. The residue numbering in (**B**) and (**D**) follows the hSERCA2b sequence.

TM11 of the Protostomia better than TM11 of the vertebrates, whereas TM11 of *Branchiostoma floridae* (Cephalochordata) takes an intermediate position (Fig. 4-6B). Note that according to a helical wheel plot analysis, the most conserved residues are mainly found on one side of the helix, suggesting that these might be important for the interaction of the 2b-tail with the pump (Fig. 4-7D).

Amongst the Deuterostomia, the most conserved residues in TM11 are Ile^{1014}, Leu^{1021}, Leu^{1025}, Val^{1026}, Val^{1029} and Tyr^{1030} (hSERCA2b numbering, supplemental Fig. 3B, *arrows*), of which Ile^{1014}, Leu^{1021}, Leu^{1025}, and Val^{1029} are grouped along one side of the helical wheel plot (Fig. 4-7D). The wheel plot further shows that the highly conserved side of the human TM11 helix contains residues Ile^{1014}, Ser^{1015}, Phe^{1018}, Leu^{1021}, Ile^{1022}, Leu^{1025}, Trp^{1028}, and Val^{1029}. This overlaps well with the interface area of the published SERCA2b model consisting of the residues Pro^{1017}, $\underline{Phe^{1018}}$, $\underline{Leu^{1021}}$, $\underline{Leu^{1025}}$, $\underline{Trp^{1028}}$, $\underline{Val^{1029}}$, and Tyr^{1030} (overlap underlined) (12).

Functional evidence further highlights the central role of some of these residues. We already reported that P1017A, W1028A, and Y1030A substitutions reduced the apparent affinity of SERCA2b (12). In contrast, F1018A and L1025A had no detectable effect (12), although these residues seem to be extremely well conserved and positioned on the conserved side of the helix for interaction (Fig. 4-6B and Fig. 4-7D). Our failure to detect a functional effect might however be due to the conservative nature of the substitutions. To test this, we now substituted Leu^{1025} and Phe^{1018} in the full-length SERCA2b by a polar glutamine. The F1018Q and L1025Q mutants were overexpressed in COS cells. The substitutions significantly increased the K_{Ca} value of Ca^{2+}-dependent ATPase activity, which is in better agreement with the model and the conservation (Fig. 4-8).

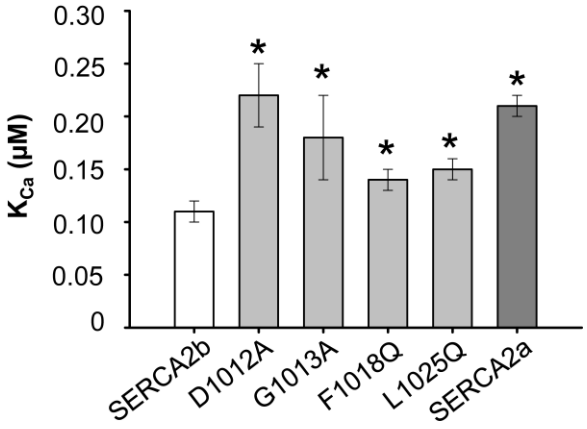

Figure 4-8. Functional features of TM11. Average ± S.E. (*error bars*) K_{Ca} value of the Ca^{2+}-dependent ATPase activity of SERCA2b wild-type and TM11 mutants. n = 3-10 independent transfections; *, $p < 0.05$.

Note that within TM11 the C-terminal part is most conserved across all species. It contains a number of conserved aromatic and/or hydrophobic residues (*arrows* in Fig. 4-7, A-C). This part of TM11 may thus hold a conserved functional feature. This is underscored by the functional effect of the W1028A and Y1030A mutations in the human SERCA2b (12). Furthermore, introduction of a free C-terminus by truncation after Tyr^{1030} leads to a complete disruption of the 2b-tail effect.

In the vertebrate TM11, the N-terminus is also remarkably well conserved (from the primitive Myxinidae *Eptatretus burgeri* to *Homo sapiens* in Fig. 4-6B), but it significantly differs from TM11 sequences in non-vertebrates and even early Deuterostomia. We previously showed that the P1017A mutation had an effect on the apparent Ca^{2+} affinity of SERCA2b (12), and now show that the D1012A and G1013A mutations in SERCA2b drastically reduce the apparent Ca^{2+} affinity of SERCA2b (Fig. 4-8). These data point also to a crucial role of the TM11 conserved N-terminal part.

Together, TM11 is the essential and oldest part of the 2b-tail. We were able to point out TM11 residues that are highly conserved, positioned at the same side of the α-helix, predicted to be in the interface area, and that are functionally important.

4-3. Discussion

4-3.1. TM11, the oldest functional region of 2b-tail. The current study demonstrates that TM11 acts as a previously unrecognized functional region of the 2b-tail. TM11 significantly increases SERCA's apparent affinity for cytosolic Ca^{2+}, but nearly halves the V_{max} of the pump. We showed that TM11 works independently from the LE, the other, earlier discovered and better described functional region of the 2b-tail. Phylogenetic analysis suggests that TM11, which is found in SERCA of most Bilateria, in fact

represents the more primitive element of the 2b-tail and that its action is secondarily reinforced by a LE only in Nematoda and Chordata.

The 2b-tail increases the apparent Ca^{2+} affinity and reduces the V_{max} of the Ca^{2+} pump, explaining the kinetic differences between the housekeeping pump SERCA2b and the muscle variant SERCA2a (7,10,13). Detailed kinetic comparisons of SERCA2b and SERCA2a already showed that the 2b-tail reduces the off-rate for Ca^{2+} from the pump transport sites and slows down the E1P to E2P and E2P to E2 conversions (10). TM11 and LE may each have a different kinetic effect, but when combined lead to the observed kinetic differences imposed by the 2b-tail. For instance, we described how LE might interact with upstream regions in the luminal domain of the pump. Modeling studies suggest that this holds the pump in the high Ca^{2+} affinity conformation E1 contributing to an increased apparent Ca^{2+} affinity with little effect on V_{max} (12).

Here, we described the functional effect of the 18-residue long TM11 via co-reconstitution with SERCA1a *in vitro*. Because of the strong V_{max} effect of TM11, it is likely that TM11 specifically affects the E1P to E2P and E2P to E2 conversions because modeling studies indicate that these slower conformational changes may significantly reduce the V_{max}(12). Future detailed kinetic measurements on SERCA2 with or without TM11 will be required to verify this by comparing the kinetic effects of LE *versus* TM11.

We further show that both the N- and C-terminal parts of TM11 are important. A more puzzling, but key observation was that the presence of a free carboxyl group after residue Tyr^{1030} in the SERCA2b-Ser^{1031*} mutant or in the pS1031-CO peptide abolishes the functional effect of TM11. However, the same peptide with an amidated carboxyl group (pS1031-CN) remains active and confers partial SERCA2b-like properties. Although pS1031-CO clearly associates with the membrane, we speculate that the

additional negative charge of the free carboxyl group might prevent the approach of pS1031-CO to its binding site, *e.g.* as a result of charge repulsion by the phospho-head groups of the lipids. Alternatively, the C-terminal part of TM11 is extremely well conserved amongst different species, pointing to a critical functional role. A C-terminal carboxyl group might therefore interfere with the action of TM11.

4-3.2. Comparison of Ca^{2+} affinity regulation by TM11 and PLN. The best described affinity regulator of the Ca^{2+} pump is PLN. In contrast to TM11, the primary effect of PLN is to reduce the apparent Ca^{2+} affinity two-fold. Earlier findings of our group showed that the presence of PLN increases the K_{Ca} of SERCA2b and SERCA2a to the same extent (*i.e.* in the presence or absence of the 2b-tail) (11,12). The opposite and independent effect of PLN and TM11 on the pump therefore strongly indicates that the 2b-tail and PLN have different binding sites and different modes of action, making it unlikely that PLN has an effect on TM11 function. The opposite effect on the apparent affinity is in part related to the fact that PLN stabilizes the E2 conformation (9), whereas the 2b-tail stabilizes E1 (11,12). An independent working mechanism of PLN and TM11 is also in agreement with our structural model of SERCA2b, postulating that TM11 interacts at site TM7, 10 (11,12), whereas the TM region of PLN presumably interacts at TM2, 4, 6, 9 (9). Note that in addition to a TM domain, PLN contains a cytosolic domain that is regulated by phosphorylation, whereas the 2b-tail contains TM11 and a LE, which are not regulated by phosphorylation.

Different from PLN, TM11 forms an intrinsic element of the SERCA2b pump, but here we show that it preserves its function when it is added *in trans*, *i.e.* uncoupled from the pump. The analysis of SERCA1a2b chimera already pointed out that the interaction site of TM11 is highly conserved in SERCA1a (12), which makes the SERCA1a proteoliposome system extremely suitable to study TM11. The maximal effect

of TM11 was observed at molar ratio 4.5, which is in the same molar range of PLN inhibition (effective SERCA:PLN molar ratio is 1:5) (15), pointing to a high affinity interaction with the pump. Note that the maximal effect occurs at a higher molar ratio than in the endogenous situation of SERCA2b where the 2b-tail is coupled to the pump in a 1:1 ratio. Several factors might explain this higher ratio. The ratio 4.5 describes the amount of peptide and pump added to the system, but the actual ratio reconstituted in the proteoliposomes is difficult to estimate. Also, as our biotinylation results indicate, half of pTM11 is inserted in the opposite orientation. Together, a higher concentration is required for a maximal effect than in the SERCA2b pump where a high local concentration of TM11 is guaranteed by the fusion of the 2b-tail to the pump.

4-3.3. Similarities between SERCA/TM11 and α/β-Na^+,K^+-ATPase interactions point to anchoring region as emerging site of regulation. Our structural model of SERCA2b predicts that TM11 occupies a binding site formed by TM7 and TM10, *i.e.* a remote and relatively immobile position in the anchoring region of the pump (12). This is somewhat difficult to reconcile with the strong functional effect of pTM11 on V_{max} and K_{Ca}. In the absence of structural information of SERCA2b, it is difficult to understand how TM11 regulates the enzymatic properties of the pump at the anchoring domain.

At least in Na^+,K^+-ATPase the anchoring region emerges as a site of regulation. Crystal structures of α,β,γ-Na^+,K^+-ATPase illustrate that the γ- (on TM9), β- (on TM7) and auto-inhibitory C-terminus (between TM7 and TM8) all interact at the anchoring region (20-22). Thus, besides a structural feature for stabilizing the pump in the lipid bilayer, the helices TM7–TM10 appear to have a dynamic role in Na^+,K^+-ATPase regulation. Indeed, the E2–E1 transition of Na^+,K^+-ATPase is accompanied by the straightening of TM5, which pushes TM7 towards TM10. Because of an extensive hydrogen-bonding network, this induces large scale structural changes involving parts of

the phosphorylation domain (P1), TM3, and the C-terminus of the α-subunit, as well as the β-subunit (21). This network might explain why mutations in the TM of the β-subunit alter the apparent K^+ affinity of the Na^+,K^+-ATPase (23).

It is difficult to overlook the striking parallel in the mode of regulation of Na^+,K^+-ATPase and SERCA by their respective TM interactors (*i.e.* the β- and γ-subunits in the Na^+,K^+-ATPase *versus* the 2b-tail and PLN in SERCA) (12). In all these cases, their single TM helix interacts with the anchoring region of the pump, which is critical for ion affinity regulation (12,23). Thus, like in Na^+,K^+-ATPase the anchoring region of the Ca^{2+}-ATPase might represent a previously unrecognized regulatory site.

4-3.4. Mechanism of TM11 regulation in the anchoring region of SERCA Ca^{2+} pump. Because the structure of the overall TM domain is remarkably conserved between Na^+,K^+-ATPase and SERCA1a, we compared the published structure of TM7 of Na^+,K^+-ATPase in the presence of the β-subunit (Fig. 4-9D) with that of SERCA1a in the absence of TM11 (Fig. 4-9C). Differences in the position of TM7 between the SERCA1a and Na^+,K^+-ATPase conformations could relate to the presence of the β-subunit. In Na^+,K^+-ATPase, the N-terminal end of TM7 bends towards TM5. This helix deformation might depend on the presence of a hinge region formed by highly conserved glycine residues ($G^{855}XXG^{858}$) (Fig. 4-9A). Moreover, the functionally important and conserved residues Phe^{39}, Phe^{43}, Tyr^{44} on the β-subunit TM region protrude toward this hinge region and might trigger the bending and partial unwinding of the cytosolic part of TM7 (Fig. 4-9D). During Metazoan evolution, the β-subunit appeared first as a regulator of the pump in Cnidaria, and at the same time Gly^{855} appeared in TM7 and remained conserved at later stages (Fig. 4-10A), suggesting that both features are related.

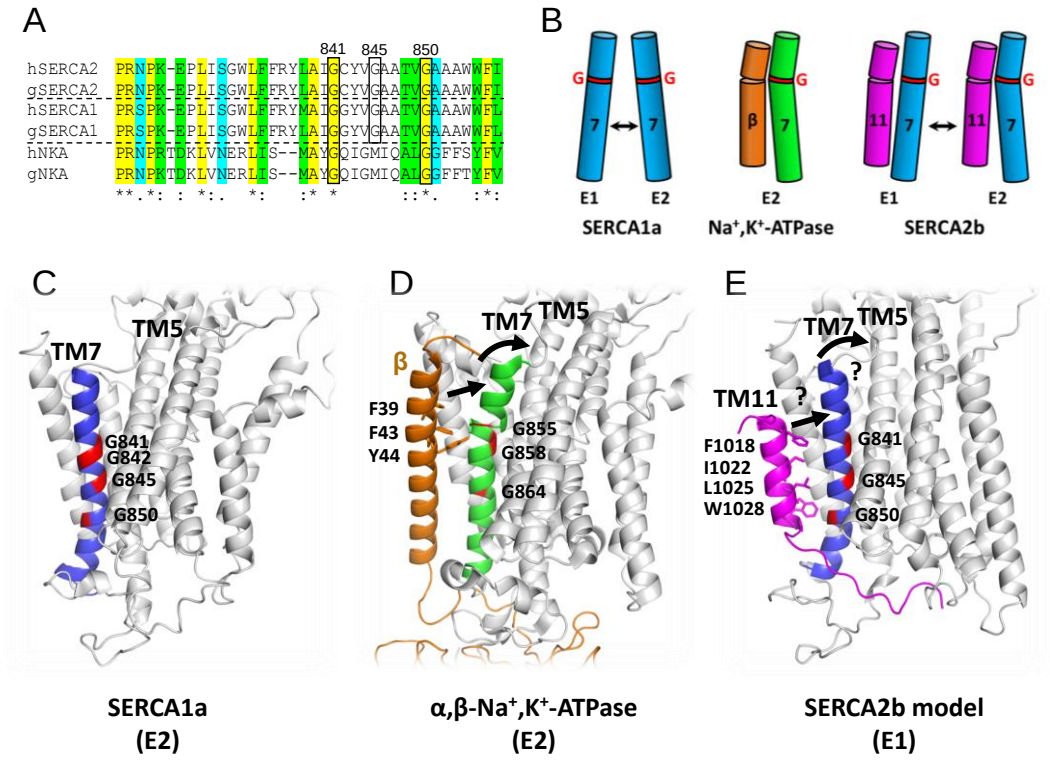

Figure 4-9. Proposed mechanism of TM11. (**A**) Amino acid sequence alignment of TM7 of human and chicken SERCA1a, SERCA2b and Na^+,K^+-ATPase. Numbers on top refer to sequence numbering of the glycines in hSERCA2. (**B**) Proposed model of TM11 mechanism. Left, in SERCA1a, TM7 undergoes a tilt between the E1 and E2 conformation. Center, in Na^+,K^+-ATPase in the presence of the β-subunit, the upper part of TM7 remains in the E1 conformation, whereas the lower part can shift to E2. The bending of TM7 might be supported by conserved glycines in TM7. Right, conserved glycines in TM7 of SERCA2b might also support the bending of TM7 in the presence of TM11. This might prevent the repositioning of TM7 during the E1-E2 conversions. (**C-E**) Schematics of the published SERCA1a structure (**C**; E2, 1WPG) (27), α,β,γ-Na^+,K^+-ATPase (**D**; E2) (20,21), and the SERCA2b structural model (**E**; E1) (12). TM7 is shown in blue for SERCA1a and SERCA2b, and in green for Na^+,K^+-ATPase. The conserved glycines are shown in red.

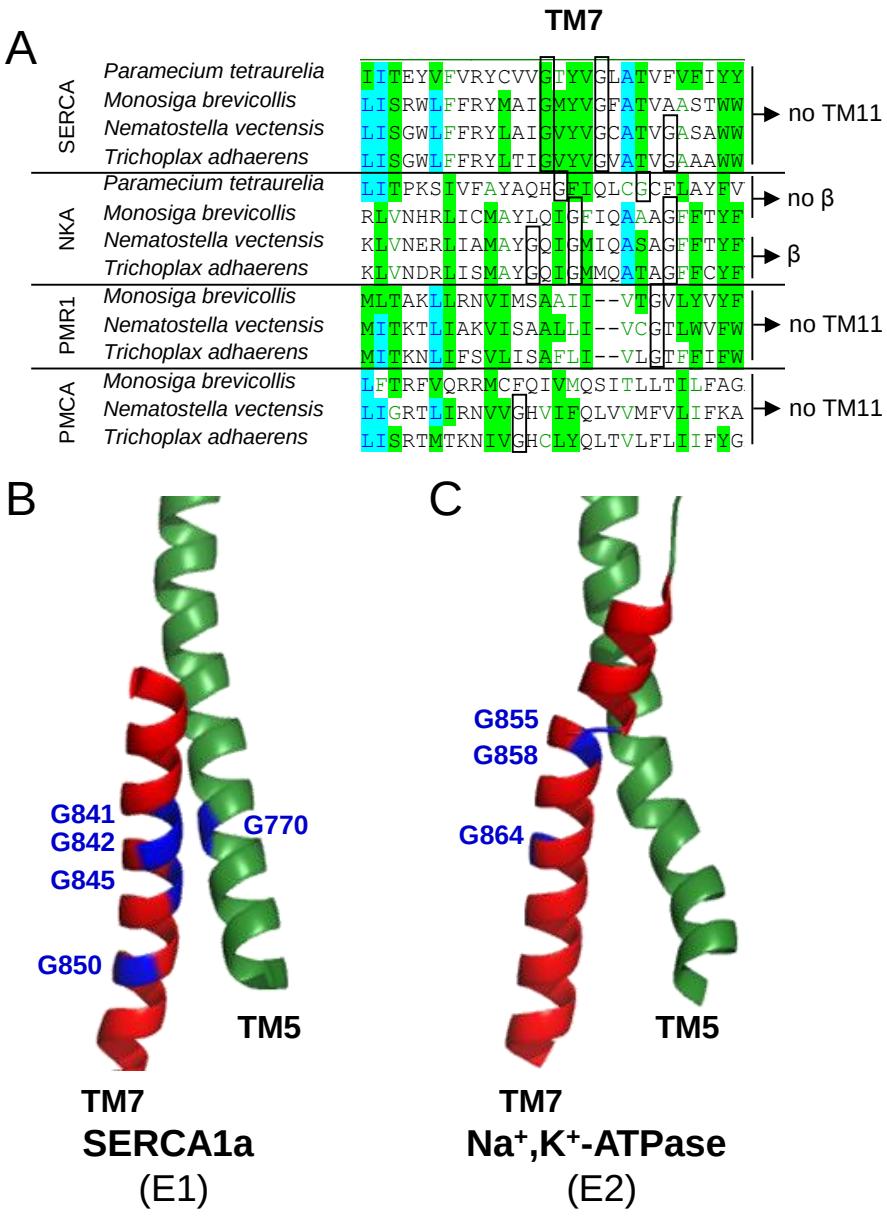

Figure 4-10. Role of the conserved glycines in TM7 of the SERCA Ca^{2+} pump. (**A**) Amino acid sequence alignment of TM7 in primitive invertebrate sequences of SERCA, Na^+,K^+-ATPase (NKA), PMR1 (secretory pathway Ca^{2+} ATPase) and PMCA (plasma membrane Ca^{2+} ATPase) (AlignX, Invitrogen). Conserved glycines are indicated by boxes. The presence or absence of TM11 or β-subunit is indicated. Yellow: 100% identical, blue: 50% identical, green: 50% conserved. (**B-C**)**.** The SERCA1a GGXXG sequence in TM7 (**B**), but not the Na^+,K^+-ATPase GXXG sequence in TM7 (**C**), is a typical helix interaction motif for TM5-TM7 interaction (glycines are indicated in dark blue).

We hypothesize that in SERCA2b, TM7 might undergo a similar bending because three extremely conserved glycine residues are found ($G^{855}XXG^{858}$ and Gly^{850}) (Fig. 4-9A). However, in the SERCA1a crystal structures, *i.e.* in the absence of TM11, TM7 is always a straight helix, which slightly shifts position between E1 (closer to TM5 as also pointed out in the E1 SERCA2b model in Fig. 4-9E) and E2 (further from TM5) (Fig. 4-9C). Note that the position of the N-terminal part of TM7 in Na^+,K^+-ATPase (Fig. 4-9D) corresponds well with the E1 position of TM7 in SERCA1a (Fig. 4-9C). We therefore hypothesize that Gly^{841} or Gly^{845} in SERCA2b facilitates the bending of TM7, which would be imposed by the presence of TM11. TM11 might keep the N-terminal part of TM7 in the E1 position, whereas the lower part of TM7 might be allowed to shift between an E1 and E2 position (Fig. 4-9B). Thus, TM11 might restrict the movement of TM7, which might reduce the maximal turnover rate and increase the apparent Ca^{2+} affinity.

TM7 bending could for instance reposition the cytosolic loops L6-7 and/or L8-9, which tightly connect the TM and phosphorylation domains via an extensive hydrogen bond network (24). Because these loops mediate the communication between both domains, their repositioning could have an impact on the kinetics of phosphorylation and dephosphorylation (24), which would be in line with the strong effect of the 2b-tail on the E1P to E2P, and E2P to E2 conversions (10). At least some mutations in L6/7 are known to affect the Ca^{2+} affinity of the pump pointing to L6/7 as a possible mediator for TM11 function (25).

Alternatively, TM11 might directly alter the packing of the other TM helices closer to the Ca^{2+}-binding sites affecting the Ca^{2+} affinity. Another possibility is that TM11 might promote the unwinding of TM7 in SERCA2b at the conserved glycines Gly^{841} and/or Gly^{845}. Indeed, in the Na^+,K^+-ATPase the β-subunit promotes unwinding of

TM7 at position Gly^{855}, which is of central importance for K^+ binding (21). Note that the glycines on TM7 of the Ca^{2+} pump are also part of a classical GXXG helix-helix interaction motif, mediating the interaction with TM5 (Fig. 4-10B). The GXXG sequence in TM7 of Na^+,K^+-ATPase is, however, not a typical helix-helix interaction motif (Fig. 4-10, A and C), and in the PMR1 and PMCA Ca^{2+} ATPases a much lower number of glycines in TM7 is found (Fig. 4-10A).

Together, the conserved glycines in TM7 of the Ca^{2+} pump and Na^+,K^+-ATPase might support important structural features as helix unwinding, bending, and TM interaction in the presence of respectively TM11 and the β-subunit. These similarities between TM11 and the β-subunit point to an interesting example of convergent evolution (12). A SERCA2b crystal structure will be required to get more detailed insight into the structural changes that accompany the TM11 interaction, but so far, purification of SERCA2b for subsequent crystallization is hindered by its low tissue expression levels (26).

4-3.5. Conclusion. We conclude that TM11 is a previously unrecognized, but highly conserved functional region of the SERCA2b Ca^{2+} pump. TM11 acts independently from PLN, presumably by restricting the movement of TM7, which could explain why TM11 exerts a strong effect on the maximal turnover rate and apparent Ca^{2+} affinity.

4-4. Experimental Procedures

4-4.1. Synthetic peptide handling. Synthetic peptides corresponding to parts of the 2b-tail were purchased from Biomatik, Wilmington, DE (95% purity grade, HPLC and MS verified). Unless otherwise specified, all synthetic peptides are acetylated at the N-terminus and amidated at the C-terminus to closely mimic the peptide backbone of the endogenous 2b-tail. Peptides were solubilized in 3:1 chloroform:trifluoroethanol at a

concentration of 0.5 – 4 mg/ml. The peptide concentration was verified by quantitative amino acid analysis.

4-4.2. Co-Reconstitution of SERCA1a and synthetic TM11 peptides. Sarcoplasmic reticulum membranes of rabbit hind limb skeletal muscle were prepared as described previously (14). The membranes were then solubilized in octaethylene glycol monododecyl ether ($C_{12}E_8$, Barnet Products), and SERCA1a was purified by affinity chromatography as in (14). Functional co-reconstitution of SERCA1a with TM11 peptides has been performed essentially as described before for SERCA1a/PLN co-reconstitution (15).

Briefly, the required amount of pTM11 was mixed with lipids (360 μg of egg yolk phosphatidylcholine, EYPC and 40 μg of egg yolk phosphatidic acid, EYPA; Avanti Polar Lipids) and dried to a thin film. The peptide/lipid film was rehydrated in water, and detergent (800 μg of $C_{12}E_8$) was added. Buffer (20 mM imidazole, pH 7.0, 100 mM KCl, 3 mM $MgCl_2$, and 0.02% NaN_3) and SERCA1a (300 μg) were added to achieve final molar stoichiometries of 1:0.5-15 SERCA1a:peptide and 1:120 SERCA1a:phospholipids. The detergent was extracted via gradual administration of SM-2 Biobeads (Bio-Rad). Finally, the SERCA1a-containing vesicles were purified via sucrose step-gradient centrifugation.

To detect the peptides in the proteoliposomes, 7.5 μl of the vesicles were loaded on Tricine-SDS-PAGE as described in (16). Proteins and peptides were visualized in the gel by silver staining.

4-4.3. Orientation of TM11 in co-reconstituted proteoliposomes via biotinylation. The orientation of pTM11 in our co-reconstituted proteoliposomes was determined using a biotin surface labeling assay as in (15). Co-reconstituted vesicles (5 μg of protein) were

mixed in labeling buffer (20 mM borate-KOH, pH 9.0) with 5 mM EZLink Sulfo-NHS-LC-Biotin (sulfosuccinimidyl-6-[biotin-amido]hexanoate; Thermo Scientific) in the absence or presence of 0.5% n-octyl-β-D-glucopyranoside (Anatrace). The mixture was incubated overnight at 4°C followed by quenching with an equal volume of SDS-PAGE sample buffer. The amount of biotin labeling was quantified on a Western blot using IRDye 800CW streptavidin conjugate and an Odyssey Infrared Imaging System (LI-COR Bioscience).

4-4.4. Ca^{2+}-dependent ATPase activity assays. Ca^{2+}-dependent ATPase activities of the co-reconstituted proteoliposomes were measured at 25°C by an enzyme-coupled assay (as in (15)) or at 37°C by an end point colorimetric measurement (as in (12)). SERCA1a activity was followed in the presence and absence of co-reconstituted synthetic peptides. A minimum of three independent reconstitutions and activity assays were performed and the Ca^{2+}-dependent ATPase activity was measured over a wide range of Ca^{2+} concentrations (from 0.1 to 10 μM).

SERCA2b mutations were introduced by site-directed mutagenesis (QuickChange). Ca^{2+}-dependent ATPase activities of the overexpressed SERCA variants in COS cells were measured using an end point colorimetric assay (12). The contribution of the endogenous SERCA2b in COS cells to the measured Ca^{2+}-dependent ATPase activity of the overexpressed SERCA variants is negligible. The K_{Ca} (Ca^{2+} concentration at half-maximal activity), the V_{max} (maximal activity), and the n_H (Hill coefficient) were calculated via nonlinear least squares fitting of the activity data to the Hill equation using Sigma Plot (SPSS Inc).

4-4.5. Statistics. Results are presented as average ± S.E. of *n* (number) independent experiments (*n* is provided in the legends). Multiple comparison statistical analysis was

carried out by one way ANOVA followed by a post hoc Fisher LSD test (Statistica 8). $p < 0.05$ was considered statistically significant.

4-5. References

1. Berridge, M. J., Bootman, M. D., and Roderick, H. L. (2003) Calcium signalling: dynamics, homeostasis and remodelling. *Nat. Rev. Mol. Cell Biol.* **4**, 517-529

2. Toyoshima, C. (2009) How Ca^{2+}-ATPase pumps ions across the sarcoplasmic reticulum membrane. *Biochim. Biophys. Acta* **1793**, 941-946

3. Olesen, C., Picard, M., Winther, A. M., Gyrup, C., Morth, J. P., Oxvig, C., Moller, J. V., and Nissen, P. (2007) The structural basis of calcium transport by the calcium pump. *Nature* **450**, 1036-1042

4. Vangheluwe, P., Sepulveda, M. R., Missiaen, L., Raeymaekers, L., Wuytack, F., and Vanoevelen, J. (2009) Intracellular Ca^{2+}- and Mn^{2+}-transport ATPases. *Chem. Rev.* **109**, 4733-4759

5. Vandecaetsbeek, I., Raeymaekers, L., Wuytack, F., and Vangheluwe, P. (2009) Factors controlling the activity of the SERCA2a pump in the normal and failing heart. *Biofactors* **35**, 484-499

6. Dally, S., Corvazier, E., Bredoux, R., Bobe, R., and Enouf, J. (2010) Multiple and diverse coexpression, location, and regulation of additional SERCA2 and SERCA3 isoforms in nonfailing and failing human heart. *J. Mol. Cell. Cardiol.* **48**, 633-644

7. Lytton, J., Westlin, M., Burk, S. E., Shull, G. E., and MacLennan, D. H. (1992) Functional comparisons between isoforms of the sarcoplasmic or endoplasmic reticulum family of calcium pumps. *J. Biol. Chem.* **267**, 14483-14489

8. MacLennan, D. H., and Kranias, E. G. (2003) Phospholamban: a crucial regulator of cardiac contractility. *Nat. Rev. Mol. Cell Biol.* **4**, 566-577

9. Toyoshima, C., Asahi, M., Sugita, Y., Khanna, R., Tsuda, T., and MacLennan, D. H. (2003) Modeling of the inhibitory interaction of phospholamban with the Ca^{2+} ATPase. *Proc. Natl. Acad. Sci. U. S. A.* **100**, 467-472

10. Dode, L., Andersen, J. P., Leslie, N., Dhitavat, J., Vilsen, B., and Hovnanian, A. (2003) Dissection of the functional differences between sarco(endo)plasmic reticulum Ca^{2+}-ATPase (SERCA) 1 and 2 isoforms and characterization of Darier disease (SERCA2) mutants by steady-state and transient kinetic analyses. *J. Biol. Chem.* **278**, 47877-47889

11. Verboomen, H., Wuytack, F., De Smedt, H., Himpens, B., and Casteels, R. (1992) Functional difference between SERCA2a and SERCA2b Ca^{2+} pumps and their modulation by phospholamban. *Biochem. J.* **286**, 591-595

12. Vandecaetsbeek, I., Trekels, M., De Maeyer, M., Ceulemans, H., Lescrinier, E., Raeymaekers, L., Wuytack, F., and Vangheluwe, P. (2009) Structural basis for the high Ca^{2+} affinity of the ubiquitous SERCA2b Ca^{2+} pump. *Proc. Natl. Acad. Sci. U. S. A.* **106**, 18533-18538

13. Verboomen, H., Wuytack, F., Van den Bosch, L., Mertens, L., and Casteels, R. (1994) The functional importance of the extreme C-terminal tail in the gene 2 organellar Ca^{2+}-transport ATPase (SERCA2a/b). *Biochem. J.* **303**, 979-984

14. Moncoq, K., Trieber, C. A., and Young, H. S. (2007) The molecular basis for cyclopiazonic acid inhibition of the sarcoplasmic reticulum calcium pump. *J. Biol. Chem.* **282**, 9748-9757

15. Trieber, C. A., Afara, M., and Young, H. S. (2009) Effects of phospholamban transmembrane mutants on the calcium affinity, maximal activity, and cooperativity of the sarcoplasmic reticulum calcium pump. *Biochemistry* **48**, 9287-9296

16. Schagger, H. (2006) Tricine-SDS-PAGE. *Nat. Protoc.* **1**, 16-22

17. Trieber, C. A., Douglas, J. L., Afara, M., and Young, H. S. (2005) The effects of mutation on the regulatory properties of phospholamban in co-reconstituted membranes. *Biochemistry* **44**, 3289-3297

18. Escalante, R., and Sastre, L. (1993) Similar alternative splicing events generate two sarcoplasmic or endoplasmic reticulum Ca^{2+}-ATPase isoforms in the crustacean *Artemia franciscana* and in vertebrates. *J. Biol. Chem.* **268**, 14090-14095

19. Zwaal, R. R., Van Baelen, K., Groenen, J. T., van Geel, A., Rottiers, V., Kaletta, T., Dode, L., Raeymaekers, L., Wuytack, F., and Bogaert, T. (2001) The sarco-endoplasmic reticulum Ca^{2+} ATPase is required for development and muscle function in *Caenorhabditis elegans*. *J. Biol. Chem.* **276**, 43557-43563

20. Morth, J. P., Pedersen, B. P., Toustrup-Jensen, M. S., Sorensen, T. L., Petersen, J., Andersen, J. P., Vilsen, B., and Nissen, P. (2007) Crystal structure of the sodium-potassium pump. *Nature* **450**, 1043-1049

21. Shinoda, T., Ogawa, H., Cornelius, F., and Toyoshima, C. (2009) Crystal structure of the sodium-potassium pump at 2.4 A resolution. *Nature* **459**, 446-450

22. Poulsen, H., Khandelia, H., Morth, J. P., Bublitz, M., Mouritsen, O. G., Egebjerg, J., and Nissen, P. (2010) Neurological disease mutations compromise a C-terminal ion pathway in the Na^+/K^+-ATPase. *Nature* **467**, 99-102

23. Hasler, U., Crambert, G., Horisberger, J. D., and Geering, K. (2001) Structural and functional features of the transmembrane domain of the Na,K-ATPase beta subunit revealed by tryptophan scanning. *J. Biol. Chem.* **276**, 16356-16364

24. Zhang, Z., Lewis, D., Sumbilla, C., Inesi, G., and Toyoshima, C. (2001) The role of the M6-M7 loop (L67) in stabilization of the phosphorylation and Ca^{2+}

binding domains of the sarcoplasmic reticulum Ca^{2+}-ATPase (SERCA). *J. Biol. Chem.* **276**, 15232-15239

25. Menguy, T., Corre, F., Bouneau, L., Deschamps, S., Moller, J. V., Champeil, P., le Maire, M., and Falson, P. (1998) The cytoplasmic loop located between transmembrane segments 6 and 7 controls activation by Ca^{2+} of sarcoplasmic reticulum Ca^{2+}-ATPase. *J. Biol. Chem.* **273**, 20134-20143

26. Vandecaetsbeek, I., Christensen, S. B., Liu, H., Van Veldhoven, P. P., Waelkens, E., Eggermont, J., Raeymaekers, L., Moller, J. V., Nissen, P., Wuytack, F., and Vangheluwe, P. (2011) Thapsigargin affinity purification of intracellular P_{2A}-type Ca^{2+} ATPases. *Biochim. Biophys. Acta.* **1813**, 1118-1127

27. Toyoshima, C., and Inesi, G. (2004) Structural basis of ion pumping by Ca^{2+}-ATPase of the sarcoplasmic reticulum. *Annu. Rev. Biochem.* **73**, 269-292

Chapter 5

Defining the multifaceted roles of the endogenous peptide modulators of SERCA

5-1. Summary of significant findings

This thesis proposes novel molecular mechanisms of SERCA regulation by endogenous peptide modulators, including SLN, zfPLN and the C-terminal extension of SERCA2b (2b-tail). The expression and regulation of SERCA activity have been widely investigated, emphasizing its central role in the regulation of calcium homeostasis during development and under a variety of pathophysiological conditions (1). Defects in calcium transport due to abnormal regulation of SERCA by its physiological regulators are of major clinical importance. However, their precise role in modulating the enzymatic properties of SERCA remains poorly defined. If the interaction between SERCA and its physiological regulators is better understood then it will contribute to the long term goal of rational therapeutic design for the improvement of clinical outcomes. This work adds to the current understanding of the mechanisms involved in SERCA regulation by endogenous peptide modulators and highlights the complexity as well as the importance of these protein-protein interactions.

The exact mechanism of SERCA regulation by SLN is unresolved. PLN and SLN have significant sequence homology in their transmembrane domains, suggesting a similar mode of binding to SERCA (2). However, unlike PLN, SLN has a highly conserved C-terminal domain that extends into the SR lumen. We found that alanine-substitution of residues in the luminal domain of SLN as well as complete removal of this domain resulted in severe loss of function (3). Furthermore, adding the luminal domain of SLN to the C-terminus of PLN resulted in super-inhibition with characteristics of both PLN and SLN. Thus, we concluded that the highly conserved C-terminal tail of SLN is a primary determinant for SERCA inhibition and that it is a distinct and transferrable functional domain.

While the mechanism of SERCA inhibition by PLN has been extensively studied, considerably less is known about the role of non-mammalian forms of PLN in SERCA regulation. Given the high sequence diversity between zebrafish and human PLN, as well as the presence of a unique zfPLN luminal extension, we were interested in studying the mechanism of zfPLN inhibition of SERCA. We found that despite the high sequence diversity, zfPLN had inhibitory properties that were similar to human PLN. Human PLN chimeras containing the cytoplasmic or linker domain of zfPLN resulted in mild loss of inhibitory function or gain of function, respectively. In addition, removal of the luminal zfPLN tail resulted in loss of function, whereas adding the zfPLN luminal extension to human PLN had a minimal effect on SERCA inhibition. From this we concluded that the luminal extensions of zfPLN and SLN have distinct functional effects, even though zfPLN appears to use a hybrid PLN-SLN inhibitory mechanism.

Lastly, the focus of this thesis was shifted towards defining the molecular mechanism of SERCA regulation by the 2b-tail of the ubiquitous SERCA2b. In contrast to SLN and PLN, the 2b-tail has been shown to increase the apparent calcium affinity of SERCA (4). While the role of the luminal extension of the 2b-tail has been already described (5), the function of the eleventh transmembrane segment (TM11) has remained elusive. We identified TM11 to be an important SERCA regulator primarily responsible for reducing the maximal activity and, to lesser extent, increasing the apparent calcium affinity of SERCA (6). Additionally, we identified TM11 as the oldest segment of the 2b-tail, signifying its important regulatory role throughout the evolution of the SERCA2 gene. We concluded that the functional difference between SERCA2a and SERCA2b are not only attributed to the luminal extension of the 2b-tail but also the TM11 segment.

In subsequent sections, a discussion on the commonalities and differences in the mechanisms of SERCA regulation by endogenous peptide regulators and their link to human diseases will be continued.

5-2. TM1-2 luminal linker region as a newly emerging site of regulation

Although highly homologous, SLN and PLN appear to use different inhibitory mechanisms to regulate SERCA (3,7). The inhibitory activity of PLN is primarily encoded by its transmembrane domain, whereas the highly conserved C-terminal luminal domain of SLN encodes ~75% of its inhibition. The luminal extension of SLN is also responsible for a drastic suppression of the maximal activity of SERCA, an effect which is not observed in the presence of PLN (2). Using kinetic simulations, we have demonstrated that SLN alters binding of the first calcium ion, thereby stabilizing a calcium-free conformation of SERCA. This is different from what is known for PLN, which is thought to slow down a SERCA conformational transition that follows binding of the first calcium ion.

Despite growing knowledge of the inhibitory properties of SLN, the exact molecular mechanism of SERCA inhibition by SLN is not fully understood. One of the remaining questions is how does the short luminal domain of SLN cause such a dramatic decrease in the apparent calcium affinity and the maximal turnover rate of SERCA? Based on modeling studies, both PLN and SLN have been proposed to bind to a groove formed by transmembrane helices TM2, TM4, TM6 and TM9 of SERCA in a calcium-free E2 conformation (8,9). Recently, two high-resolution structures of the SERCA-SLN complex confirmed the modeled SLN binding site (10,11). These structures provided valuable information regarding the binding of the transmembrane domain of SLN to SERCA; however, due to poorly defined electron density of the C-terminal region of

SLN, they did not reveal the nature of interactions between the luminal domain of SLN and SERCA. Nevertheless, these structures show that the C-terminal end of the transmembrane domain of SLN interacts with the base of TM2, suggesting that the luminal domain of SLN is in proximity to the TM1-2 linker region of SERCA. This is in agreement with our proposed model of the interactions between SLN and SERCA, which suggests that the essential luminal residues of SLN (Arg^{27}, Tyr^{29} and Tyr^{31}) form functionally important contacts with the highly conserved aromatic residues found in the TM1-2 luminal linker region of SERCA (3). We proposed that Arg^{27} of SLN may form a cation-π interaction with Phe^{92} of SERCA or aid in positioning of SLN relative to SERCA and the lipid bilayer, whereas Tyr^{29} and/or Tyr^{31} of SLN may form a cation-π or π-π interactions with Phe^{88} of SERCA.

So the question that follows is how do the interactions between the luminal domain of SLN and the TM1-2 linker region of SERCA, which is located far away from the calcium binding sites, cause SERCA inhibition? To answer this question, it is necessary to take the conformational changes of SERCA into consideration. Comparison of the high-resolution crystal structures of SERCA representing different conformational states of the enzyme clearly shows that the TM1-2 region undergoes drastic structural rearrangements during the calcium transport cycle (Fig. 5-1) (12). The cytoplasmic ends of the TM1 and TM2 helices are connected to the highly mobile A-domain of SERCA via flexible linkers, suggesting that the movement of the TM1-2 region is largely dependent on the conformation of the A-domain. In fact, shortening or elongation of these linker regions has been shown to dramatically affect SERCA function (13,14). Thus, there is a dynamic interplay between the rotation of the A-domain and the movements in the TM1-2 region, which is imperative for proper SERCA function. The TM1-2 region appears to undergo the largest conformational changes as SERCA transitions from the calcium-free

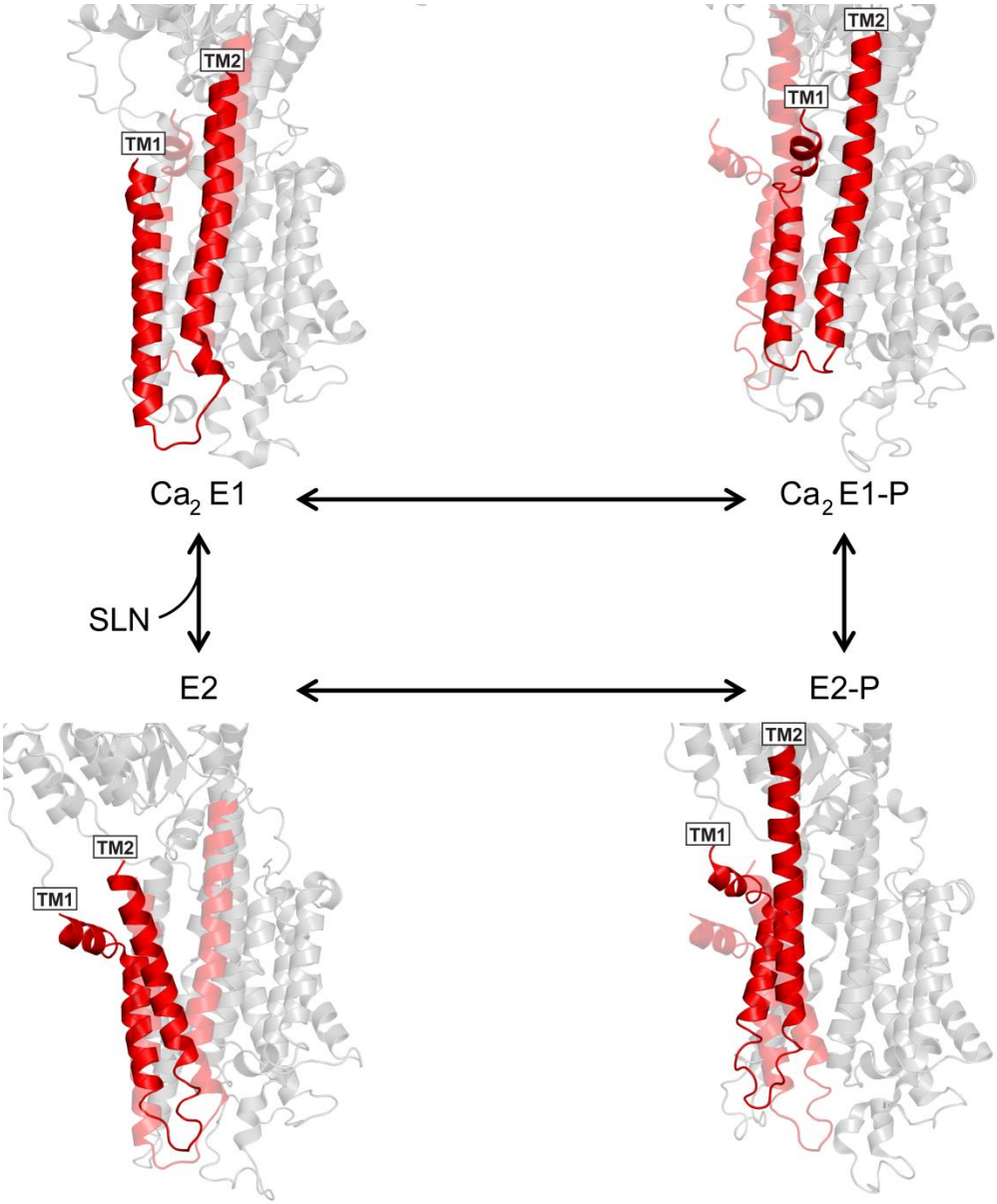

Figure 5-1. Conformational changes of the TM1-2 region of SERCA during the reaction cycle. SERCA structures representing key conformational states in the calcium transport cycle are shown in cartoon representations. SERCA is shown in grey except for the TM1 and TM2 helices which are shown in red. The TM1-2 region representing the subsequent conformation is shown in transparent red. (PDBs: 1SU4, 1T5S, 3B9B, 1IWO)

E2 state to the calcium-bound E1 state, and from the E1-P to the E2-P state. Given that SLN binds to SERCA in the calcium-free state, it is possible for the SLN tail to bind to the TM1-2 luminal linker region and prevent the large structural rearrangements necessary for the rotation of the A-domain and opening of the cytoplasmic calcium ion access channel. This provides a possible explanation as to how SLN traps SERCA in a calcium-free state.

The interaction of the luminal domain of SLN with the TM1-2 linker region in SERCA might also explain the differences in the inhibitory mechanisms of SLN and PLN. Functional and modeling studies have shown that PLN forms most interactions with residues on TM4 and TM6 and fewer interactions with TM2 and TM9 of SERCA (8,15). In fact, only two C-terminal residues of PLN have been proposed to form interactions with residues in the luminal end of TM2 of SERCA (Val^{49} and Leu^{52} of PLN with Val^{89} and Ile^{85} of SERCA, respectively) (16). In the case of SLN, however, the luminal domain forms extensive interactions with the TM1-2 linker region, perhaps preventing TM1 and TM2 from undergoing large conformational changes. Moreover, recent cross-linking studies have shown that mutations of SERCA residues responsible for binding the N-terminal part of the transmembrane domain of PLN had almost no effect on the cross-linking efficiency of SLN to SERCA, suggesting that the interaction between SERCA and the transmembrane domain of SLN are distinct from that of SERCA and PLN (7). Therefore, lack of the luminal extension in PLN could suggest that PLN has a much weaker association with TM2 of SERCA than SLN, which could allow for more conformational freedom in the TM1-2 region of SERCA. This could also be the explanation as to why SLN lowers the maximal activity of SERCA even at high calcium concentrations and PLN does not. In addition, this hypothesis further explains why most

of the PLN inhibitory activity is encoded by its transmembrane domain while most of the inhibitory activity of SLN is encoded by its luminal domain.

The importance of the TM1-2 linker region as a site of SERCA regulation is corroborated by the fact that SLN is not the only membrane protein to use this site to modulate SERCA activity. In chapter 3, we have shown that zfPLN might also use this site to regulate SERCA. Unlike most known PLN proteins, zfPLN has an additional five amino acid luminal extension, which is reminiscent of the luminal domain of SLN. Although there is little similarity between the luminal domains of zfPLN and SLN, we have shown that they both contribute to SERCA inhibition. However, the inhibitory properties of these luminal domains are significantly different. The luminal domain of zfPLN provides much less inhibition (~40% of the zfPLN inhibitory activity) as compared to the luminal domain of SLN (~75% of the SLN inhibitory activity), and it does not appear to have a significant effect on the maximal activity of SERCA. These observed functional differences must be attributed to the differences in sequence composition of the luminal domains. Nonetheless, an interesting commonality between these luminal extensions is that Phe^{54} in zfPLN assumes the same position as the essential Tyr^{31} in SLN. This suggests that both of these aromatic residues interact in a similar manner with the TM1-2 linker region and that the luminal extension of zfPLN uses Phe^{54} to exhibit most of its inhibitory activity.

Interestingly, proteins other than transmembrane regulators of SERCA have also been shown to interact with the TM1-2 linker region of SERCA. This region has also been found to interact with a histidine-rich calcium binding protein (HRC) found in the lumen of cardiac SR (17). HRC is a low affinity but high capacity calcium binding protein involved in SR calcium cycling. Studies in transgenic mice have shown that overexpression of HRC in the heart results in depressed SR calcium uptake rates,

suggesting that HRC inhibits SERCA function (18). More recent studies have demonstrated that HRC specifically interacts with residues 74-90 in the TM1-2 luminal region of SERCA2a and this interaction is decreased at higher calcium concentrations (17). By binding to the TM1-2 linker region, HRC most likely hinders the conformational changes of TM1 and TM2, thereby preventing structural rearrangements necessary for calcium binding. Thus, this is an additional and distinct example of how interactions with the TM1-2 linker region of SERCA can greatly influence SERCA activity.

5-3. TM11 versus other transmembrane peptide regulators of SERCA

Depending on the physiological requirements, SERCA proteins use different regulators to modulate its affinity for calcium. While the muscle-specific SERCA1a and SERCA2a isoforms are regulated by SLN and/or PLN, the enzymatic properties of the housekeeping SERCA2b isoform are modulated by its unique C-terminal extension (2b-tail). The 2b-tail consists of an eleventh TM segment (TM11) and a luminal extension (LE), which together increase the calcium affinity and decrease the maximal turnover rate of SERCA (4). In chapter 4, we have demonstrated that TM11 acts independently from the LE and is an important functional region of the 2b-tail. TM11 significantly increases the apparent calcium affinity and lowers the maximal activity of SERCA. This is in contrast to the primary effect of SLN and PLN, which is to reduce the apparent calcium affinity of SERCA (2). It is well accepted that SLN and PLN exert their function by binding to a hydrophobic grove formed by the TM2, TM4, TM6 and TM9 helices of SERCA, thereby stabilizing the enzyme in a calcium-free E2 state (9). Since this region of SERCA undergoes large conformational changes throughout the calcium transport cycle, it is easy to envision how binding of SLN or PLN could have an effect on calcium affinity. In contrast, the TM11 interactions with SERCA are much different. According to a structural model of SERCA2b, TM11 interacts with TM7 and TM10 helices in the

seemingly immobile anchoring region (TM7-10) of the pump (Fig. 5-2) (19). This site of interaction is distant from where SLN and PLN bind, which at least in part explains the opposite effect this peptide has on the apparent calcium affinity of SERCA. TM11 is thought to restrict the movement of TM7 of SERCA, which would increase the apparent calcium affinity and lower the maximal activity (6). It is noteworthy to mention that TM11 preserves its function when uncoupled from SERCA2b, which suggests that the TM7 and TM10 helices form a highly specific site for interaction with TM11. In fact, residues in the proposed binding site of TM11 (TM7 & TM10) and the binding site of PLN and SLN (TM2, TM4, TM6 & TM9) are highly conserved among SERCA1 and SERCA2 isoforms. This specificity is also reflected by the high sequence divergence between the TM11 segment and the transmembrane domains of SLN and PLN. Thus, TM11 is an active regulator of SERCA that functions independently from SLN and PLN.

The finding that TM11 is not just a passive transmembrane segment but a modulator of SERCA function adds to our understanding of the complex mechanisms used to regulate SERCA activity. It appears that SERCA utilizes multiple sites on the periphery of its transmembrane domain to interact with different regulatory proteins. While SLN and PLN form inhibitory interactions with the mobile part of the transmembrane domain of SERCA, our study demonstrated that the anchoring region of SERCA can also serve as a site of regulation (6). Furthermore, recent EM studies have revealed another important site of intramembrane interactions between SERCA and its regulators (20,21). The PLN pentamer was observed to form interactions with TM3 of SERCA, which is located away from the regulatory SLN/PLN and TM11 binding sites (Fig. 5-2). This interaction has been proposed to facilitate delivery or removal of the monomeric form of PLN from the putative inhibitory site, making it an important part of the mechanism used by PLN to regulate SERCA activity. Interestingly, the use of

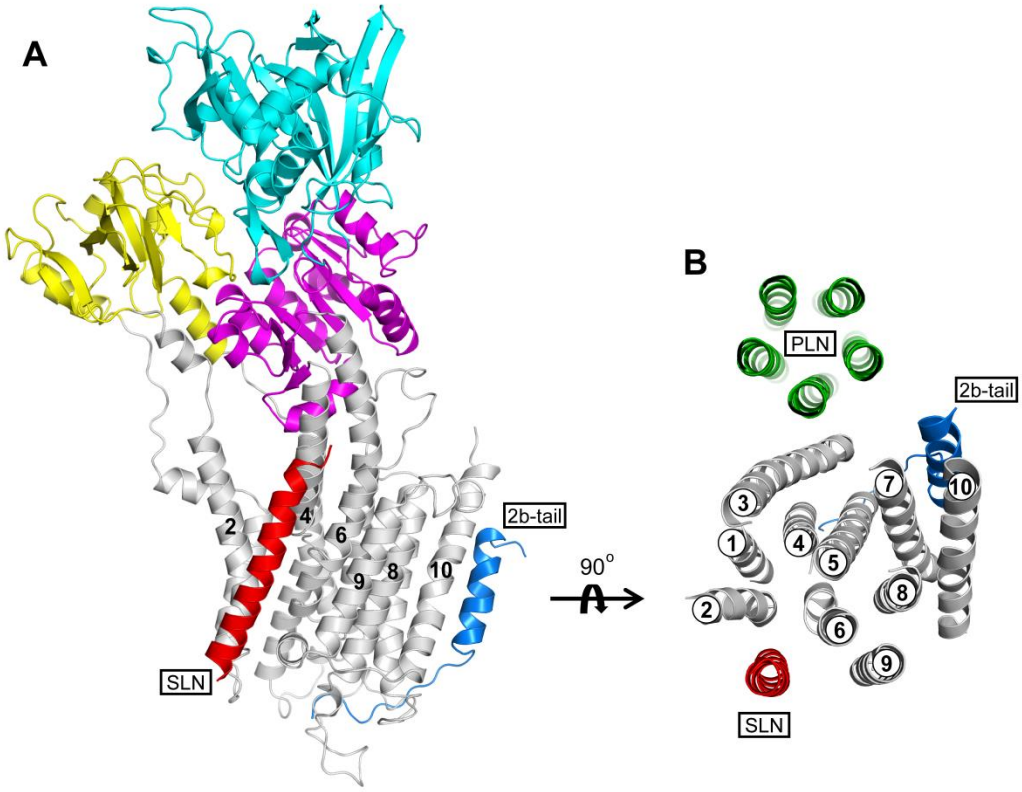

Figure 5-2. Model of transmembrane interactions between SERCA and its endogenous regulators. (A) SERCA (15) in a calcium-free E2 conformation is shown in cartoon representation with the P-domain in magenta, N-domain in cyan, A-domain in yellow, and helices TM1-10 in grey. SLN is shown in red (can also represent the TM domain of PLN) and the 2b-tail of SERCA in blue (19). **(B)** Rotation of panel A by 90° around the x-axis (top-down view). SERCA, SLN and the 2b-tail are colored as in panel A. The transmembrane segment of the PLN pentamer is shown in green (PDB: 2KYV).

multiple sites of regulation is also evident in other P-type ATPases. For example, Na^+/K^+-ATPase is known to associate with two transmembrane regulators, the β- and γ-subunits, which regulate its affinity for ions (22). In fact, the position and mode of binding of the β- and γ-subunits to Na^+/K^+-ATPase highly resemble the binding of TM11 and PLN to SERCA, respectively. This could suggest that important sites of regulation are conserved among the members of the P-type ATPase family. Taken together, SERCA utilizes multiple binding sites in its transmembrane domain to interact with small intramembrane regulatory proteins. These interactions are specific and are used to fine tune the activity of SERCA based on its physiological requirements.

5-4. SERCA regulation from the luminal side of the membrane

As described in the preceding section, physical interactions between the transmembrane domains of SERCA and its endogenous peptide regulators are imperative for their function. Similarly, the cytoplasmic domains of PLN and SLN have been shown to be important in proper regulation of SERCA activity (2). However, less is known about the particular role of the luminal domains of SERCA regulators. The work presented in this thesis focused on functional characterization of SLN, zfPLN and the 2b-tail of SERCA2b, all of which contain unique luminal extensions (Fig. 5-3). We have shown that the luminal extensions of SLN and zfPLN function as independent domains which significantly contribute to their inhibitory activity. Earlier work demonstrated that the luminal extension of the 2b-tail is imperative for increasing the apparent calcium affinity of SERCA (5). Thus, it is evident that the luminal domains of these endogenous regulators play an important part in modulating SERCA activity.

Since the luminal domains of SLN and zfPLN result in the inhibition of SERCA and the luminal extension of the 2b-tail increases the apparent calcium affinity of

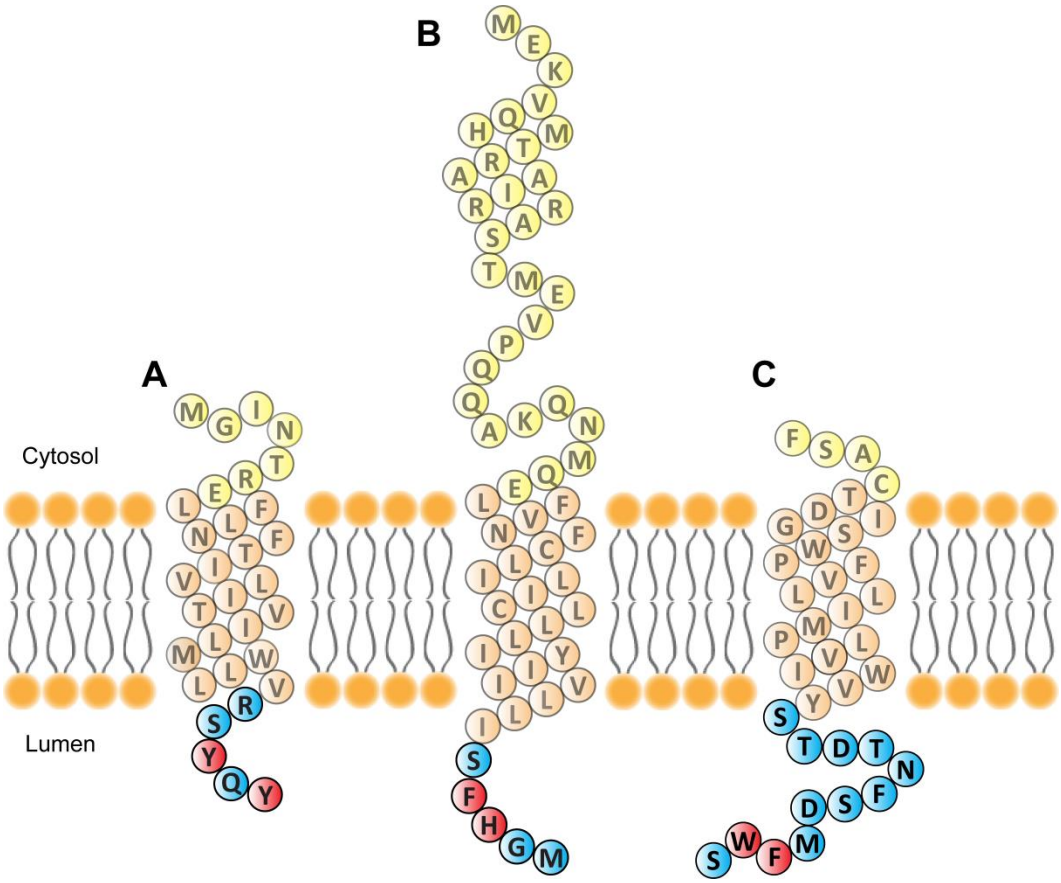

Figure 5-3. Topology models of SERCA regulatory peptides. Topology models for **(A)** SLN, **(B)** zfPLN and **(C)** 2b-tail of SERCA2b. The cytoplasmic domains are yellow, transmembrane domains are orange and luminal domains are blue. Functionally important aromatic residues in the luminal domains are shown in red.

SERCA, they must use different mechanisms to exert their respective roles. In section 5-2, we discussed a probable mechanism of how the luminal domains of SLN and zfPLN can exert their inhibitory properties through the possible interactions with the TM1-2 luminal region of SERCA. The opposite functional effect of the luminal domain of the 2b-tail can also be addressed by examining its interactions with SERCA. The luminal extension of the 2b-tail is much longer than that of SLN or zfPLN, suggesting that its interactions with the luminal part of SERCA are more extensive. Indeed, a structural model of SERCA2b infers a direct interaction of this luminal extension with a luminal cavity formed by the TM1-2, TM3-4, TM7-8 and TM9-10 luminal linker regions of SERCA (19). These interactions are thought to stabilize the calcium-bound E1 conformation of the enzyme. Interestingly, the luminal binding cavity appears to be only formed in the E1 conformation and becomes gradually distorted as the pump transitions toward the calcium-free E2 state (Fig. 5-4). Kinetic analyses revealed that the 2b-tail as a whole is critical for several steps in the reaction cycle, including the steps of calcium dissociation (E1-P to E2-P) and dephosphorylation (E2-P to E2) (4). More recent kinetic studies revealed that the luminal extension of the 2b-tail preferentially stabilizes the calcium-bound E1 and E1-P conformations, whereas TM11 is of particular importance for the rate of the E2-P to E2 transition (23). These results are in line with the structural model of SERCA2b and also explain why, in our studies, TM11 had a more pronounced effect on maximal activity than the apparent calcium affinity of SERCA (6). Moreover, this suggests that the interactions between SERCA and the luminal extension of the 2b-tail are disrupted after the release of calcium. However, it is still unknown whether the luminal extension of the 2b-tail completely dissociates from the enzyme upon release of calcium or remains bound throughout the reaction cycle.

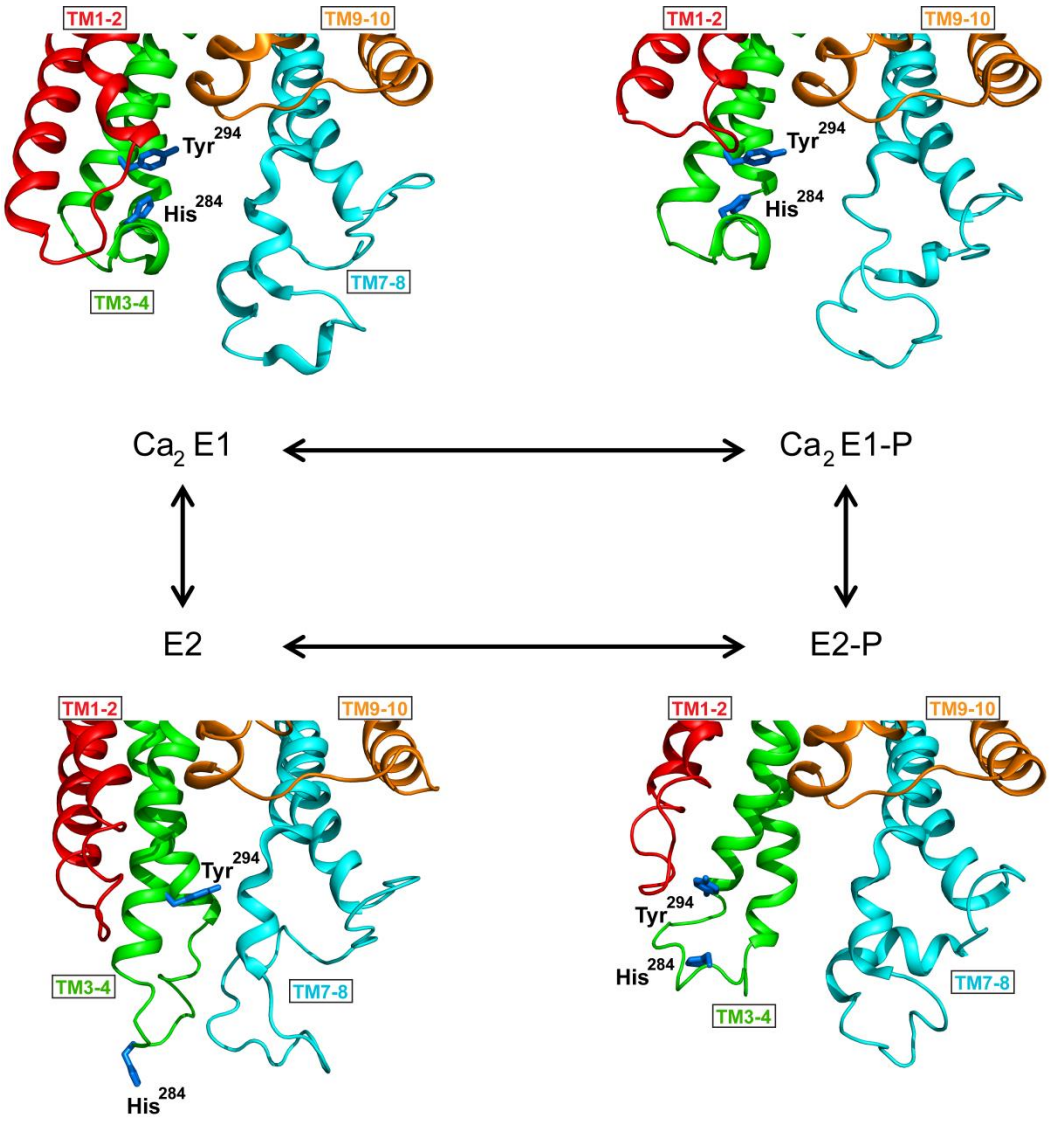

Figure 5-4. Conformational changes in the luminal region of SERCA during the reaction cycle. SERCA structures representing key conformational states in the calcium transport cycle are shown in cartoon representations. The TM1-2 region is shown in red, TM3-4 in green, TM7-8 in cyan and TM9-10 in orange. The TM5-6 region was removed for clarity purposes. Aromatic residues in the TM3-4 luminal region of SERCA proposed to form functional interactions with the luminal extension of the 2b-tail are shown as blue sticks. (PDBs: 1SU4, 1T5T, 3B9B, 1IWO)

Even though the luminal domains of these regulators can be described to have either an inhibitory or stimulatory effect on the apparent calcium affinity of SERCA, they appear to have a common theme with their respective mechanisms of modulation. In section 5-2, we discussed the importance of aromatic residues residing in the luminal domain of SLN in SERCA inhibition. Based on these findings, we proposed that the two aromatic residues in the luminal domain of zfPLN might form similar interactions with the TM1-2 linker region in SERCA. Interestingly, the luminal extension of the 2b-tail also contains two aromatic residues (Phe^{1040} and Trp^{1041}) near the C-terminal end which are crucial for its function (Fig. 5-3C). In fact, a peptide corresponding to the last four C-terminal residues of the 2b-tail (^{1038}Met-Phe-Trp-Ser^{1042}) was shown to be sufficient to significantly increase the apparent calcium affinity of SERCA (19). A molecular model of SERCA2b indicates that Phe^{1040} and Trp^{1041} of the 2b-tail might form important interactions with Tyr^{294} and His^{284} in the TM3-4 luminal linker region of SERCA, respectively (Fig. 5-5C). These interactions appear to be strong enough to prevent movement of the luminal loops necessary for the release of calcium. It is noteworthy to point out that the TM3-4 luminal linker region of SERCA is more disordered in the calcium-free states than in the calcium-bound states of the enzyme (Fig. 5-4). This causes His^{284} to be facing away from the luminal binding cavity, which prevents interactions with the aromatic residues of the 2b-tail. Thus, the luminal extensions of SLN and zfPLN form interactions with the TM1-2 luminal region of SERCA to stabilize the enzyme in a calcium-free E2 state, whereas the luminal extension of the 2b-tail interacts with luminal loops of SERCA to stabilize the enzyme in a calcium-bound E1 state (Fig. 5-5). Moreover, interactions between aromatic residues in the luminal extensions of these peptide regulators and the aromatic residues in the luminal loops of SERCA are essential for their regulatory function.

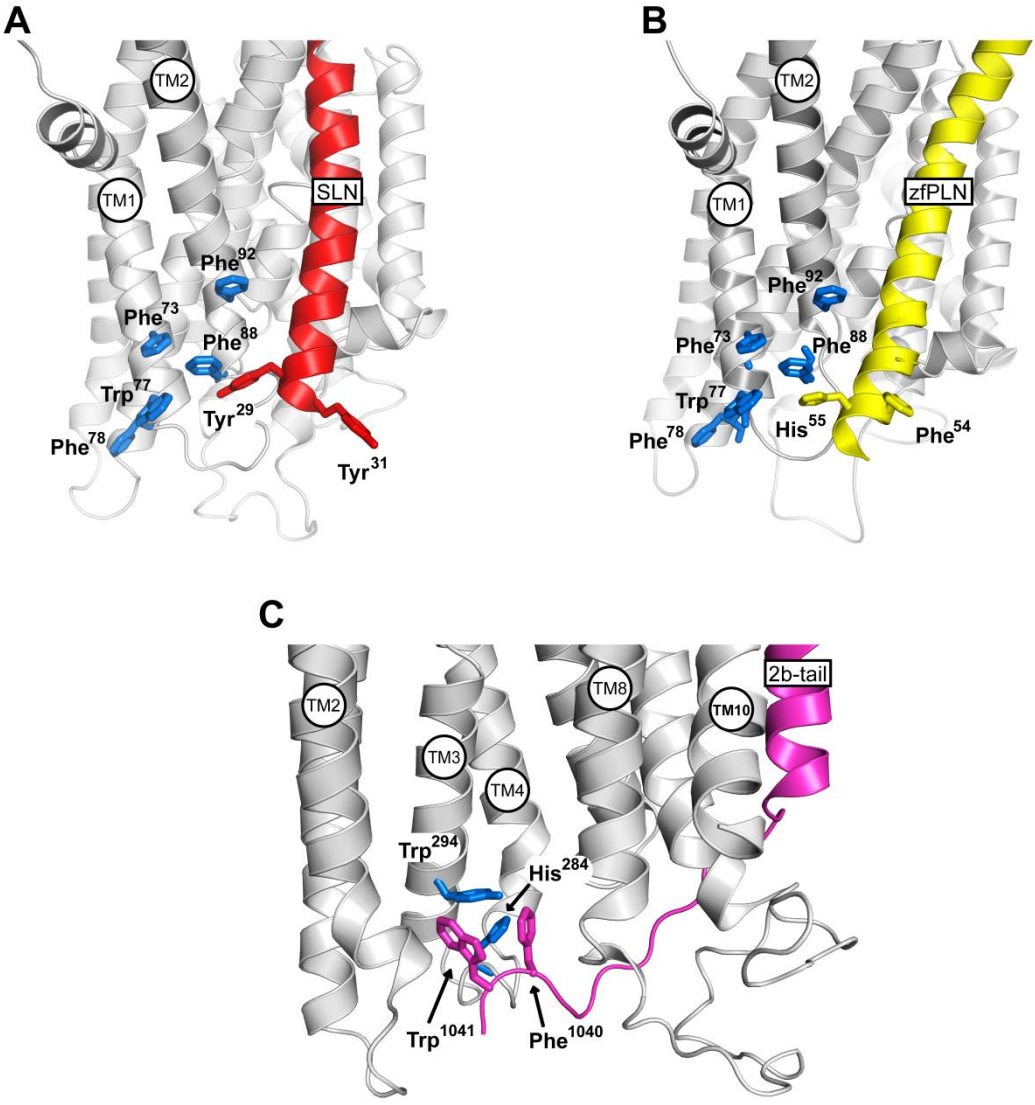

Figure 5-5. Interactions between SERCA and the luminal extensions of its peptide regulators. Molecular models of SERCA (grey) in complex with (A) SLN (red, (15)), (B) zfPLN (yellow, (15)) and (C) 2b-tail (magenta,(19)). SERCA residues proposed to interact with the aromatic residues in the luminal extensions of the peptide regulators are shown as blue sticks. Functionally important aromatic residues in the luminal extensions of SLN, zfPLN and the 2b-tail are shown as sticks.

5-5. Disease relevance

The role of SERCA pumps in maintaining optimal calcium homeostasis is of great physiological importance (24). Defects in the calcium pump function and regulation have been linked to many human diseases, including heart failure, cancer, as well as rare forms of skin and skeletal muscle diseases (25). While the pathophysiology associated with this family of proteins has been well documented, the molecular etiology is still to be fully understood.

Abnormal calcium handling is a hallmark of human heart failure (26). Decreases in SERCA expression level and activity have been shown to directly contribute to the deteriorated cardiac function (27). Increasing the activity of SERCA in order to stimulate SR calcium uptake, is therefore considered as a potential therapeutic strategy to improve contractility of a failing heart. This can be achieved by elevating SERCA2a expression levels, which has been shown to improve cardiac contractility in animal models (28,29). In fact, overexpression of SERCA2a using adenoviral (AAV) gene transfer has recently been tested as a treatment in clinical trials (30). While there are drawbacks to this therapy, such as immunity to the adenovirus, most treated patients demonstrated overall improvement in cardiac contractility. An alternative approach is to increase the apparent calcium affinity of SERCA2a. Our studies show that the 2b-tail increases the apparent calcium affinity, suggesting that its interaction site may serve as a novel drug target to increase the calcium affinity of malfunctioning SERCA2a in the failing heart as a mechanism for improving cardiac contractility.

The regulation of SERCA2a by PLN plays a critical role in cardiac contractility and in mediating the β-adrenergic response (31). Several genetic mutations in PLN have already been found to cause dilated cardiomyopathy in humans (1). Since SLN is

abundantly expressed in the atria of the heart it can also be a major factor in heart disease development and progression. In fact, expression of SLN at both mRNA and protein levels has been shown to be down-regulated in the atria of patients with chronic atrial fibrillation which appears to contribute to atrial remodeling (32-34). Although no disease associated mutations have been described for SLN, it is likely that mutations will be found in SLN that cause heart failure. Given that the luminal domain of SLN encodes for most of its inhibitory activity, this region of SLN could be a hotspot for disease causing mutations.

Aside from being an active regulator of cardiac SERCA2a, SLN is the primary regulator of SERCA1a in fast-twitch skeletal muscle, where it was recently shown to play an additional role in thermogenesis (35). SLN is thought to promote uncoupling of SERCA1a, which causes an increase in ATP hydrolysis and leads to muscle dependent non-shivering thermogenesis (NST). Thus, SERCA1a-SLN interaction could be a potential pharmacological target to increase energy expenditure as a strategy to treat obesity.

Taken together, the molecular details of SERCA regulation by endogenous peptide modulators outlined in this work provide important insights that might be beneficial to the long term goal of rational therapeutic design.

5-6. References

1. Kranias, E. G., and Hajjar, R. J. (2012) Modulation of cardiac contractility by the phospholamban/SERCA2a regulatome. *Circulation research* **110**, 1646-1660

2. Bhupathy, P., Babu, G. J., and Periasamy, M. (2007) Sarcolipin and phospholamban as regulators of cardiac sarcoplasmic reticulum Ca2+ ATPase. *Journal of molecular and cellular cardiology* **42**, 903-911

3. Gorski, P. A., Glaves, J. P., Vangheluwe, P., and Young, H. S. (2013) Sarco(endo)plasmic reticulum calcium ATPase (SERCA) inhibition by sarcolipin is encoded in its luminal tail. *The Journal of biological chemistry* **288**, 8456-8467

4. Dode, L., Andersen, J. P., Leslie, N., Dhitavat, J., Vilsen, B., and Hovnanian, A. (2003) Dissection of the functional differences between sarco(endo)plasmic reticulum Ca2+-ATPase (SERCA) 1 and 2 isoforms and characterization of Darier disease (SERCA2) mutants by steady-state and transient kinetic analyses. *The Journal of biological chemistry* **278**, 47877-47889

5. Verboomen, H., Wuytack, F., Van den Bosch, L., Mertens, L., and Casteels, R. (1994) The functional importance of the extreme C-terminal tail in the gene 2 organellar Ca(2+)-transport ATPase (SERCA2a/b). *The Biochemical journal* **303 (Pt 3)**, 979-984

6. Gorski, P. A., Trieber, C. A., Lariviere, E., Schuermans, M., Wuytack, F., Young, H. S., and Vangheluwe, P. (2012) Transmembrane helix 11 is a genuine regulator of the endoplasmic reticulum Ca2+ pump and acts as a functional parallel of beta-subunit on alpha-Na+,K+-ATPase. *The Journal of biological chemistry* **287**, 19876-19885

7. Sahoo, S. K., Shaikh, S. A., Sopariwala, D. H., Bal, N. C., and Periasamy, M. (2013) Sarcolipin protein interaction with sarco(endo)plasmic reticulum Ca2+ ATPase (SERCA) is distinct from phospholamban protein, and only sarcolipin can promote uncoupling of the SERCA pump. *The Journal of biological chemistry* **288**, 6881-6889

8. Toyoshima, C., Asahi, M., Sugita, Y., Khanna, R., Tsuda, T., and MacLennan, D. H. (2003) Modeling of the inhibitory interaction of phospholamban with the Ca2+ ATPase. *Proceedings of the National Academy of Sciences of the United States of America* **100**, 467-472

9. Asahi, M., Sugita, Y., Kurzydlowski, K., De Leon, S., Tada, M., Toyoshima, C., and MacLennan, D. H. (2003) Sarcolipin regulates sarco(endo)plasmic reticulum Ca2+-ATPase (SERCA) by binding to transmembrane helices alone or in association with phospholamban. *Proceedings of the National Academy of Sciences of the United States of America* **100**, 5040-5045

10. Toyoshima, C., Iwasawa, S., Ogawa, H., Hirata, A., Tsueda, J., and Inesi, G. (2013) Crystal structures of the calcium pump and sarcolipin in the Mg2+-bound E1 state. *Nature* **495**, 260-264

11. Winther, A. M., Bublitz, M., Karlsen, J. L., Moller, J. V., Hansen, J. B., Nissen, P., and Buch-Pedersen, M. J. (2013) The sarcolipin-bound calcium pump stabilizes calcium sites exposed to the cytoplasm. *Nature* **495**, 265-269

12. Moller, J. V., Olesen, C., Winther, A. M., and Nissen, P. (2010) The sarcoplasmic Ca2+-ATPase: design of a perfect chemi-osmotic pump. *Quarterly reviews of biophysics* **43**, 501-566

13. Daiho, T., Yamasaki, K., Wang, G., Danko, S., Iizuka, H., and Suzuki, H. (2003) Deletions of any single residues in Glu40-Ser48 loop connecting a domain and the first transmembrane helix of sarcoplasmic reticulum Ca(2+)-ATPase result in almost complete inhibition of conformational transition and hydrolysis of phosphoenzyme intermediate. *The Journal of biological chemistry* **278**, 39197-39204

14. Daiho, T., Yamasaki, K., Danko, S., and Suzuki, H. (2007) Critical role of Glu40-Ser48 loop linking actuator domain and first transmembrane helix of Ca2+-ATPase in Ca2+ deocclusion and release from ADP-insensitive phosphoenzyme. *The Journal of biological chemistry* **282**, 34429-34447

15. Seidel, K., Andronesi, O. C., Krebs, J., Griesinger, C., Young, H. S., Becker, S., and Baldus, M. (2008) Structural characterization of Ca(2+)-ATPase-bound phospholamban in lipid bilayers by solid-state nuclear magnetic resonance (NMR) spectroscopy. *Biochemistry* **47**, 4369-4376

16. Chen, Z., Akin, B. L., Stokes, D. L., and Jones, L. R. (2006) Cross-linking of C-terminal residues of phospholamban to the Ca2+ pump of cardiac sarcoplasmic reticulum to probe spatial and functional interactions within the transmembrane domain. *The Journal of biological chemistry* **281**, 14163-14172

17. Arvanitis, D. A., Vafiadaki, E., Fan, G. C., Mitton, B. A., Gregory, K. N., Del Monte, F., Kontrogianni-Konstantopoulos, A., Sanoudou, D., and Kranias, E. G. (2007) Histidine-rich Ca-binding protein interacts with sarcoplasmic reticulum Ca-ATPase. *American journal of physiology. Heart and circulatory physiology* **293**, H1581-1589

18. Gregory, K. N., Ginsburg, K. S., Bodi, I., Hahn, H., Marreez, Y. M., Song, Q., Padmanabhan, P. A., Mitton, B. A., Waggoner, J. R., Del Monte, F., Park, W. J., Dorn, G. W., 2nd, Bers, D. M., and Kranias, E. G. (2006) Histidine-rich Ca binding protein: a regulator of sarcoplasmic reticulum calcium sequestration and cardiac function. *Journal of molecular and cellular cardiology* **40**, 653-665

19. Vandecaetsbeek, I., Trekels, M., De Maeyer, M., Ceulemans, H., Lescrinier, E., Raeymaekers, L., Wuytack, F., and Vangheluwe, P. (2009) Structural basis for the high Ca2+ affinity of the ubiquitous SERCA2b Ca2+ pump. *Proceedings of the National Academy of Sciences of the United States of America* **106**, 18533-18538

20. Stokes, D. L., Pomfret, A. J., Rice, W. J., Glaves, J. P., and Young, H. S. (2006) Interactions between Ca2+-ATPase and the pentameric form of phospholamban in two-dimensional co-crystals. *Biophysical journal* **90**, 4213-4223

21. Glaves, J. P., Trieber, C. A., Ceholski, D. K., Stokes, D. L., and Young, H. S. (2011) Phosphorylation and mutation of phospholamban alter physical interactions with the sarcoplasmic reticulum calcium pump. *Journal of molecular biology* **405**, 707-723

22. Morth, J. P., Pedersen, B. P., Toustrup-Jensen, M. S., Sorensen, T. L., Petersen, J., Andersen, J. P., Vilsen, B., and Nissen, P. (2007) Crystal structure of the sodium-potassium pump. *Nature* **450**, 1043-1049

23. Clausen, J. D., Vandecaetsbeek, I., Wuytack, F., Vangheluwe, P., and Andersen, J. P. (2012) Distinct roles of the C-terminal 11th transmembrane helix and luminal extension in the partial reactions determining the high Ca2+ affinity of sarco(endo)plasmic reticulum Ca2+-ATPase isoform 2b (SERCA2b). *The Journal of biological chemistry* **287**, 39460-39469

24. Carafoli, E. (2002) Calcium signaling: a tale for all seasons. *Proceedings of the National Academy of Sciences of the United States of America* **99**, 1115-1122

25. Periasamy, M., and Kalyanasundaram, A. (2007) SERCA pump isoforms: their role in calcium transport and disease. *Muscle & nerve* **35**, 430-442

26. Morgan, J. P. (1991) Abnormal intracellular modulation of calcium as a major cause of cardiac contractile dysfunction. *The New England journal of medicine* **325**, 625-632

27. Kranias, E. G., and Bers, D. M. (2007) Calcium and cardiomyopathies. *Sub-cellular biochemistry* **45**, 523-537

28. Miyamoto, M. I., del Monte, F., Schmidt, U., DiSalvo, T. S., Kang, Z. B., Matsui, T., Guerrero, J. L., Gwathmey, J. K., Rosenzweig, A., and Hajjar, R. J. (2000) Adenoviral gene transfer of SERCA2a improves left-ventricular function in aortic-banded rats in transition to heart failure. *Proceedings of the National Academy of Sciences of the United States of America* **97**, 793-798

29. del Monte, F., Williams, E., Lebeche, D., Schmidt, U., Rosenzweig, A., Gwathmey, J. K., Lewandowski, E. D., and Hajjar, R. J. (2001) Improvement in survival and cardiac metabolism after gene transfer of sarcoplasmic reticulum Ca(2+)-ATPase in a rat model of heart failure. *Circulation* **104**, 1424-1429

30. Jaski, B. E., Jessup, M. L., Mancini, D. M., Cappola, T. P., Pauly, D. F., Greenberg, B., Borow, K., Dittrich, H., Zsebo, K. M., Hajjar, R. J., and Calcium Up-Regulation by Percutaneous Administration of Gene Therapy In Cardiac Disease Trial, I. (2009) Calcium upregulation by percutaneous administration of gene therapy in cardiac disease (CUPID Trial), a first-in-human phase 1/2 clinical trial. *Journal of cardiac failure* **15**, 171-181

31. MacLennan, D. H., and Kranias, E. G. (2003) Phospholamban: a crucial regulator of cardiac contractility. *Nature reviews. Molecular cell biology* **4**, 566-577

32. Uemura, N., Ohkusa, T., Hamano, K., Nakagome, M., Hori, H., Shimizu, M., Matsuzaki, M., Mochizuki, S., Minamisawa, S., and Ishikawa, Y. (2004) Down-regulation of sarcolipin mRNA expression in chronic atrial fibrillation. *European journal of clinical investigation* **34**, 723-730

33. Shanmugam, M., Molina, C. E., Gao, S., Severac-Bastide, R., Fischmeister, R., and Babu, G. J. (2011) Decreased sarcolipin protein expression and enhanced

sarco(endo)plasmic reticulum Ca2+ uptake in human atrial fibrillation. *Biochemical and biophysical research communications* **410**, 97-101

34. Xie, L. H., Shanmugam, M., Park, J. Y., Zhao, Z., Wen, H., Tian, B., Periasamy, M., and Babu, G. J. (2012) Ablation of sarcolipin results in atrial remodeling. *American journal of physiology. Cell physiology* **302**, C1762-1771

35. Bal, N. C., Maurya, S. K., Sopariwala, D. H., Sahoo, S. K., Gupta, S. C., Shaikh, S. A., Pant, M., Rowland, L. A., Bombardier, E., Goonasekera, S. A., Tupling, A. R., Molkentin, J. D., and Periasamy, M. (2012) Sarcolipin is a newly identified regulator of muscle-based thermogenesis in mammals. *Nature medicine* **18**, 1575-1579

Appendix I

Probing the oligomeric state of sarcolipin

Acknowledgements: Dr. C. Trieber functionally characterized the PLN alanine mutants and Dr. D. Ceholski functionally characterized the PLN truncation constructs. Dr. JP Glaves helped in designing SLN mutants.

I-1. Introduction

Phospholamban (PLN) and sarcolipin (SLN) are small integral membrane proteins that regulate the enzymatic activity of the sarco(endo)plasmic reticulum calcium ATPase (SERCA). PLN is expressed in cardiac, smooth and slow-twitch skeletal muscle, while SLN is expressed in fast-twitch skeletal muscle and the atria of the heart (1). PLN has 52 amino acids and consists of a cytoplasmic domain (domain I; residues 1-29) and a transmembrane domain (domain II; residues 30-52) (2). The cytoplasmic domain is further divided into domain Ia (N-terminal cytoplasmic helix) and domain Ib (a flexible linker connecting the two helices). SLN is made up of 31 amino acids, consisting of a short cytoplasmic domain (residues 1-6), a transmembrane helix (residues 7-26), and a luminal extension (residues 27-31) (3). The homology of the two peptides is readily apparent in their membrane regions, with many identical or conserved residues (Fig. I-1).

The regulation of SERCA by PLN or SLN is determined by the phosphorylation states of these proteins as well as the cytosolic calcium concentration. Both PLN and SLN are inhibitors of SERCA in their dephosphorylated states and it has been shown that phosphorylation of the peptides reverses SERCA inhibition (1). It is well documented that the inhibitory PLN monomer can self-associate to form pentamers, which is considered as a functionally inactive storage form of the peptide (4). Site-specific mutagenesis experiments revealed that the PLN pentamer is stabilized by a leucine-isoleucine zipper motif (4,5). This was later supported by NMR structures of the PLN pentamer which revealed that the transmembrane leucine residues (Leu^{37}, Leu^{44}, and Leu^{51}) in one transmembrane helix of PLN form hydrophobic interactions with isoleucine residues (Ile^{40} and Ile^{47}) in the neighboring PLN monomer (6,7). In addition to the leucine and isoleucine residues, cysteine residues (Cys^{36}, Cys^{41} and Cys^{46}) in the transmembrane domain of PLN have also been shown to play an important role in structural stability of

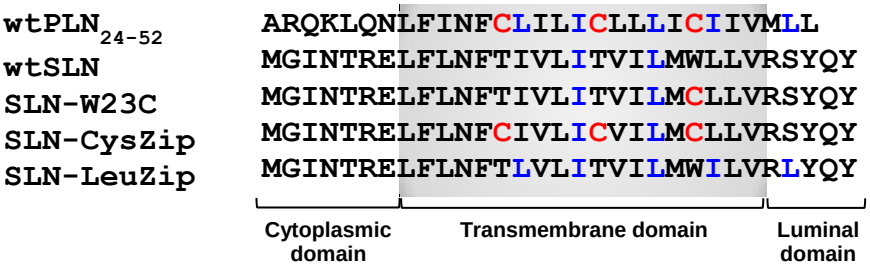

Figure I-1. Amino acid sequence alignments for PLN and various SLN constructs. The cytoplasmic, transmembrane, and luminal domains are indicated. Transmembrane cysteine residues are shown in red and the transmembrane leucine-isoleucine residues involved in PLN pentamer formation are shown in blue.

the pentamer. Mutation of the transmembrane cysteines in PLN has been shown to completely prevent pentamer formation without having a major effect on its ability to inhibit SERCA (5,8,9). In contrast to PLN, SLN is thought to exist primarily as a monomer, although several studies have shown that SLN can also oligomerize. Analytical ultracentrifugation experiments revealed that SLN oligomerizes in the presence of nonionic detergents and cross-linking showed that SLN has the ability to self-associate in liposomes (10). Recently, a fluorescence study done in insect cells demonstrated that SLN monomers associate into dimers and higher order oligomers, whereas mutant Ile^{17}-to-Ala SLN only formed monomers and dimers (11). Furthermore, when incorporated in thiolipid bilayers, SLN has been shown to form channels selective toward chloride and phosphate anions (12).

Given the marked differences in their ability to form oligomers, we decided to investigate sequence elements in SLN and PLN that might be important in controlling their ability to oligomerize. We chose to sequentially introduce residues important for the PLN pentamer formation into SLN and examine their effect on SERCA activity and oligomer formation. To summarize our findings, incorporation of the leucine-isoleucine zipper motif into SLN resulted in a mild loss-of-function and did not enhance its ability to form oligomers. SLN mutants containing either one or all three transmembrane cysteines known to be important for the PLN pentamer stability resulted in a mild gain of inhibitory function but were completely monomeric. Interestingly, the C-terminal ^{50}Met-Leu-^{52}Leu motif of PLN is known to play a role in pentamer formation. Since this motif is replaced by a polar ^{27}Arg-Ser-Tyr-Gln-^{31}Tyr sequence in SLN, it could suggest that the luminal domain of SLN largely interferes with oligomerization of SLN. Based on our results, we propose that the presence of polar and aromatic residues at key positions in

the transmembrane and luminal domains of SLN reduce the stability of its oligomeric forms.

I-2. Results and Discussion

I-2.1. Incorporation of the PLN leucine-isoleucine zipper motif into SLN. Although highly homologous, the transmembrane domains of PLN and SLN contain several amino acid differences which could be responsible for the observed oligomeric states of these peptides (Fig. I-1). Several studies have shown that the leucine-isoleucine zipper motif in PLN is a crucial sequence element responsible for pentamer formation (5,8). Mutation of any of the leucine or isoleucine residues in the zipper motif of PLN has been shown to greatly destabilize the pentamer. Since the residues that make up the leucine-isoleucine zipper motif are not fully conserved in SLN, this could be a potential explanation as to why SLN exists primarily as a monomer. To test this hypothesis, we decided to introduce the leucine-isoleucine zipper motif into SLN and examine the ability of this new construct (designated SLN-LeuZip) to regulate SERCA activity and form oligomers. Given that two of the five PLN zipper motif residues are conserved in SLN (Ile^{17} and Leu^{21}), we mutated the remaining three residues to generate SLN-LeuZip (two conservative mutations, Ile^{14}-to-Leu and Leu^{24}-to-Ile; and Ser^{28}-to-Leu). Next, we co-reconstituted SLN-LeuZip with SERCA into proteoliposomes and measured its effect on the calcium-dependent ATPase activity of SERCA. Compared to wild-type SLN, SLN-LeuZip resulted in a significant loss of inhibitory function (K_{Ca} of 0.64 μM compared to 0.80μM calcium for wild-type) and almost a complete recovery of the maximal activity of SERCA (V_{max} of 3.9 μmol mg^{-1} min^{-1}; i.e. no reduction in the V_{max} of SERCA as seen for wild-type SLN) (Fig. I-2 and Table I-1). Perhaps it is not surprising that SLN-LeuZip

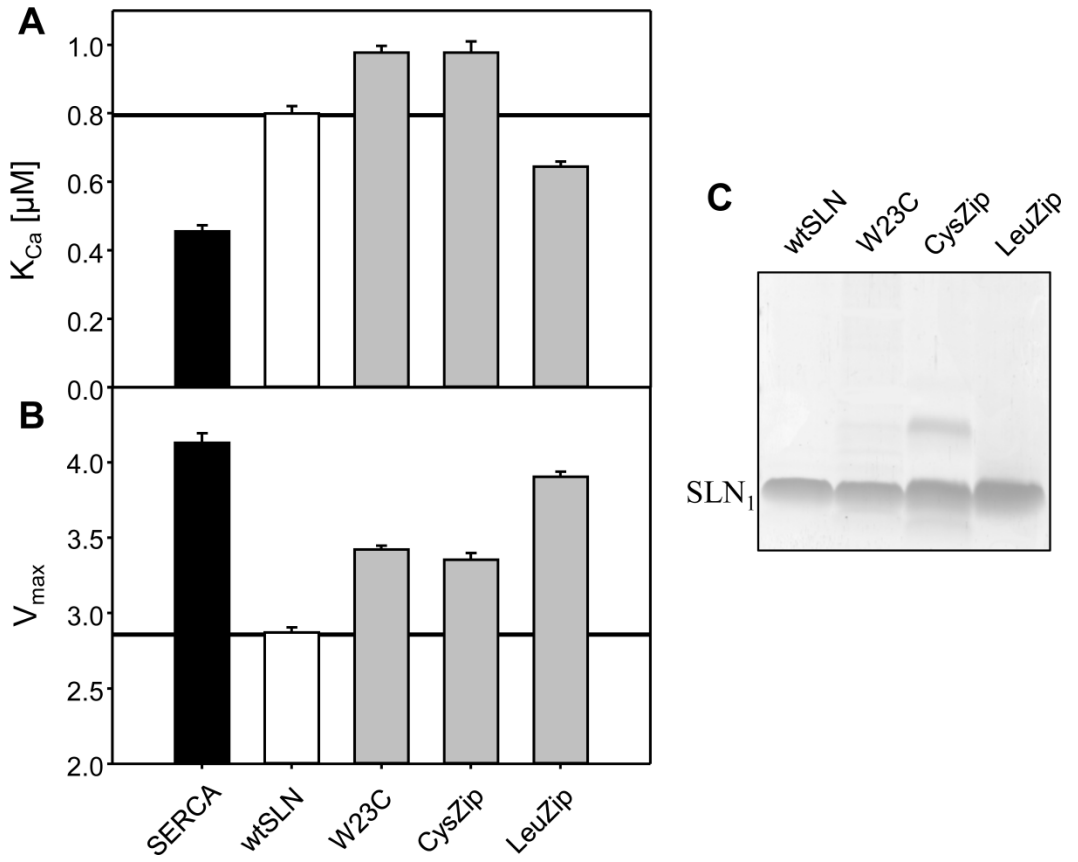

Figure I-2. The effects of mutation in the transmembrane domain of SLN on the K_{Ca} and V_{max} of SERCA. K_{Ca} **(A)** and V_{max} **(B)** values for were determined from ATPase activity measurements for SERCA in the absence and presence of wild-type and mutant forms of SLN. Each data point is the mean ± S.E. (*error bars*) ($n \geq 3$). The V_{max}, K_{Ca}, and n_H are given in Table II-1. **(C)** SDS-PAGE of wild-type and mutant forms of SLN (5 μg per lane; 16% acrylamide gel).

Table I-1. Kinetic parameters from Hill plots.

	V_{max} (μmol mg^{-1} min^{-1})	K_{ca} (μM)	n_H	n
SERCA	4.1 ± 0.1	0.46 ± 0.02	1.7 ± 0.1	32
wtSLN	2.9 ± 0.1	0.80 ± 0.02	1.4 ± 0.1	10
W23C	3.4 ± 0.1	0.98 ± 0.02	1.4 ± 0.1	4
CysZip	3.4 ± 0.1	0.98 ± 0.03	1.5 ± 0.1	3
LeuZip	3.9 ± 0.1	0.64 ± 0.01	1.5 ± 0.1	3
wtPLN	6.1 ± 0.1	0.88 ± 0.03	2.0 ± 0.1	9
M50A[a]	4.6 ± 0.1	0.69 ± 0.02	1.9 ± 0.1	8
L51A[a]	4.3 ± 0.2	1.12 ± 0.08	1.9 ± 0.2	4
L52A[a]	5.0 ± 0.1	0.69 ± 0.04	1.9 ± 0.2	5
L52stop	5.6 ± 0.2	0.73 ± 0.04	1.8 ± 0.1	5
M50stop	6.7 ± 0.2	0.69 ± 0.05	1.7 ± 0.2	6

[a] The kinetic data were taken from Trieber *et al* (13).

is a loss-of-function construct as it has one of SLN's essential C-terminal residues mutated to leucine (Ser^{28}-to-Leu). We have recently shown that alanine substitution of any residue within the ^{27}RSYQY motif had a negative impact on the ability of SLN to alter the apparent calcium affinity of SERCA (14). Finally, we used SDS-PAGE to examine the oligomeric state of SLN-LeuZip. SLN-LeuZip appeared to be completely monomeric and indistinguishable from wild-type SLN (Fig. I-2C), indicating that introduction of the leucine-isoleucine zipper motif into SLN did not increase its propensity to form oligomers.

I-2.2. Incorporation of the PLN transmembrane cysteines into SLN. Previous studies have shown that mutation of the three cysteines in the transmembrane domain of PLN (Cys^{36}, Cys^{41} and Cys^{46}) to alanine, serine, or phenylalanine disrupts the pentameric structure of PLN, suggesting that cysteine side chains are crucial for the oligomeric stability of PLN (5,8). Interestingly, the transmembrane domain of SLN does not contain any cysteines. Instead, the homologous positions in SLN are occupied by two threonines (Thr^{13} and Thr^{18}) and an aromatic tryptophan (Trp^{23}) (Fig. I-1). In order to test whether these residues interfere with formation of SLN oligomers, we decided to introduce cysteines into the transmembrane domain of SLN to more closely mimic the transmembrane domain of PLN. To this end, two SLN mutants were constructed, one with just the aromatic Trp^{23} mutated to cysteine (SLN W23C) and one with Thr^{13}, Thr^{18} and Trp^{23} mutated cysteines (designated SLN-CysZip). The calcium-dependent ATPase activity was measured for SERCA in the presence of the SLN mutants, where SERCA alone served as a negative control and SERCA in the presence of wild-type SLN served as a positive control. Compared to wild-type SLN, including SLN-W23C into proteoliposomes resulted in a significant gain-of-function (K_{Ca} of 0.98 μM compared to 0.80μM calcium for wild-type) and a V_{max} value halfway between that of SERCA alone

and SERCA in the presence of wild-type SLN (V_{max} of 3.4) (Fig. I-2 and Table I-1). Interestingly, including SLN-CysZip had virtually identical effect on the apparent calcium affinity and the maximal activity of SERCA as SLN-W23C (Fig. I-2 and Table I-1). This suggests that unlike Thr^{13} and Thr^{18}, Trp^{23} of SLN might play an important role in modulating the SERCA-SLN inhibitory complex.

The ability of the cysteine mutants of SLN to form oligomers was tested by SDS-PAGE. Similar to SLN-LeuZip, SLN-W23C and SLN-CysZip appeared to be completely monomeric (Fig. I-2C). This was a surprising finding, given that SLN-CysZip contains almost all of the PLN residues responsible for pentamer formation (three cysteines and almost completely conserved leucine-isoleucine zipper motif; Fig. I-1). Thus, introducing the essential PLN sequence motifs responsible for pentamer stability into SLN does not enhance its ability to form oligomers, suggesting that SLN has other sequence elements which prevent it from forming stable oligomers.

I-2.3. The C-termini of PLN and SLN play an important role in defining their oligomeric states. The C-terminal sequences of PLN and SLN represent a marked difference between these two proteins, where the hydrophobic Met^{50}-Leu-Leu^{52} in PLN is replaced by the more polar Arg^{27}-Ser-Tyr-Gln-Tyr^{31} in SLN. Since introducing the leucine-isoleucine zipper motif and the native PLN cysteines into the transmembrane domain of SLN did not enhance its ability to form oligomers, we hypothesized that the differences in the C-termini of SLN and PLN might play an important role in determining their oligomeric states. Therefore, we decided to examine the role of the last three C-terminal residues of PLN in maintaining pentamer stability. In an earlier study, we mutated residues 50-52 of PLN to alanine, co-reconstituted each mutant with SERCA, and measured the calcium-dependent ATPase activity of the proteoliposomes (Fig. I-3 and Table I-1) (13). We reported Met^{50}-to-Ala (M50A) and Leu^{52}-to-Ala (L52A) as mild loss-

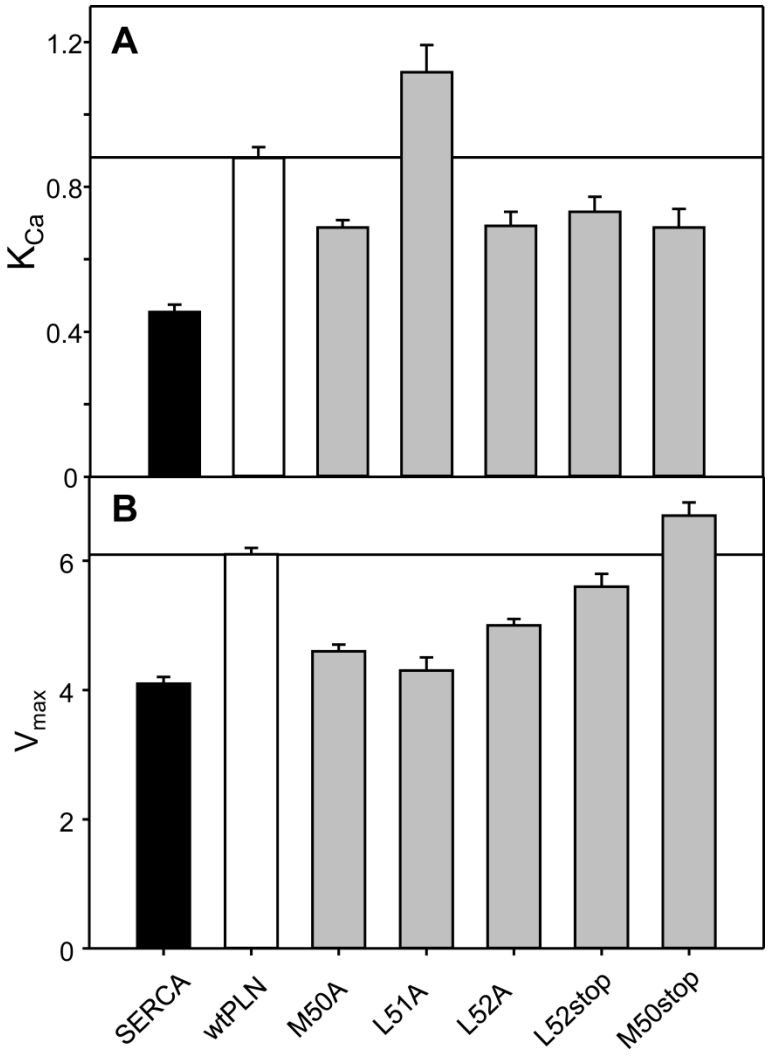

Figure I-3. The effects of mutation and truncation of the C-terminal end of PLN on the K_{Ca} and V_{max} of SERCA. K_{Ca} **(A)** and V_{max} **(B)** values for were determined from ATPase activity measurements for SERCA in the absence and presence of wild-type and various PLN constructs. Each data point is the mean ± S.E. (*error bars*) ($n \geq 4$). The V_{max}, K_{Ca}, and n_H are given in Table I-1.

of-function mutants and Leu^{51}-to-Ala (L51A) as a mild gain-of-function, as compared to wild-type PLN. Herein, we decided to examine the effects of these mutations on the pentamer stability. To this end, we used quantitative gel electrophoresis to determine the total percent of pentamer and monomer of wild-type and mutant forms of PLN at different SDS concentrations (2% and 6% SDS final concentrations). While the L52A mutant was indistinguishable from wild-type PLN, M50A and L51A formed less stable pentamers (Fig. I-4 and Table I-2). Compare the % pentamer values in the presence of 2% SDS for M50A (49%), L51A (23%), and wild-type PLN (63%). Since Leu^{51} is part of the leucine-isoleucine zipper motif, it was not surprising that alanine substitution at this position had the most negative impact on the ability of PLN to form pentamers (Fig. I-5A).

As a next step in examining the role of the C-terminal residues of PLN in pentamer stability, we chose to generate truncated variants of PLN, one missing the last C-terminal amino acid (L52stop) and one missing the last three C-terminal amino acids (M50stop). Similar to the alanine mutants, removal of either one or three C-terminal amino acids resulted in a mild loss of PLN function (K_{Ca} of 0.73 μM for L52stop and 0.69 μM calcium for M50stop; Fig. I-3 and Table I-1). The pentamer stability of these truncated constructs was examined in the same fashion as the alanine mutants described above. Removal of the last C-terminal residue in PLN had no effect on its ability to form pentamers. The pentamer and monomer composition of L52stop at low and high SDS concentrations did not significantly differ from what was observed for wild-type PLN (Fig. I-4 and Table I-2). This is not surprising considering that Leu52 is located on the opposite side of the PLN transmembrane helix as the leucine-isoleucine zipper residues (Fig. I-5A). Removal of the last three C-terminal residues of PLN, however, had a drastic effect on the pentamer stability. At high SDS concentrations, M50stop appeared to be

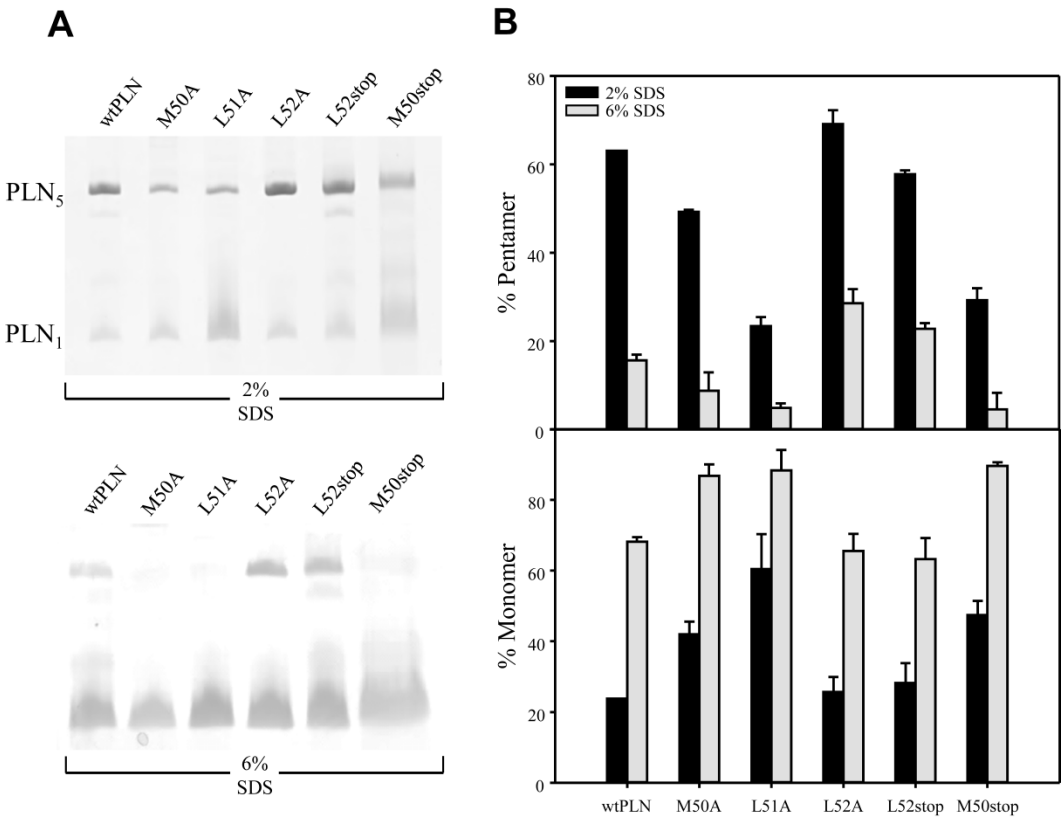

Figure I-4. The effect of mutation and truncation of the C-terminal end of PLN on the pentamer stability. (A) SDS-PAGE of wild-type and various PLN constructs in the presence of 2% SDS (top) and 6% SDS (bottom). The PLN pentamer (PLN_5) and monomer (PLN_1) are indicated. **(B)** Quantification of pentameric stabilities of PLN constructs at low (2% SDS, black bars) and high (6% SDS, grey bars) SDS concentrations. The percentage of total PLN in the pentameric (top) and monomeric (bottom) forms for wild-type and various PLN constructs.

Table I-2. Quantification of pentameric stabilities of various PLN constructs.

	Percentage pentamer			Percentage monomer		
	2%	-SDS-	6%	2%	-SDS-	6%
wtPLN	63.0 ± 0.0		15.6 ± 1.3	23.8 ± 0.0		68.1 ± 1.4
M50A	49.2 ± 0.5		8.8 ± 4.1	42.0 ± 3.6		86.8 ± 3.3
L51A	23.4 ± 2.1		4.8 ± 1.1	60.4 ± 9.9		88.3 ± 5.7
L52A	69.1 ± 3.1		28.5 ± 3.3	25.7 ± 4.1		65.5 ± 4.9
L52stop	57.8 ± 0.8		22.8 ± 1.3	28.3 ± 5.6		63.3 ± 5.9
M50stop	29.2 ± 2.7		4.6 ± 3.7	47.5 ± 3.9		89.6 ± 1.0

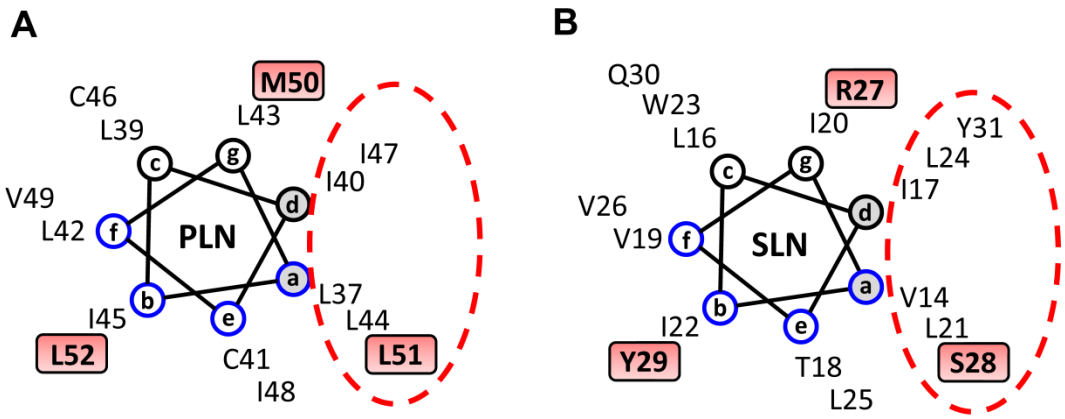

Figure I-5. Helical wheel diagram of the transmembrane and luminal domains of PLN and SLN. Residues 37-52 of PLN **(A)** and 14-31 of SLN **(B)** are indicated**.** The residues at positions highlighted in blue (a, b, e and f) have been proposed to directly interact with SERCA. The leuicine-isoleucine zipper residues of PLN (positions a and d) involved in pentamer formation are indicated with a red dashed circle. The C-terminal Met^{50}-Leu-Leu^{52} residues of PLN are shown in red boxes. The corresponding SLN residues are indicated as in panel A.

almost completely monomeric and the determined pentamer and monomer composition was indistinguishable from that of L51A mutant (Fig. I-4 and Table I-2).

Thus, alanine mutation and truncation data are in strong agreement and indicate that the C-terminal ^{50}MLL motif of PLN is very important in maintaining the pentamer stability, especially Met^{50} and Leu^{51}. Since this hydrophobic motif is replaced by a more polar ^{27}RSYQY sequence in SLN, it is likely that this region interferes with the oligomer assembly of SLN. Interestingly, Met^{50} and Leu^{51} of PLN are the equivalent positions of a positively charged Arg^{27} and a small polar Ser^{28} of SLN, respectively, suggesting that these polar residues might be the key in preventing oligomer formation (Fig. I-5B). This also agrees with our previous studies on the PLN/SLN chimeras which have shown that replacing the C-terminal ^{50}MLL sequence of PLN with the ^{27}RSYQY sequence of SLN resulted in a chimera which was completely monomeric by SDS-PAGE (14). Based on these results, we wanted to replace the ^{27}RSYQY sequence of SLN with the C-terminal ^{50}MLL motif of PLN. Unfortunately, attempts to express or synthesize this construct were unsuccessful. Taken together, we conclude that the presence of a polar luminal extension and lack of key transmembrane residues in SLN make this protein unable to form stable oligomers.

I-3. Experimental Procedures

I-3.1. Expression and Purification of Recombinant SLN. Recombinant SLN and PLN chimeras were expressed and purified as described previously (15) with the exception of an additional organic extraction step for SLN purification. Briefly, following protease digestion of the maltose-binding protein and SLN fusion protein, trichloroacetic acid was

added to a final concentration of 6%. This mixture was incubated on ice for 20 min. The precipitate was collected by centrifugation at 4 °C and subsequently homogenized in a mixture of chloroform:isopropanol:water (4:4:1) and incubated at room temperature for 3 h. The organic phase, which was highly enriched in recombinant SLN, was removed, dried to a thin film under nitrogen gas, and resuspended in 7 M guanidine hydrochloride. Reverse-phase HPLC was performed as described (15), and the molecular mass was verified by MALDI-TOF mass spectrometry (Institute for Biomolecular Design, University of Alberta).

I-3.2. Co-reconstitution of SERCA and Recombinant SLN. Routine procedures were used to purify SERCA1a from rabbit skeletal muscle SR vesicles and functionally reconstitute it into proteoliposomes with SLN. SERCA, SLN, egg yolk phosphatidylcholine, and egg yolk phosphatidic acid were solubilized with octaethylene glycol monododecyl ether ($C_{12}E_8$) to achieve final molar stoichiometries of 1 SERCA, 6 SLN, and 195 lipids. The co-reconstituted proteoliposomes containing SERCA and SLN were formed by the slow removal of detergent (with SM-2 Biobeads, Bio-Rad) followed by purification on a sucrose step gradient. The purified co-reconstituted proteoliposomes typically yield final molar stoichiometries of 1 SERCA, 4.5 SLN, and 120 lipids. This same procedure was used for the co-reconstitution of SERCA with PLN constructs.

I-3.3. Activity Assays. Calcium-dependent ATPase activities of the co-reconstituted proteoliposomes were measured by a coupled enzyme assay (16). The coupled enzyme assay reagents were of the highest purity available (Sigma-Aldrich). All co-reconstituted peptide constructs were compared with a negative control (SERCA reconstituted in the absence of SLN) and a matched positive control (SERCA co-reconstituted in the presence of either wild-type SLN or wild-type PLN). A minimum of three independent reconstitutions and activity assays were performed for each peptide, and the calcium-

dependent ATPase activity was measured over a range of calcium concentrations (0.1–10 μM) for each assay. This method has been described in detail (17). The calcium concentration at half-maximal activity (K_{Ca}), V_{max}, and Hill coefficient (n_H) were calculated based on nonlinear least square fitting of the activity data to the Hill equation using Sigma Plot software (SPSS Inc., Chicago, IL). Errors were calculated as the S.E. for a minimum of three independent measurements.

I-3.4. Quantitative gel electrophoresis. Lyophylized PLN samples were solubilized in an SDS-PAGE sample buffer containing either 2% or 6% SDS (0.5 mg/ml final protein concentration). 5 μg of each PLN construct was loaded onto 16% SDS-PAGE. Proteins were visualized in the gel by Coomassie staining. Quantification of percentages of PLN pentamer and monomer formation was performed on the scanned gel images using the Image Quant software.

I-4. References

1. Bhupathy, P., Babu, G. J., and Periasamy, M. (2007) Sarcolipin and phospholamban as regulators of cardiac sarcoplasmic reticulum Ca2+ ATPase. *J Mol Cell Cardiol* **42**, 903-911

2. Fujii, J., Ueno, A., Kitano, K., Tanaka, S., Kadoma, M., and Tada, M. (1987) Complete complementary DNA-derived amino acid sequence of canine cardiac phospholamban. *J Clin Invest* **79**, 301-304

3. Wawrzynow, A., Theibert, J. L., Murphy, C., Jona, I., Martonosi, A., and Collins, J. H. (1992) Sarcolipin, the "proteolipid" of skeletal muscle sarcoplasmic reticulum, is a unique, amphipathic, 31-residue peptide. *Arch Biochem Biophys* **298**, 620-623

4. Kimura, Y., Kurzydlowski, K., Tada, M., and MacLennan, D. H. (1997) Phospholamban inhibitory function is enhanced by depolymerization. *J. Biol. Chem.* **272**, 15061-15064

5. Simmerman, H. K., Kobayashi, Y. M., Autry, J. M., and Jones, L. R. (1996) A leucine zipper stabilizes the pentameric membrane domain of phospholamban and forms a coiled-coil pore structure. *The Journal of biological chemistry* **271**, 5941-5946

6. Oxenoid, K., and Chou, J. J. (2005) The structure of phospholamban pentamer reveals a channel-like architecture in membranes. *Proceedings of the National Academy of Sciences of the United States of America* **102**, 10870-10875

7. Traaseth, N. J., Verardi, R., Torgersen, K. D., Karim, C. B., Thomas, D. D., and Veglia, G. (2007) Spectroscopic validation of the pentameric structure of phospholamban. *Proceedings of the National Academy of Sciences of the United States of America* **104**, 14676-14681

8. Fujii, J., Maruyama, K., Tada, M., and MacLennan, D. H. (1989) Expression and site-specific mutagenesis of phospholamban. Studies of residues involved in phosphorylation and pentamer formation. *The Journal of biological chemistry* **264**, 12950-12955

9. Karim, C. B., Marquardt, C. G., Stamm, J. D., Barany, G., and Thomas, D. D. (2000) Synthetic null-cysteine phospholamban analogue and the corresponding transmembrane domain inhibit the Ca-ATPase. *Biochemistry* **39**, 10892-10897

10. Hellstern, S., Pegoraro, S., Karim, C. B., Lustig, A., Thomas, D. D., Moroder, L., and Engel, J. (2001) Sarcolipin, the shorter homologue of phospholamban, forms oligomeric structures in detergent micelles and in liposomes. *The Journal of biological chemistry* **276**, 30845-30852

11. Autry, J. M., Rubin, J. E., Pietrini, S. D., Winters, D. L., Robia, S. L., and Thomas, D. D. (2011) Oligomeric Interactions of Sarcolipin and the Ca-ATPase. *The Journal of biological chemistry* **286**, 31697-31706

12. Becucci, L., Guidelli, R., Karim, C. B., Thomas, D. D., and Veglia, G. (2007) An electrochemical investigation of sarcolipin reconstituted into a mercury-supported lipid bilayer. *Biophys J* **93**, 2678-2687

13. Trieber, C. A., Afara, M., and Young, H. S. (2009) Effects of phospholamban transmembrane mutants on the calcium affinity, maximal activity, and cooperativity of the sarcoplasmic reticulum calcium pump. *Biochemistry* **48**, 9287-9296

14. Gorski, P. A., Glaves, J. P., Vangheluwe, P., and Young, H. S. (2013) Sarco(endo)plasmic reticulum calcium ATPase (SERCA) inhibition by sarcolipin is encoded in its luminal tail. *The Journal of biological chemistry* **288**, 8456-8467

15. Afara, M. R., Trieber, C. A., Ceholski, D. K., and Young, H. S. (2008) Peptide inhibitors use two related mechanisms to alter the apparent calcium affinity of the sarcoplasmic reticulum calcium pump. *Biochemistry* **47**, 9522-9530

16. Warren, G. B., Toon, P. A., Birdsall, N. J., Lee, A. G., and Metcalfe, J. C. (1974) Reconstitution of a calcium pump using defined membrane components. *Proceedings of the National Academy of Sciences of the United States of America* **71**, 622-626

17. Trieber, C. A., Douglas, J. L., Afara, M., and Young, H. S. (2005) The effects of mutation on the regulatory properties of phospholamban in co-reconstituted membranes. *Biochemistry* **44**, 3289-3297